

Investigating Seamless Handover in VANET Systems



**Middlesex
University**

A thesis submitted to Middlesex University in partial fulfilment of
the requirements for the degree of

Doctor of Philosophy

Arindam Ghosh

Department of Computer Science
School of Science and Technology

Middlesex University

June 2016

I would like to dedicate this thesis to my loving parents ...
For their endless love, support and encouragement.
And to ALMIGHTY GOD (Goddess DURGA Maa)!
who always shower's her blessings upon us!

Declaration

I hereby declare that except where specific reference is made to the work of others, the contents of this thesis are original and have not been submitted in whole or in part for consideration for any other degree or qualification in this, or any other university. This thesis is my own work and contains nothing which is the outcome of work done in collaboration with others, except as specified in the text and Acknowledgements. This thesis contains fewer than 55,000 words including appendices, bibliography, footnotes and equations and has fewer than 100 urefigures and tables.

[Arindam Ghosh](#)

June 2016

Acknowledgements

A wise man once said... Time flies! and it flies never to be regained! the only thing you regain with time is Knowledge! This is first thing that comes to my mind after looking back at the journey i have made towards my PhD degree.

This thesis exhibits not only my work behind the keyboard, by spending late hours in the networking labs and PhD research office, but it is also a milestone of achievements in my life at Middlesex University and specifically within the School of Science and Technology. My experience at Middlesex University has been nothing short of an amazing one. Since my first day as a PhD student, I have felt at home at Middlesex University. I have been given many unique opportunities and met some really extraordinary people. Throughout the PhD years, I have learned that there are those who are good in maths and there are those who are good in writing, but my passion is certainly in gadgets used in new technologies by implementation of a real-time VANET Testbed at MDX used in cutting edge research. This thesis also symbolizes the lessons learned in the PhD path through various ups and downs. But this thesis is also the result of many experiences, that I have encountered at Middlesex University through many remarkable individuals who I also wish to acknowledge.

First of all, I would like to acknowledge my debt of gratitude towards my supervisors, Dr Glenford Mapp and Professor Orhan Gemikonakli for their continuous guidance, kind support and great zeal for excellent research. It has been a great motivation and pleasure to work with them. During my studies, both have been instrumental in setting a stepping stone towards my career path as an independent researcher. I have also greatly benefited from their invaluable advice on my research. In particular, I am also thankful to Dr Enver Ever and Dr Jonathan Loo for enlightening me the first glance of research in this particular field. Further, I would also like to express my humble respect and sincere gratitude to the Dean of School of Science and Technology (SAT) Prof Martin Loomes and to the Deputy Dean Prof Balbir Barn, without whom the MDX VANET Testbed (a major part of my work contributing towards my final PhD thesis) wouldn't have been possible.

Also, a special thanks to Dr Purav Shah and Dr Ramona Trestian for their generous support in interpreting some of the results and many useful discussions.

My list of thanks wouldn't be complete without having a special mention for Prof Richard Comley (Director of Research, RKTO) who has been greatly constitutional towards chairing my PhD from the start by welcoming us into this PhD program and later at every milestone (e.g., registration, transfer and final viva).

I also would like to thank the technical staff of Middlesex University for their support during my studies especially Barry Harte, Louis Slabbert and Leonard Miraziz, Jairam Reddy, Simon Hinks and Bilal Hashmi. My sincere appreciation goes to Terri Demetriou, Alex Fogdon and Nicholas Nikeforou for ensuring the countless number of forms, and paperwork for registration, transfer and viva were correctly completed and led. I am deeply indebted to my friends, in particular Kiishi, Irina Alexandra Titi, Aiden Mullet, Niovi and my research office colleagues Vishnu Vardhan Paranthaman, Ammar Zayouna, Yongpil Yoon, for their help with my research, and more for their great friendship and encouragement during my studies. A special thanks to Nicolae Starciuc, Govar Abdulkarim and Kajanthan Rajalingam (undergraduate students involved in the VANET Project) for your endless support in making the Testbed successful. To all my friends, thank you for understanding and encouragement in my many moments of crisis. Your friendship makes my life a wonderful experience. The number of people i want to thank is countless and my humble apologies, if i have missed out on anyone, therefore, i would like to deeply thank everyone with whom i might have come across in some or the other way in this journey.

I would like to thank my sister Priyanca Ghosh Sinha, Sandeep Sinha (brother-in-law) and my nephew Aabir Sinha, for their extra care and affection (via skype sessions) during my studies. Their continued love and support helped me through hard times while in London.

Lastly and most importantly, my deepest gratitude, love and affection to my parents, Tarun Kanti Ghosh and Misti Rani Ghosh, to whom I owe alot for all that I have ever accomplished. Their endless love, patience, encouragement, and their never ending support pulled me through in times when it was most needed. I owe everything to my parents, I have ever achieved in my life. Without their love and support, it wouldn't have been possible to complete my PhD degree.

Finally I would like to Thank, Almighty Lord, for always being there for me. This thesis is only a beginning of my journey.

Abstract

Wireless communications have been extensively studied for several decades, which has led to various new advancements, including new technologies in the field of Intelligent Transport Systems. Vehicular Ad hoc Networks or VANETs are considered to be a long-term solution, contributing significantly towards Intelligent Transport Systems in providing access to critical life-safety applications and infotainment services. These services will require ubiquitous connectivity and hence there is a need to explore seamless handover mechanisms. Although VANETs are attracting greater commercial interest, current research has not adequately captured the real-world constraints in Vehicular Ad hoc Network handover techniques. Due to the high velocity of the vehicles and smaller coverage distances, there are serious challenges in providing seamless handover from one Road Side Unit (RSU) to another and this comes at the cost of overlapping signals of adjacent RSUs. Therefore, a framework is needed to be able to calculate the regions of overlap in adjacent RSU coverage ranges to guarantee ubiquitous connectivity. This thesis is about providing such a framework by analysing in detail the communication mechanisms in a VANET network, firstly by means of simulations using the VEINs framework via OMNeT++ and then using analytical analysis of the probability of successful packet reception. Some of the concepts of the Y-Comm architecture such as Network Dwell Time, Time Before Handover and Exit Times have been used to provide a framework to investigate handover issues and these parameters are also used in this thesis to explore handover in highly mobile environments such as VANETs. Initial investigation showed that seamless communication was dependant on the beacon frequency, length of the beacon and the velocity of the vehicle. The effects of each of these parameters are explored in detail and results are presented which show the need for a more probabilistic approach to handover based on cumulative probability of successful packet reception. In addition, this work shows how the length of the beacon affects the rate of change of the Signal-to-Noise ratio or SNR as the vehicle approaches the Road-Side Unit. However, the velocity of the vehicle affects both the cumulative probability as well as the Signal-to-Noise ratio as the vehicle approaches the Road-Side Unit. The results of this work will enable systems that can provide ubiquitous connectivity via seamless handover using proactive techniques because

traditional models of handover are unable to cope with the high velocity of the vehicles and relatively small area of coverage in these environments. Finally, a testbed has been set-up at the Middlesex University, Hendon campus for the purpose of achieving a better understanding of VANET systems operating in an urban environment. Using the testbed, it was observed that environmental effects have to be taken into considerations in real-time deployment studies to see how these parameters can affect the performance of VANET systems under different scenarios. This work also highlights the fact that in order to build a practical system better propagation models are required in the urban context for highly mobile environments such as VANETs.

Table of contents

List of figures	xiii
List of tables	xvi
List of Abbreviations	xvii
1 Introduction	1
1.0.1 Current Trends in the VANET Technology	5
1.0.2 Constraints in the Vehicular Networks	7
1.0.3 IEEE 1609.4 Broadcasting Limitations	7
1.0.4 Beacon Collision due to lack of Congestion Control	8
1.0.5 Interference Issues in dense Urban Environemtns	9
1.1 Research Aims and Objectives	9
1.1.1 Key Research Questions	10
1.1.2 Hypothesis and Approach	11
1.1.3 List of Publications	12
1.1.4 Organization of the thesis	13
2 Literature Review	16
2.1 State of the Art - VANET Applications	16
2.1.1 Safety-Related Applications	16
2.1.2 Local Traffic Information Systems	18
2.1.3 Automated Highway and Cooperative Driving	18
2.1.4 IP-Based Applications	19
2.2 Standards and Protocol Architecture	20
2.2.1 WAVE-Protocol Stack	20
2.2.2 Data Plane Services	22
2.2.3 Management Plane Services	24
2.3 IEEE 802.11p	27
2.3.1 MAC Sub layer in IEEE 802.11p	27

2.3.2	PHY Layer in IEEE 802.11p	30
2.4	WAVE WSMP	32
2.5	Understanding Handover in Detail	33
2.5.1	Handover Concepts	33
2.5.2	General Characteristics of Handover	33
2.5.3	Advanced Classification of Handover	35
2.6	Related Works	38
2.6.1	Handover based Related Works	38
2.6.2	Analytical Model based Related Works	40
2.6.3	Testbed based Related Works	42
2.7	Propagation Model based Related Works	43
2.7.1	Propagation Models: An Overview	43
2.8	Existing Path Loss Models used in VANETs	44
2.8.1	Free Space Path Loss Model	44
2.8.2	Two-Ray Ground Model	45
2.8.3	Rayleigh and Rician Fading Model	45
2.8.4	Log-Normal Path Loss Model	46
2.8.5	Nakagami Model	47
2.8.6	The Okumura Model	47
2.8.7	Hata Models	48
2.8.8	CORNER Propagation Model	49
2.8.9	Finite Propagation Model	50
2.9	Current Trends in VANET Simulation Techniques	54
2.9.1	Mobility Simulator	55
2.9.2	Network Simulator	55
2.9.3	VANET Simulator	55
2.10	Which is the Most Suitable Simulator?	56
2.11	Summary	60
3	Preliminary Investigation for Providing Ubiquitous Communication using Road-Side Units in VANET Systems	61
3.1	Introduction	61
3.2	Research Methodology: Simulation	62
3.2.1	Simulation approach in OMNeT++	63
3.2.2	The Simulation tool - OMNeT++	64
3.3	Simulation Scenario	64
3.3.1	SUMO simulation files	64
3.3.2	Simulation with the Veins Framework	66

3.3.3	Running the simulation	66
3.4	Analysis of RSU Coverage Area	67
3.4.1	Reception Power	68
3.4.2	Beaconing & Beacon Generation Rate	69
3.4.3	Detection Range Formula	69
3.5	Why Network Dwell Time (NDT)?	70
3.6	Simulation Results and Discussions	71
3.6.1	Simulation Detection Range	74
3.6.2	Analysis of Network Dwell Time (NDT)	74
3.6.3	Analysis of Exit Time (ET)	75
3.6.4	Minimum Overlapping distance for Handover	76
3.7	Summary	77
4	Detailed Investigation of the Communication Mechanisms in VANET Systems	78
4.1	Introduction	78
4.2	Further Analysis of Coverage Range	78
4.2.1	Calculation of Successful Packet Reception in Simulation	78
4.2.2	Further Investigation into PHY layer for Beacon size	83
4.3	Summary	86
5	Exploring Cummulative Probability to understand Communication Dynamics in VANETs	87
5.1	Introduction	87
5.2	Overview of Cumulative Probability Approach	87
5.2.1	The Effect of Beacon Frequency on Cumulative Probability	89
5.2.2	The Change in Beacon Reception Probability	94
5.2.2.1	The Change (ΔP) at Entry	94
5.2.2.2	The Change (ΔP) at Exit	94
5.3	Handover Policy Based on CP Approach	95
5.4	Analysis of Overlapping Region	100
5.5	Summary	103
6	Development of an Approximate Model of Communications in VANET Systems	104
6.1	Introduction	104
6.2	The Essence of SNR on ΔP for CP	105
6.2.1	Equation for Calculating $dP/dSNR$	105

TABLE OF CONTENTS

6.3	The Impact of Beacon Length on Delta P (ΔP)	108
6.4	The relation of ΔP with respect to Velocity	111
6.4.1	Calculation for P with respect to velocity using dP/dR	113
6.5	Impact of Velocity of the Vehicle on P and CP	114
6.6	Summary	117
7	MDX-VANET TESTBED	119
7.1	Introduction	119
7.2	MDX-VANET Testbed	120
7.3	Investigating previous deployments in VANET	120
7.4	Steps Before Deployment - MDX VANET Testbed	122
7.4.1	Initial Scenario Problem	122
7.4.2	Initial testbed Coverage Analysis	122
7.4.3	Description of the testbed Deployment	123
7.4.4	FSPL calculations for our MDX testbed	132
7.5	Initial Coverage Testing before Deployment	135
7.5.1	Hatchcroft Building	135
7.5.2	William Building	136
7.5.3	Middlesex University Car Park	136
7.5.4	Grove Building	137
7.6	Overlapping Regions in MDX VANET testbed	138
7.7	The Final Deployment of the MDX VANET Testbed	140
7.8	MDX VANET Trial	142
7.9	Results - MDX VANET Testbed Deployment	144
7.9.1	Coverage Graph	144
7.9.2	Live Vehicle Tracking	146
7.10	General Observations from the MDX VANET Trial	147
7.11	Extended VANET Testbed Project - DfT	148
7.11.1	Recommendations for Future Testing and Implementation	149
7.12	Summary	151
8	Conclusion and Future Works	152
8.0.1	Summary of the Work Done	152
8.0.2	Contribution to Knowledge	152
8.0.3	Thesis Contributions	155
8.0.4	Summary	155
8.1	Conclusion	156
8.2	Suggestions for Future Work	156

TABLE OF CONTENTS

8.3	Final Statement	158
	References	159
	Appendix A	171
A.1	Equations	171
A.1.1	Equation for Calculating $dP/dSNR$	171
A.1.2	Calculation for P with respect to velocity using dP/dR . .	174
	Appendix B	176
B.1	Abstract of Publications	176

List of figures

1.1	An Intelligent Transport System Scenario	1
1.2	A VANET scenario	2
2.1	An example of a Safety Application.	17
2.2	An example of a Non-Safety Application	19
2.3	WAVE Protocol Architecture.	21
2.4	WAVE reference model.	22
2.5	TDMA Channel Time.	23
2.6	Channel Access.	23
2.7	Channel Intervals.	24
2.8	Guard Interval.	25
2.9	Different Channel Access Options.	26
2.10	Prioritization Mechanism.	28
2.11	Inter-frame Space.	29
2.12	Channel Allocation.	31
2.13	WSMP Packet Format.	33
2.14	Handover Concepts.	34
2.15	YComm Architecture	35
2.16	Illustrating TBVH and NDT	37
2.17	CORNER Propagation Model	49
2.18	Taxonomy of VANET Simulators.	58
3.1	Simulation Process.	65
3.2	Coverage Segmentation.	67
3.3	Handover process and corresponding messages.	68
3.4	Handover Procedures in Simulation Scenario.	71
3.5	Beacons Received at Vehicle.	72
3.6	Received Power at Vehicle.	73
3.7	Received Power at the Vehicle in the Overlapping Region.	74

4.1	PHY and MAC Segmentation.	79
4.2	PacketOK vs DbIRand.	80
4.3	NDTi vs NDTr.	81
4.4	NDTr with different Beacon Sizes (10m/s).	81
4.5	NDTr with different Beacon Sizes (30m/s).	82
4.6	Entry Side of Coverage Area (10m/s).	83
4.7	Entry Side of Coverage Area (30m/s).	84
4.8	First & Last Beacon received at PHY & MAC layers.	84
4.9	Exit Side of Coverage Area (10m/s).	85
4.10	Exit Side of Coverage Area (30m/s).	85
5.1	CP reaching 1 (Entry Region - 10m/s).	89
5.2	CP reaching 1 (Entry Region - 30m/s).	90
5.3	CP_n reaching 0 (Exit Region - 10m/s).	90
5.4	CP_n reaching 0 (Exit Region - 30m/s).	91
5.5	NDT of Probability vs NDT of Cumulative Probablity (10m/s).	91
5.6	NDT of Probability vs NDT of Cumulative Probablity (30m/s).	92
5.7	Comparision of P NDT vs CP NDT vs NDTr vs NDTi (10m/s).	93
5.8	Comparision of P NDT vs CP NDT vs NDTr vs NDTi (30m/s).	93
5.9	ΔP vs SNR.	95
5.10	Traditional and Probabilistic Segmentation.	96
5.11	NDT - From Concept to Reality	97
5.12	Overlapping Scenarios	101
5.13	Overlapping Distance.	102
6.1	Comparison of Simulation vs. Analytical Model.	108
6.2	Comparison of Analytical Model vs. Approximation.	109
6.3	Approximate with different Packet Lengths.	109
6.4	Rate of change vs. Packet Length.	110
6.5	Comparison of dSNR vs. dR.	112
6.6	Comparison of dP vs. dR.	112
6.7	Comparison of P and CP for 30 m/sec.	115
6.8	Comparing P and CP for 1Hz.	115
6.9	Comparison of P and CP for 10Hz.	116
6.10	Comparison of P of 1Hz and 10Hz.	116
6.11	Comparison of CP of 1Hz and 10Hz.	117
7.1	MDX VANET Testbed.	120
7.2	MDX Campus Coverage Map of RSUs range of each Spot	123

7.3	An Example: Free Space Pathloss Model in Line-of-Sight	132
7.4	Comparison of RSSI from testbed and FSPL for Hatchcroft	135
7.5	Comparison of RSSI from testbed and FSPL for Williams	136
7.6	Comparison of RSSI from testbed and FSPL for Car Park	137
7.7	Comparison of RSSI from testbed and FSPL for Grove	138
7.8	Map with Overlapping Coverage Ranges of all RSUs.	139
7.9	NETWORK DIAGRAM.	140
7.10	Data forwarding from RSU to Server.	141
7.11	MDX VANET Trial Photos.	143
7.12	Coverage Map.	144
7.13	Coverage of each RSU.	145
7.14	Live Tracking Screen shot.	146
7.15	Extended Scenario for MDX VANET testbed.	148
7.16	Network Diagram of a LTE Backhauled Mobile RSU.	149
7.17	Building LTE Backhauled Mobile RSU in Lab.	150

List of tables

2.1	The default EDCA parameters in IEEE 802.11p	27
2.2	Spectrum Allocation for DSRC/WAVE: An Overview	31
2.3	The Comparison of WAVE and Wi-Fi Parameters.	32
2.4	Summary of Propagation Models used in VANETs.	52
2.5	Summary of Propagation Models used in VANETs.	53
3.1	RSU Configuration Parameters.	71
3.2	OBU Configuration Parameters.	72
3.3	Comparison of NDT: Simulaiton vs. Theoretical	75
3.4	Exit Time from Simulation.	75
3.5	Overlapping Distance ($\lambda=1\text{Hz}$).	76
3.6	Overlapping Distance ($\lambda=5\text{Hz}$).	76
3.7	Overlapping Distance ($\lambda=10\text{Hz}$).	76
5.1	Communication Time (secs) between the Segments	98
7.1	Field Measurements from RSU-1 on Hatchcroft Building	125
7.2	Field Measurements from RSU-2 on Williams Building	126
7.3	Field Measurements from RSU-3 on MDX Car Park	127
7.4	Field Measurements from RSU-4 on Grove Building	128
7.5	Field Measurements from RSU-1 (Inside Pathway)	129
7.6	Field Measurements from RSU-2 (Inside Pathway)	130
7.7	Field Measurements from RSU-3 (Inside Pathway)	131

List of Abbreviations

Greek Symbols

μ_{ml}	is the Mobility leave rate
CP	Cumulative Probability
CP_{EN}	Cumulative Probability at Entry
CP_{EX}	Cumulative Probability at Exit
CP_n	Negative Cumulative Probability, (Exit Side)
$dPDR$	is defined as the rate of change with respect to Packet Delivery Ratio and is further abbreviated to dP
dR	is defined as the rate of change with respect to Radius (R)
$dSNR$	is defined as the rate of change with respect to Signal-to-Noise Ratio
E_{vel}	Expected Velocity of the vehicle.
NDT_{CP}	Cumulative Probability of Network Dwell Time
NDT_P	Probability of Network Dwell Time
P	Probability, Probability of Individual Successful Beacon Reception.
P_L	Power of Path Loss
P_N	Power of Noise
P_n	Negative Probability, (Exit Side)
P_S	Power of Signal
P_T	Power of Transmitter

List of Abbreviations

$pMAX$	Maximum Transmission Power Possible.
R_H	Handover radius.
sat	Minimum signal attenuation threshold.
T_{EH}	Time taken to Handover to the next network.
V_{max}	Maximum velocity of the vehicle.
α	Minimum path loss coefficient.
Δ_{ENTRY}	$P_N - P_{N-1}$, The rate of change (Entry Side)
Δ_{EXIT}	$P_N - P_{N+1}$, The rate of change (Exit Side)
Δ_P	The Rate of Change
Λ	Wavelength = (speedOfLight/carrierFrequency)
λ	Beacon frequency
π	$\simeq 3.14 \dots$
A	Area of the cell.
ET	$NDT - T_{EH}$
NDT	$1/\mu_{ml} = (\pi \times R_H)/V_{max}$, where, μ_{ml} = Mobility leave rate.
NDT	NDD/E_{vel} , where, NDD is Network Dwell Distance travelled along a motorway that is in coverage of a given network.
P	Perimeter of the cell.
PDR	$[1 - 1.5erfc(0.45\sqrt{SNR})]^L$, where, L is the length of the packet.
SNR	(SignaltoNoiseRatio) = $10^{SNR_{dB}/10}$ (This is from the Simulation)

Acronyms / Abbreviations

AC	Access Categories
AIFS	Arbitration Inter-Frame Spacing
BER	Bit Error Rate

List of Abbreviations

BS	Base Station
BSM	Basic Safety Message
BSS	Basic Service Set
CAMs	Cooperative Awareness Messages
CCH	Control Channel
CP	Cyclic Prefix
CSMA/CA	Carrier Sense Multiple Access/Collision Avoidance
CTS	Clear to Send
CW	Contention Window
CW _{max}	Contention Window Maximum
CW _{min}	Contention Window Minimum
DCC	Decentralized Congestion Control
DCF	Distributed Coordination Function
DEMs	Decentralised Environmental Messages
DIFS	DCF Inter-Frame Space
DSRC	Dedicated Short Range Communication
EDCA	Enhanced Distributed Channel Access
EDCAF	Enhanced Distributed Channel Access Function
EIFS	Extended Inter-Frame Space
ET	Exit Time
ETSI	European Telecommunications Standards Institute
FCC	Federal Communications Commission
FDMA	Frequency Division Multiple Access
GDP	Gross Domestic Product

List of Abbreviations

GI	Guard Interval
GPS	Global Positioning System
ICI	Inter-Carrier Interference
IFS	Inter-Frame Space
IPv4	Internet Protocol version 4
IPv6	Internet Protocol version 6
ISI	Inter-Symbol Interference
ITS	Intelligent Transport System
IVC	Inter-Vehicular Communication
LLC	Logical Link Control
MAC	Medium Access Control
MIB	Management Information Base
MLME	MAC sub-Layer Management Entities
MS	Mobile stations
MSDU	MAC Service Data Unit
NDT	Network Dwell Time
NDTi	Network Dwell Time (Idealised - Theoretically Calculated)
NDTr	Network Dwell Time (Realistic - Simulation Calculated)
NLOS	Non Line-of-Sight
OBUs	On-Board Units
OFDM	Orthogonal Frequency Division Multiplexing
PCF	Point Coordination Function
PDR	Packet Delivery Ratio
PHY	Physical Layer

List of Abbreviations

PIFS	PCF Inter-Frame Space
PLME	PHY Layer Management Entities
PPS	Pulse Per Second
PSID	Provider Service ID
QoS	Quality of Service
RCR	Reliable Connectivity Range
RSSI	Received Signal Strength Indicator
RSUs	Road-Side Units
RTS	Request to Send
RX	Reception
SCH	Service Channel
SIFS	Short Inter-Frame Space
SIGs	Special Interest Groups
TA	Timing Advertisement
TBH	Time Before Handover
TBVH	Time Before Vertical Handover
TCP/IP	Transmission Control Protocol/Internet Protocol
TDMA	Time Division Multiple Access
TraCI	Traffic Control Interface
TX	Transmission
TXOP	Transmission Opportunities
UCR	Unreliable Connectivity Range
UDP	User Datagram Protocol
UTC	Coordinated Universal Time

List of Abbreviations

V2I	Pedestrian to Infrastructure
V2I	Vehicle to Infrastructure
V2R	Vehicle to RoadSide
V2V	Vehicle to Vehicle
VANET	Vehicular Ad hoc Network
WAVE	Wireless Access in Vehicular Environment
WBSS	WAVE Basic Service Set
WME	WAVE Management Entity
WPCF	WAVE Point Coordination Function
WSAs	WAVE Service Advertisements
WSM	WAVE Short Message
WSMP	WAVE Short Message Protocol
Y-Comm	Y-Communication

Chapter 1

Introduction

In this era of globalization, transport efficiency plays an important part in the economic growth of a flourishing country in today's world. Thus, an efficient transport system, is a key requirement for the community for better sustainable resources (i.e for commuting, employment and trade). However, this transport efficiency presently comes at a very substantial cost because of excessive use of pollutants like oil, coal, etc., which leads to heavy CO₂ emissions in the air. Statistics from the European Commission show that the European transport industry constitutes about 6.3% of the Gross Domestic Product (GDP) which alone comes from transport industry itself. It is also considered the most employable sector which gives employability to nearly 13 million people. Various European research efforts show that our transport system itself, consumes about 63% of the oil, which produces about 29% of the CO₂ emissions alone (European Commission, 2015). Figure 1.1 represents an Intelligent Transport Systems (ITS) scenario cited

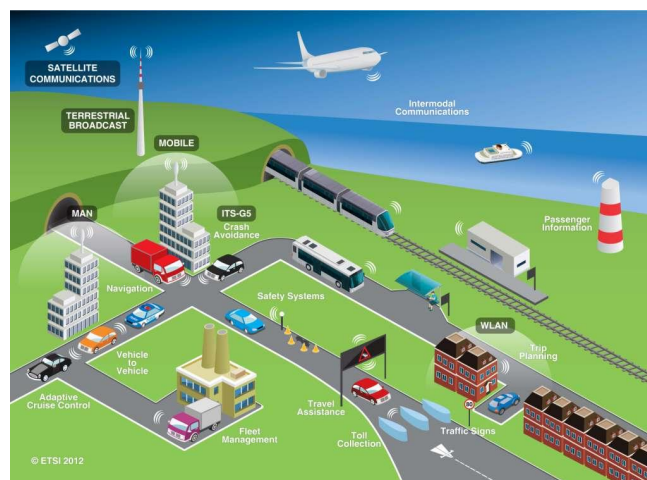


Fig. 1.1 An ITS Scenario. (European Standards Organization, 2015)

from (European Standards Organization, 2015). According to this scenario, reducing oil reserves will be the main cause for the oil prices to go higher to about 50% by 2050. This calls for an urgent change in the current tendencies, otherwise the social costs of the accidents and pollution will continue to rise (European Commission, 2015).

This rapid growth in the number of vehicles on the roads has created a plethora of challenges for road traffic management authorities such as, traffic congestion, increasing number of accidents, air pollution, etc. Over the last decade, significant research efforts from both the automotive industry and academia have been undertaken to accelerate the deployment of a wireless network, based on a short-range communication among moving vehicles (Vehicle-to-Vehicle, V2V) and roadside infrastructure (Vehicle-to-Infrastructure, V2I). This network is called a Vehicular Ad Hoc Network (VANET) and is characterized by high node speed, rapidly changing topologies, and short connection lifetimes. A typical VANET scenario, taken from the work in (Eiza et al., 2013) has been highlighted in Figure 1.2.

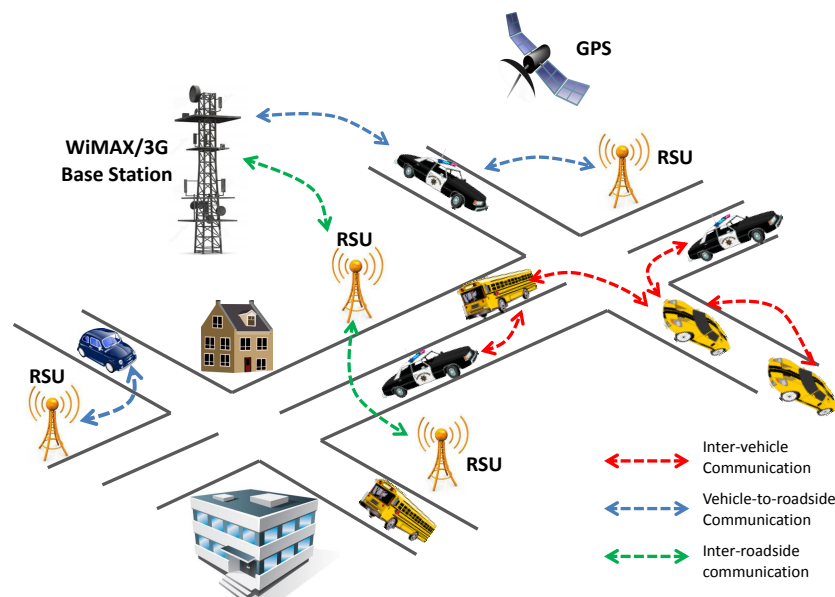


Fig. 1.2 A VANET scenario as illustrated by ITS.

Several applications for VANETs have been categorized for road-safety, traffic efficiency, and infotainment applications (i.e. information and entertainment applications). The latter two can be typically referred to as non-safety applications as they aim to provide information and comfort/ entertainment to travellers and have the great potential to increase the chances of success for VANETs and to accelerate their market penetration (Karagiannis et al., 2011).

Road traffic management for Smart Cities involves monitoring of the actual traffic situation in real-time (i.e., speeds, incidents, traffic flow etc.) with the aim of controlling of this real-time information from the vehicles or influencing the traffic flow using this information in order to reduce traffic congestion. This real-time information is then used to efficiently deal with accidents and provide an accurate and reliable traffic information in order to make predictions for drivers and transport authorities (Ghosh et al., 2013).

In VANETs, vehicles periodically broadcast beacons that are essentially status messages used to discover and maintain neighbor relationships (Reinders et al., 2011), (Van Eenennaam et al., 2010), (Campolo et al., 2011b) and (Van Eenennaam et al., 2009). The European ITS VANET Protocol (EIVP) defines beacons as Cooperative Awareness Message (CAM). Beacons also include a security component and the size of a beacon is approximately 400 bytes long (Reinders et al., 2011), (Van Eenennaam et al., 2010) and (Campolo et al., 2011b). Beaconing can be used for reliability due to the lack of acknowledgements and reservation by means of RTS/CTS (Ganan et al., 2012). Beacon messages are generated and issued periodically between the vehicle (V2V) and the RSUs (V2I) communications. The beacon generation rate is the rate at which beacons are sent to the Medium Access Control (MAC) layer for transmission, since they are used to create Cooperative Awareness. The beacon generation rate should be in the order of several beacons per second to provide the system with accurate information about the close surroundings (Ganan et al., 2012), (Chung et al., 2011), (Reinders et al., 2011) and (Campolo et al., 2011b). The beacon frequency is the beacon generation rate which is denoted by λ . Though some research efforts consider a fixed λ of 10Hz (Van Eenennaam et al., 2009), it was shown in (Ganan et al., 2012) that generation rate adaptation as a network layer mechanism is one of the instruments to make beaconing more scalable. Increasing λ results in more beacons being sent and a higher temporal resolution. But this comes at the price of an increase in collision probability, especially in dense traffic situation. Hence, an adaptive mechanism for beaconing is desirable and this needs consideration in order to have seamless connectivity for life critical safety applications used in VANETs (Campolo et al., 2011b).

In the next couple of years, it is evident that Intelligent Transport Systems (ITS) will entail the deployment of VANETs especially for Smart Cities. For this purpose it is not only imperative to have proper infrastructure with several Road-Side Units (RSUs) being placed in a resourceful and cost-effective manner, but also to serve the main purpose of ITS in order to have seamless connectivity for optimum coverage with ideal channel utilization where vehicles are able to access applications and

services quickly (Ghosh et al., 2013). The paradox of deployment issues are, that on one hand ITS demands the deployment of infrastructure in such a way that it supports seamless connectivity but on the other hand, this comes at the cost of having many RSUs placed along the road-side leading to possible interference issues. Hence, in order to achieve seamless connectivity, the placement of RSUs within the general infrastructure needs to be fully investigated (Ganan et al., 2012).

Though other research efforts have looked at many issues in VANET networks, very few research work have looked at handover issues. Most researchers assume that handover does not take a significant time and does not affect overall VANET operation. However, this thesis also shows that by using a simulation approach to analyse the effects of handovers, providing ubiquitous communication for VANET systems is a non-trivial task and a proactive approach is needed which must take several factors into account. Thus, previous work in this on-going research in (Ghosh et al., 2013), (Ghosh et al., 2014a) and (Ghosh et al., 2014b) has highlighted the challenges in providing a ubiquitous communication using RSU in VANETs. The Y-Comm Architecture (Mapp et al., 2012) was developed to explore proactive handover issues in future mobile networks. It has introduced an advanced handover classification system as well as new concepts such as Network Dwell Time (NDT), Time Before Handover (T_{BH}) and Exit Time (ET) (Shaikh et al., 2007) have been used to analyse the handover issues in VANET systems and the overall performance of VANET systems. Y-Comm has been used to study seamless handover in both homogeneous and heterogeneous networks (Mapp et al., 2012) and (Shaikh et al., 2007). This thesis demonstrates the importance of these concepts in achieving a seamless communication. In this context, NDT is the time the vehicle spends in a RSU's coverage range. This thesis provides a more comprehensive analysis involving the beacon frequency, size of the beacon and the velocity of the vehicle, and how they influence the handover characteristics as highlighted in Y-Comm framework.

In traditional mobile and wireless communication systems, mobility is considered to be a fundamental challenge to overcome. Hence, many research efforts have stressed on mobility issues. In the case in VANET systems, the constant movement of the vehicle is one of the major challenges, which, in turn affect the reliability of the communication. Therefore, reliable communication is the key source for VANETs in providing ubiquitous communication for critical life-safety applications. This encourages us to not only further examine different handover techniques, but also forces us to re-consider the classification of handovers in VANETs i.e., how the handovers can be classified according to VANET characteristics?

The process of transferring an active call or communication from one cell (in this case coverage areas of the RSUs) to another is called *handover*. There are different types of handovers, which have been defined in the Y-Comm architecture (Mapp et al., 2012). There are two general classification of handover according to wireless mobile communications that can be applied to VANETs systems, one is *Vertical handover* and the other is *Horizontal handover*.

In Vertical handover, the communication switches between different, network types, (e.g., Mobile networks to WLAN and vice versa). Likewise, in Horizontal handover, the communication takes place between similar network infrastructures (i.e., WLAN to WLAN). Vertical handover is out of the scope of this thesis. Therefore, in this thesis, we aim to look at horizontal handover rather than vertical handover. Though, many argue that vertical handover is essential for mobile and wireless communications where there is a need to maintain certain standard of Quality-of-Service (QoS), as the mobile user is required to switch between cellular towers or base stations (BS). However, in VANET systems the beaconing mechanism, which is unique to this new technology, enforces broadcasting of these short-lived beacons for seamless connectivity. Hence, it is evident that to achieve this seamless communication for supporting critical life-safety applications in VANETs, it is necessary to understand the V2I handover mechanism, thus, making horizontal handover ideal option for VANET systems. This entails the Y-Comm concepts to be carefully studied under different scenarios, in order to predict the handover times and thus making proactive handover possible.

This thesis is driven by the challenges that arise when handover occurs in vehicular environments. Some of the features that directly influence these challenges have been categorised in the next section.

1.0.1 Current Trends in the VANET Technology

With the ever growing popularity in wireless and mobile communications standards, Special Interest Groups (SIGs), technical experts and standardization bodies across United States, Europe and Japan acknowledged the need to develop new specialised standards for vehicular communications. The standards were then formalised on the perquisites from vehicular networks based on their explicit features. Therefore, these standards are essential for validating the interoperability between different equipments developed in U.S and Europe and Japan for ITS purposes (IEEE-Std., 2010) and (ETSI-Std., 2009).

On one hand, the Federal Communications Commission (FCC) in the United States, allocated a spectrum of 75 MHz in the 5.9 GHz frequency band specially

designed for Dedicated Short-Range Communications (DSRC) applications for ITS. In this 75 MHz band, seven 10 MHz channels and 5 MHz guard band are defined. Out of these seven channels, one of the channel is a Control Channel (CCH) and rest of the six channels are Service Channels (SCH) (Uzcategui and Acosta-Marum, 2009) and (IEEE-Std., 2010).

However, the Europe Telecommunications Standard Institute (ETSI), allocated a spectrum of 30 MHz in the 5.895 - 5.925 GHz frequency band. Out of which one physical channel is dedicated to be the control channel (CCH), which is also termed as G5-CCH. And seven fixed service channels and one variable physical service channel are identified as G5-SCHs (ETSI-Std., 2009) and (ETSI-Std., 2011). According to the ETSI standards, the usage of G5-CCH and G5-SCH1 to G5-SCH2 are dedicated basically to ITS road safety (i.e., safety applications) and G5-SCH3 to G5-SCH5 are essentially dedicated to ITS road traffic efficiency (i.e., non-safety applications) (ETSI-Std., 2009) and (ETSI-Std., 2011). Nonetheless, in the European standards the ITS-G5C specifies that the communication is suppose to only take place between infrastructure and vehicle and hence eliminating the possibility of V2V communication (ETSI-Std., 2009). This justifies the reason why, in this thesis we only focus on V2I communications as the research work accomplished in implementing the VANET Testbed is around Middlesex University London campus which is situated in the United Kingdom, hence maintaining the European standards for ITS research.

In VANETs, the rest of the protocol stack is defined by the IEEE 802.11p (i.e., the lower layers) standards and the Wireless Access in Vehicular Environment (WAVE) 1609 standards family (i.e., mainly the upper layers). The PHY layer of IEEE 802.11p uses the Orthogonal Frequency Division Multiplexing (OFDM) transmission technique. IEEE 802.11p is designed based on the modifications to the existing IEEE 802.11a in PHY layer. This means that the IEEE 802.11p has the capability of sending data at higher rates ranging from 3 to 27 Mbps over a 10 MHz bandwidth unlike the traditional IEEE 802.11a (Wi-Fi) which operates with 20 MHz bandwidth. This reduction in the bandwidth is due to the halved subcarrier spacing but this comes at the cost of higher inter-symbol interferences which is caused from its own transmissions in dynamic vehicular environments. Theoretically IEEE 802.11p standard aims to provide communication ranges up to 1000 meters (1 km) for both V2V and V2I communications. Moreover, there are also some provision in the OFDM techniques for effective channel selection in order to reduce the outside channel interferences and hence increasing the channel resistance for IEEE 802.11p. The MAC layer in VANETs is based on the amendments

to the IEEE 802.11e standards (IEEE-Std., 2005). The IEEE 802.11e was developed for the Enhanced Distributed Channel Access (EDCA) mechanism which is based on the user priority services to support QoS (IEEE-Std., 2005). There are four Access Categories (AC) in EDCA mechanism which supports and prioritizes the data traffic. In vehicular environments, due to the short communication time, it is not possible to perform the authentication and association procedures between vehicles or RSUs and vice-versa. Therefore traditional Basic Service Set (BSS) were a bad choice, hence the IEEE 802.11p MAC layer uses Wave Basic Service Set (WBSS) which authenticates with just a single beacon message which contains all the necessary information, hence reducing additional overheads.

The rest of upper layers in the standard encompasses the IEEE 1609 WAVE family which defines the management entities and multichannel switching operations (IEEE-Std., 2010). This feature distinguishes it from the traditional wireless IEEE 802.11 standard family, which is specially designed for vehicular environments. Most of the networking services, resource management services and security modules are defined in this IEEE 1609 stack. It also outlines the Wave Short Message (WSM) and the Wave Short Message Protocol (WSMP). Moreover, in WAVE, both Internet and Non-IP based protocols are supported for both safety and non-safety applications respectively. Due the multichannel switching operation the WSMP protocol can uniquely tune the communication channel to Control Channel (CCH) which not only prioritises the message but also propels full power to the communication channel capitalizing on the likelihood of vehicles receiving the packets successfully.

1.0.2 Constraints in the Vehicular Networks

In VANETs, the current standards were initially developed based on the existing IEEE 802.11 family standards which are specifically designed to cater for the needs of a mobile environment (in this case vehicular networks). Therefore, there are many limitations in the current standard which restrict our use of this emerging technology. Some of them have been illustrated in the next couple of sections.

1.0.3 IEEE 1609.4 Broadcasting Limitations

In Vehicular environments, traffic density varies from very dense urban areas to sparse highways. Therefore, the MAC layer of the VANET is required to be scalable. Distributed Coordination Function (DCF) mechanism is adopted by the IEEE 1609.4 (IEEE-Std., 2010) at MAC layer which operates on CSMA/CA with

binary exponential backoff algorithm. Further this MAC layer mechanism uses the traditional IEEE 802.11e (IEEE-Std., 2005), which is an improved version of the Hybrid Coordination Function (HCF). Fundamentally, the HCF MAC technique works with a variable for prioritization of the packet, which is called the Arbitration Interframe Space (e.g. AIFS[i]). This makes priorities differ with different contention window sizes (Ganan et al., 2012). However, this MAC mechanism is neither secure nor efficient for dense networks. Therefore, while broadcasting, this CSMA/CA cannot avoid collisions entirely. This leads to severe drops in throughput in dense urban environments. Additionally, due the lack of a RTS/CTS handshake, there are no acknowledgements and more likely that there is no error-handling, hence increasing the possibility of beacons colliding. This is also witnessed in the case of hidden node problem when beacons are broadcasted without RTS/CTS handshake. Furthermore, safety applications require reliable and timely broadcasting of beacons in control channel, which is given full transmission power for optimal coverage but this comes at the cost of an increased interference (Ganan et al., 2012).

1.0.4 Beacon Collision due to lack of Congestion Control

On one hand, the beaconing in VANET systems is described as a principal attribute that has been designated as the Basic Safety Messages (BSMs) and Cooperative Awareness Messages (CAMs) in both the IEEE 802.11p in U.S and ETSI standards in Europe to cope with highly mobile environments. But at the same time this also raises the issues of traffic congestion caused due to the periodic broadcasting of the beacons and also due to the ad hoc nature of communication that occur among vehicles. It has been anticipated that periodic switching between the control channels and services channels for every 50ms period over a combined interval of 100ms including the guard intervals, is required in order to achieve time synchronization for timely updating the beacons for timely delivery for life-safety applications. They are tuned to the CCH to exchange CAMs at every 100 ms. This will not only generate a great deal of beacon overheads but also possibly use the whole channel bandwidth. Therefore, this problem has been highlighted in the European ETSI standards for ITS but to the best of our knowledge, there has been no such concern emphasised in the IEEE standards in the U.S. Currently, there is some provision which is being considered with a mechanism called the Decentralised Congestion Control (DCC) according to the European standards to deal with these kind of technical challenges (Osafune et al., 2015) and (Autolitano et al., 2013).

1.0.5 Interference Issues in dense Urban Environemtns

In the near future, the deployment of RSUs can be foreseen. This will require RSUs being placed next to each other in order to have maximum coverage. Perhaps, this could be achieved in a more pragmatic fashion, meaning, positioning of several RSUs close to each other in a crowded manner, hence generating severe interferences due to signal overlap. Conversely, this could also mean blind-spots on the roads (especially in urban road intersections) which will be wasting of resources. The current IEEE WAVE standards are unable to provide concrete solutions for these kinds of problems due to the lack of RTS/CTS handshake and authentication. In addition, from previous sections we have carefully observed that most of the applications for vehicular communication is envisaged for environments which require periodic broadcasting of the beacons in the form of WAVE Service Advertisements (WSA). And we have previously witnessed how beaconing is used for this purpose. Usually, 1-10Hz beacon frequency is used in such cases. In such, dense urban environments, it is possible that beacons will suffer severe collisions, not only because of high beacon generation rates but also due dense environmental factors due to the non-existence of MAC layer acknowledgements. This brings another, interesting technical anomaly due to the lack of authentication of beacons, is the denial of service attacks that can be placed by emulating a device acting as a RSUs on the road. Thus, there are no provisions in IEEE 1609.4 ([IEEE-Std., 2010](#)) to cope with these types of attacks, hence bringing security issues which directly affects the overall network performance ([Ganan et al., 2012](#)).

1.1 Research Aims and Objectives

The main aim of this thesis addresses the issues highlighted above by looking at developing mechanisms for seamless handover in vehicular environments that fulfil the requirements of both safety and non-safety applications. Even though, there are many other important technical challenges such as interference, beacon collisions, routing protocols and security issues, they are out of the scope of this thesis. In this thesis, we primarily focus our efforts on techniques for seamless handover in order to achieve seamlessly connectivity in dense urban environments. Further, we restrict the research capacity of this work to vehicle-to-infrastructure (V2I) communication, by anticipating the presence of infrastructure that benefits from the local data from other RSUs in the vicinity. This is also supported by the fact that in urban scenarios early deployment will be witnessed, it is aimed that proactive handover techniques will work better in the presence of infrastructure to

support WAVE advertisements that are required for status updates of the vehicles as demonstrated in (Campolo and Molinaro, 2011b) and (Campolo and Molinaro, 2011a). This is quite a challenge in itself. Some literature in this context, which indirectly validates our argument where only V2V communication is explored, i.e., by studying broadcasting of beacons in VANETs, and thus ignoring the role of RSUs (Vinel et al., 2009a), (Vinel et al., 2009b), (Campolo and Molinaro, 2011a) and (Campolo and Molinaro, 2011b). Another example where only V2V perspective has been exemplified is exhibited in (Campolo et al., 2011a) and (Vinel et al., 2009a) where the broadcasting techniques for transmissions has been analytically modeled while taking into account the channel switching operation (Campolo et al., 2011a) and (Vinel et al., 2009a).

Also, WAVE services will be announced by the infrastructure during the control channel this requires timely information exchange between RSUs and the vehicles. In dense urban environments this will be difficult to achieve. Therefore, the frequency at which the beacons are transmitted will be an important factor contributing to the overall VANET performance. This thesis, not only looks at one element affecting seamless handover such as beacon frequency, but also the size of the beacon and the velocity of the vehicle. Additionally, it is necessary to provide a reliable broadcasting service via RSUs in order to support the streaming multimedia applications (Bai and Krishnamachari, 2010). Unlike safety applications, non-safety applications, are mainly aimed for Service Channels (SCH), which also have strict requirements and necessitates a more reliable handover as depicted in (Esposito et al., 2010) and (Bai and Krishnamachari, 2010) (i.e., infotainment applications). Hence an insight into the relationship between beacon frequency, the size of the beacon and velocity of the vehicle is imperative to study handover techniques in VANETs.

These key parameters that have been stressed in this thesis for exploring handovers in VANET Systems along with probability distributions that accentuates the urge to recognise these critical times for understanding the establishment of reliable communication. Hence this helped to predict the handover times and thus making proactive handover possible.

Considering the scope above, the main research question of this thesis have been underlined in the next subsection.

1.1.1 Key Research Questions

Some of the key Research Questions that have been highlighted in this Thesis:

1. Can handover in VANET systems happen without any interruption in the communication?
2. Can these factors be explored using analytical models?
3. What factors affect the ability to achieve seamless handover in VANET environments?

1.1.2 Hypothesis and Approach

We approach the research questions of this thesis by exploring using mechanisms for seamless handover placed on top of the WAVE protocol stack. Therefore, no modification is required in the IEEE 802.11p standard for vehicular communication. In view of the separation of safety and non-safety radio channels and underlying network protocols in the standard. This thesis provides a more comprehensive analysis involving the beacon frequency, size of the beacon and the velocity of the vehicle. Some of the concepts of Y-Comm architecture such as Network Dwell Time (NDT), Time Before Handover(T_{BH}) and Exit Times (ET) have been used to provide a framework to investigate handover issues. Y-Comm has been used to study seamless handover in both homogeneous and heterogeneous networks. This thesis, also explains our overall approach by describing the VANET Testbed and articulates that in vehicular environments it is necessary to consider a new handover model which is based on a probabilistic rather than a fixed coverage approach. Finally, a new performance model is developed for proactive handover which is then compared with traditional approaches.

A testbed is set-up at the Middlesex University, Hendon Campus for the purpose of achieving a better understanding of VANET systems operating in an urban environment. In addition, environmental factors have to be taken into considerations in real-time deployment studies, to see how these affect the performance of VANET systems under different scenarios. Eventually, this can be achieved by looking at some of existing propagation models in wireless communications. However some of the existing pathloss models do not cater to the specifications of VANETs standards, hence this is a potential research area for future studies. The MDX-VANET Testbed, has been set-up to demonstrate infrastructure-to-vehicle (I2V) communications. Furthermore, this thesis, postulates more insight on how to support life critical applications, using seamless handover techniques. This is achieved by comparing results from analytical model, simulation and the real-time values collected from the VANET Testbed which further helped address the challenges while fulfilling the requirements of both safety and non-safety applications. Therefore,

understanding handover issues is critical in supporting life-safety applications and services in VANETs.

1.1.3 List of Publications

This thesis has resulted in four fully (peer-reviewed) conference papers, two journal articles and two (peer-reviewed) book chapters. This research work also resulted in real-time deployment of VANET Testbed, (VANET Project) which is under progress as part of the T-TRIG grant from Department for Transport (DfT). The publications (Ganan et al., 2012, Ghosh et al., 2013, Ghosh et al., 2014a, Ghosh et al., 2014b) were submitted to International Conferences, out of which, one of them was invited journal article for EURASIP Journal on Wireless Communications and Networking, another an IEEE Communications Magazine journal article and one of them was a contribution towards Springer book chapter. All of these are full papers/journals and are published.

- Vishnu, Vardhan., Arindam, Ghosh., Glenford, Mapp., Victor, Iniovosa., Purav, Shah., Huan, X. Nguyen., Orhan, Gemikonakli and Shahedur, Rahman. **Building a Prototype VANET Testbed to Explore Communication Dynamics in Highly Mobile Environments**, in Proceeding of 11th EAI International Conference on Testbeds and Research Infrastructures for the Development of Networks & Communities, Springer-Digital Library/EAI Endorsed Transactions on Future Internet. China, Hangzhou, June 14-15th 2016 (Accepted and in prints).
- Arindam, Ghosh., Vishnu, Vardhan., Glenford, Mapp., Orhan, Gemikonakli, and Jonathan, Loo. **Enabling Seamless V2I Communications: Towards Developing Cooperative Automotive Applications in VANET Systems**, Communications Magazine, IEEE, vol. 53, issue no. 12, pp. 80–86, December 2015 (Published).
- Arindam, Ghosh., Glenford, Mapp., Vishnu, Vardhan., Victor, Iniovosa., Jonathan, Loo, and Alexey, Vinel. **Exploring Seamless Connectivity and Proactive Handover Techniques in VANET System**. In Springer Book Chapter - *Dependable Vehicular Communications for Improved Road Safety* (Published).
- Vishnu, Vardhan., Glenford, Mapp., Purav, Shah., Huan, X, Nguyen., Arindam, Ghosh. **Exploring Markov Models for the Allocation of Resources for**

Proactive Handover in a Mobile Environment, in Local Computer Networks Workshops (LCN Workshops), 2014 IEEE 40th Conference on, October 2015, Clearwater Beach, Florida, USA. (Published).

- Arindam, Ghosh., Vishnu, Vardhan., Glenford, Mapp., and Orhan, Gemikonakli. **Exploring Efficient Seamless Handover in Vanet Systems Using Network Dwell Time**, EURASIP Journal on Wireless Communications and Networking, vol. 2014, no. 1, p. 227, 2014 (Published).
- Arindam, Ghosh., Vishnu, Vardhan., Glenford, Mapp., and Orhan, Gemikonakli. **Providing Ubiquitous Communication Using Handover Techniques in VANET systems: Unveiling the Challenges**, in Proceeding of Ad Hoc Networking Workshop (MED-HOC-NET), In Ad Hoc Networking Conference (MED-HOC-NET), 2014 13th IEEE/IFIP Annual Mediterranean Conference on, pp. 195–202, Slovenia, Piran, June 2-4th 2014, (Published).
- Arindam, Ghosh., Vishnu, Vardhan., Glenford, Mapp., Orhan, Gemikonakli, and Jonathan. Loo. **Providing Ubiquitous Communication Using Road Side Units in VANET systems: Unveiling the Challenges**, in Proceeding ITS Telecommunications (ITST), 2013 13th IEEE International Conference on, pp. 74-79, Finland, Tampere, November 2013 (Published).
- Carlos, Ganan., Arindam, Ghosh., Jonathan, Loo., Oscar, Esparza., Sergi, Rene., and JoseL, Munoz. **Analysis of Inter-RSU Beaconing Interference in VANETs**. In Boris Bellalta, Alexey Vinel, Magnus Jonsson, Jaume Barcelo, Roman Maslennikov, Periklis Chatzimisios, and David Malone, in Multiple Access Communications, volume 7642 of Lecture Notes in Computer Science, pages 49-59. Springer, Berlin, Heidelberg, 2012 (Published).

1.1.4 Organization of the thesis

The organisation of the chapters in this thesis is structured as shown below

- Chapter 2 highlights the Literature Review in three parts; firstly by an overview, describing the characteristics of the VANET architecture and the WAVE protocol stack. Secondly, it culminates in a critical review of the existing solutions and approaches produced by researchers, scientists and groups by highlighting on the arguments which emphasis more on some of our research questions on prediction techniques for achieving proactive handover in VANET systems. Thirdly, it describes the state-of-art in VANET

applications by giving examples of some real-time safety and non-safety applications. Finally, this Chapter, interprets the methods and approaches used for conducting simulation studies by providing comprehensive grounds for justifying why we chose the simulation environment for this work.

- Chapter 3 interprets the methods and approaches used for conducting simulation studies by providing comprehensive grounds for justifying why we chose the simulation environment for this work introduces the Y-Comm concepts of Network Dwell Time (NDT), Exit Time (ET), and Time before Handover (T_{BH}) and the initial investigation using extensive packet-level simulation studies explaining why in certain cases overlapping is necessary phenomenon. This chapter also demonstrates that how simulations in VANET systems depends critically upon the calculation of the probability of a successful transmission. The current formulas used to calculate this parameter do not take into account the frequency of the beacon or the velocity of the vehicle. This chapter validates that these factors are significant and justifies need for a more complete analytical model.
- In chapter 4 a more comprehensive analysis involving the beacon frequency, size of the beacon and the velocity of the vehicle to provide a complete framework for investigating the handover issues is highlighted. In addition, this chapter explains the need to understand the cumulative effect of beaconing in addition to the probability of successful reception as well as how these probability distributions are affected by the velocity of the vehicle, which provides a broad insight into probabilistic approach on how to support life critical applications using proactive handover techniques.
- Chapter 5, highlights results that focus more on a probabilistic approach to handover using cumulative probabilities which give a better understanding of how seamless handover can be achieved in highly mobile environments such as VANETs. However, some of the results also demonstrate that the frequency of the beacon only affects the cumulative probability and hence it validates that the frequency, the length of the beacon and velocity of vehicle affect different aspects of the probability space with regard to the Network Dwell Time. Furthermore, this Chapter emphasizes that these results can be used to develop a probabilistic proactive handover approach based on cumulative effects of beaconing.
- Chapter 6 describes the probabilistic approach by showing that the length of the beacon contributes significantly to the rate of change of P, the individual

probability as the vehicle approaches the RSU. Then, the newly proposed probabilistic analytical model for handover process is explored further by showing how communication changes as the vehicle approaches a new RSU. An approximate model is then developed to examine these issues further. However, in the case of velocity of the vehicle, the results show that this affects the difference between the CP and individual probabilities. The results also show that these effects are reduced for higher beacon frequencies. Overall this Chapter, shows how this work explains the effects of beaconing and the velocity of the vehicle on the overall communication dynamics in VANET systems.

- Chapter 7 discusses the VANET Testbed in detail by comparing the simulation and real-time calculations and also highlighting the need for a more realistic propagation model especially designed to capture the dense urban environments in VANET systems.
- Finally, Chapter 8 concludes this thesis with a summary and directions for future work, in order to ensure continual improvement in the current and related field of study.

Chapter 2

Literature Review

2.1 State of the Art - VANET Applications

Many applications are to be used in Intelligent Transport Systems (ITS). For many of these applications, VANETs will be the supporting technology. These applications are particularly useful in vehicular environments to cater the need, provided by the VANET protocol stack. Therefore, these can be specifically categorized into four types as shown below:

1. Safety-related Applications
2. Local traffic information systems
3. Automated highways and cooperative driving
4. IP-based Applications

2.1.1 Safety-Related Applications

For emergency warnings human drivers rely on visual signals, for example, break lights. The reaction time of a driver ranges from 0.7 to 1.5 seconds which is slow. There might also be unavoidable collisions due to the warning signals not being in the line of sight which results in huge delay in getting the warning signals. This line of sight problem and delay in receiving the warning signals can be greatly reduced using VANET technologies. Using IVC (Inter-Vehicular Communication), a vehicle recognizing an emergency warning or dangerous situation can immediately report it to the neighbouring vehicles which will facilitate a decreased reaction time to the situation. Recognition of dangerous situations can be performed by the on-board sensors in the vehicle ([Artimy et al., 2008](#)).

The interest in improving the safety of public on transport system has recently led to a considerable amount of safety-related application research. Proximity warnings, intersection collision warnings and road obstacle warnings are some of the safety-related application examples. The objective of these applications is to warn the driver when a collision is likely using IVC to collect surrounding vehicles dynamics and location (Artimy et al., 2008).

Collision warning systems can adopt two different approaches and they are passive and active approaches. An accurate knowledge must be maintained about all the vehicles position in a Passive approach. An algorithm is used on the gathered data like speed, position, acceleration and directions to analyze and assess the risk of a collision. In the active approach, warning packets are sent during occurrences of an emergency event. On-board sensors are used to detect the emergency events. The practical systems can and will combine both approaches (Artimy et al., 2008). Similarly, Figure in 2.1 illustrates an example of a critical life-safety application scenario where, a child is seen to have mistakenly jumped onto the road while playing and hence, how the on-coming vehicles need to suddenly apply on their brakes to avoid an accident situation (Vegni et al., 2013). This situation could be avoided if these braking messages can be passed onto the speeding vehicles behind it reliably and efficiently.

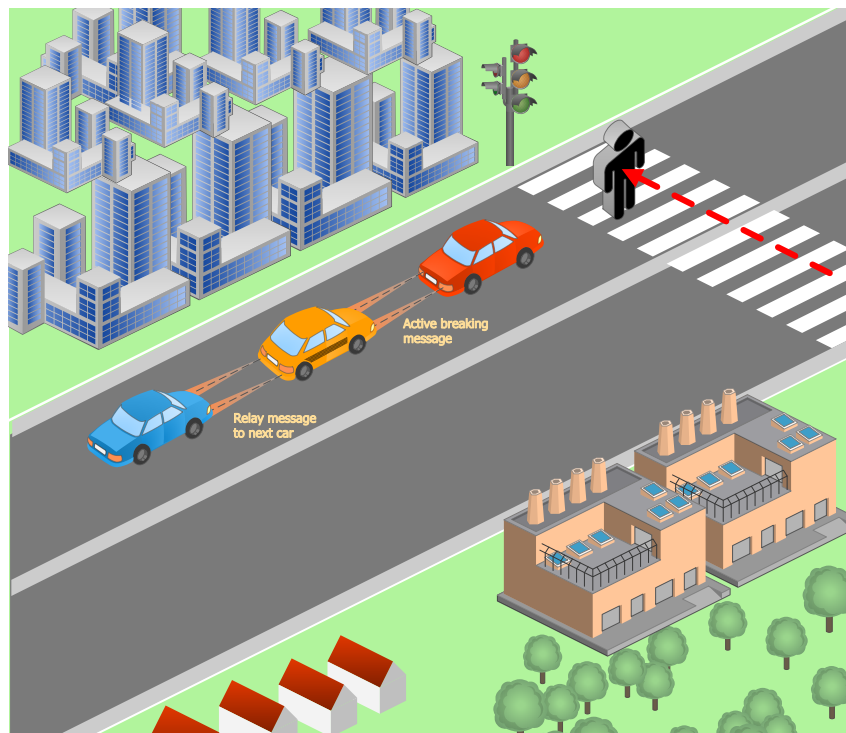


Fig. 2.1 An example of a Safety Application.

Therefore, in fast changing environments, network topology and unreliability of wireless communication in vehicular environment creates challenges in satisfying reliability and latency constrains in collision warning system. Hence, collision warning systems rely on repeated broadcast of warning messages as a delivery mechanism. Since, there is no feedback or acknowledgement from the receiver after delivery of message via RTS/CTS handshake, it is difficult in a mobile environment to identify all the receivers of broadcast message and to obtain their feedback. Thus, several copies of message are broadcasted in combination with CSMA mechanism of IEEE 802.11 standard to ensure the delivery of messages (Artimy et al., 2008).

2.1.2 Local Traffic Information Systems

Traditional traffic information systems are based on centralized architectures. Road side sensors are used to collect traffic data which is then processed at the central unit. This processed information is then sent to the user through on demand via cellphone or through radio broadcast. Using on-board sensors, digital maps and GPS in VANETs, a powerful traffic information system can be realized without expensive infrastructure as the traditional traffic information systems (Guo et al., 2011).

If about 40-50% of all vehicles are equipped with the VANET Onboard Unit an effective communication system can be created (EuropeanCommission, 2015). Once a higher market penetration is reached then scalability becomes an issue due to data overload conditions. The traffic information can be transmitted to the vehicles only if that information is relevant to the route that the vehicle is likely to go (Artimy et al., 2008).

2.1.3 Automated Highway and Cooperative Driving

In order to increase safety of driving and improve the highway capacity, applications concerned with automation of some driving functions will be helpful. Some of the applications are automated/assisted takeover, automatic cruise control, platooning and emergency vehicles announcements. The highway capacity can be increased by reducing the spacing between the vehicles travelling at high speed also known as automated vehicle platooning. Due to the slow reaction time of drivers, vehicles must operate under automatic control. Other applications using Vehicle to RoadSide (V2R) are intersection collision warning, work zone warning, hidden driveway warning, railroad crossing warning, electronic road signs, automated driving and

highway merge assistance (Guo et al., 2011). Safe platooning requires reliable and high bandwidth wireless communication (Artimy et al., 2008).

2.1.4 IP-Based Applications

IP-Based applications mainly deal with entertainment and passenger comfort. Some of the examples are internet and online games. These require a fixed infrastructure to provide these services hence road side units becomes a necessity. Handover of connection from one gateway to another and the discovery of Internet Gateway are important in these kind of applications. In addition, due to the highly dynamic topology in VANETs, the classic routing protocols which are required for basic service route discovery are not efficient for optimum performance in VANETs. Thus, some of the key Ad hoc routing protocols with multiple hop capability will increase the communication range significantly and this reduces the number of Internet Gateways thus reduces the cost. Vehicles can use fuzzy logic to choose the most suitable Internet Gateway among many that are available and accessed at the same time (Artimy et al., 2008).

Cellular networks which are long range wireless technologies can be used to provide Internet access to VANETs. Some can act as gateways to other vehicles which help in reducing the cost of this architecture. By routing of packets through gateways other vehicles can access the Internet (Artimy et al., 2008). Figure 2.2 (a) and (b) demonstrate a non-safety (infotainment) application for passengers ease in the vehicle. The image has been taken from the book chapter presented in (Vegni et al., 2013).

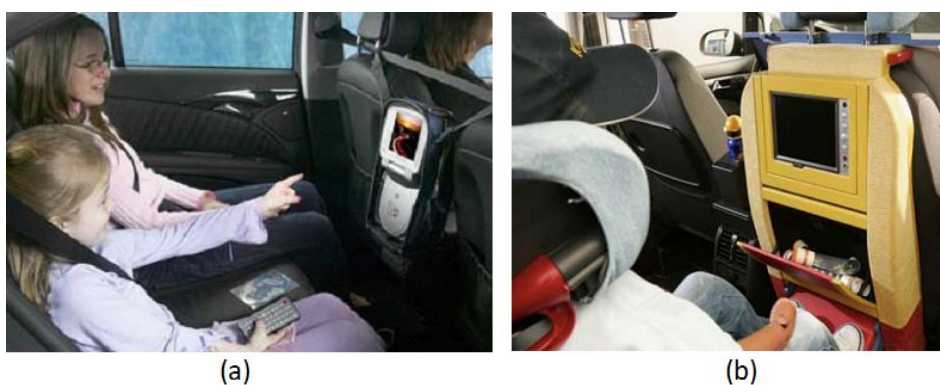


Fig. 2.2 An example of a Non-Safety Application (Infotainment Applications).

2.2 Standards and Protocol Architecture

2.2.1 Wireless Access in Vehicular Environments (WAVE) - Protocol Stack

WAVE standards are proposed using the Dedicated Short Range Communication (DSRC) frequency bands. Road safety and messaging and control require an extremely short latency wireless communication technology which can only be met by DSRC/WAVE. In WAVE there are two classes of devices i.e. On-board Units (OBUs) and Road Side Units (RSUs). This RSU and OBU are similar to the Base Stations (BS) and Mobile stations (MS) in cellular systems respectively. A Base Station (BS) is used by a Mobile Station (MS) in cellular networks to communicate with another mobile station but in WAVE, an OBU can communicate directly with another OBU. There are several technical challenges in WAVE, such as collision avoidance between vehicles moving with high velocity. The communication between two vehicles moving in opposite directions at high velocity is another challenge. The environments in which the WAVE networks may operate can be of wide range. Density of the vehicles can vary from very few to tens of thousands of vehicles in a single radio coverage area. To meet these requirements and challenges the WAVE solution must be robust, scalable, high throughput, low latency and cognitive (Li, 2012).

The major components of the WAVE protocol architecture and its associated standards are summarized below and also depicted in Figure 2.3 (Li, 2012):

- IEEE P1609.0 “Draft Standard for WAVE – Architecture”
- IEEE 1609.1 “Trial Use Standard for WAVE – Resource Manager”
- IEEE 1609.2 “Trail Use Standard for WAVE – Security Services for Applications and Management Messages”
- IEEE 1609.3 “Trail Use Standard for WAVE – Networking Services”
- IEEE 1609.4 “Trail Use Standard for WAVE – Multi Channel Operation”
- IEEE P1609.11 “Over-the-Air Data Exchange Protocol for ITS (Intelligent Transport System)”
- IEEE 802.11p Part 11 “ Wireless LAN MAC (Medium Access Control) and PHY (Physical Layer) specifications - Amendment : WAVE

Non-Safety Application		Safety Application
Transport	UDP/TCP	WSMP IEEE 1609.2 (Security) IEEE 1609.3
Networking	IPv6	
LLC		IEEE 802.2
MAC		IEEE 802.11p IEEE 1609.4 (Multi-Channel)
PHY 802.11p		IEEE

Fig. 2.3 WAVE Protocol Architecture.

An optimized communication protocol stack is provided by WAVE for vehicular communication. Descriptions of architecture and operations are provided by IEEE P1609.0. Multiple wireless channel operation with OCBAEnabled operation needs channel coordination. OCBAEnabled is operation outside context of the basic service set as defined and specified in IEEE 802.11p standard (IEEE-Std., 2010). The reference model of this standard is shown below in Figure 2.4.

WAVE supports both IP based and Non-IP based data transfer, although only one networking protocol might be supported by an individual device. WAVE Short Message Protocol (WSMP) supports non-IP based data transfer specified in IEEE 1609.3 standard. In IEEE 802.11 MAC channel coordination is a set of enhancements and interacts with the IEEE 802.11 PHY and IEEE 802.2 Logical Link Control (LLC). In IEEE 1609.3 standard WME (WAVE Management Entity) and network services corresponding to it are specified (IEEE-Std., 2010).

PHY layer management entities (PLME) and MAC sub-layer management entities (MLME) are the management entities conceptually included in PHY and MAC layers respectively. Layer management service interfaces are provided by these management entities through which layer management functions can be invoked. MSDU (MAC service data unit) delivery and management of channel coordination are the services provided by this standard. The data plane features and the management plane features are described in detail below (IEEE-Std., 2010).

2.2.2 Data Plane Services

Data plane services consist of channel coordination, channel routing and user priority. Data frames, Management frames and control frames are the three types of information exchanged on WAVE medium. Control frames are not addressed in this standard and may be used as per IEEE 802.11 standard. Management frame enters the data plane at the MAC layer. TA (Timing Advertisement) frame specified in IEEE 802.11p standard and WSA frame specified in IEEE 802.11 standard and amended by IEEE 802.11p standard are the primary management frames. Time synchronization information is distributed using Timing Advertisement frames. WAVE Service Advertisements (WSAs) are the management information which is exchanged using WSA frames. TAs and WSAs can be transmitted on any channel (IEEE-Std., 2010).

IEEE 1609.4 makes use of FDMA/TDMA (Frequency/Time division multiple access). The TDMA channel time is divided into 100ms time periods as shown in Figure 2.5. For each 100ms, 50ms is allocated for CCH and another 50ms is allocated for SCH. This 50ms includes the 4ms guard interval (GI) which is used for switching between CCH and SCH. The purpose of this switching is for accommodating both CCH and SCH services on a single channel in the WAVE system. During the 46ms of the CCH time only two kinds of message can be sent (Li, 2012).

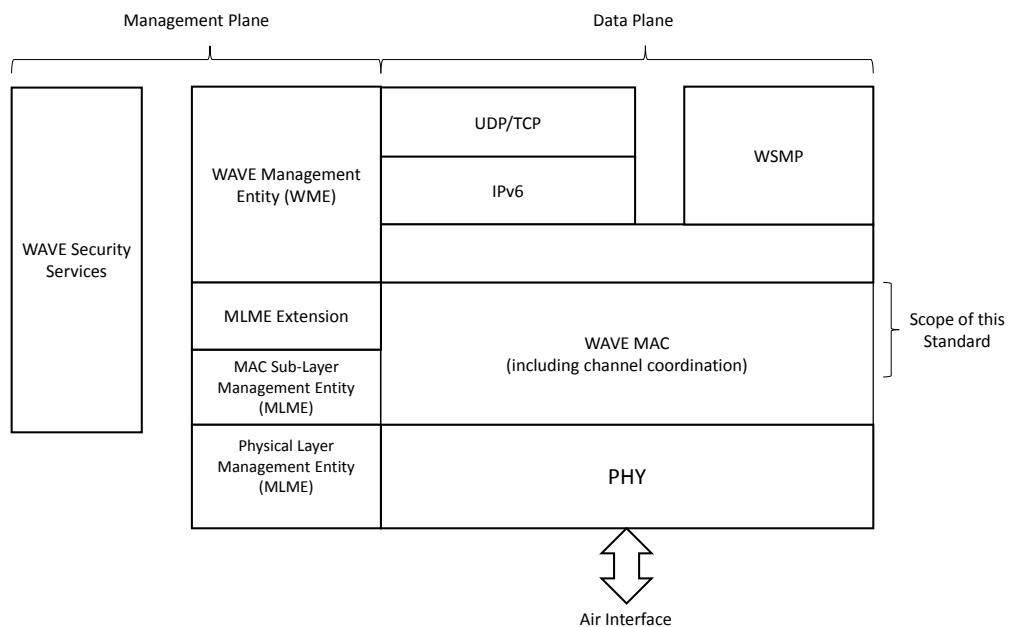


Fig. 2.4 WAVE reference model.

1. WSMP - WAVE Short Message Protocol, Short messages primarily meant for safety applications.
2. WSA - WAVE Service Advertisement messages which is used for advertising the services available on other SCH channels.

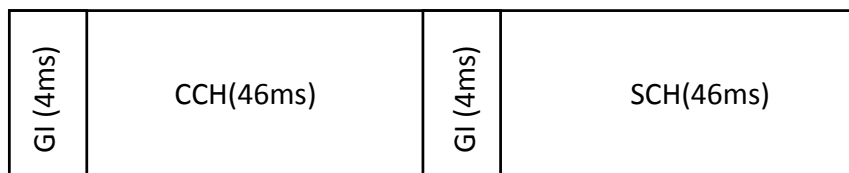


Fig. 2.5 TDMA Channel Time.

Both IPv6 and WSMP specified in IEEE 1609.3 standard are supported by WAVE. WSMPs in data frames can be exchanged between devices on either SCH or on CCH, whereas IP datagrams in a data frames are allowed only in SCH (“IEEE Standard for Wireless Access in Vehicular Environments (WAVE)– Multi-channel Operation,” 2011).

Channel coordination is designed for exchange of data support for one or more switching devices with alternating operation on SCH and CCH concurrently. The illustrations in Figure 2.6 show the continuous channel access and alternating channel access (IEEE-Std., 2010): Continuous channel access doesn’t require channel

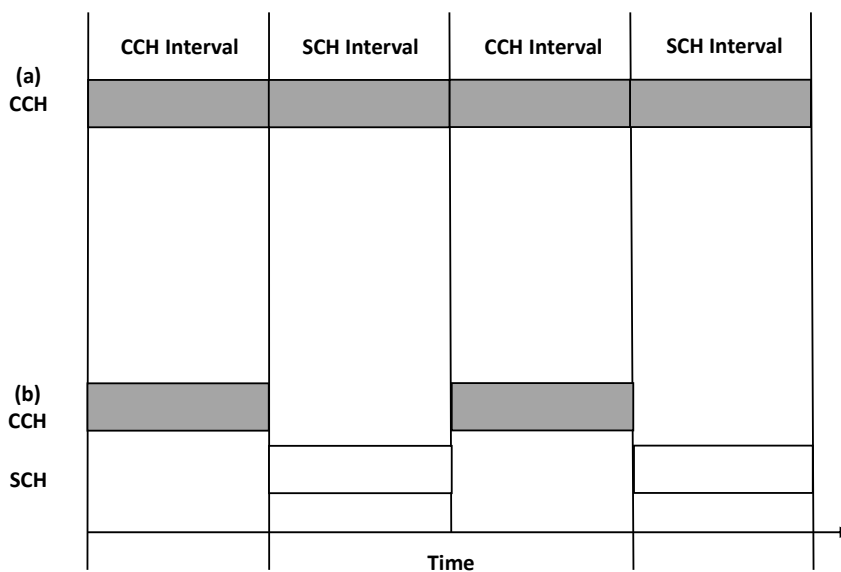


Fig. 2.6 Channel Access.

coordination and alternating channel access requires channel coordination ([IEEE-Std., 2010](#)). The time duration of the SCH and CCH intervals are specified in the draft standards and stored in the MIB attributes SchInterval and CchInterval respectively. Sync interval is the sum of SCH interval and CCH interval. The Guard interval is at the beginning of each SCH and CCH interval. The Guard interval time is used for radio switching and to manage the inaccurate device timing among different devices. CCH interval, SCH interval, guard interval and sync interval are shown in Figure 2.7 below ([IEEE-Std., 2010](#)).

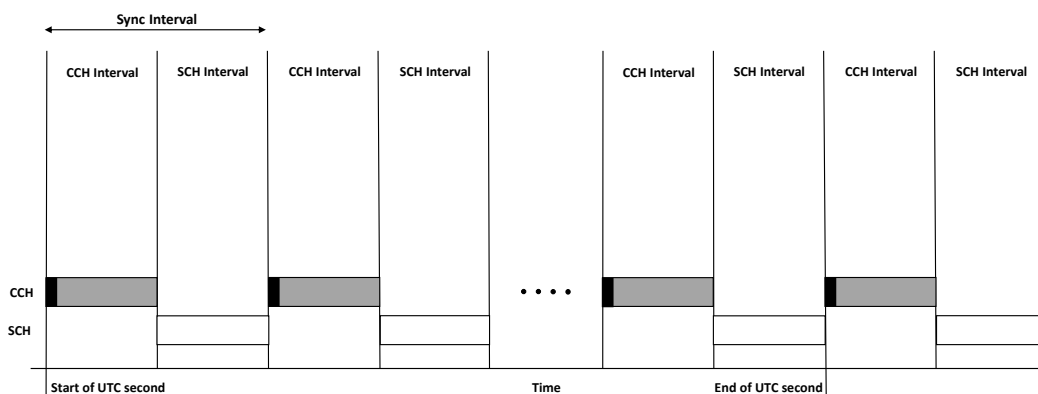


Fig. 2.7 Channel Intervals.

2.2.3 Management Plane Services

Management plane services consist of the Multi-Channel synchronization and Channel access. To perform the channel coordination function in WAVE devices, the common time reference is used which is a synchronization function. Timing information can be acquired over the air for the devices without local time from other WAVE devices. Time Advertisement and Timestamp field information in the Timing Advertisement (TA) frame are used by synchronization procedures as inputs in estimating UTC. For WAVE devices channel switching on channel interval boundaries, synchronization to UTC is mandatory. Timing management function is used to derive Time information from the received information over the air is used for synchronization or may be obtained from local reference time. UTC time is maintained by the MLME which is used for channel coordination. UTC is derived from the Timing management function and this function can be external or internal to the MLME. That is an external function can be set for MLME UTC estimate through `MLMEX-SETUTC TIME.request` ([IEEE-Std., 2010](#)).

UTC can be obtained from many sources and GPS (Global Positioning System) is one which provide a precise time. It provides a 1 PPS (Pulse per Second) UTC signal which can be used for timing and synchronization. Here the obtained value has an error less than 100 ms (IEEE-Std., 2010).

An estimator of UTC time and standard deviation estimator of the error in the estimate of UTC time are implemented when MLME synchronizes to UTC time this is done while performing synchronization. This permits transmission synchronization with channel intervals. For a simple estimator, a GPS can be used as an input for calculating the necessary offset value of TSF timer and the standard deviation is set to that of the time output of GPS devices' standard deviation under the given operating condition. To update a UTC time's internal estimator along with an estimator error the Time Advertisement information from a received Timing Advertisement Frame can be used but it would be a slightly complex implementation (IEEE-Std., 2010).

The Timing Advertisement Frame is an element called Time Advertisement information and it has Timing Capabilities subfield, a Time Error subfield, and a Time Value subfield which can be used by recipients to estimate UTC. Along with a Local TSF time an estimate of UTC at any time can be provided. The transmitting device TSF timer value is conveyed in the Timestamp field. Source of external timing of the transmitting device is indicated by the Timing Capabilities subfield. An estimate of the time standard at the time, the frame was transmitted for a receiving STA can be obtained when the Time Value is conjugated with the Time Stamp. Standard deviation of the error is indicated by Time Error sub-field. Receiving and sending timing information are optional (IEEE-Std., 2010).

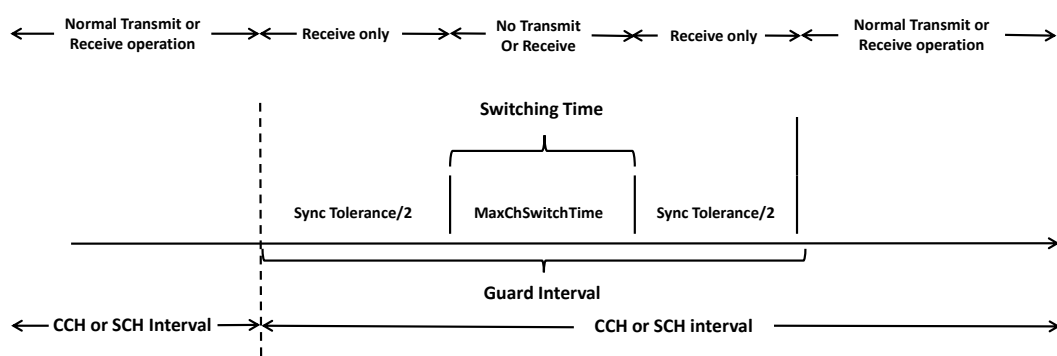


Fig. 2.8 Guard Interval.

The sum of Management Information Base (MIB) system parameters is known as the Guard interval. The system parameters are MaxChSwitchTime and SyncTolerance. Whether the WAVE device is synchronized to UTC or not is determined

by the value of SyncTolerance/2. Communication will not happen for a switching device during the guard interval time. The activities in the MAC of the previous channel may be suspended during the start of the guard interval time and prioritized access activities shall be started on the next channel or resumed if they were suspended. During the guard interval, a medium busy shall be declared so that all transmission attempts at the start of each channel interval are subjected to a random back-off. This is for preventing the multiple switching devices from simultaneously transmitting at the end of a guard interval (IEEE-Std., 2010). The components of the guard interval are shown Figure 2.8.

There are different Channel Access options and they are alternating service channel, continuous access and CCH access, extended SCH access and immediate SCH access. A combination of both Immediate and extended options can be used in a single access. The channel access options are represented in the Figure 2.9 where (a) continuous access, (b) alternating, (c) immediate and (d) extended (IEEE-Std., 2010).

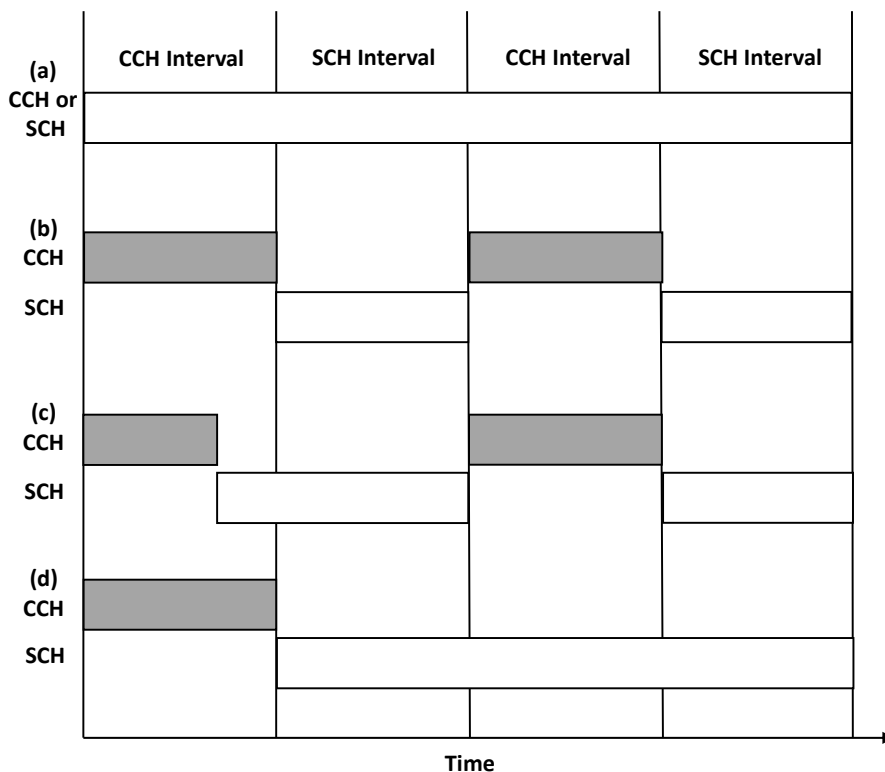


Fig. 2.9 Different Channel Access Options.

Communication access to the SCH immediately without waiting for the next SCH interval is known as Immediate SCH access. Communication access to the SCH

without any pauses for CCH access is known as Extended SCH access (IEEE-Std., 2010).

2.3 IEEE 802.11p

Due to the rapid topological change of the network and propagation environment characteristics, the application requirements in such networks will be different from the traditional network. Hence for Wireless Access in vehicular environments, the IEEE 802.11p has been proposed (Han et al., 2012).

EDCA - Enhanced Distributed Channel Access MAC sub-layer protocol is used in IEEE 802.11p. EDCA is designed based on modifying transmission parameters of existing IEEE 802.11e. The physical layer is developed similar to IEEE 802.11a standard. The transmission rates supported by IEEE 802.11p are from 3 to 27 Mb/s over a 10 MHz bandwidth, which is half the bandwidth of IEEE 802.11a. The IEEE 802.11p standard aims to provide communication ranges up to 1000 meters for both V2V and V2I with vehicles velocities up to 30m/s in a variety of environments such as motorway, rural, urban and suburban. The characteristics which are important in VANETs include low latency as safety-related applications require high reliability, high resource utilization, low packet loss rate, high throughput, and fairness. These are the main concerns of applications in VANET, so for the applications different QoS (Quality-of-Service) metrics need to be considered are discussed in (Han et al., 2012). The MAC sub-layer and the PHY (physical) layer of IEEE 802.11p are discussed below:

2.3.1 MAC Sub layer in IEEE 802.11p

IEEE 802.11e has the EDCA mechanism which is designed based on contention prioritized QoS support. There are four Access Categories (AC) in EDCA mechanism which supports and prioritizes the data traffic. The default EDCA parameters in IEEE 802.11p are shown in Table 2.1 below.

Table 2.1 The default EDCA parameters in IEEE 802.11p .

AC	CWmin[AC]	CWmax[AC]	AIFSN [AC]
AC_BK	CWmin	CWmax	9
AC_BE	$(CWmin+1)/2-1$	CWmax	6
AC_VI	$(CWmin+1)/4-1$	CWmin	3
AC_VO	$(CWmin+1)/4-1$	$(CWmin+1)/2-1$	2

Access Channels (AC) works independently to contend for TXOP (Transmission Opportunities) using EDCAF (Enhanced distributed channel access function). Each independently working AC is like a DCF station (STA)(Han et al., 2012).

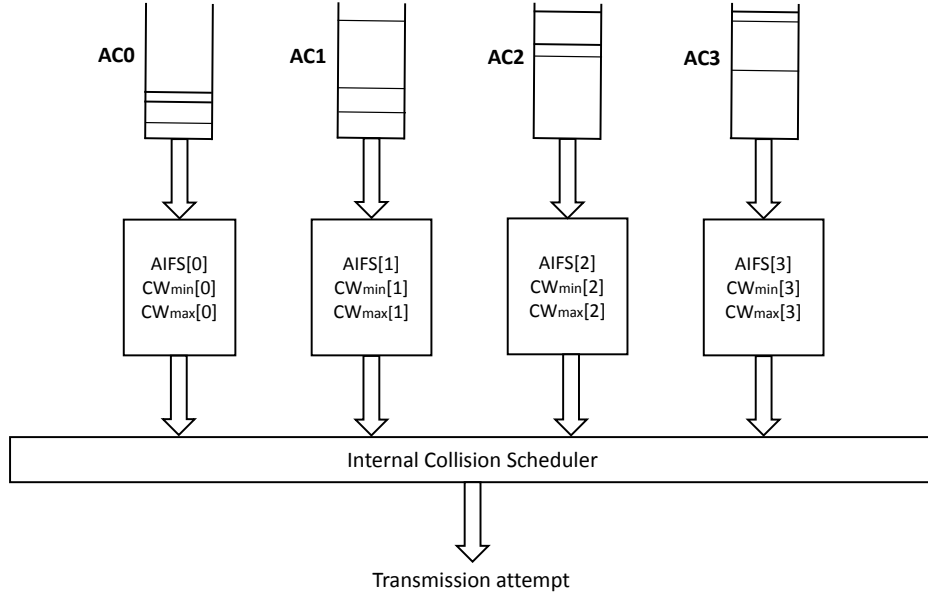


Fig. 2.10 Prioritization Mechanism.

Figure 2.10 shows the mechanism of prioritization inside each station. It illustrates four different transmit queues for four different access channels in a STA and four independent EDCAF's for traffic categories of different types. For each AC, the AIFS value is denoted by AIFS[AC]. Each access channel queue uses different CWmin, CWmax and AIFS values. AIFS is a new Inter frame space (IFS) that is used to implement the prioritization of transmission. The extension of the backoff procedure in DCF can also be considered as AIFS (Han et al., 2012).

The illustration in Figure in 2.11 shows the relationships of different inter-frame space. Here apart from the original inter-frame spacing (SIFS), DCF IFS (DIFS) and PCF IFS (PIFS), in EDCA they have introduced a new AIFS values for different ACs. AIFS[AC] duration is derived from the AIFSN[AC] value by the relation given below.

$$\Rightarrow \text{AIFS[AC]} = \text{AIFSN[AC]} \times \text{aSlotTime} + \text{aSIFSTime}$$

Where MAC protocol in EDCA parameter table sets the AIFSN[AC] value, aSlotTime is the slot time duration and aSIFSTime is the SIFS length. Different AIFSNs are allocated to different ACs. Smaller AIFSN values of an AC have higher priority for channel access. Different ACs are assigned with different CWmin and

CWmax sizes. When a shorter CW size is assigned to a AC with higher priority, then it ensures that AC with higher priority will have higher chance to access the channel than a AC with lower priority. Latest version of the IEEE 802.11p draft the CWmin is 15 and CWmax is 1023 (Han et al., 2012). Here are some of the Inter Frame Space relationships as shown in Figure 2.11

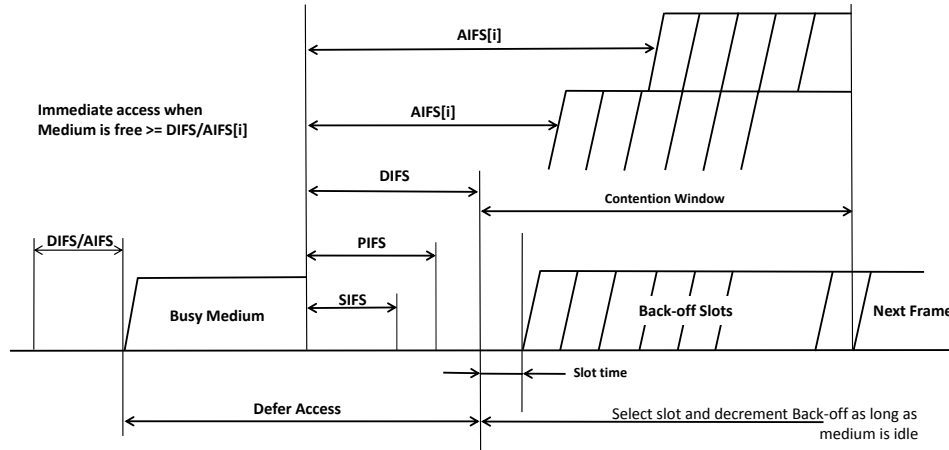


Fig. 2.11 Inter-frame Space.

As per the above Figure 2.11, there are four AC queues in each station which will act as four independent stations. For duration of $AIFS[x]$ if the channel is sensed idle and if there is backlogged data for transmission in AC_x queue, the EDCAF's back-off timer will be checked. Otherwise, the transmission sequence shall be initiated by EDCAF. The back-off timer shall be decreased by the EDCA if there is a non-zero value. Since there are four EDCAF's in a STA, there is a probability of transmission at the same time. Hence, inside a single STA a collision may occur. Inside STA there is a scheduler which will avoid this kind of internal collision by granting a highest propriety AC with an EDCF-TXOP. At the same time, a back-off procedure will be invoked at the other colliding ACs due to internal collision and behaves as if an external collision on the wireless medium has occurred. For internal collision the retry bit in the MAC headers of low-priority queues are not set by the STA. If the TXOP is granted for more than one AC by different STAs then an external collision will occur. STAs have equal opportunity to compete for channel access, since there is no priority among stations. The back-off procedure is invoked after the collided frame is deferred (Han et al., 2012).

According to the actual standard drafted in the year 2010, when a vehicle tries to send multiple packets at once, the EDCA scheduling system is said to be used at the MAC layer which is similar to the one defined in IEEE 802.11e. But in IEEE 802.11p, there are eight internal queues (i.e.) one queue per combination of channel

type and AC and each queue is controlled by one EDCAF (EDCA Function). The back-off counter for the transmission initiation of a packet as well as for each queue is controlled by the EDCAF. When a queue's back-off counter is 0 and also the PHY channel is idle for a given particular AIFS then at least one of the packet can be sent from that queue (Eckhoff and Sommer, 2012).

A queue will be changed to back-off mode when one of the following cases occur (Eckhoff and Sommer, 2012), hence, the cases are as follows:

- (i) When back-off counter is 0, then the channel goes busy.
- (ii) A different channel was active or a packet was ready to be sent in guard interval.
- (iii) A packet of higher AC was ready to be sent at the same time.
- (iv) Failed transmission of a packet.

The back-off time is determined by IEEE 802.11p slot length and a random number multiplication between $[0, CW]$. In cases (i) and (iii) the CW values are unchanged. In case (iv) CW value is doubled or set to CWmax whichever value is smaller. The back-off counter is reduced by EDCAF at each slot boundary (Eckhoff and Sommer, 2012).

2.3.2 PHY Layer in IEEE 802.11p

The Physical layer was developed in a similar to IEEE 802.11a standard and operates at 5.9 GHz compared to IEEE 802.11a which operates at 5 GHz. Orthogonal frequency division multiplexing (OFDM) transmission techniques are used in PHY layer of IEEE 802.11p which is similar to IEEE 802.11a. IEEE 802.11p channel bandwidth is scaled down to 10 MHz which is not the same in IEEE 802.11a. This is motivated by the propagation environment characteristics in Hybrid vehicular communication (HVC). The reason for choosing 10 MHz bandwidth is due to the high velocity of the vehicle which is not the same in the traditional wireless networks and thus there is a high delay spread of multiple paths. The inter symbol interference will be high if the bandwidth is high hence it is a reasonable choice of choosing a 10 MHz bandwidth for vehicular environments (Han et al., 2012).

In US, for DSRC applications 75 MHz of spectrum in the 5.9 GHz frequency band has been allocated. In this 75 MHz band, seven 10 MHz channels and 5 MHz guard band are defined. Out of these seven channels, one channel is a Control Channel (CCH) and rest of the six channels are Service Channels (SCH) (Li, 2012). A diagram of channel allocation and channel numbers are shown in Figure 2.12:

Frequency (MHz)	5850	5855	5865	5875	5885	5895	5905	5915	5925
Channel Number	Guard Band	172	174	176	178	180	182	184	
		175		181					
Channel Usage		SCH	SCH	SCH	CCH	SCH	SCH	SCH	

Fig. 2.12 Channel Allocation.

As depicted in the above Figure 2.12 a pair of channels can be combined to form a 20 MHz Channel. The transmission (TX) power ranges from 0 to 28.8dBm for four classes of devices (Li, 2012). The spectrum allocation for DSRC/WAVE applications in different regions of the world are shown in the Table 2.2.

Table 2.2 Spectrum Allocation for DSRC/WAVE in different regions of the world.

Region/Country	Frequency Bands (MHz)	Reference Documents
ITU-R (ISM band)	5725-5875	Article 5 of Radio regulations
Europe	5795-5815, 5855/5875-5905/59251	ETSI EN 202-663, ETSI EN 302-571, ETSI EN 301-893
North America	902-928, 5850-5925	FCC 47 CFR
Japan	715-725, 5770-5850	MIC EO Article 49

Normally, in Wi-Fi 20-MHz channel with OFDM PHY is used. Compared to Wi-Fi the supported data rate and subcarrier spacing of IEEE 802.11p are halved while its cyclic prefix (CP) including symbol interval is doubled (Li, 2012). The comparison of WAVE and Wi-Fi parameters are shown Table 2.3.

WAVE receivers need special design considerations due to the changing channel environment. In WAVE, receiver Inter-carrier interference (ICI) are caused due to much higher Doppler spread compared to Wi-Fi. The WAVE receiver is more sensitive to Doppler shifts and carrier frequency offsets due to halved subcarrier spacing. Channel becomes faster fading and more frequency selective due to the higher multi-path delay spread and higher Doppler spread (Li, 2012).

For high performance WAVE receiver designing following questions must be addressed (Li, 2012):

- In most harsh environments with high multi-path delay spread, is CP sufficient to remove the inter-symbol interference (ISI)?

Table 2.3 The Comparison of WAVE and Wi-Fi Parameters.

Parameters	WAVE	Wi-Fi
Frequency Band	5.9 GHz	2.4/5 GHz
Channel Bandwidth	10 MHz	20 MHz
Supported Data Rate (Mbps)	3, 4.5, 6, 9, 12, 18, 24 and 27	6, 9, 12, 18, 24, 36, 48, and 54
Modulation	Same as Wi-Fi	BPSK, QPSK, 16QAM, and 64QAM
Channel Coding	Same as Wi-Fi	Convolution coding rate: 1/2, 2/3, 3/4
No of Data Subcarriers	Same as Wi-Fi	48
No of Pilot Subcarriers	Same as Wi-Fi	4
No of Virtual Subcarriers	Same as Wi-Fi	12
FFT/IFFT Size	Same as Wi-Fi	64
FFT/IFFT Interval	64 μ s	32 μ s
Subcarrier Spacing	0.15625 MHz	0.3125 MHz
CP Interval	1.6 μ s	0.8 μ s
OFDM Symbol Interval	8 μ s	8 μ s

- During one OFDM interval can the channel remain constant which is a fundamental requirement?
- Is there a large enough channel coherence bandwidth so that channel estimation on the pilot carriers can be done and effective interpolation of these estimates to data subcarriers can be done?
- Is there a large enough channel coherence time to enable effective channel tracking? The fact that the symbol interval of the OFDM is doubled and fading of channel is faster, work against this condition.

Further research, field measurement and even parameters of existing standard might need to be changed in order to achieve the satisfactory outcome (Li, 2012).

2.4 WAVE WSMP

WSMP is a WAVE Specific protocol which has been developed to carry messages on both SCHs and CCH. The lower layer parameters such as channel number, TX power, data rate and receiver MAC addresses can be directly controlled by

applications through WSMP which is not possible in standard IP protocol. In CCH the WSMP can skip the steps for forming a WBSS (WAVE BSS) that delivers IP and WSM (WAVE short message) traffic on SCHs for reducing the latency. Reducing the overload is the primary motivation for developing WSMP (Li, 2012). A diagram of the WSMP packet is shown in Figure 2.13.

WSM Version (1 Octet)	Security Type (1 Octet)	Channel Number (1 Octet)	Data Rate (1 Octet)	TX Power (1 Octet)	PSID (4 Octets)	Length (2 Octets)	WSM Data (Variable)
-----------------------------	-------------------------------	--------------------------------	---------------------------	--------------------------	--------------------	----------------------	------------------------

Fig. 2.13 WSMP Packet Format.

Packet overhead of WSMP packet is 11 bytes which is much less compared to the UDP/IPv6 packets which has a minimum size of 52 bytes. The received WSMP packet will be disvehicled if the packet is not a supported WSM version. Security Type identifies if the packet is Signed, Unsecured or Encrypted. The Channel Number, TX power and Data Rate allow the WSMP to control the radio parameters directly. The PSID (Provider Service ID) parameter performs the similar function of the UDP/TCP packet's port number i.e. to identify the applications which will process the WSM Data. As specified in IEEE 1609.2 the Length field which indicated the number of bytes in WSM Date might be security protected (Li, 2012).

2.5 Understanding Handover in Detail

2.5.1 Handover Concepts

In this section, different types of handovers are shown. Handover is a process of transferring an active call or communication from one cell to another. There are different types of handover as defined by the Y-Comm framework (Dr.Glenford Mapp, 2014). The hierarchy of the Proactive handover (Mapp et al., 2009) is as depicted in Figure 2.14.

2.5.2 General Characteristics of Handover

Handover is defined as the changing of the Point of Attachment (PoA) of a Mobile Node (MN) to a network. Handovers may generally be categorised as follows:

- Horizontal vs Vertical: In horizontal handovers, the point of next attachment is of the same technology as the previous PoA. For example, 3G to 3G or

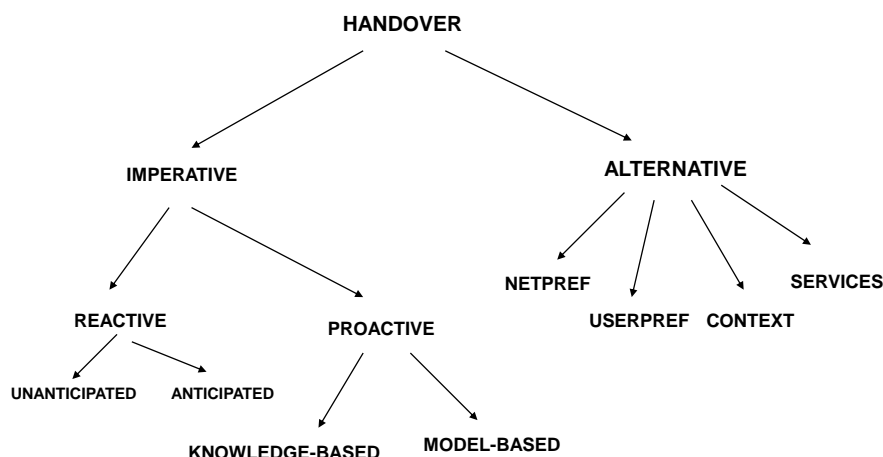


Fig. 2.14 Handover Concepts.

WiFi to WiFi. By contrast, in vertical handovers the new PoA is of different technology compared with previous PoA. Hence, vertical handovers are challenging because when they occur they can be accompanied by huge changes in the Quality of Service (QoS) of the two networks involved in the handover. The management of the different QoS is an important part of providing seamless communication.

- **Hard vs Soft:** In hard handovers, the connection to the previous PoA is broken before the connection to the new PoA is established (i.e., break before make). By contrast, in soft handovers the connection to the new PoA is established before the connection to the previous PoA is broken (i.e., make before break). Compared to hard handovers, soft handovers, therefore, result in less disruption.
- **Upward vs Downward:** In upward handover, the communication on the MN is moving from a network of small coverage to a network of larger coverage (e.g., going from a WiFi network to a LTE/3G network). By contrast, in downward handovers, the MN is going from a network of large coverage to a network of smaller coverage (i.e., going from a LTE/3G network to a WiFi network).
- **Network-based vs Client-based:** In network-based handover the network is responsible for executing the handover, while in a client-based handover the client is responsible for executing the handover. This means that for client-based handovers, the MN must acquire all the relevant network resources to achieve handover.

2.5.3 Advanced Classification of Handover

Y-Comm is an architecture (shown in Figure 2.15) that has been designed to build future mobile networks by integrating communications, mobility, QoS and security. It accomplishes this by dividing the Future Internet into two frameworks: Core and Peripheral Frameworks. The researchers of Y-Comm have made major contributions in the areas of proactive handover to provide seamless communication, QoS, as well as security (Mapp et al., 2007).

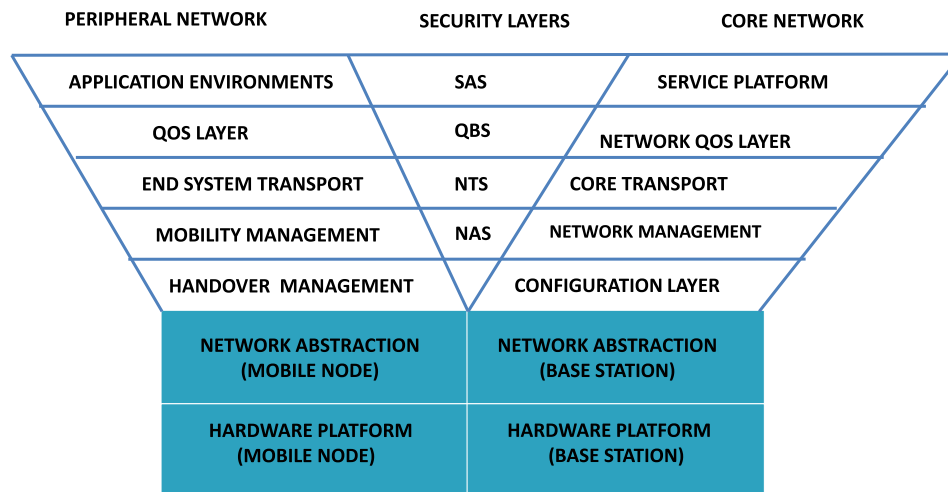


Fig. 2.15 YComm Architecture

An advanced classification of handover has been proposed by the Y-Comm Project (Mapp et al., 2009) and is shown in Figure 2.14. Handovers can also be divided into two advanced types. Imperative handovers occur due to technological reasons only. Hence the MN changes its network attachment because it has determined by technical analysis that it is good to do so. This could be based on parameters such as signal strength, coverage, and the quality-of-service offered by the new network. These handovers are imperative because there may be a severe loss of performance or loss of connection if they are not performed. In contrast, alternative handovers occur due to reasons other than technical issues (Mapp et al., 2012). The factors for performing an alternative handover include a preference for a given network based on price or incentives. User preferences based on features or promotions as well as contextual issues might also cause handover.

Imperative handovers are, in turn, divided into two types. The first is called reactive handover. This responds to changes in the low-level wireless interfaces as to the availability or increasing non-availability of certain networks. Reactive handovers can be further divided into anticipated and unanticipated handovers (Mapp et al., 2012). Anticipated handovers are therefore soft handovers that describe the

situation where there are alternative base-stations to which the mobile node may handover (Augusto et al., 2014). With unanticipated handover, the mobile node is heading out of range of the current PoA and there is no other base-station to which to handover.

The other type of imperative handover is called proactive handover. These handovers use soft handover techniques. Presently, two types of proactive handovers are being developed. The first is knowledge-based, where the MN attempts to know, by measuring beforehand, the signal strengths of available wireless networks over a given area such as a city. This most likely will involve physically driving around and taking these readings. The second proactive policy is based on a mathematical model which calculates the point when handover should occur and the time that the mobile would take to reach that point based on its velocity and direction. The accuracy of this approach is dependent on various factors including location technology, the propagation model used, network topology, and specific environments, for example, whether the MN is indoor or outdoor as well as the quality of the receiver (Mapp et al., 2012).

Proactive handover policies attempt to know the condition of the various networks at a specific location before the MN reaches that location (Almulla et al., 2014). Two key parameters are used to develop algorithms for proactive handover: Time Before Vertical Handover (TBVH) which is the time after which the handover should occur, and Network Dwell Time (NDT) which is the time the MN spends in the coverage of the new network as shown in Figure 2.16. According to the article (Mapp et al., 2012), with an accurate measurement of the handover radius, it is possible to accurately estimate TBVH as well as NDT. By using these mechanisms, it is possible to minimize packet loss and service disruption as an impending handover can be signalled to the higher layers of the network protocol stack.

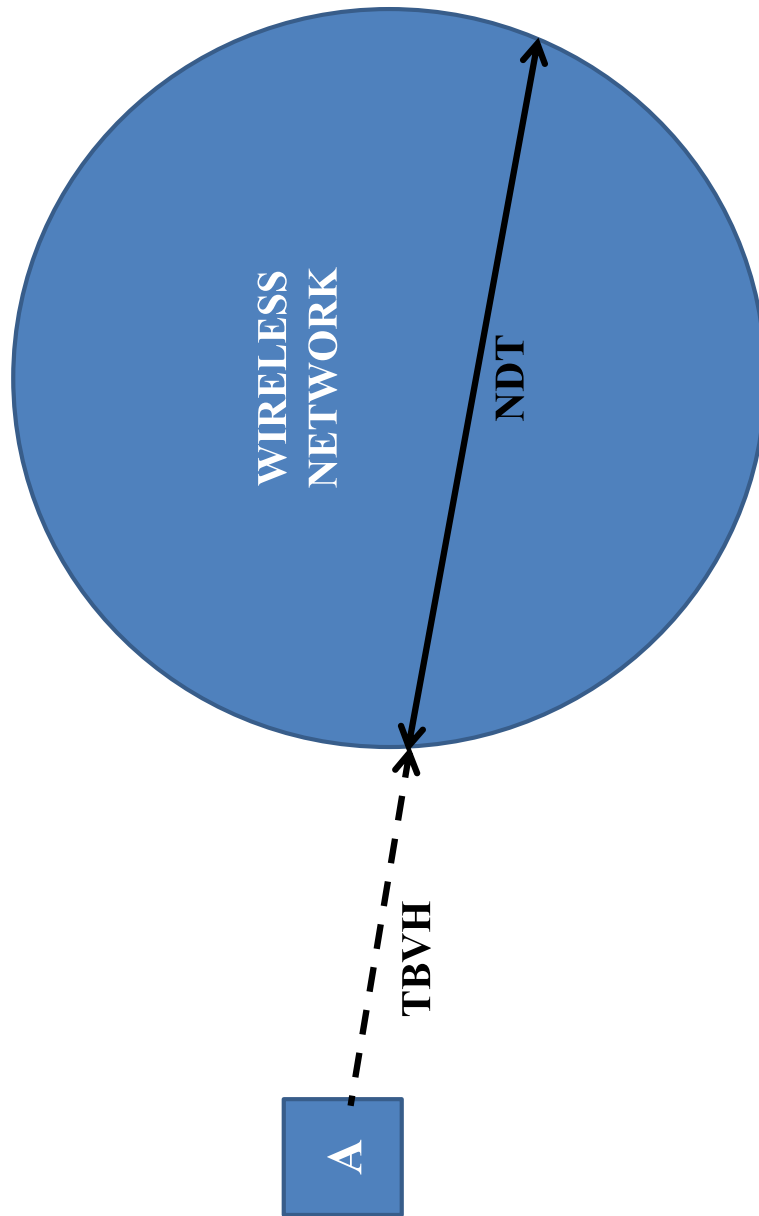


Fig. 2.16 Illustrating Time Before Vertical Handover and Network Dwell Time.

2.6 Related Works

2.6.1 Handover based Related Works

This related works section demonstrates literature review, which emphasizes on the impact of handovers especially in V2I communications. But at the same time, this section not only exemplifies the need of a good critical review of the current literature in handover techniques but it also focuses on the literature which show a wide range of testbed, simulation and benchmarking works that have been considered in this thesis. Hence, below are some of the works and findings that have been considered in this thesis:

The work in (Van Eenennaam et al., 2010), the authors highlighted the importance of scalable beaconing and the fact that power control alone will not be sufficient if the requirement of the application has to be met. Hence, the rate at which beacons are generated must also be controlled. The authors proposed an adaptive architecture and an adaptive timing aspects of beacon generation.

The authors in (Sheu et al., 2011), proposed a distributed routing protocol and focused on two kinds of handovers: inter RSU handover and intra RSU handover. The approximate location of the vehicles is found using the link quality based on Received Signal Strength Indicator (RSSI) from the Timing Advertisement from RSU.

A multi-technology seamless handover mechanism for vehicular networks is explored (Dias et al., 2012). The authors looked at integrating other technologies like 3G to achieve seamless communication between the vehicles and the infrastructure without breaking an active session. Using the extended mobility protocols of MIPv6 and PMIPv6, a test was performed to measure the handover latency for different bit rates between the same communication technology and between different communication technologies. Here speeds of the vehicles considered were 50 and 60 Km/h respectively.

In (Chung et al., 2011), a time coordinated medium access control (MAC) protocol named WAVE point coordination function (WPCF) for vehicle to infrastructure (V2I) communication was investigated. The service disconnection time of various channel access technique for V2I handover was shown. In order to reduce the handover delay and for a soft handover to happen, additional messages were added.

In (Bohm and Jonsson, 2009), the authors referred and criticized the efforts of (Tseng et al., 2005), (Montavont and Noel, 2006) and (Paik and Choi, 2003) where a predictive and proactive handover approach was proposed for 802.11 networks. The authors proposed a proactive polling mechanism where the information about the

approaching vehicles are forwarded to the next RSU, where the vehicles became part of the communication schedule even before entering the next RSU's transmission range. The next RSU starts polling early enough to account for a 20% increase in average speed over the distance between the two access points. When a vehicle experiences a significant decrease in average speed or leaves the highway entirely, the RSU cannot continue sending out proactive polling messages indefinitely. Hence a decrease in average speed of 20% is allowed. The polling by the next RSU stops after this threshold. A new RSU after this should go through the regular connection setup process.

The work of (Lee et al., 2013), proposed a seamless handover scheme based on proactive caching of data packets. Here when an OBU is about to leave the coverage area of an RSU, the buffered packets will be forwarded to the entire candidate RSUs. The new RSU which is one of the candidates will transmit the buffered packets to the OBU and a message is sent to the rest of the candidate RSU's to disvehicled the cached packets.

(Augusto et al., 2014), proposed a new architecture called the MYHand Architecture for providing extended information in Next Generation Networks (NGN) scenarios is detailed. By using the IEEE 802.21 protocol basic schema(IEEE-Std., 2013) and part of the Y-Comm architecture (Mapp et al., 2007), MYHand improves the handover managed by mobile devices (user centric management). A scenario with three access providers and a mobile user walking through the avenue was simulated by using NS2 (Network Simulator2).

The work in (Shaikh et al., 2007) proposed a proactive handover policy using a simple mathematical model. Proactive handover facilitates minimize disruption due to service degradation or packet loss during handover by signalling to the higher layers that a handover is about to happen. This work shows how the Network Dwell Time (NDT) and Time Before Vertical Handover (TBVH) are calculated in heterogeneous environments. TBVH is the time a mobile node has got to hit the circle for handover given the velocity and direction. The paper analysed various vertical handovers (WLAN-3G, 3GWLAN) in their work.

In (Salam et al., 2011), a seamless proactive vertical handover algorithm was proposed which took into account the users preferences, network conditions, velocity of the mobile station and application requirements for selecting a candidate network for handover which is stable. The proposed algorithm calculates the residence time in a candidate network which is already been proposed and highlighted in (Shaikh et al., 2007). This shows the importance of NDT in achieving a proactive handover.

The work in (Shaikh et al., 2007) proposes a proactive handover policy using a simple mathematical model. Proactive handover facilitates minimize disruption due to service degradation or packet loss during handover by signalling to the higher layers that a handover is about to happen. This work shows how the Network Dwell Time (NDT) and Time Before Vertical Handover (TBVH) are calculated in heterogeneous environments. TBVH is the time a mobile node has got to reach the circle for handover given the velocity and direction. The paper analysed various vertical handovers (WLAN-3G, 3G-WLAN) in their work.

Many papers have looked at VANETs as well as handover in essentially isolated or loosely coupled ways. But to the best of our knowledge no work has considered the importance of lower layers (i.e. PHY and MAC) in achieving an effective proactive handover. From a communications point-of-view, this thesis extends the work done in (Shaikh et al., 2007) and (Augusto et al., 2014) by analysing the effects of Network Dwell Time, Time Before Handover and Exit Times in the context of VANET to provide ubiquitous communication in VANET systems.

2.6.2 Analytical Model based Related Works

There have been various analytical models that have been developed to study the beaconing in VANET systems. In this thesis, we have described the advantages that come with this unique characteristics of beaconing in VANETs in the previous chapter. Hence, in this section, we will highlight on some of the existing analytical models that have been developed or optimised to study this beaconing effect and hence, are highlight below:

The authors in (Vinel et al., 2008) have depicted that VANET is a new vehicular communication system, which is being considered for Intelligent Transport Systems. The work, not only emphasizes that extra research efforts are being made by countries like USA, Japan and Europe, but there are more efforts being put in deploying such active systems. This work referred to the new IEEE 802.11p communication standards and have recently been in the limelight. Therefore, in this context, the authors emphasized on the lower layer of the communication standards as periodic beaconing is a key feature in VANETs. This periodic beaconing is seen as a key aspect for providing reliable communication for life critical safety messages in order to stop accidents. Hence, there is a need to analytical model and analyse the probability of successful beacon reception and message transmission delays. Further, this work showed a performance evaluation of such metrics.

The work in (Vinel et al., 2009a) is a continuation of the work presented in (Vinel et al., 2008). Hence, in this work the authors further extend the beaconing com-

munication mode and a new analytical model for investigating the influence of beacon generation rate in vehicle-to-vehicle (V2C) context was presented. The analysis from the new analytical model demonstrated that the numerical results gathered can be used as a method to estimate the probability of successful beacon delivery and mean delay in transmission. It was also noted from the results that the proposed Markov chain analysis is not feasible for unsaturated case due to the large amount of states involved and hence, for this reason non-saturated case should be investigated in the future.

Van Eenennam et al. in (van Eenennaam et al., 2012) designed an analytical model to model the beaconing influence used in VANETs. The authors adapted this behaviour from the existing analytical model presented in (Engelstad and Østerbo, 2006), which emphasized on the IEEE 802.11e EDCA mechanism for traditional WLANs. This work also showed the importance of beaconing taking into account the broadcasting technique widely used for beacon transmission. This is very much required for reliable and efficient communication in vehicular networks. Thus, the authors, argued that CSMA/CA method is used for broadcasting beacons, thus it is very critical to model the backoff mechanism and the blocking behaviour used in the MAC layer very aptly. Hence, the results analysed in this work showed that the analytical model presented closely best fits the simulation results.

The work in (Vinel, 2012) proposed a theoretical framework to compare and contrast the two main technologies currently being considered for vehicular applications. The work critically highlights on the mathematical models developed for both IEEE 802.11p/WAVE and 3GPP LTE technologies. The author conducted several parallel experiments with the developed analytical models and the corresponding simulators in order to correctly model the beaconing parameter required probabilistic calculations. Therefore, the results emphasized that the 3GPP LTE technology faces serious challenges while coping with overloading of the network with beacons. So consequently, 3GPP LTE needs to be modelled more accurately for future considerations in vehicular communication and hence, VANETs or the IEEE802.11p/WAVE protocol stack on the other hand has been designed to cater these challenges appropriately. But still dedicated dual radios, each for safety and non-safety application should be considered in the future.

The works highlighted in the above section were taken into consideration for studying and modeling the beacon parameters used in this thesis. Some of the arguments discussed above enabled us to come to some constructive decision-making while considering the models and simulations used for this study.

2.6.3 Testbed based Related Works

Several field tests have explored various communication scenarios in Vehicular Ad hoc Networks. The work described in (Gozalvez et al., 2012), conducted a field experiment which extensively analysed the performance of V2I communication in an urban environment for an effective and reliable RSU deployment. The field testing was conducted in the city of Bologna with four key scenarios. Three urban and a high way scenario were considered. The communication performance was measured in terms of the packet delivery ratio (PDR) as a function of the distance of the Onboard Unit (OBU) to the communicating RSU. The authors presented the Reliable (RCR) and Unreliable Connectivity Range (UCR) as the distance to the RSU up to which the experienced PDR is above 0.7 and below 0.1 respectively. The study was performed for two transmission power levels i.e., 10dBm and 20dBm, and showed that high transmission power levels can significantly increase the RCR and UCR distances. The study also showed the effects of NLOS, Antenna Heights, Traffic and Heavy Vehicles. Non Line-of-Sight (NLOS) had a significant impact on the communication. The minimum and maximum reliable communication range distance was 400m and 800m (approx.) respectively.

The study reported in (Lin et al., 2012) presented simulation results and field trials were conducted in an internationally standardised laboratory at the ARTC in Taiwan. The work investigated critical parameters such as packet loss, latency and delay spread for DSRC in a controlled environment. The conducted experiments focused on the vehicles speed and its distance from RSU in order to evaluate packet loss and latency. The field measurements of this study showed that if the velocity of a vehicle is 100km/h, then 30% packet loss for safety orientated applications was experienced.

Although, in this thesis we focus mainly into V2I communications, it is worthwhile reviewing some of the main points obtained in V2V field tests. The work depicted in (Jerbi et al., 2007) demonstrates a thorough experimental measurements of V2V communications in various scenarios in order to highlight important factors that influence multimedia applications over an IEEE 802.11p in vehicular networks. The authors aimed to evaluate the effects of speed and distance on the quality of received traffic which emulated a video transmission. The results in the work demonstrated that the performance of the network and signal strength greatly depends on the velocity of the vehicle, as well as the distance between each vehicle.

The field trails presented in (Paier et al., 2010) was conducted in Austria. The authors examined the performance of vehicle to infrastructure communications in an highway environment using IEEE 802.11p prototype. This work presented

the results of average downstream performance of the physical layer. The study analysed the physical layer of IEEE 802.11p without the MAC layer. Investigating the physical layer alone highlights the strengths of the layer as well as pointing out weaknesses, furthermore, improvements can be suggested for a better layer design in order to have more robust vehicle to infrastructure communications. The RSUs in this experiment were set up to broadcast meaning only one way transmission took place and retransmission was disabled. The research proved that environmental effects such as electromagnetic wave propagation and traffic density had significant influence on transmission performance, in particular for big packets and high speed transmission.

The studies examined in this literature have provided valuable information on V2I and V2V communications performance. However, most studies tend to focus on simulation rather than real-time testing because of high associated cost. In this context, we present real-time field experiments which extensively evaluates V2I performance in urban environment. The key purpose of this study is to investigate the deployments issues of RSUs in urban environment which has been further explored in depth in Chapter 7.

2.7 Propagation Model based Related Works

2.7.1 Propagation Models: An Overview

In telecommunications, it is a quite common practice to model the disparities in the amplitude of the received signals. This is done by means of modeling the small or large disparities of fading, shadow fading or by modeling path loss calculations (Raymond and Lajos, 1999). These efforts have been studied in telecommunications for a long time. Some of the common existing models for such path loss variants include Walfisch-Ikegami and Okumura and Hata models. Similarly, there are a few famous statistical fading models such as Rician and Rayleigh for such small scale fading. The most recent and the latest statistical model studied for such small scale fading effects is the Nakagami M-distribution. It best suits most cases as it considers the shape parameter and the spread controlling parameters. Additionally, there are also some realistic empirical models for studying shadow fading effects such as the famous log-normal distribution. Although, these shadow fading effects form a key feature in telecommunication studies, it is quite astonishing that very few cases have been presented using this particular distribution. Therefore, this shadow fading attribute is quite extensively used in developing a comprehensive

network simulation tools for analysing various handover techniques and as well as interferences issues for modeling the realistic environment.

Most wireless system use propagation models for urban environments in order to consider non line of sight (NLOS) or obstacle problems with respect to received signal; these NLOS problems could be caused by the environmental factors such as tall building, trees, large obstacles and etc. The propagation model is used to predict the received signal strength based on calculation from the transmitter and the receiver. There are many models developed for this purpose, but very few consider both issues of line of sight and Non line of sight (Rappaport, 2012). Path loss is also known as path attenuation can be defined as the drop/reduction in the density of power (attenuation) of an electromagnetic wave when it is being propagated through space. It is also defined in some cases as the difference (in dB) between the power transmitted and the power received. Path loss plays a major role in the analysis and design of the link budget of a telecommunication system. The term Path Loss is mostly is used in wireless communications and is basically signal propagation. There are numerous contributing factors which lead to Path loss. These effects include but are not limited to; free-space loss, refraction, diffraction, reflection, aperture-medium coupling loss, and absorption. Path loss is also influenced by terrain contours, environment (urban or rural, vegetation and foliage), propagation medium (dry or moist air), the distance between the transmitter and the receiver, and the height and location of antennas.

2.8 Existing Path Loss Models used in VANETs

For this research work, a specific propagation models were taken into consideration. Some of them have been previously used for VANET studies and have been highlighted and explained in detail below.

2.8.1 Free Space Path Loss Model

The free space path loss model is used in mobile and wireless communication to predict the signal strength between the transmitter and receiver in clear line of sight. As the name implies, the model deals with path loss in free space. In this model, the attenuation is proportional to the square of the distance between the transmitter and the receiver and also to the square of the frequency of the radio signal(Rappaport, 2012).

For free space path loss (FSPL) in decibels, it can be mathematically represented as:

$$(FSPL) = 20\log_{10}(d) + 20\log_{10}(f) + 32.44 - G_t - G_r$$

where d is the distance from the antenna in kilometres, f is the frequency of the signal in MHz , G_t is the gain at the transmitter and G_r is the gain at the receiver. The free space path loss model is highly effective where multipath effects are at minimal such as for satellites in space. This model lacks accuracy in the sense that the received signal power is only dependant on the transmitted power, the antenna gains and the distance between the sender and the receiver. Obstacles are not taken into consideration.

2.8.2 Two-Ray Ground Model

This propagation model takes into account the fact that radio propagation will normally get affected by at least one significant interference namely the ground reflection (Sommer and Dressler, 2011). To archive a physically more correct path loss approximation (Rappaport, 2012), it must be based on the phase difference of interfering rays φ and reflection coefficient γ_{\perp} , leading to a Two-Ray Interference Model (Rappaport, 2012),

$$L_{tri}[dB] = 20\log\left(4\pi\frac{d}{\lambda}\left|1 + \Gamma_{\perp}e^{i\varphi}\right|^{-1}\right), \text{ substituting}$$

$$\sin\theta_i = (h_t + h_r)/d_{ref}, \cos\theta_i = d/d_{ref}$$

The problem with this model is the fact that it assumes that the received energy is the sum of the direct line of sight path and the reflected path from the ground taking no account for obstacles and the sender and receiver are required to be on the same height (Martinez et al., 2009).

2.8.3 Rayleigh and Rician Fading Model

These models are based on a standard normal distribution. Clarke's model for Rayleigh fading (Xiao et al., 2003) is given as

$$g(t) = \frac{1}{\sqrt{N}} \sum_{n=1}^N e^{j(\omega_{at} \cos \theta_n + \phi_n)}$$

Where N represents the number of reflections, ω_d is the maximum radian Doppler frequency and θ_n and ϕ_n are the angle of arrival and initial phase of the n^{th} propagation path. This equation can be broken down into its real and imaginary components. $g_c(t)$ and $g_s(t)$ respectively.

The Rayleigh Fading path loss model is calculated in dB as shown in (Rappaport, 2012)

$$Rayleigh_{dB} = 10\log_{10}\left(\frac{[g_c(t)^2] + [g_s(t)^2]}{2}\right)$$

The Rician fading model is obtained by adding a dominant signal to Clarke's model. The ratio of the power of the dominant signal to that of the sum of the reflected signals is represented by Rician parameter K (Mukunthan et al., 2012). The path-loss due to Rician fading in dB is given as (Xiao et al., 2003)

$$Rician_{dB} = 10\log_{10}\left(\frac{[g_c(t) + \sqrt{2K}]^2 + [g_s(t)]^2}{2(k+1)}\right)$$

Both models would not be entirely suitable for VANET communication because both models simply describe the time correlation of the received signal power. Rician Model considers indirect paths between the sender and the receiver while Rayleigh fading considers when there is one dominant path and multiple indirect signals (Martinez et al., 2009).

2.8.4 Log-Normal Path Loss Model

The log-normal path loss model is a model which can predict the propagated signal in a dense urban environment even inside a building as defined in (J. Salo and Vainikainen, 2005). In Log-Normal model, the path loss can be mathematically represented as follows:

The probability density for the log-normal distribution is:

$$P(x) = 1/(S\sqrt{2\pi})e^{-\frac{(\ln x - M)^2}{2S^2}}$$

And the cumulative distribution functions for the log-normal distribution is:

$$D(x) = 1/2[1 + \text{erf}((\ln x - M)/(S\sqrt{2}))]$$

where, $\text{erf}(x)$ is the erf function.

2.8.5 Nakagami Model

This model is a well defined radio propagation model as described in (Nakagami, 1960). The Nakagami model incorporates more parameters than usual models, and hence can model the real-world constraints more efficiently. The uniqueness of this model is that it aptly models the fading effects for multipath scattering of large delay-time spreads, with different clusters of reflected signals. This models can also be used for both urban and motorway scenarios along with channel fading effects (Nakagami, 1960). Further, this model is more identical to Rayleigh fading signals as they have the same amplitude distribution as the Nakagami model. Nakagami-m distribution has the following advantages versus the other models:

1. It is a generalized distribution which can model different fading environments.
2. It has greater flexibility and accuracy in matching some experimental data than the Rayleigh, log-normal or Rice distributions .
3. Rayleigh and one-sided Gaussian distribution are special cases of Nakagami-m model.

Therefore, this model is more generally accepted for practical fading channels.

Nakagami distribution is defined by the following equation as the probability density function:

$$f(x; m, \Omega) = \frac{2m^m}{\Gamma(m)\Omega^m} x^{2m-1} \exp\left(-\frac{m}{\Omega}x^2\right)$$

Its cumulative distribution function is:

$$F(x; m, \Omega) = P\left(m, \frac{m}{\Omega}x^2\right)$$

where, P is the incomplete gamma function.

2.8.6 The Okumura Model

In urban and suburban areas, it is necessary to take into consideration the effects of multipath(Okumura, 1968). The Okumura model is mostly used model especially for the urban areas (Okumura, 1968). For Okumura model, the path loss is mathematically represented as:

$$PL = L_f + A_{mu} - G_{ht} - G_{hr} - G_{area}$$

where L_f is the free propagation path loss, A_{mu} is the attenuation of the medium relative to free space, G_{ht} is the gain due to the height of the base station antenna, G_{hr} is the gain due to the height of the mobile node receiver and G_{area} is the gain due to the type of environment.

Some of the key points which need to be followed in order to use this radio propagation model in an urban environment are as follows:

1. This model can only be considered in cases where the channel operates on the frequency band between 150 - 1920 MHz.
2. The height of the Base station antenna needs to be between: 30 meters - 1000 meters.
3. The mobile node can be at a height between: 1 meters to 3 meters.
4. Link distance should be between: 1 km to 100 km.

2.8.7 Hata Models

The Hata model is more or less based on the Okumura model which can be deployed for urban and suburban environments (Hatay, 1980). After changing a few configurable parameters on the Okumura model, for urban areas the Hata model can be represented as:

$$L_u = 69.55 + 26.16 \log_{10} f - 13.82 \log_{10} h_b - C_H + (44.9 - 6.55 \log_{10} h_b) \log_{10} d$$

where h_b is the height of the base station, h_m is the height of the mobile node, and C_H is the antenna height correction factor.

For small or medium cities (Hatay, 1980),

$$C_H = 0.8 + (1.1 \log_{10} f - 0.7) h_m - 1.56 \log_{10} f$$

For large cities, the formula is dependent on two frequency ranges (Hatay, 1980);

So for $150 \text{ MHz} \leq f \leq 200 \text{ MHz}$

$$C_H = 8.29(\log_{10}(1.54h_m))^2 - 1.1$$

and for $200\text{MHz} \leq f \leq 1500\text{MHz}$

$$C_H = 3.2(\log_{10}(11.75h_m))^2 - 4.97$$

For Suburban areas,

$$L_{su} = L_u - 2(\log_{10}(\frac{f}{28}))^2 - 5.4$$

where L_u is the path loss in urban areas, f is the transmission frequency in MHz , and all path loss values are in dB .

Therefore, this model cannot be used in VANETs because of the frequency band concerns. The Frequency band at which VANETs operate is 5.9 GHz, which operates at a much higher frequency band for considering such models.

2.8.8 CORNER Propagation Model

This type of propagation model is a low computational light weight model, which operates by using the use of information about the road topology. CORNER benefits from the attenuation between two nodes taking into account the presence of buildings (Giordano et al., 2010). This model also takes into account three possible cases namely:

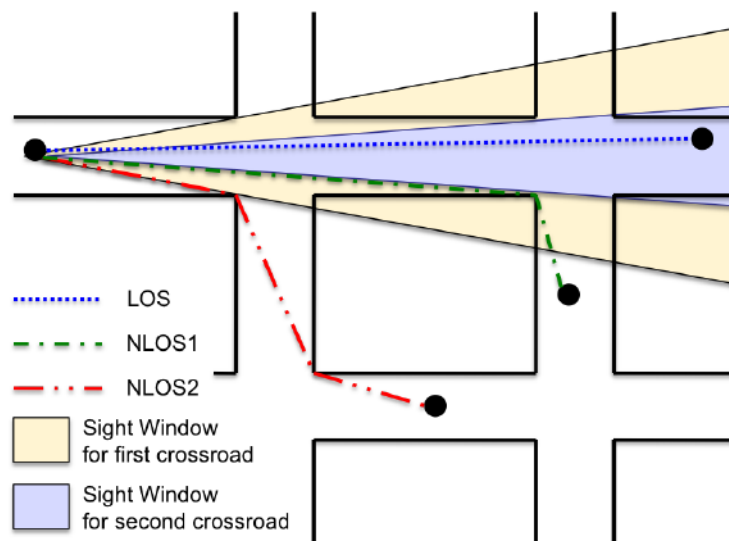


Fig. 2.17 Illustration of CORNER Propagation as defined in (Giordano et al., 2010).

Line Of Sight (LOS): assuming that the vehicle is in direct line of sight with the RSU and the free space path loss can be assumed given as

$$PL = 20\log_{10}\left(\frac{\lambda}{4\pi d}\right)$$

Non Line Of Sight with one corner along the path (NLOS1): This assumes that two nodes are not in line of sight but separated by one corner, this is illustrated mathematically as

$$PL = 10\log_{10}\left(10\frac{PL_D}{10} + 10\frac{PL_R}{10}\right)$$

where PL_D represents diffraction around the corner and PL_R represents reflection around the corner (Mukunthan et al., 2012).

Non Line Of Sight with two corners along the path (NLOS2): It assumes that two nodes do not have direct line of sight and are separated by two corners and mathematically illustrated as

$$PL = 10\log_{10}\left(10\frac{PL_{DD}}{10} + 10\frac{PL_{DR}}{10} + 10\frac{PL_{RD}}{10} + 10\frac{PL_R}{10}\right)$$

where PL_{DD} represents a diffraction around a corner followed by diffraction around another corner, PL_{DR} represents a diffraction around a corner followed by a reflection around another corner, PL_{RD} represents a reflection around a corner followed by a diffraction around another corner and PL_R represents a reflection around a corner (Mukunthan et al., 2012).

To enable differentiate between these three possible cases, a width is assigned to each road segment and is computed as:

$$Width = (NoL * LW) + 10$$

Where NoL is represents the number of lanes expressed in meters. (Note, the number of lanes is double of the segment is part of a two way road). LW represents the width of the lane which is assumed to be constant. An additional 10 meters is added taking the side walks into consideration.

2.8.9 Finite Propagation Model

This propagation model talks about solving the problem of radio coverage in the urban areas and the troposphere and of all the available propagation models, seems

to be the closest to solving the problem of propagation models associated with VANET. One of the persistent challenges in the urban areas and the troposphere is the ability to get the required radio coverage (Hall et al., 1997). Researchers in the area of wave propagation have been in search of efficient mathematical models for describing the problem of electromagnetic wave propagation in the atmosphere. There are various methods available for the prediction of electromagnetic waves propagation in the atmosphere (Craig and Levy, 1991). Nevertheless, there are a few complications in the application of some methods due to the presence of vertical refractive stratification in the atmosphere (Hitney, 1994).

A while ago, geometrical optics (GO) techniques and modal analysis were given a lot of emphasis (Arshad et al., 2007). GO provides a general geometrical description of ray families, propagating through the atmosphere. Ray tracing methods present many disadvantages; for example, the radio-wave frequency is not accounted for and it is not always clear whether the ray is trapped by specific duct structure (Slingsby, 1991) and (Arshad et al., 2007)

A different form of approach for tropospheric propagation modelling was implemented by Baumgartner (Baumgartner et al., 1983) and later extended (Shellman and CA., 1986) and is generally identified as the Wave guide Model or Coupled Model Technique.

Most of the current available prediction models for VANET are majorly based on simplified Deygout solution for multiple knife-edge diffraction (Deygout, 1991). But this model proposes a solution which tackles the full vector problem i.e the three dimensional variations in refraction. At the long run, this solves the problem of electromagnetic propagation problems in the presence of an irregular terrain (Arshad et al., 2007).

Therefore, the table 2.5 shows a simple comparison of some of the existing and most widely used models in wireless and mobile communications such as Free Space Path Loss model, Two-Ray Ground model (Khan and Qayyum, 2009), Shadowing model, Rician and Rayleigh model, RPMO model (Marinoni and Kari, 2006), Mahajan et al. (Mahajan et al., 2007) model and Nakagami model (Nakagami, 1960). Since, this thesis's sole focus is not on the radio propagation models, hence we just describe them briefly, that have been used previously for VANET studies.

Table 2.4 Summary of Propagation Models used in VANETs.

Propagation Models	Descriptions	Significance of the Propagation Model in Vehicular Communications
Free Space Pathloss Model	<p>This model is purely based on the received signal strength of the receiver i.e., the received power is calculated based on the distance between the transmitter and the receiver and potential antenna gains and hence no obstacles are considered or modeled. Therefore, the distance plays an important role in this model.</p>	<p>This model is can be considered for VANETs. But this model is the most simplistic model to be considered for VANETs, hence not quite adequate for the dynamically changing environment in VANETs.</p>
Two-Ray Ground Model	<p>This model is basically based on the height factor of the sender and the receiver; thus, both need to be at the same level in order to consider this model. This model is based on the principles of received signal strength being calculated as sum of the reflected path from the ground and a clear line of sight, between the sender and receiver. Again no obstacle model is considered.</p>	<p>This model can be considered for VANETs, but it is not as realistic for vehicular environments. For example, if the transmission range of a node is 450 meters, then the receiving end of the nodes could very well be placed anywhere within that range. Therefore, it means that probability of receiving a packet will be the same, whether or not a node is placed 450 metres away or 20 metres away from the sender (doesn't consider any fading effects).</p>
Shadowing Model	<p>The shadowing model is best suited for the cases where there are environmental constraints being considered. This model takes into account a gaussian variable to the calculated pathloss.</p>	<p>This model can be considered for VANETs, taking into account the environmental constraints.</p>

Table 2.5 Summary of Propagation Models used in VANETs.

Propagation Models	Descriptions	Significance of the Propagation Model in Vehicular Communications
Rician and Rayleigh Fading Model	<p>One of the features about this Rician model is that it considers reflected orscattered paths (no one particular paths or multiple paths) but this comes at the cost of multipath interferences. In short, line of sight being as a dominant factor for calculating fading in the Rician model. But, the Rayleigh Fading model on the other hand considers at least one prevailing path and multiple reflected paths. Consequently, both these models are based on the received power based on the time association between the sender and the receiver.</p>	<p>This model is can be considered for VANETs, as it is a more realistic model with fading considerations.</p>
RPMO Model	<p>This model is a simple radio propagation model # which models an obstacles for its evaluation. The obstacle factor is the main key this model. Hence, if there are no obstacles then this model behaves just like the Two-ray Ground.</p>	<p>This model is can be considered for VANETs, but again not as realistic to be considered for vehicular environments.</p>
Mahajan et al., Model	<p>This model behaves like Two-ray Ground, adding the influence of obstacles and the distance attenuation, but it is designed for the 802.11b environment.</p>	<p>This model is cannot be considered for VANETs, as it can only be used for IEEE 802.11b technology.</p>
Nagakami Model	<p>Nagakami propagation model occurs when there is multipath scattering with larger delay-time spreads compared to other models and for different clusters of reflected waves.</p>	<p>This model is can be used for VANETs. As it interprets more realistic parameters than other models.</p>

2.9 Current Trends in VANET Simulation Techniques and Tools

VANETs are based on the basic principles of connecting vehicles to RSUs and to other adjacent vehicles in the vicinity. The basic operation is to send and receive information over wireless communication channel. One of the most important characteristics of VANETs is that the vehicles are anticipated as mobile nodes and the RSUs as access points. This feature also comes in handy as an advantage to the VANET systems as both the RSUs and the OBUs can act as an access point or a mobile node and vice-versa. However, most of the time the RSUs are standalone and operate as fixed nodes. Due to this unique characteristic, the mobile nodes in VANET systems are considered to be fast moving resulting in a highly dynamic environment i.e., continuously changing network topology.

In order to study VANET systems it is necessary to look into different simulation techniques. This requires emulating the fast moving mobile nodes (the mobility side) and the highly dynamic environment (the network topology side). Therefore, VANET simulation identifies this criteria and distinguishes VANET simulation into two different simulation categories: (a) Mobility Simulators and (b) Network Simulators. Since, the wide spread of VANET research and standardization of the VANET protocols, there had been a considerable amount of increase in extensive use of simulation tools for studying VANET systems. This has led the scientific community and researchers to explicitly develop and use of a third component which is being now categorised as VANET Simulators or frameworks. A framework generally is regarded as being a middleware/software which incorporates components from several different independent modules, for example one such framework being used to vehicular communications is the VEINS framework (VEHICLES In Network Simulation): This is a good example of how it connects and uses different modules from a Network simulator such as OMNET++ and a Mobility simulator such as SUMO (Simulation in Urban Mobility) and produces a complete simulation environment for vehicular communications studies.

A simple block diagram has been depicted in Figure 2.18 displaying various currently available simulators for studying vehicular communications. On one hand, mobility simulators, (also known as traffic generators) are responsible for generating realistic mobility traces for vehicles, which are then fed into vehicular sub-modules available in network simulators. On the other hand, network simulators are accountable for creating the entire vehicular networks along with physical wireless communication channel and all the network level components required for

achieving vehicular communications. These have been further explored in detail, in the sections below (Noori and Olyaei, 2013).

2.9.1 Mobility Simulator

There are many mobility simulators that have been categorised for wireless communications in general, but for vehicular communications this has been divided into two main categories - 1) Microscopic and 2) Macroscopic. The first category highlights on the vehicle and the vehicular communications parameters itself (Harri et al., 2009). A typical example of a microscopic description used in VANET simulation are the vehicle parameters such as speed, acceleration, the times each vehicle departs and its arrival rate and road dynamics etc. The second category focuses more on the flow of the mobility of the vehicle (flow patterns), in particular the broader picture i.e., the traffic density and the traffic flow. In addition, the microscopic description of the mobility models, where each vehicle's parameters such as vehicle acceleration and speed can be controlled and captured at every instant by means of parallel simulation (also known as micro-level simulation) such as SUMO (Behrisch et al., 2011). In this thesis we mainly look at SUMO traces. Some of the other mobility simulation softwares are listed here: CityMob, VanetMobiSim, CORSIM, FreeSim, PARAMICS, VISSIM, STRAW and Netstream (Noori and Olyaei, 2013).

2.9.2 Network Simulator

Network simulators are typically computer programs or tools developed to imitate the behaviour of a real communication network environment (infrastructure) to measure and quantify the overall network performance metrics. Traditionally, there are several network simulators for wired, wireless and ad hoc communication which are freely available on-line and/or are licensed such as OPNET, Qualnet, NCTUns and NS-2. Among these network simulators there are some which support VANET simulation. Most of the network simulators are designed to support MANET simulations but some of them have been currently optimised to support VANET simulations by using extended frameworks, for example: OMNeT++, NS-2, GloMoSim, JiST/SWANS, GTNetS, J-SIM, SNS and NS-3 (Noori and Olyaei, 2013).

2.9.3 VANET Simulator

As discussed in the above sections, VANET simulators are middleware entities which use a framework to connect the mobility simulators to network simulators by means

of providing inputs from parameters used in VANET simulation (Christoph Sommer, 2014). Some most famous VANET simulations which are currently being used have been listed here, for example: Veins, NCTUns, MOVE, TraNS, etc (Noori and Olyaei, 2013). In recent times, the Veins Framework has gathered more attention from many researchers and scientists as being the most widely used open source framework for vehicular communications. The Veins framework is based on two well-established simulators: OMNeT++, an event-based network simulator (Andras Varga, 2014), and SUMO, a road traffic simulator (Krajzewicz, 2010), which extends these to offer a more comprehensive suite of models for vehicular communication simulation.

2.10 Which is the Most Suitable Simulator?

In this section of the thesis, we highlight some of the key factors that has led us to select and justify our choice of simulation tools used for this study. In this thesis, we conduct several simulation experiments for that we mainly focus only on OMNeT++ (the Network Simulator) and SUMO (the Mobility Simulator) along with the extended Veins framework (VANET Simulator) for our experiments.

As mentioned in the previous sections, there are many popular simulators for conducting VANET research. There is no single comprehensive simulation tool/software that incorporates all the VANET features, for instance there is no one network simulator or mobility traffic regenerator that can achieve this; nor is there any one single software or middleware that exists that does the job. Therefore, it is imperative to first learn how to select the best set of simulation tools for VANET research. Previously, there has been some research done in this area and some of the literature clarify on how to achieve the best possible combination of simulation tools for VANET research. Therefore, this thesis will also enlighten on some of the key work which identifies this problem and concludes that it is a best practice to use a combination bidirectionally coupled simulation techniques rather than using one single simulator or simulation software.

In order to select the perfect combination of simulation tools for VANET research, one must begin to look into an efficient and resourceful network simulator. Some of the most widely used network simulator for VANET research are: GloMoSim, NS-2 or NS-3 (now) and OMNeT++. In (Hassan and Larsson, 2011), the authors have clearly highlighted on some of the key advantages and more on limitations of GloMoSim, NS-2, NS-3, CANUMobiSim, NCTUns simulators compared to OMNeT++. OMNeT++ for that matter is a newer simulator that has been able to integrate the VANET technology, the protocol stack (architecture) and the stan-

dards itself appropriately. This has been emphasized more in (Weingartner et al., 2009), where the authors compare the same simulation experiment with similar performance metrics to evaluate five simulators, in order to compare and contrast on which of the simulator outperforms the other. The authors, concluded that JiST, NS-3 and OMNeT++ were much more capable of performing efficiently in a large scale network simulation.

Moreover, OMNeT++ delivers a more rich graphical user interface (GUI), that eases the user experience and hence there has been more widespread use of OMNeT++ in recent times. Also OMNeT++ is a more open-source and portrays a more abstract modeling language than NS-3 and JiST. Whereas, JiST and NS-3 depend more on the command-line source codes for the entire simulation development. It is also a good practice to investigate in detail some the middlewares or interfaces that can couple these simulators. Hence, the work in (Harri et al., 2009), demonstrates a typical example of how an interface interacts with both the network and traffic simulator, but it was not able to completely mimic the simultaneous interactions between both the micro-level and macro-level simulation i.e., the SUMO and the NS-2. Similarly, the same is seen in the work presented in (Piórkowski et al., 2007) where the authors developed a GUI tool called TraNS, which integrates both traffic and network simulators such as SUMO and NS-2. However, the lower layer models in NS-2 don't really interact with the traffic generator (dynamically), how a realistic mobility model should interact with the lower layers of the protocol stack as defined by the radio models of IEEE 802.11p standards.

There are many similar comparative evaluation studies done in this area, highlighting the most widely accepted interface for VANET studies, some of them have been presented in (Karnadi et al., 2007), (Fiore et al., 2007), (Choffnes and Bustamante, 2005), (Karnadi et al., 2007), (Fernandes et al., 2010), (Conceição et al., 2008) and (Fernandes and Ferreira, 2012). For example, the work in (Choffnes and Bustamante, 2005) demonstrates the use of real maps for realistic traffic generation and mobility traces. Similarly, the authors in (Karnadi et al., 2007), illustrate an easy solution for integrated simulation by the use of a simple Java program for users that can generate realistic mobility model based on real maps. Another, Java written simulator interface is the VanetMobiSim extension which focuses more on vehicular mobility, and features new realistic automotive motion models at both macroscopic and microscopic levels (Fiore et al., 2007). Among these simulation interfaces or middlewares, one such new VANET simulators is worth mentioning, is the DIVERT project (Conceição et al., 2008), which integrates DIVERT with NS-3. This was more elaborated in the work in (Fernandes et al., 2010) and later extended

in the work in (Fernandes and Ferreira, 2012). Hence, in conclusion it can be said that from the highlighted works, it is quite evident from the above analysis that one major common constraint of such interfaces or middlewares is the lack of two-way communication (lack of bidirectionally coupled simulation). The reason being it is easy for network simulators to get inputs from the micro-level simulators like SUMO and DIVERT etc., but not the other way round.

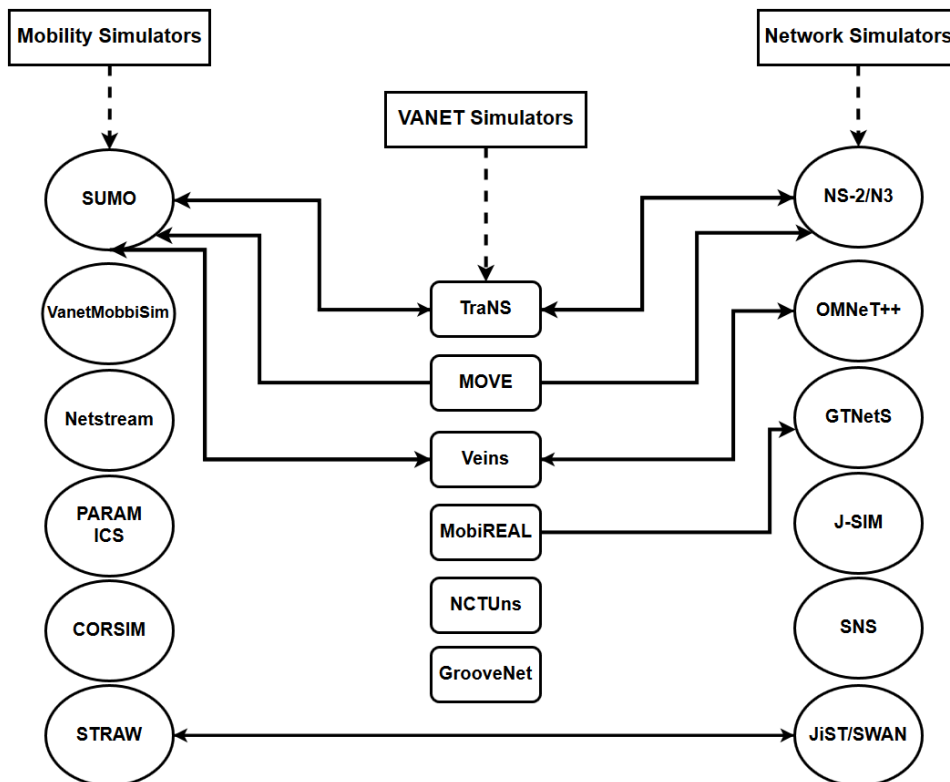


Fig. 2.18 Taxonomy of VANET Simulators.

Therefore, in this thesis we select the Veins framework that integrates the OMNeT++ and SUMO, which also demonstrates a bidirectionally coupled road traffic and network simulation. This bidirectionally coupled attribute has a number of advantages to it. Firstly, this bidirectionally coupled attribute enables the simulation to interact both ways i.e., it can achieve re-routing of the vehicles based on re-configuration at the network-level simulation while both simulations are running. Secondly, the Veins framework is capable of generating realistic traffic based on real-maps which are generated from SUMO and feeds it live to the network simulator. This also enables it to run parallel simulation at both micro and macro-levels via a TCP socket. Unlike, other frameworks or middlewares, the Veins framework minutely models the channel switching techniques of the IEEE

1609.4 DSRC/WAVE stacks. It even models carefully the behaviours of lower layers i.e., is of the IEEE 802.11p radios as specified in the standards. Initially, the Veins framework was based on the MiXiM framework but now the newer versions of the Veins framework that incorporate more added features such as more parameters for both the RSUs and the vehicles. MiXiM framework was developed to model the detailed wireless communication and the interaction of the communication channel which has been depicted in (Köpke et al., 2008). MiXiM framework provides a more detailed model of the wireless communication channel and the connectivity. This enabled early researcher in the VANET community to further explore and develop more accurate MAC protocols for VANETs. The mobility attribute was added later with the increase in vehicular communication studies using OMNeT++. Moreover, SUMO is an open source continuous road traffic simulator at microscopic level geared to mimic the large road networks (Noori and Olyaei, 2013).

Finally, we can conclude by noting some of the key advantages of the Veins framework that have been highlighted in (Sommer et al., 2011), in order to support bidirectionally coupled road traffic and network simulations. It was observed that simple mobility generators cannot model the real-time traffic based on real maps and hence, making generated traffic models unsuitable for such micro-level simulations whereas the Veins framework, connects these micro-level road traffic simulator such as SUMO via TCP socket with OMNeT++ for realistic interactions (Yoon et al., 2003). The newer versions of the Veins framework provide a more comprehensive model of the lower layer, which helps to replicate the urban setting which includes obstructions from the buildings and road infrastructures. There is an obstacle module present in the Veins framework which helps in providing such inputs considering realistic radio propagation models and surrounding buildings position on the maps from SUMO. Hence, these types of inputs are very much needed for evaluating realistic vehicular communications in developing more realistic radio propagation models and routing protocols (Lochert et al., 2005) and (Sommer and Dressler, 2007). Furthermore, using bidirectional coupled simulation can achieve direct performance evaluation on the microscopic simulation parameters without needing to evaluate them separately for example in SUMO simulation one can not only record traffic related parameters i.e., speed, acceleration, deceleration and etc. but also record environmental attributes, i.e. CO₂ emission from the vehicles and vehicle behaviour which will help environmental evaluation to decide whether the drivers can indirectly affect the environment (Sommer et al., 2008) and (Wang et al., 2007).

2.11 Summary

In this Chapter, the state of art VANET applications was discussed. These applications were categorised into four major types, which highlighted the applicability of safety (life-critical) and non-safety applications in VANET systems. Further, an overview of the VANET architecture along with protocol stack was discussed in detail. A thorough critical review was presented, looking into the communication mechanisms in VANETs which were used to determine the parameters that affect the seamless communication especially handover techniques. The literature also looked into the current state of art simulation techniques and tools used for studying vehicular communications. A thorough evaluation was conducted in order to determine which simulation tools are best suited for this study. Finally, it was evident from literature reviewed that in order to achieve ubiquitous connectivity, it requires a proactive approach towards handover which takes into account the nature of the wireless communications and the velocity of the vehicles.

It is therefore, necessary to conduct preliminary investigation looking into the parameters particularly beaconing that affect the handover in order to achieve seamless communication. Further, Y-Comm concepts are introduced in depth. This is discussed in the next Chapter of this work.

Chapter 3

Preliminary Investigation for Providing Ubiquitous Communication using Road-Side Units in VANET Systems

3.1 Introduction

This chapter is about an initial investigation into providing ubiquitous communication using Road-Side Units in VANET systems because current research has not adequately captured the real-world constraints in VANET handover techniques. Our investigation begins by looking at a simple scenario involving a single vehicle and a Road-Side Unit (RSU) to understand the communication mechanism in a VANET environment, in particular, we will examine the effects of beaconing to signal the presence of a new RSU network to the vehicle and how the beacon is processed by the different layers of the networking stack. In order to do this, we use concepts such Network Dwell Time, Time Before Handover and Exit Times which were explored in the Y-Comm Framework. We first develop the concept of idealised Network Dwell Time (NDTi) from the Y-Comm framework and compare it with measured NDT which involves the difference between when the first and last beacons of the current network are received. We study the impact of beacon frequency and velocity on the measured NDT, Exit Times and the minimum overlapping distance required for soft handover.

3.2 Research Methodology: Simulation

Simulation refers to an imitation of a real-world process. There has to be a set of assumptions which can be expressed logically or symbolically to achieve the reproduction of a prototype or an existing system. Once the simulation process is run, the events have to be observed and registered for future consideration. In the simulation framework, several factors such as state, activity and events must be included. The importance of using realistic mobility model for VANET simulation so that it can show the real-world performance is reflected by traffic guidance, coordination, traffic management and safety, driver behaviour and node mobility. The work in (Krajzewicz et al., 2012) reflects the importance of using realistic mobility model for VANET simulation. Following their research traffic guidance and management, coordination, safety, node mobility and driver behaviour reflects the importance of using realistic mobility model for VANET simulation.

The simulation process consists of two parts: the building of the model (pre-simulation) and simulation. More tools have to be used and these have to be compatible with each other. The most popular tools are SUMO (mobility simulator) (Krajzewicz, 2010), OMNeT++ (network simulator), and Veins which is used to link the previous two. The tools mentioned above can be incorporated in order to form a mesoscopic simulator (Krajzewicz et al., 2012). This is done to achieve closer to real-life results which can further be used in VANET research.

There are three kinds of simulation models of traffic. The first one is microscopic and it can show the location of the vehicle and its speed and the vehicle's state. The second type is called macroscopic and it focuses on traffic flow which includes speed and density. The third type is called mesoscopic and it comprises the other two types: microscopic and macroscopic.

However in Zhiyuan and Jinhongs' research paper on the Framework of Real VANET Simulation Research it is mentioned that VANET simulation consists of two main parts: the vehicular mobility model and the simulation of self-organizing wireless mobile network.

In VANET simulation there are three steps to be completed and each one in a defined order as the output of one step becomes the input for the next step. For the purpose of this research Ubuntu 14.04 LTS operating system has been used. The project requires downloading a map as part of pre-simulation procedure. The map can be downloaded from www.openstreetmap.org. The map can be exported once it meets all the requirements in the sense of the needed territory. A file with ".osm" extension will be downloaded.

The “.ned.xml” and “.edg.xml” are used for creating the “.net.xml” file with the help of netconvert:

netconvert -osm-files testmdx.osm -o testmdx.net.xml Further with the help of polyconvert the “.net.xml” file is converted into “.poly.xml”.

Polyconvert -net-file testmdx.net.xml -osm-files testmdx.osm -type-file typemap.xml -o testmdx.poly.xml

The “.sumo.cfg” file uses the “.net.xml”, “.poly.xml” and “.rou.xml” files. This is done to include additional information such as traffic events. To import the mapping data SUMO has been used (Krajzewicz, 2010) and (Krajzewicz et al., 2012). It generates traffic and allows the evaluation of traffic management. It is also designed for simulation of multimodal traffic, including vehicles, public transport and pedestrians and is able to handle the integration with other software.

3.2.1 Simulation approach in OMNeT++

OMNeT++ (Objective Modular Network TESTBED) is component based C++ simulation library, open source and supports the integration of other tools. Each vehicle represents a mobile wireless node. For the simulation of this research movement paths generated by mobility simulator, SUMO (Krajzewicz, 2010), are integrated into the network simulator, OMNeT++, which will manage the communication between the nodes, both mobile (OBUs) and immobile (RSUs). The network simulator contains many features and these are built with Network Description files (NED). Any simulation is initialized with a file called “omnetpp.ini”.

The network simulator and the traffic generator have to be connected using a bidirectional coupled simulator such as Veins framework. The advantages are free parameterization and realistic node movement. It provides feedback on vehicle behaviour. Veins is designed for running vehicular network simulations and includes a comprehensive suite of models. It uses Python scripts (sumo-launchd.py) and TCP connection to enable SUMO to act as a mobility model in OMNeT++ which can be run either via graphical user interface or command line use interface. The only disadvantage is the traces cannot be reused (Krajzewicz et al., 2012).

3.2.2 The Simulation tool - OMNeT++

For this work, OMNeT++ version 4.6. (Andras Varga, 2014) has been used. It is component-based C++ simulation framework designed primarily for building network simulations. It includes many networking features such as wireless and queuing networks. This tool has a graphical runtime environment, it is very flexible in adding extra features for real-time simulation, and it is open-source for academic and non-profit use. In order to have a better representation of a realistic environment, SUMO version 0.22.0 (Simulation of Urban Mobility) has been used (Krajzewicz, 2010). Though OMNeT++, also supports other frameworks Veins (Christoph Sommer, 2014) is a platform for running vehicular network simulations. Veins extends OMNeT++ and SUMO to deliver a comprehensive combination of models for IVC (Inter Vehicle Communication) simulation. The software tools can be easily combined to run simulations interactively (Christoph Sommer, 2014).

3.3 Simulation Scenario

For this research, the map of Hendon Campus of Middlesex University, London was exported from www.openstreetmap.org. The territory has the following coordinates: latitudes from 51.5868 to 51.5950 and altitudes from -0.2392 to -0.2174.

3.3.1 SUMO simulation files

- **Network file:** Using NETCONVERT tool demonstrates the creation of the network file. It contains the road infrastructure which is used in SUMO. The road infrastructure is directed graph. The road infrastructure includes the edges (streets) and junctions. The network file ends with “.xml” extension.
- **Routes file:** The routes file is used as input in the mobility simulator (SUMO). The vehicle moves following a defined route. The routes file ends with “.xml” extension. In SUMO there are four applications which generate the routes. These are OD2TRIPS, DFROUTER, JTRROUTER, and DUAROUTER (please see Figure 3.1) and each one has a different feature. For example DUAROUTER generates routes based on shortest path search.
- **Configuration file:** It contains all the parameters that are needed and define the simulation. The configuration file contains the start and end simulation times, steps, input file etc.

Additional files. The additional files contain any additional data, such as events, which is needed for the simulation. It ends with “.xml” extension.

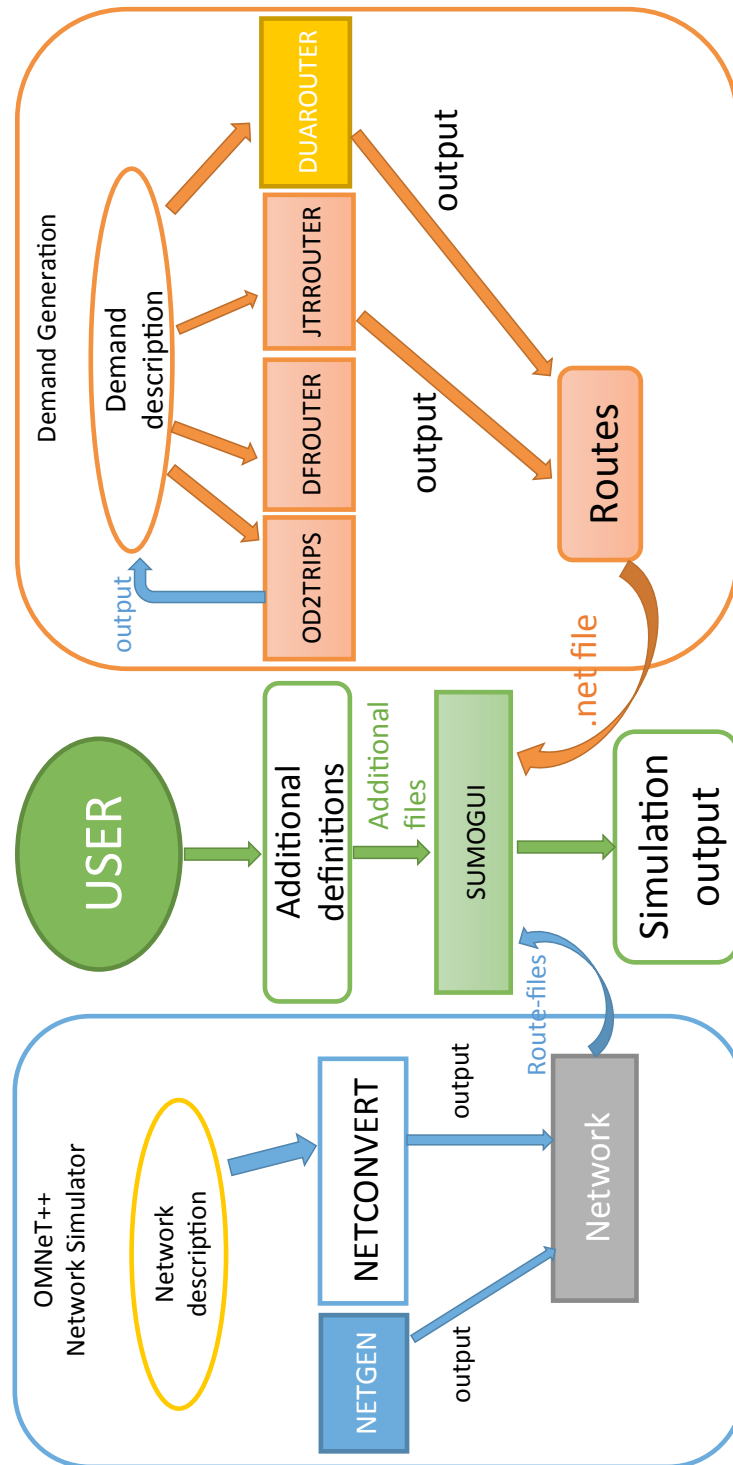


Fig. 3.1 Simulation Process.

3.3.2 Simulation with the Veins Framework

The Veins framework requires the following steps to run the simulation:

- **Building the network:** It contains the vehicles and road infrastructure map. It includes the channel control module. This module identifies if a node is within the communication range based on its movement and location. All the information is used at transmissions.

TraCI scenario manager is the module which connects the network simulator (OMNeT++) to a server running traffic simulations. TraCI scenario manager manages the simulation with the help of another model inside the vehicle model called TraCIMobility.
- **Designing the vehicle sample/model:** Using Veins examples the vehicles can facilitate TCP and UDP applications.
- **Launch configuration file:** It copies all the files which are needed for the mobility simulator (SUMO). These files include routes file, net file, and additional files. It has the “.xml” extension.
- **Initialization file:** All the simulation parameters which are needed for the simulation are included in the initialization file (omnetpp.ini). These are the network parameters, channel control modules and all the additional parameters.

3.3.3 Running the simulation

The traffic generator (SUMO) can be launched in two ways. The first is to launch it manually every time. The second way requires the Python interpreter in order to be able to use the Python script called sumo-launchd.py. It opens a port before the simulation starts. OMNeT++ MinGW command line should be run first in order to write the following command:

```
$/c/Users/user/src/omnetpp-4.5/bin/omnetpp/samples/sumo-launchd.py -vv -c /c/Users/user/src/sumo-0.22.0/sumo.exe
```

Next step is to start OMNeT++ IDE and right-click on **omnetpp.ini** and choose **Run As > OMNeT++ simulation**. This should start the simulation using both the network simulator (OMNeT++) and the mobility simulator (SUMO) running concurrently.

3.4 Analysis of RSU Coverage Area

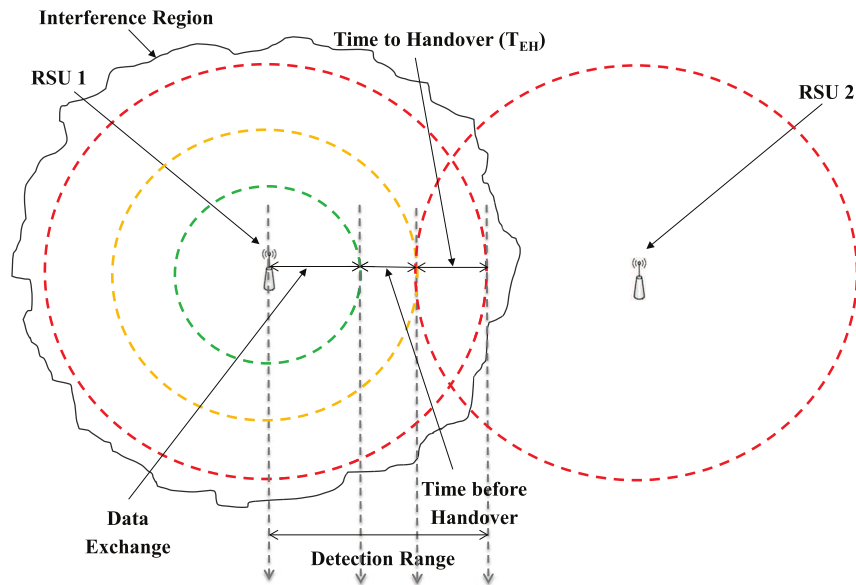


Fig. 3.2 Coverage Segmentation.

The Figure in 3.2 demonstrates diagrammatic representation of the Segmentation of the RSU's Coverage area:

- Detection range: is the region where both the vehicle's receiver sensitivity threshold and the SINR are met for the payload. Vehicles within this range of the transmitting RSU are able to decode packets.
- Data Exchange range: is the region where the actual data transmission takes place.
- Time before Handover: is the region where the OBU gets ready for handover.
- Time to Handover: is the region where the actual handover takes place.

The Figure in 3.3 shows the scenario represented in Figure 3.2, which is simulated below.

The handover procedures and messages exhibits:

- 1) *When the vehicle enters the detection range of RSU1 i.e. T1, it receives a beacon with a timing advertisement.*
- 2) *The vehicle then sends a Respond Beacon back to RSU1.*
- 3) *Consequently, the connection between RSU1 and vehicle is established and Data Exchange takes place.*

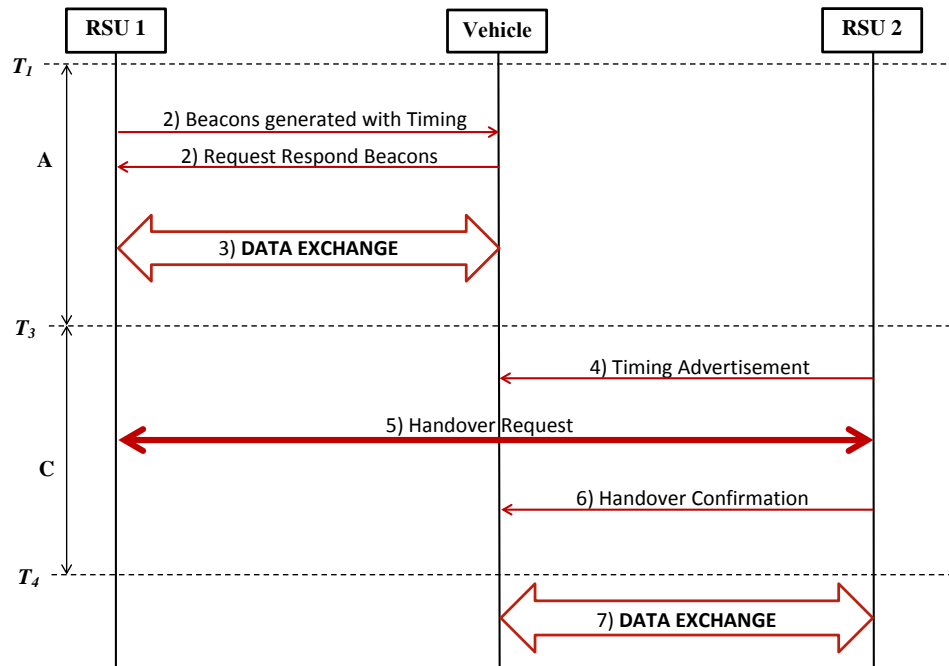


Fig. 3.3 Handover process and corresponding messages.

- 4) As the vehicle moves along, it receives timing advertisements from RSU2 after entering the Time to Handover region i.e. T_3 to T_4 .
- 5) Further into this region, the vehicle sends Handover request to both the RSUs.
- 6) Handover confirmation is sent from RSU2.
- 7) Finally Data Exchange starts with RSU2 as soon as the handover is finished.

3.4.1 Reception Power

The Reception power is the power at which vehicles will receive the beacons, but this is dependent on the power at which the signal is transmitted. With low transmission power, only the closest neighbor may receive the beacon, a more remote node might not. With high transmission power, a significant number of vehicles might receive the beacon, but the collision probability is also higher (Reinders et al., 2011) and more vehicles will receive interference. The goal of transmission power control is to increase spatial frequency reuse. The power control method must be fair: a higher transmission power of a sender should not be selected at the expense of preventing other vehicles to send/receive their beacons. In (Ganan et al., 2012) and (Reinders et al., 2011) adaptive solutions to transmission power control are explored in detail.

The minimum received Power is calculated in the OMNeT++ simulation module named Connection Manager (Andras Varga, 2014) i.e. it is the minimum power level at the vehicle to be able to physically receive a signal from the RSU is as shown below,

$$\text{minRecvPow} = 10^{\text{sat}/10} \quad (3.1)$$

Where,

sat → Minimum signal attenuation threshold and;

minRecvPow → Minimum power to be able to physical receive a signal.

3.4.2 Beaconsing & Beacon Generation Rate

Beaconsing can be used for reliability due to the lack of acknowledgements and reservation by means of RTS/CTS (Ganan et al., 2012). Beacon messages are generated and issued periodically. The generation rate, λ , is the rate at which beacons are sent to the MAC for transmission. Since they are used to create a Cooperative Awareness, λ should be in the order of several beacons per second to provide the system with accurate information about the close surroundings (Ganan et al., 2012), (Chung et al., 2011), (Reinders et al., 2011) and (Campolo et al., 2011b). Though some research efforts consider a fixed λ of 10Hz (Van Eenennaam et al., 2009), in (Ganan et al., 2012) the generation rate adaptation as a network layer mechanism is one of the instruments to make beaconsing more scalable. Increasing λ results in more beacons being sent and a higher temporal resolution. But this comes at the price of an increase in collision probability, especially in dense traffic. Hence, an adaptive beaconsing is preferable.

3.4.3 Detection Range Formula

Calculation of the detection range (Christoph Sommer, 2014) and (Andras Varga, 2014) based on transmitter power, wavelength, path loss coefficient and a threshold for minimal receives power for a communication to take place is shown below.

$$DR = ((\Lambda^2 \times pMax)/(16.0 \times \pi^2 \times \text{minRecvPow}))^{1/\alpha} \quad (3.2)$$

Where,

Λ → Wavelength = (speedOfLight/carrierFrequency)

pMax → Maximum Transmission Power Possible

Value = 16.0 → Constant (according to simulation based on lab test settings)

α → Minimum path loss coefficient

minRecvPow → Minimum power level to be able to physically receive a signal.

3.5 Why Network Dwell Time (NDT)?

NDT is the time a vehicle spends in a RSU's network range. NDT in a wireless network is given by the reciprocal of the mobility leave rate. In the literature (Shaikh et al., 2007), the mobility leave rate is given by

$$\mu_{ml} = E_{vel} \times P / (\pi \times A) \quad (3.3)$$

Where,

$E_{vel} = \frac{V_{max}}{2}$ → Expected Velocity of the vehicle

P → Perimeter of the cell, in this case = $2 \times \pi \times r$

A → Area of the cell, in this case = $2 \times \pi \times r^2$

r → Radius,

$$NDT = 1/\mu_{ml} = (\pi \times R_H) / V_{max} \quad (3.4)$$

Where, μ_{ml} → Mobility leave rate from equation (3.3)

R_H → Handover radius

V_{max} → Maximum velocity of the vehicle

In motor way context, the distance between two travelling points can be directly calculated. Hence NDT is given as shown below

$$NDT = NDD / E_{vel} \quad (3.5)$$

Where, NDD is Network Dwell Distance travelled along a motorway that is in coverage of a given network (Mapp et al., 2012). The exact distance between two points on a motorway can be calculated using GPS.

$$ET = NDT - T_{EH} \quad (3.6)$$

Where,

T_{EH} → Time taken to Handover to the next network.

For VANETs we assume that the RSU is alongside the road hence NDD is approximately equal to 2R where R is the radius of coverage.

3.6 Simulation Scenario, Results and Discussions

For the simulation experiments, the discrete event simulation environment OM-NeT++ (Andras Varga, 2014) is used in conjunction with the Veins framework (Christoph Sommer, 2014). This is a mobility simulation framework for wireless and mobile networks. A beaconing model using IEEE 802.11p was implemented in the Veins framework by (Christoph Sommer, 2014). A scenario as similar to the Figure in 3.4 is created.

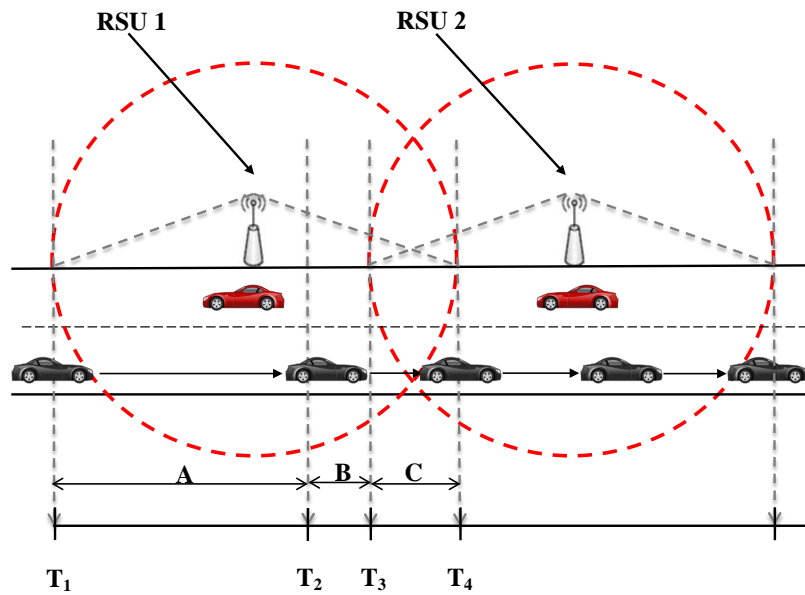


Fig. 3.4 Handover Procedures in Simulation Scenario.

The simulation parameters with which the experiments were carried out are shown in the Tables in 3.1 and 3.2.

Table 3.1 RSU Configuration Parameters.

Parameter	Values
Transmission Power	20mW
Bit rate	18Mbps
Sensitivity	-94.0dBm
Thermal Noise	-110.0dBm
Header Length	256 bits
Beacon Length	400 bits
Send Data	False

All the PHY and MAC properties used in the IEEE 802.11p simulation model conform to (IEEE-Std., 2010) and (IEEE-Std., 2005). Two RSUs are placed such

Table 3.2 OBU Configuration Parameters.

Parameter	Values
Speed	10, 20, 30, 40, 50 m/s, (36, 72, 108, 144, 180 Km/h)
Channel bandwidth	10MHz
OBU receiver sensitivity	-94.0dBm

that the detection range of both RSU overlaps with each other in order to have a soft handover. The nodes remain stationary during each simulation run. Another mobile node (i.e., vehicle) is made to run over the ranges of two RSUs for collecting various values for our study.

During simulation, the mobile node is run at different velocities and different beacon generation rates. Beacons are sent to the vehicle from RSU at the rate of λ , which is varied in the different simulation experiments. An overview of the different simulation parameter values used is shown in Tables 3.1 and 3.2. Note that these parameters contain the EDCA default values as highlighted in (Ganan et al., 2012). The experiment is carried out with one vehicle and with different velocities ranging from 10m/s to 50m/s. The remaining parameters are set according to the default values used by the Veins framework (Christoph Sommer, 2014). The beacon length was set to 656 bits. The data received in bits at the vehicle from RSU is shown in the graph in Figure 3.5 for different velocities of vehicle.

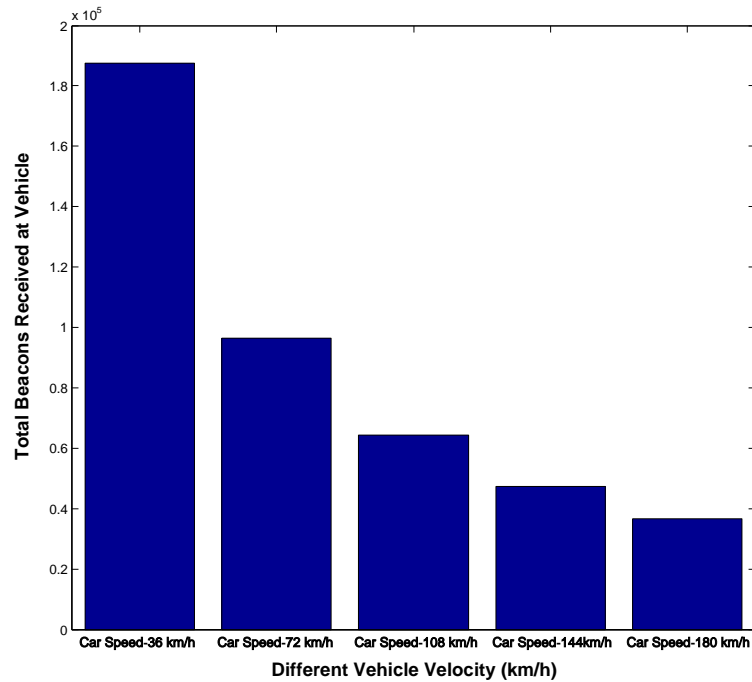


Fig. 3.5 Beacons Received at Vehicle.

The graph in Figure 3.5 clearly shows that the amount of beacons received for a fixed distance is reduced as the velocity of the vehicle increases. This is because the time spent in the data exchange region is significantly reduced at higher velocities. Hence more priority must be given to high velocity vehicles compared with low speed moving vehicles to achieve fairness.

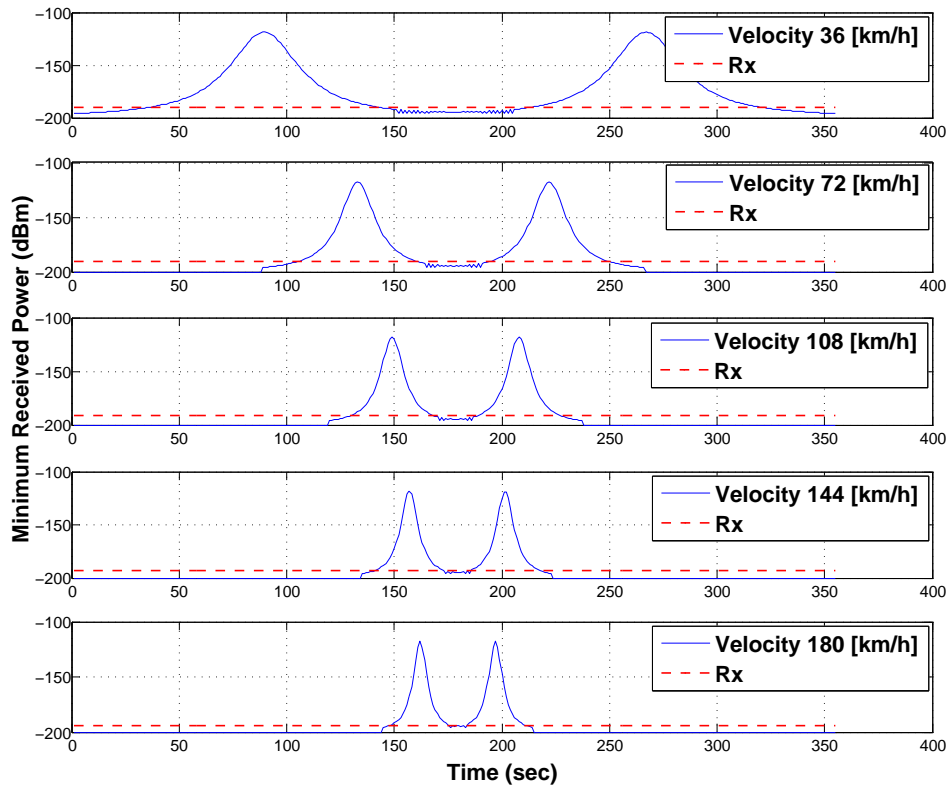


Fig. 3.6 Received Power at Vehicle.

The power received at the vehicle from the RSU is shown in the graph in Figure 3.6 for different velocities of the vehicle. While, the graph in Figure 3.7 shows the time spent in the overlapping region between the two RSUs, which is a much enhanced version of the graph presented in Figure 3.6, where the handover should take place. However, this is greatly reduced as the velocity increases.

Hence, the reception of packets is less. Thus a fast and an efficient handover is required in order to achieve an ubiquitous communication.

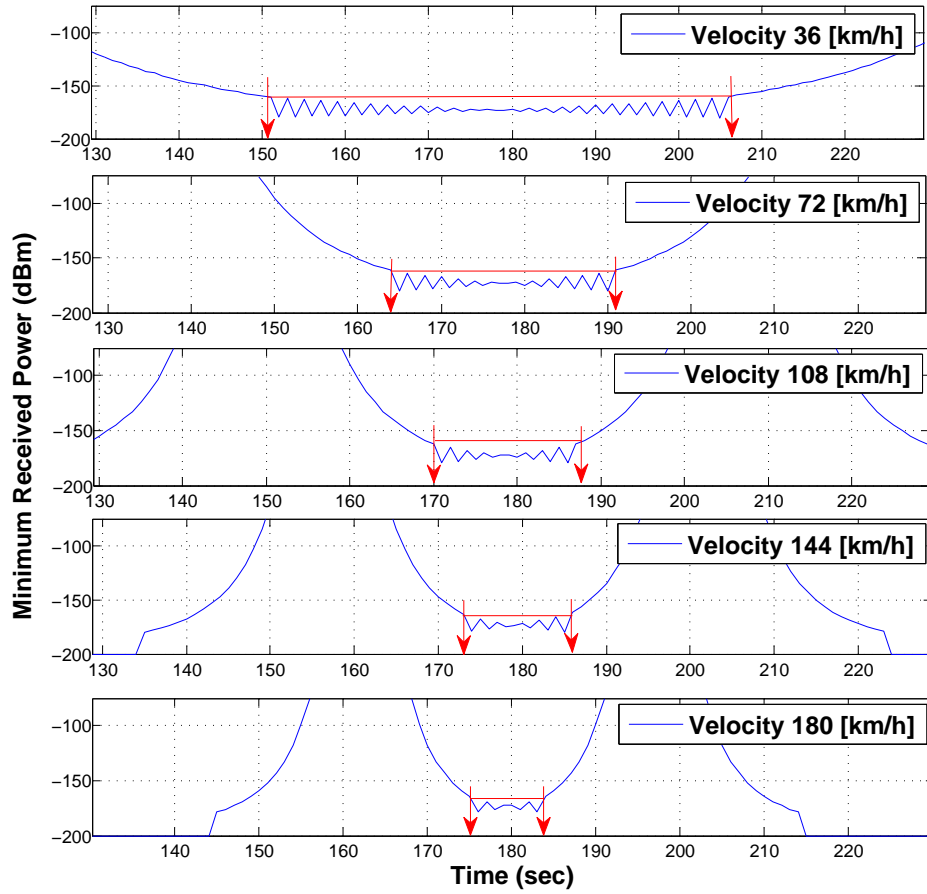


Fig. 3.7 Received Power at the Vehicle in the Overlapping Region.

3.6.1 Simulation Detection Range

Based on the simulation parameters, the detection range is calculated in the simulation. The outcome from the formula suggests 907.84 meters i.e. the radius (R) of the coverage. This confirms the radius using the original analysis for NDTi.

3.6.2 Analysis of Network Dwell Time (NDT)

In Intelligent Transport Systems, we assume that the RSUs are placed very close to the road infrastructure so that NDD is approximately equal to $2R$ (where R is the radius of coverage). So the NDT formula in equation in represents a way of calculating an upper bound on the value of NDT at different speeds.

Table 3.3 shows the NDT values from simulation experiments with different λ at the RSU and using the formula in equation 3.5 to calculate the upper bound. This upper bound does not consider any factors like contention, it assumes the medium or channel is ideal and that the only loss is due to propagation. A more accurate

Table 3.3 Comparison of Network Dwell Time from Simulation vs. Theoretical Calculation.

Speed	NDTi	NDTr				
		$\lambda=1\text{Hz}$	$\lambda=5\text{Hz}$	$\lambda=10\text{Hz}$	$\lambda=20\text{Hz}$	$\lambda=40\text{Hz}$
0-108 km/h	60s	54s	55s	57s	57s	57s
144 km/h	45s	37s	39s	43s	43s	43s
180 km/h	36s	30s	31s	34s	34s	34s

analytical calculation of NDT is dependent on the exact position of the RSU with respect to the road infrastructure as shown in (Mapp et al., 2012). However, we know that any simulation results should not exceed the upper bound for a given speed.

The NDT in simulation is calculated by measuring the time between the first reception of packet in a coverage area when a mobile node moves in and the last packet received in that coverage area, i.e. (T_4-T_1).

The NDT increases as the λ increases i.e. reaching closer to the upper bound value. But increasing λ beyond 10 Hz clearly shows that there is no increase in NDT and simulation results show that there is an increase in packet loss. Therefore, for handover management it is good to only consider λ from 1 to 10. This finding is different from other papers that have considered much higher values of beacon frequencies.

3.6.3 Analysis of Exit Time (ET)

The table in 3.4 shows the Time to Handover (T_{EH}) and the Exit Time (ET) values from simulation. The results show that increasing the beacon frequency results in a reduced handover time which in turn increases the Exit time including the Data Exchange region.

Table 3.4 Exit Time from Simulation.

Speed	T_{EH} (Simulation)			ET (Simulation)		
	$\lambda=1\text{Hz}$	$\lambda=5\text{Hz}$	$\lambda=10\text{Hz}$	$\lambda=1\text{Hz}$	$\lambda=5\text{Hz}$	$\lambda=10\text{Hz}$
0-108 km/h	6.98s	2.19s	1.89s	47.01s	52.80s	55.10s
144 km/h	5.98s	1.99s	0.89s	31.01s	37.00s	42.10s
180 km/h	3.98s	0.99s	0.69s	26.01s	30.00s	33.03s

However, the way T_{EH} is calculated from the simulation is that the two RSU's were moved close enough in order to receive a fair amount of beacons at the moving vehicle in the overlapping region from both the RSU's simultaneously. In order to have a reliable communication between both the RSUs, it was made sure that

at least a minimum average of five beacons were successfully received from the second RSU in order to handover. Therefore, it is this time in seconds which is the T_{EH} (please refer to Figure 3.2), the time taken to handover which has been illustrated in table 3.4.

3.6.4 Minimum Overlapping distance for a soft handover

The simulation experiments were conducted for three different beacon generation rates at RSU and with different velocities of the vehicle. Here the two RSU's were moved closer from a far distance until a fair amount of beacons are received by the moving vehicle in the overlapping region from both the RSU's simultaneously which will ensure a soft handover.

Table 3.5 Overlapping Distance ($\lambda=1\text{Hz}$).

Speed	Min. Overlapping Needed	Data Recieved	Total Packets Recieved	Total Packets Lost
0-108 km/h	415m	64944 bits	99	22
144 km/h	445m	50512 bits	77	13
180 km/h	525m	38048 bits	58	15

Table 3.6 Overlapping Distance ($\lambda=5\text{Hz}$).

Speed	Min. Overlapping Needed	Data Recieved	Total Packets Recieved	Total Packets Lost
0-108 km/h	215m	329968 bits	503	102
144 km/h	285m	251904 bits	384	69
180 km/h	315m	200736 bits	306	58

Table 3.7 Overlapping Distance ($\lambda=10\text{Hz}$).

Speed	Min. Overlapping Needed	Data Recieved	Total Packets Recieved	Total Packets Lost
0-108 km/h	136m	662560 bits	1010	200
144 km/h	186m	497248 bits	758	147
180 km/h	206m	398848 bits	608	117

The above tables (i.e. Tables 3.5, 3.6 and 3.7) show the result of the simulation experiments with beacon generation rates of 1Hz, 5 Hz and 10 Hz. It is clearly evident that when the beacon generation rate is increased then the overlapping distance needed for soft handover is decreased.

3.7 Summary

In this Chapter, a preliminary investigation into communication mechanisms in VANETs was carried out to determine the parameters that need to be considered in order to achieve a seamless communication. The results, however, highlight the need to consider these factors in order to achieve ubiquitous connectivity requires a proactive approach which takes into account the nature of the wireless communications such as the location of the Roadside Units (RSUs), the velocity the vehicle as well as operational issues such as the beaconing frequency.

It is therefore, necessary to look at how these factors interact with each other and to develop good analytical models to help in the implementation of intelligent mechanisms that would ensure ubiquitous communication. This is discussed in the next Chapter of this work.

Chapter 4

Detailed Investigation of the Communication Mechanisms in VANET Systems

4.1 Introduction

In the previous Chapter, we investigated the issues involved in providing ubiquitous connectivity in VANET systems. We concluded that the velocity of the vehicle and the effects of beaconing played a major role in the communication between the vehicle and the RSU. In this Chapter, these findings are further explored. Firstly, we break down this communication into several distinct interactions in the PHY and MAC layers of the network stack. Secondly, the probability of successful handover is used to explain how communication is achieved within these regions. Finally, we introduce the concept of cumulative probability to take into account the effects of beacon frequency on communication dynamics.

4.2 Further Analysis of Coverage Range

4.2.1 Calculation of Successful Packet Reception in Simulation

In Figure 4.1, T_1 and T_2 is the time when the first packet at PHY and MAC layer are received respectively. Between T_3 and T_4 is the region where the packet is always successfully received i.e., where Probability (P) of successful packet reception is '1'. T_5 and T_6 is the time when the last packet at MAC and PHY layer are received. All the packets between $T_1 - T_2$ and $T_5 - T_6$ are lost due to bit errors. Figure 4.1

also shows that the reliable communication starts only when the packet reaches the MAC layer. The reason and the way the packets are dropped by the simulation in the PHY layer is explained below.

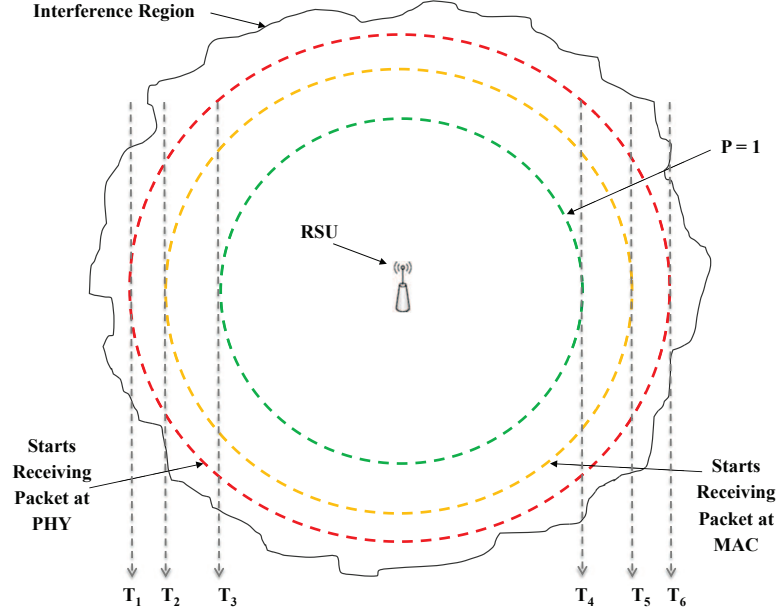


Fig. 4.1 PHY and MAC Segmentation.

In the simulation, T2 is the time where the actual communication starts and we know that we receive packet at T1 but these received packets are discarded due to bit errors, hence the question which has to be asked here is, can this time T2 be determined given that the vehicle receives the first packet in PHY layer at time T1? To analyse this effect, we further carefully investigate the calculation of the successful packet reception. Figure 4.1 shows that the communication starts only when the packet reaches the MAC layer.

The graph, shown in Figure 4.2, has been simulated in OMNeT++ using the Veins Framework. The graph shows the PacketOk and a randomly generated double number. This simulation was carried out with only one RSU and one vehicle moving at 30m/s as depicted in the scenario in Figure 4.1. Each beacon is of size 100 bytes with a beacon generation frequency of 1Hz, generated by the RSU. The PacketOk is calculated and defined as shown in equations 4.1 and 4.2:

$$PacketReceptionProbability = [1 - 1.5erfc(0.45\sqrt{SNR})]^L \quad (4.1)$$

where,

$$SNR(SignaltoNoiseRatio) = 10^{SNR_{dB}/10} \quad (4.2)$$

and

$L \rightarrow$ Length of the packet.

In Figure 4.2 the lower (red) line is the randomly generated double number and the upper (blue) line is the computed PacketOk. The PacketOk number below the randomly generated number curve is assumed as error and is dropped at the PHY layer. Packet Reception Probability Ratio in Veins for 18Mbps bit rate is calculated using the formula in 4.1 which has been modeled using (Fuxjager et al., 2010). For each beacon received at the PHY layer, a PacketOk number is computed which is a packet reception ratio. This number is computed based on Bit Error Rate (BER) and length of the beacon. This computed double number is then compared against a randomly generated double number ranging between 0 and 1. If the computed number is less than the randomly generated number then that respective beacon is dropped at the PHY layer, reason assumed that there is an error in the packet.

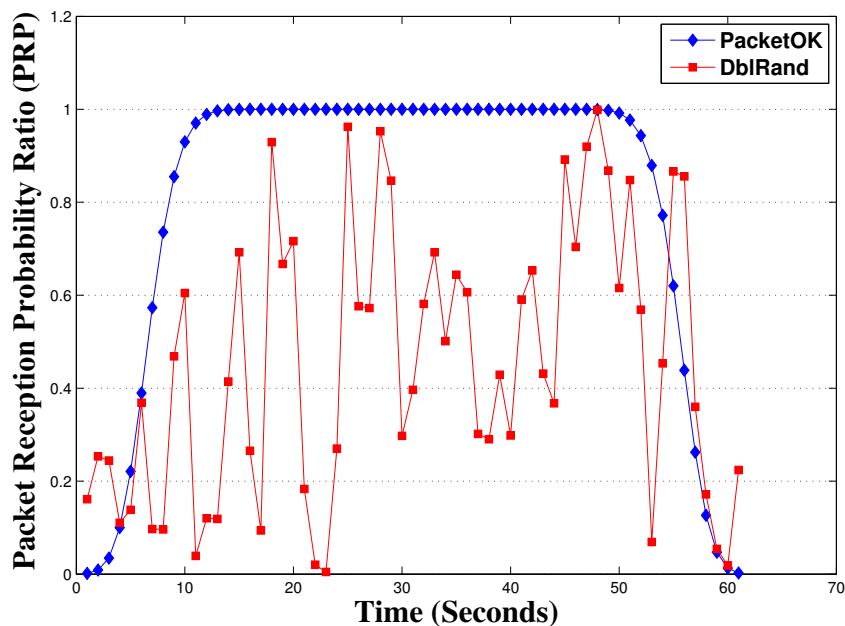


Fig. 4.2 PacketOK vs DbIRand.

In Figure 4.2, from the graph we can observe that as the vehicle is heading towards the RSU, the packet reception probability increases and reaches to a point until 1, which means there is no possibility of error in the packet. In other words, we can say that the region where the $P = 1$ is a very reliable communication region. This is the time T_3 to T_4 which has been shown in the Figure 4.1.

In Chapter 3, Network Dwell Time (NDT) is defined as the time a vehicle spends in a RSU's network range. In this Chapter, we will now examine these concepts in

more detail and the concepts of idealised NDT ($NDTi$) and measured NDT, ($NDTr$) are introduced.

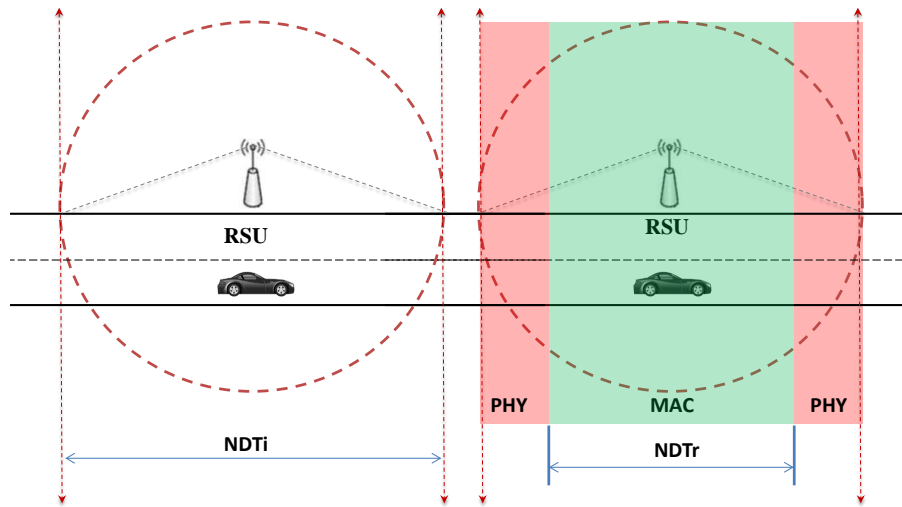


Fig. 4.3 $NDTi$ vs $NDTr$.

With ideal NDT denoted as ($NDTi$), it is assumed that the communication starts as soon as the vehicle hits the edge of the coverage of a communication range. However, in real time the measured definition of NDT, which is denoted by $NDTr$, can be defined as the time between the first and the last beacon reaching the MAC layer without being dropped in the PHY layer due to bit error as shown in Figure 4.3.

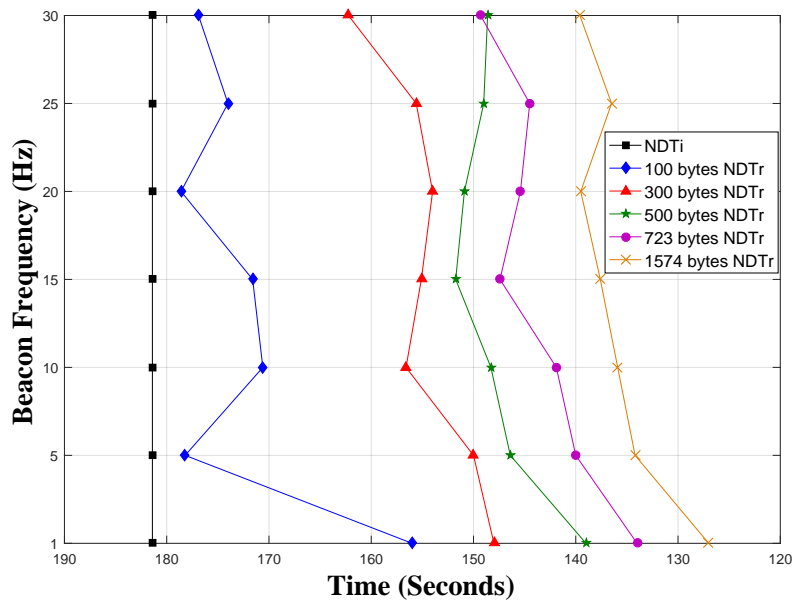


Fig. 4.4 $NDTr$ with different Beacon Sizes (10m/s).

The graph in Figure 4.4 shows the NDT_r for different size of beacon broadcasted to the vehicle moving at a constant speed (10m/s) with different λ . Figure 4.5 shows the same but with different speed (30 m/s). The NDT_i is also plotted in this graph. It shows that as the size of the beacon increases the NDT_r is reduced i.e. the communication time is reduced. NDT also reduces (comparing Figures 4.4 & 4.5) as the velocity of the vehicle increases.

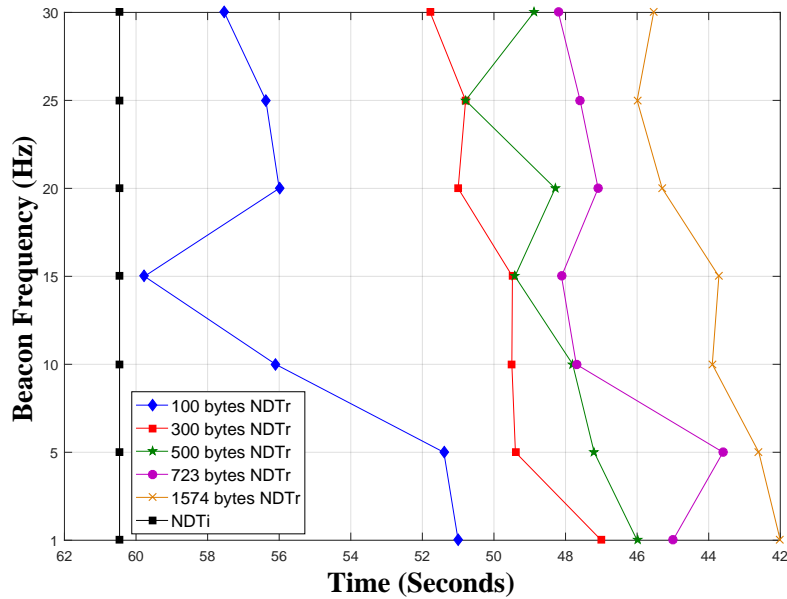


Fig. 4.5 NDT_r with different Beacon Sizes (30m/s).

This clearly shows that the size of the packet is an important factor in determining the NDT_r. The graphs also illustrate that there is no peak increase in NDT_r after 10Hz and it is also evident that some beacons are being dropped which causes this difference between NDT_r and NDT_i. The reason and the way the beacons are dropped by the simulation in the PHY layer is explained in the next section.

4.2.2 Further Investigation into PHY layer in relation to Beacon size

Hence for further investigation, simulation was carried out but this time monitoring the beacons received at the lower layer (i.e., PHY). We considered different beacon sizes for the simulation experiments. This is due to the fact that each beacon in

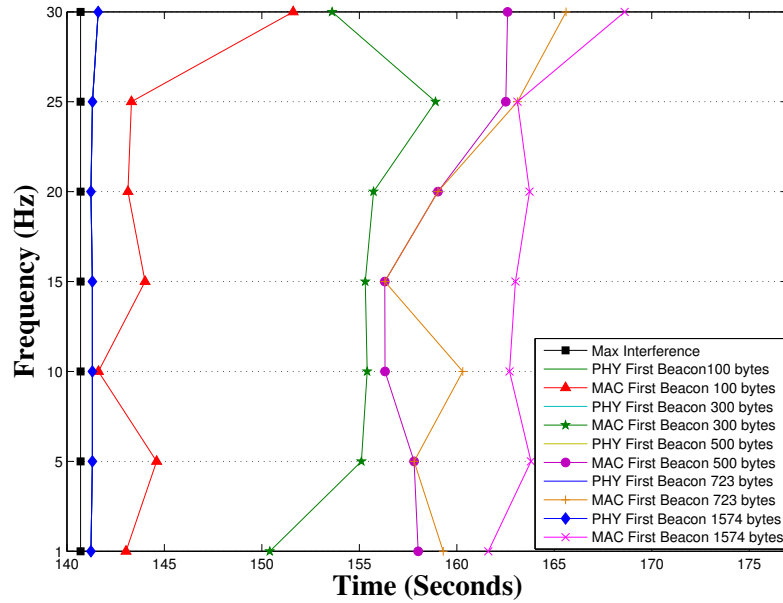


Fig. 4.6 Entry Side of Coverage Area (10m/s).

general contains the PHY and MAC parameters, however, it may also contain some additional information based on the message type and the application. Hence, this may vary in length. Therefore, in this thesis we considered a wide range of beacon sizes (in bytes) in order to achieve a complete understanding of different beacon lengths for imitating different message types used in different applications. The graphs in Figures 4.6 and 4.7 show the first beacon reception at both PHY and MAC layers against simulation time during the entry by the vehicle in the coverage region.

The simulation was carried out for different sizes of beacon with different beacon frequencies with two different velocities of the vehicle. It also shows the actual interference range or detection range calculated in the Veins framework comparing with actual time the beacon was received. This clearly showed that the vehicle starts receiving the beacon at the PHY layer as soon as it enters the detection range. This detection range is the place where the minimum criteria for the communication to happen are met. The time delay between the PHY layer first beacon and the MAC layer first beacon is due to the loss of those beacons i.e. those

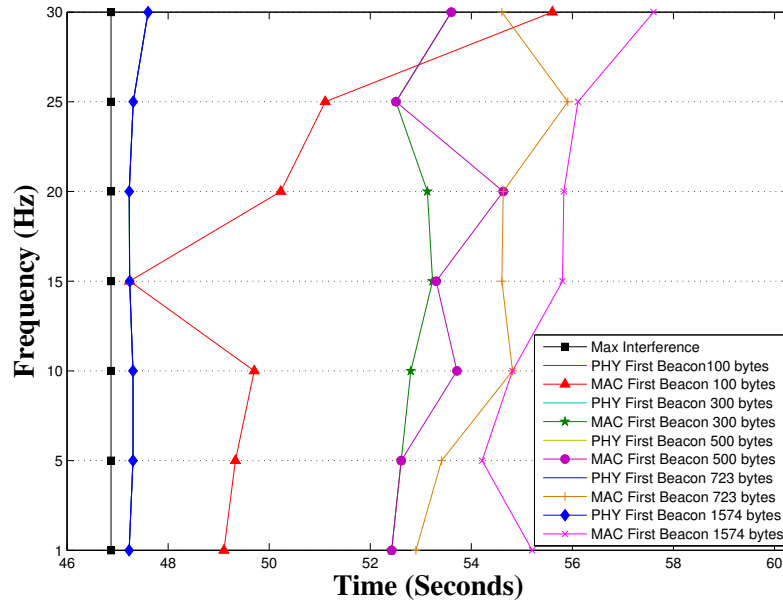


Fig. 4.7 Entry Side of Coverage Area (30m/s).

beacons are received by the PHY layer but with errors in the beacon and hence dropped at the PHY layers as depicted in Figure 4.8.

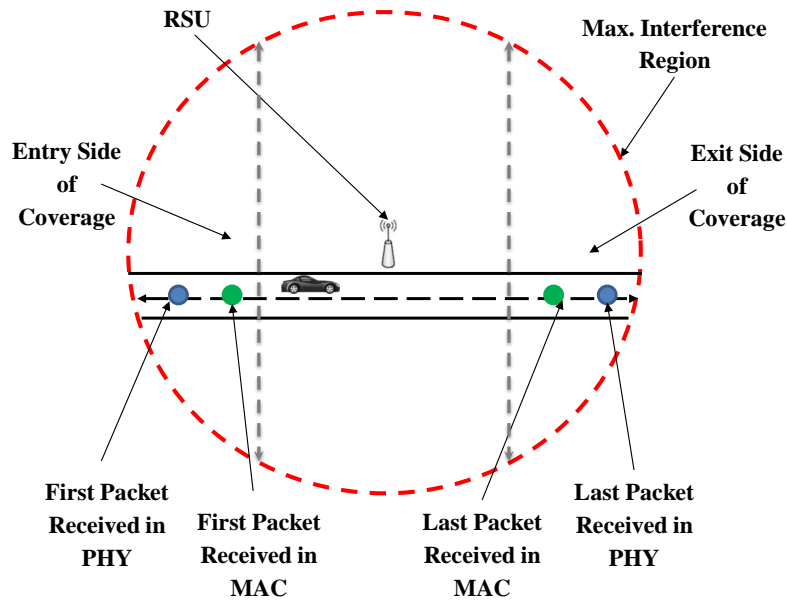


Fig. 4.8 First & Last Beacon received at PHY & MAC layers.

We can also see that when there is an increase in size of the beacon there is a delay in reception of the beacon at MAC layer i.e., more beacons are lost due to

error at the PHY layer. When comparing the graphs in Figures 4.6 and 4.7 with the graphs in Figures 4.4 and 4.5 respectively, we can conclude that the increase in size of beacon will push the NDT down.

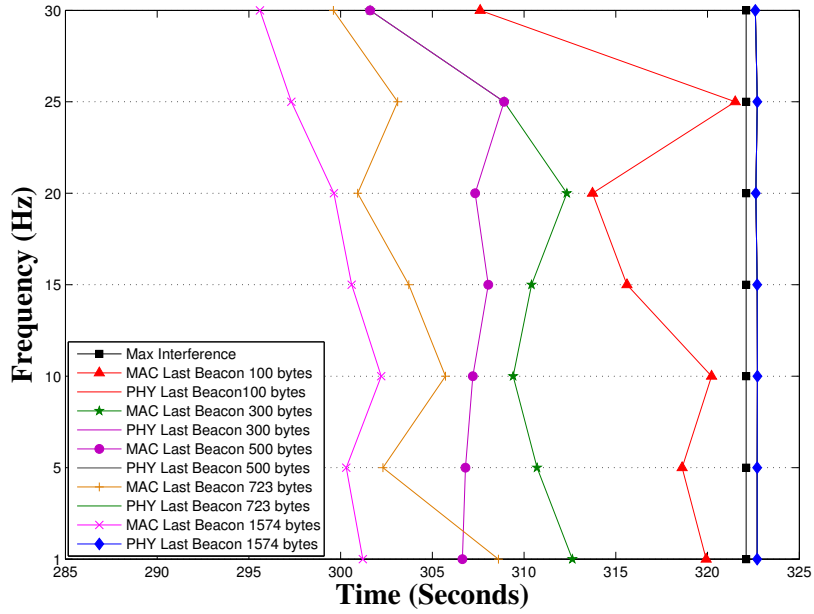


Fig. 4.9 Exit Side of Coverage Area (10m/s).

Figures 4.9 and 4.10 show the last beacon reception at both PHY and MAC layers against simulation time during the Exit by the vehicle from the coverage region.

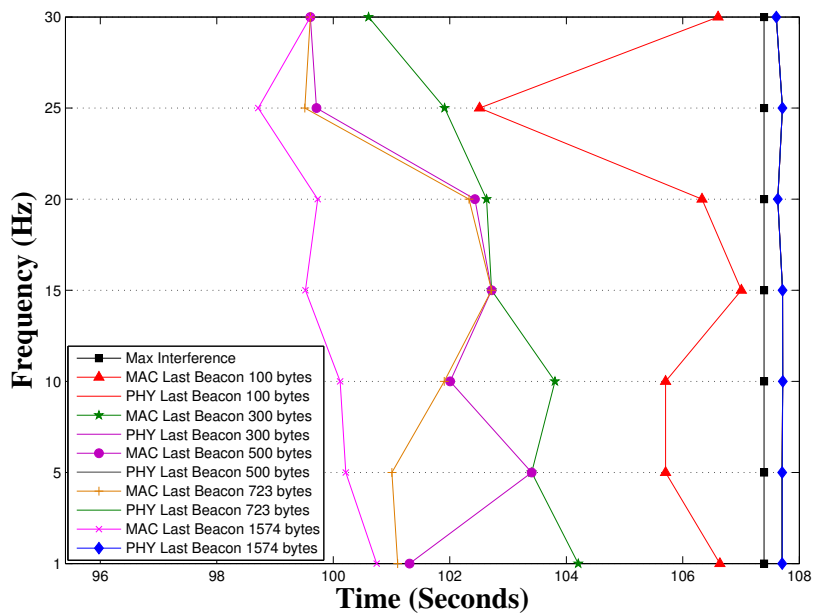


Fig. 4.10 Exit Side of Coverage Area (30m/s).

4.3 Summary

In this Chapter, a more in-depth analysis was conducted by investigating the effects of beacon size and beacon frequency as well as the velocity of the vehicle in order to achieve seamless handover. This was done by further exploration of the estimated Network Dwell Time for different beacon sizes, frequency and velocity of the vehicle. The PacketOK formula appears to directly take into account only the size of the beacon but the results from this chapter show that the frequency of the beacon and the velocity of the vehicle does also need to be taken into account.

In order to look at how the frequency of beaconing affects overall communication, it is necessary to consider a cumulative probability approach, rather than just individual probabilities. This is challenging because the probability of a successful reception increases as the vehicle get closer to the RSU and hence this is a non-stationary scenario. This is explored fully in the next Chapter.

Chapter 5

Exploring Cumulative Probability to understand Communication Dynamics in VANETs

5.1 Introduction

In the previous Chapter, it was established that a cumulative approach needs to be considered in order to take into account the frequency of beaconing. This is explored in detail in this Chapter. The results show that a more probabilistic approach to handover using cumulative probabilities would give better understanding of how seamless handover can be achieved in highly mobile environments such as VANETs.

5.2 Overview of Cumulative Probability Approach

In order to investigate the effect of beacon frequency we also need to look at the cumulative probability of a successful packet reception, in addition to calculating the probability of a successful packet reception for an individual packet at a given time 't'. Since we know the single packet reception probability using equation (5.1) from the simulation, the cumulative probability can be calculated.

Therefore, if P is the probability of receiving one successful beacon and $(1-P)$ is the probability of not successfully receiving a beacon then the cumulative

probability for a sequence of N receptions is given by:

$$P + (1 - P)P + (1 - P)^2P + \dots + (1 - P)^{N-1}P \quad (5.1)$$

In probability theory P is constant and cumulative probability (CP) tends to 1 as N tends to infinity. In this case it means that successful reception of the beacon is guaranteed once the CP reaches 1. But in this scenario because the vehicle is moving towards the RSU, P increases for every sequence. Therefore for N receptions the CP is:

$$CP = P_1 + (1 - P_1)P_2 + (1 - P_1)(1 - P_2)P_3 + \dots \quad (5.2)$$

Where, P_N is greater than P_{N-1}

Since P is increasing because the vehicle is moving towards the RSU, hence the cumulative probability reaches 1 long before infinity and therefore affects the successful reception of the beacon. This analysis applies to when the vehicle enters the network.

For Exit times we consider the probability of not receiving the packet $P_n = 1 - P$ from the RSU as we drive away i.e., the negative cumulative probability. If P is the probability of successful reception the negative cumulative probability (CP_n) is given by:

$$CP_n = (1 - P_1) + P_1(1 - P_2) + P_1.P_2(1 - P_3) + \dots \quad (5.3)$$

For the Exit scenario P the probability of the successful reception decreases as we move away from the RSU, hence 1-P is increasing. Once the vehicle does not hear the beacon after the period T, the inverse of the beacon frequency, it immediately hands over to the next RSU. Our results considers the effect of the cumulative probability on entrance and exit region of RSU coverage.

5.2.1 The Effect of Beacon Frequency on Cumulative Probability

To understand the effect of frequency in determining the NDT, the cumulative probability (CP) of the packet reception rate reaching 1 (i.e., vehicle moving towards RSU) has been calculated for different frequencies and different sizes of beacon for the entry region. The cumulative probability (CP) of this entry region for two different velocities (10 m/s and 30 m/s) of vehicle is as shown in Figures 5.1 and 5.2 respectively.

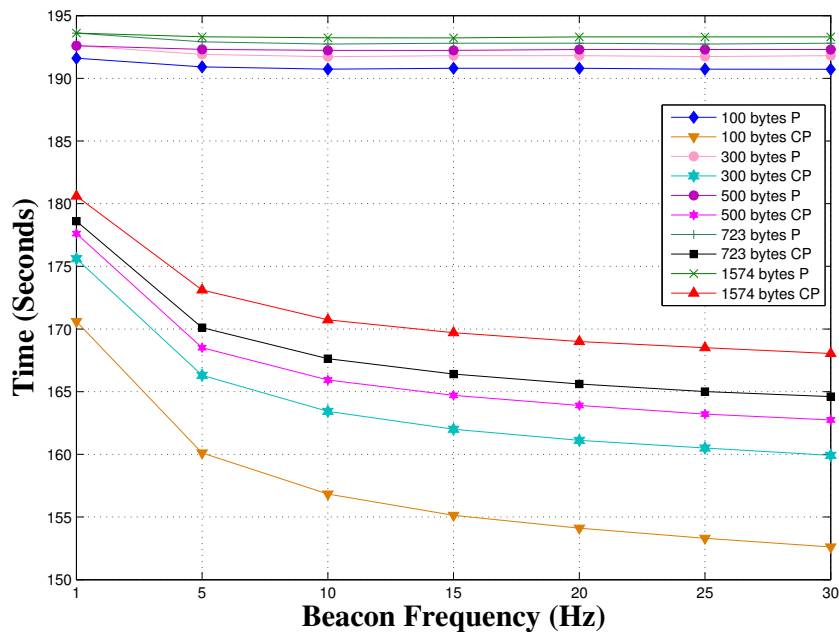


Fig. 5.1 CP reaching 1 (Entry Region - 10m/s).

The result presented as graphs in Figures 5.1 and 5.2 show that the cumulative probability reaches 1 long before the probability of an individual successful beacon reception and therefore this parameter better explains the relationship between beacon frequency and successful reception and not the individual probability.

The graphs in 5.3 and 5.4 show that as the frequency increases the cumulative probability (CP) is reaching 1 much before the actual probability. Here after 10Hz to 15Hz there is not much decrease in the time. This shows the impact of the frequency on the NDT. The first result shows that the cumulative probability reaches 1 long before the probability of an individual successful reception and therefore it is the parameter that explains the relationship between beacon frequency and successful reception and not the individual probability.

The negative cumulative probability is the cumulative probability of no longer hearing (i.e., Vehicle driving away from RSU) the beacon as the vehicle exits the

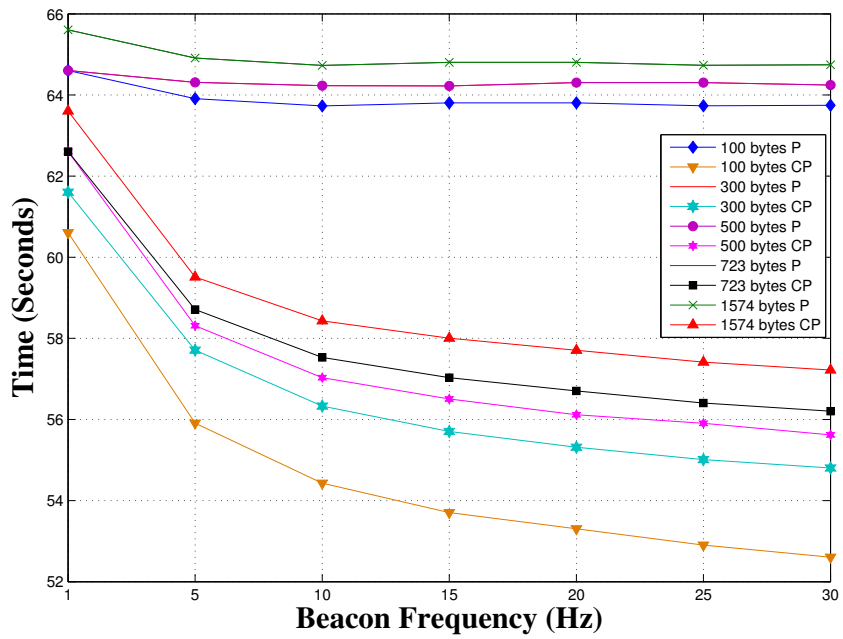


Fig. 5.2 CP reaching 1 (Entry Region - 30m/s).

coverage area. It could be thought of as the opposite of the positive cumulative probability when the vehicle enters the area. So the negative cumulative probability is the cumulative probability of (1-P) where P is the probability of successful packet reception. The graphs in Figures 5.3 and 5.4 shows the negative cumulative probability and single packet reception probability for two velocities of vehicle.

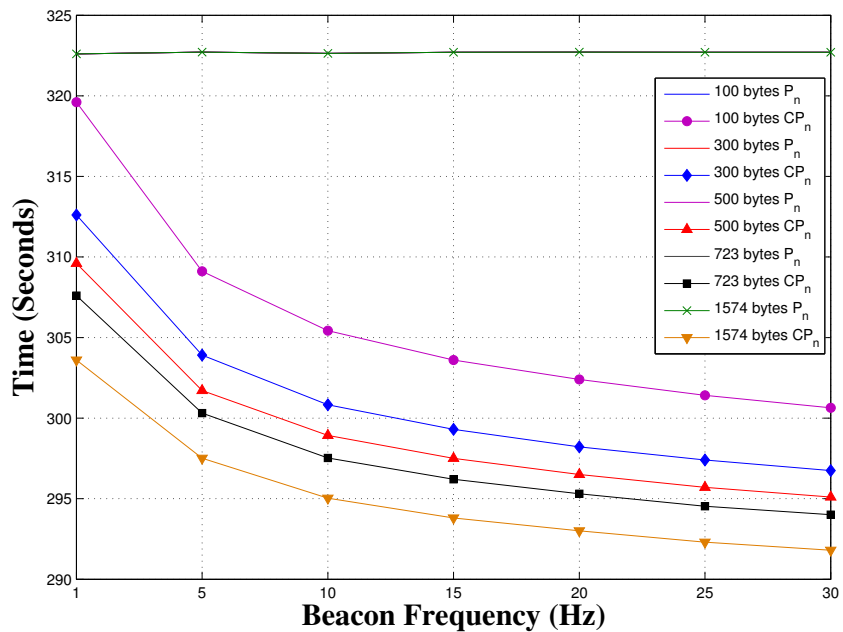


Fig. 5.3 CP_n reaching 0 (Exit Region - 10m/s).

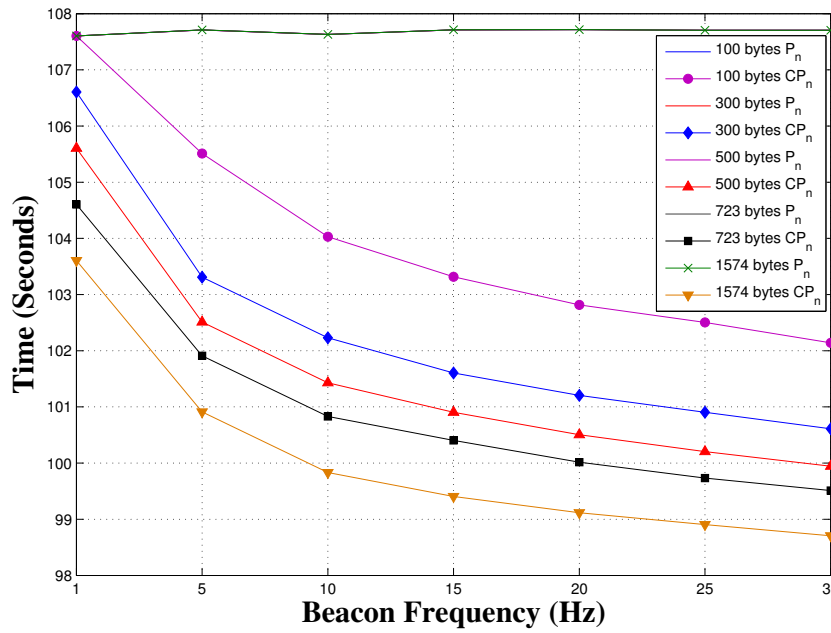


Fig. 5.4 CP_n reaching 0 (Exit Region - 30m/s).

The exit graphs shown in Figure 5.3 and 5.4 also depict exit times for different frequencies and different sizes so they clearly show that the size of the packet affects the exit times due to fact that the probability of error and hence not hearing the packet increases with packet size and so the larger the packet size, the lower the exit times.

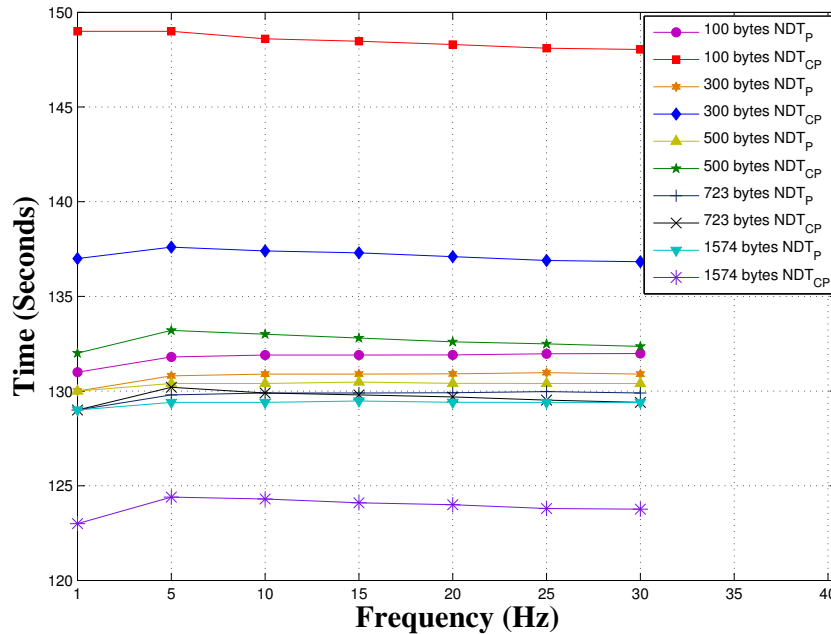


Fig. 5.5 NDT of Probability vs NDT of Cumulative Probability (10m/s).

To obtain the NDT from our model, we subtract the exit times from the entry times of CP reaching 1 and this NDT is called as Cumulative Probability NDT (NDT_{CP}) (i.e., NDT derived from CP). This means that NDT is being calculated based on the cumulative and single packet reception probabilities (NDT_P) with the above results and depicted as a graphs in Figures 5.5 and 5.6.

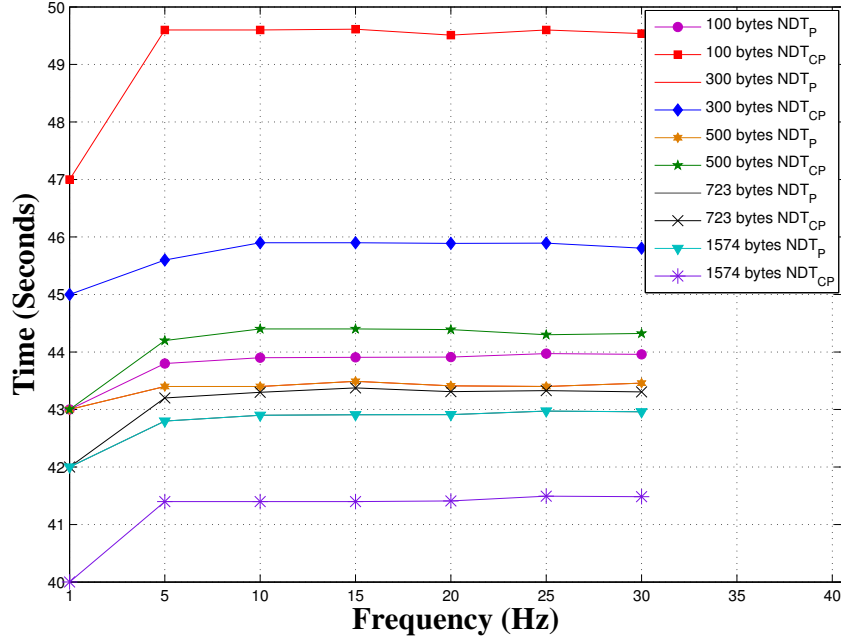


Fig. 5.6 NDT of Probability vs NDT of Cumulative Probability (30m/s).

The graphs in Figures 5.7 and 5.8 show NDT_r , NDT_i , NDT_P and NDT_{CP} for two different sizes of beacon. It is clear that these values are affected by the sizes of beacon. For relatively small beacon sizes, the difference between NDT_{CP} and NDT_P is greater but for larger beacon sizes, the trend seems to be much smaller. For beacon sizes around 723 bytes the NDT_{CP} and NDT_P are almost equal. This indicates that for handover where predictability is important, maximum beacon sizes around 600 – 800 bytes (approx.) could give best chance for seamless communication.

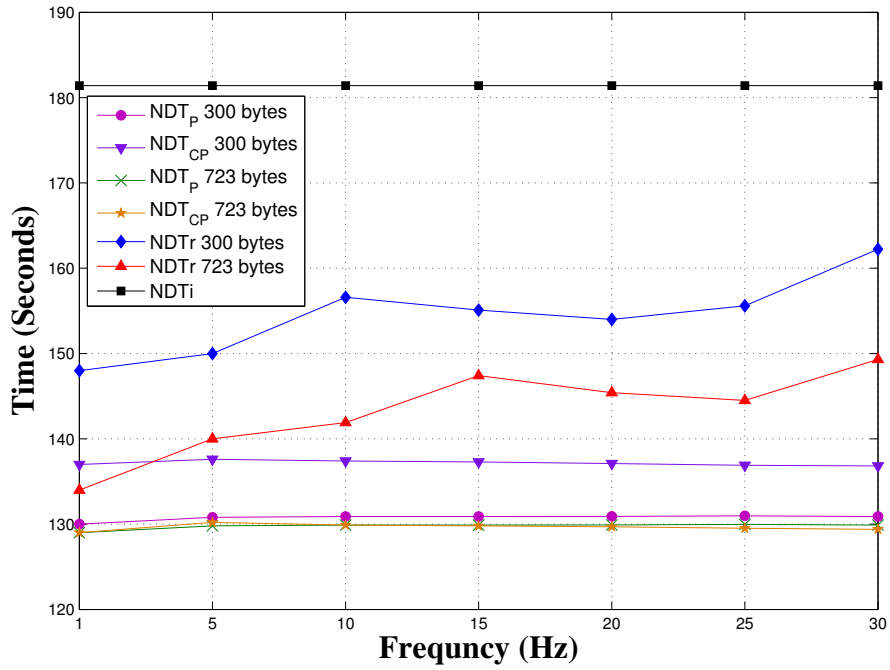


Fig. 5.7 Comparison of P NDT vs CP NDT vs NDTTr vs NDTi (10m/s).

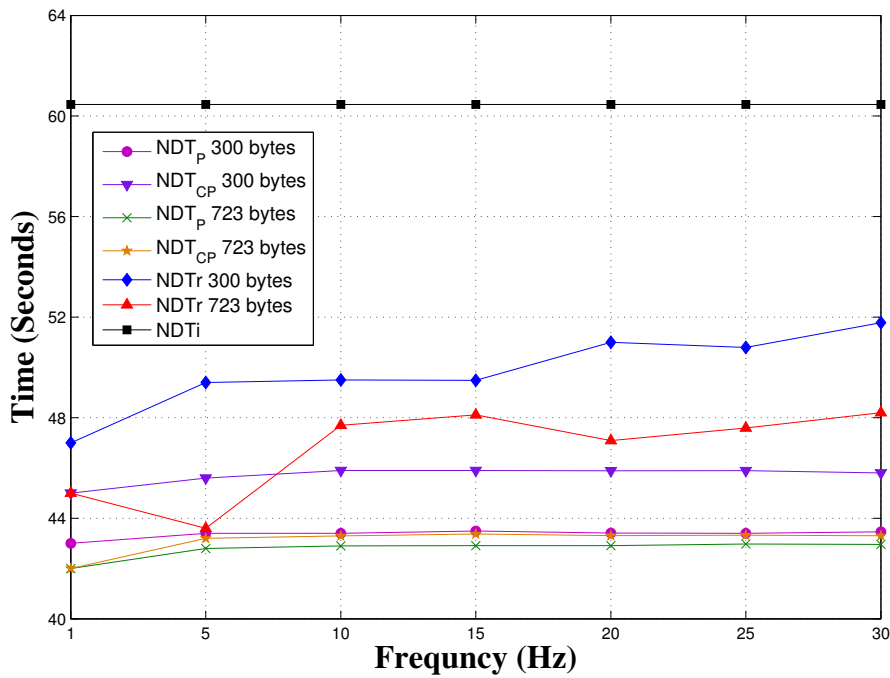


Fig. 5.8 Comparison of P NDT vs CP NDT vs NDTTr vs NDTi (30m/s).

5.2.2 The Change in Probability of Successful Beacon Reception (ΔP)

5.2.2.1 The Change (ΔP) at Entry

For the Entry Region the rate of change in P i.e. Probability of successful beacon reception is shown in the equation (5.4).

$$\Delta P_{ENTRY} = P_N - P_{N-1} \quad (5.4)$$

ΔP is significant because the SNR changes more rapidly with the increased velocity of the vehicle. Hence, ΔP increases significantly as the velocity of the vehicle increases. Where, P_N is the probability of packet reception of an individual packet 'N' and 'N-1' is the previous packet. ΔP is calculated until P reaches 1.

5.2.2.2 The Change (ΔP) at Exit

For the Exit Region the rate of change in P is as shown in the equation (5.5).

$$\Delta P_{EXIT} = P_N - P_{N+1} \quad (5.5)$$

Where, P_N is the probability of packet reception of an individual packet 'N' and 'N+1' is the next packet. ΔP is calculated until P reaches 0.

The change in probability of successful beacon reception, i.e. ΔP vs SNR (dB), for beacon sizes 300 bytes and 723 bytes is illustrated as a graph in Figure 5.9. The graph is generated using the equation (5.6) which do not take into account the velocity of vehicle. We know that ΔP for second packet (i.e, N+1) with respect to first packet (i.e, N) can be calculated as,

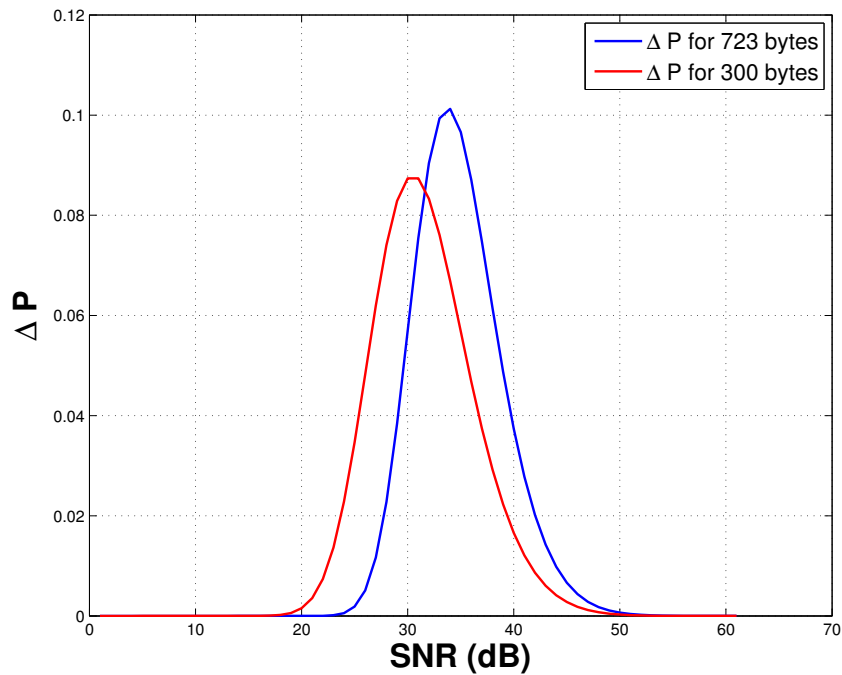
$$\Rightarrow \Delta P = P_2 - P_1$$

We know the formula for P i.e.

Hence,

$$\Delta P = [1 - 1.5erfc(0.45\sqrt{SNR_2})]^L - [1 - 1.5erfc(0.45\sqrt{SNR_1})]^L \quad (5.6)$$

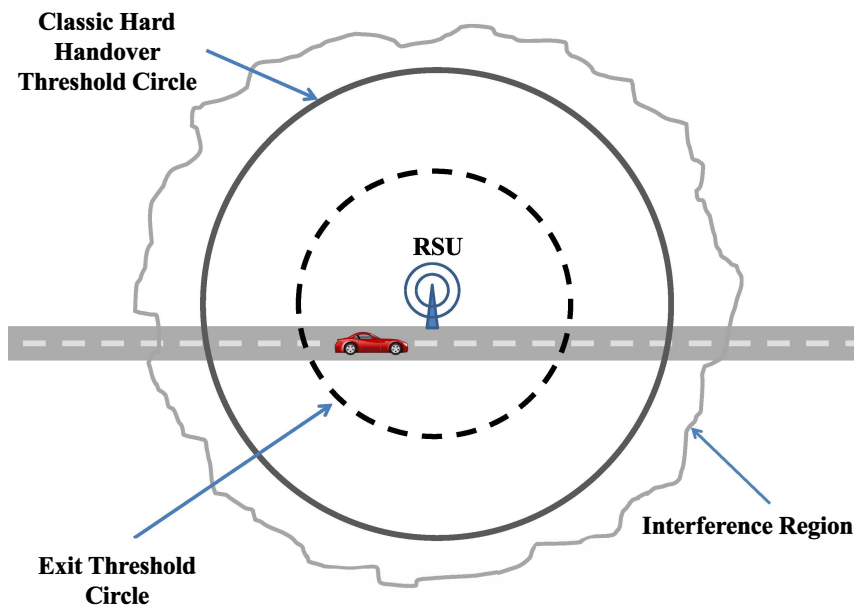
The simulation experiments were conducted to analyze the change in P with respect to different velocities and different beacon frequencies.

Fig. 5.9 ΔP vs SNR.

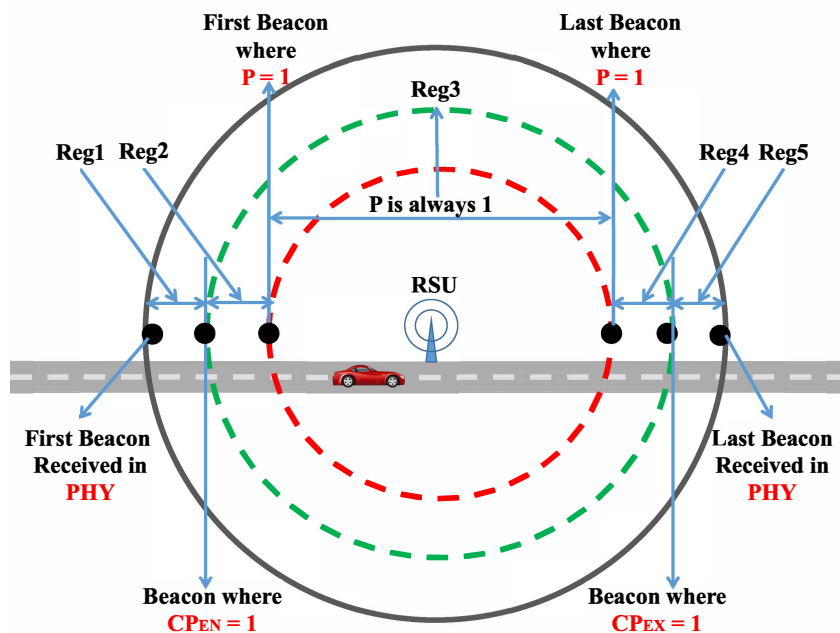
The results highlighted in graphs from Figures 5.1 through to 5.8 show the effects of the size of the beacon, the velocity of the vehicle as well as the beacon frequency. Therefore, if a formula is being modeled based on these results then for a given velocity of the vehicle, for a given beacon size and for a given beacon frequency; the rate of change of P can be calculated using the modeled formula in equation (5.6). With this rate of change being known the P and CP at any given point can be calculated, which can be used to predict the $NDTr$ more accurately. Hence, this approach will allow us to further explore how it can be used to achieve a better handover policy.

5.3 Handover Policy Based on Cumulative Probability Approach

Handover in mobile environments such as VANETs can be depicted as shown in Figure 5.10 (a). There is a hard handover threshold circle depicted by hard barrier and there is a dotted circle within the hard barrier representing the exit threshold. The exit threshold circle is the boundary to start the handover in order to finish the handover before reaching the hard barrier, which is needed for a successful soft handover. If the handover is not successful before the hard barrier then there is a break in the communication which leads to a hard handover. Though this



(a)



(b)

Fig. 5.10 Traditional and Probabilistic Segmentation.

approach is currently being used for mobile communications, in highly mobile environments such as VANETs, it presents two challenges: firstly, the exit radius is dependent on the velocity of the MN and hence at high velocities there will be no time to do a soft handover. Secondly, the hard or fixed handover circle represents the area of coverage but at this outer region, actual communication is difficult due

to the probability of packets been received with error due to low Signal to Noise (SNR) ratio. Hence a more probabilistic approach is required which makes use of Cumulative Probability to provide a realistic boundary for handover (Ghosh et al., 2015).

Let the probability (P) represent the probability of a successful reception of beacon at the Physical (PHY) layer. This probability can be calculated for each beacon with the knowledge of the SNR and the length of the beacon (Sjöberg et al., 2010), (Fuxjager et al., 2010). In probability theory, P has a stationary distribution i.e., the possible outcomes are constant over time. Hence, we can define the Cumulative Probability as the probability of the event occurring - in this case, a successful beacon reception - before a given time or sequence number. In addition, when CP is 1, then we are sure that the event has occurred. If P is constant, then CP is normally 1 at infinity. In this case however, P does not have a stationary distribution because as the MN moves towards the RSU, P increases significantly and hence, CP will become 1 long before infinity and, in fact, may become 1 before P becomes 1. Hence this shows that we can be certain of receiving a successful transmission before P becomes 1 due to CP . This means that it is necessary to use the CP approach to determine the regions of reliable communication. Therefore, we need to calculate CP for a sequence of N beacon receptions and compare it to when P is 1.

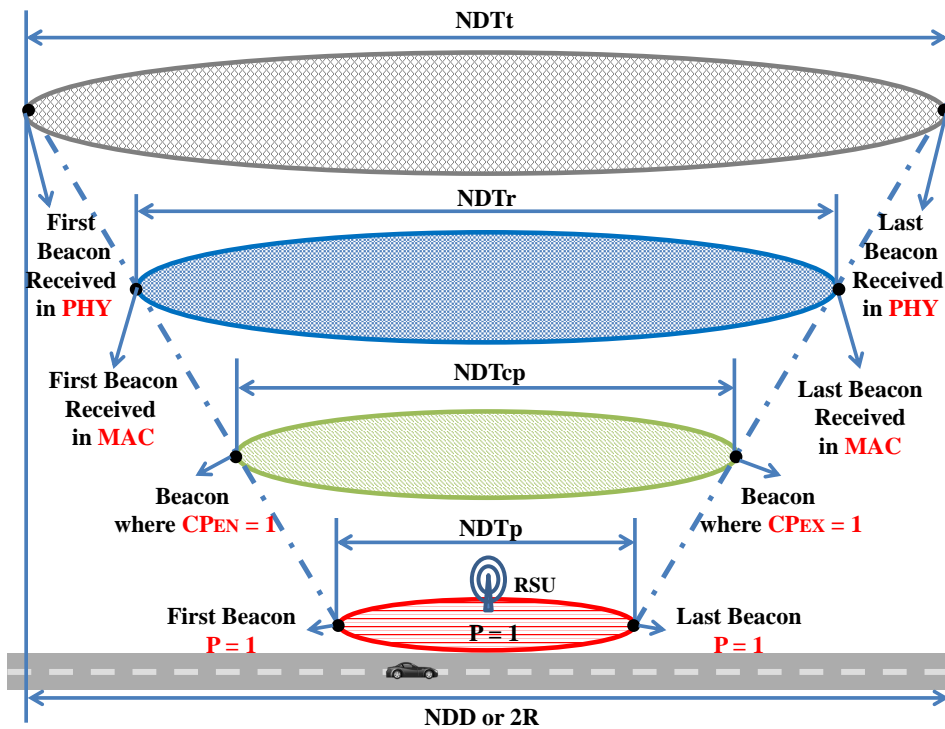


Fig. 5.11 NDT - From Concept to Reality

We define, the CP as the vehicle enters a new network as the Cumulative Entrance Probability (CP_{EN}). For Exit scenarios, we consider the probability of not receiving the beacon P_n from the RSU as we drive away i.e., the Exit Cumulative Probability, (CP_{EX}). For the Exit side, P the probability of the successful reception decreases as we move away from the RSU, hence $1-P$ is increasing. Our results therefore consider the effect of the cumulative frequencies on entrance and exit regions of RSU coverage.

To obtain the Network Dwell Times from our model, we subtract the exit times from the entry times to obtain the values for NDT_{CP} . This means that NDT_{CP} and NDT_P are being calculated based on the cumulative and single beacon reception probability respectively with the approach described above. Figure 5.11 represents a conical view of NDT_r , NDT_t , the single beacon probability NDT_P and the cumulative probability NDT NDT_{CP} in order to understand the difference.

NDT_P shown in Figure 5.11, is the time when the vehicle travels in a coverage receives the beacon with Probability (P) = 1 where the communication is highly reliable.

Table 5.1 presents the communication time between the segments or regions named as Reg_1 , Reg_2 , Reg_3 , Reg_4 and Reg_5 as shown in Figure 5.10 (b). These regions are the communication times i.e., the time duration when beacons are received by the vehicle in a particular segment of RSU coverage.

Table 5.1 Communication Time in Seconds between the Segments.

S.No	Beacon Size (bytes)	Beacon Frequency (Hz)	Reg_1 (seconds)	Reg_2 (seconds)	Reg_3 (seconds)	Reg_4 (seconds)	Reg_5 (seconds)
10 m/s							
1	300	10	41.8	8.9	80.5	46.1	4.6
2	300	15	38.46	12.73	81.26	43.73	7.4
3	300	20	35.85	14.75	80.5	41.5	9.1
4	500	10	43.3	7.9	79.5	43.2	8.0
5	500	15	40.13	11.53	80.33	41	10.6
6	500	20	37.6	13.5	79.5	38.95	12.15
7	723	10	44.2	7.5	78.5	41.4	10.3
8	723	15	41.26	10.93	79.26	39.4	12.73
9	723	20	38.75	12.85	78.5	37.45	14.15
30 m/s							
10	300	10	17.1	0.0	26.5	17.1	0.0
11	300	15	16.46	0.86	26.73	17.26	0.0
12	300	20	15.3	1.8	26.5	16.55	0.55
13	500	10	17.1	0.0	26.5	17.1	0.0
14	500	15	16.83	0.46	26.73	16.13	1.2
15	500	20	15.7	1.4	26.5	15.3	1.8
16	723	10	17.1	0.0	26.5	16.1	1.1
17	723	15	17.13	0.2	26.73	15.26	2.06
18	723	20	16	1.1	26.5	14.5	2.6

- Reg_1 : Is the region between the first beacon being heard in the PHY layer and the point when $CP_{EN}=1$.
- Reg_2 : Is the region between $CP_{EN}=1$ and the point where P is first equal to 1.
- Reg_3 : Is the region where P is always equal to 1.
- Reg_4 : Is the region between the last beacon where $P = 1$ and $CP_{EX}=1$
- Reg_5 : Is the region between $CP_{EX}=1$ and the last beacon being heard at the PHY layer for that RSU.

Another important observation which is perceived from the Probabilistic Segmentation as shown in Figure 5.10 (b) and from table 5.1, is that the CP on exit and entry regions (i.e. Reg_1 = "Entry Region for the vehicle" and Reg_5 = "Exit Region for the vehicle") are not symmetrical. Hence, once we have different values of P, it will be asymmetric. In addition, the key factor in the Probabilistic Segmentation is that at any given time the P and (1-P) are not equal and the CP reaches 1 before P. However, this is even more significant with increased velocity of the vehicle, therefore, CP has a positive effect at the entry region as the vehicles enter the coverage area and a negative effect at the exit region as the vehicle leaves the coverage area, hence the different times observed particularly in regions Reg_1 and Reg_5 unlike in regions Reg_2 and Reg_4 .

In order to explore these concepts, a simulation was carried out with one RSU and one vehicle moving along the road using Veins Framework in OMNeT++. The Framework supports IEEE 802.11p and the coverage radius of the RSU was 907m with 20mW transmission power and the minimum receiver gain was set to -94 dBm (Sommer et al., 2011). For the simulation two different velocities were considered, 10 m/s (i.e., 36km/h) for urban speed and 30 m/s (i.e., 108km/h) for motorway speed. The results in (Ghosh et al., 2014b) also showed that for handover, a maximum beacon size between approximately 600 to 800 bytes as shown in Table 5.1 could give the best chance for seamless communication. Hence, beacon sizes of 300, 500 and 723 bytes have been considered to conduct our study.

In addition to this, the work in (Ghosh et al., 2014b) also showed that an ideal range of beacon frequency for vehicular communication is between 10 to 20 Hz. Hence beacon frequencies of 10, 15 and 20 Hz are considered in this article. When there is an increase in beacon frequency, a considerable amount of communication time is achieved between $CP_{EN} = 1$ and $P = 1$ (i.e. Reg_2) and between $CP_{EX} = 1$ and $P = 0$ (i.e. Reg_5). This clearly indicates that a high beacon frequency should

result in an increased NDT as the beacon is heard almost as soon the vehicle enters the coverage area.

5.4 Analysis of Overlapping Region

In order to verify our handover policy based on the CP approach, we have come up with three different scenarios of overlapping two RSUs as shown in Figure 5.12. A mobile node (i.e. in our case a vehicle) is made to travel over the coverage range of these two RSUs with velocities of 10 m/s and 30 m/s for collecting various values for our study. The same parameter settings were used as done for the one RSU simulation experiment setup for calculating CP.

Case (i) The two RSUs are overlapped such that RSU 1's last beacon received by the vehicle with $P = 1$ and RSU 2's first beacon with $P = 1$ are received one after another. The time difference between these two beacons is very small and hence the Figure 5.12 shows these two beacons at the same point.

Case (ii) The two RSUs are overlapped such that RSU 1's last beacon with $P = 1$ and RSU 2's first beacon reaching $CP_{EN} = 1$ are received one after another.

Case (iii) The two RSUs are overlapped such that RSU 1's beacon reaching $CP_{EX} = 1$ and RSU 2's beacon reaching $CP_{EN} = 1$ are received one after another.

Since the transmission power of the RSU is set 20 mW, the maximum interference distance according to Veins framework is 907.843 m (Andras Varga, 2014) and (Ghosh et al., 2014b). Hence all the mathematical calculations in this work has considered 907 m as the radius of the coverage. During simulation, the RSU broadcasts the beacon with different beacon generation rates and with different beacon sizes as considered in Table 5.1.

The simulation results for each case are illustrated as graphs in Figure 5.12. In Case (i) as mentioned earlier the overlapping of two RSUs are setup such that P is 1 for both RSUs at the overlapping region. Hence it is clearly evident from the graph that once the vehicle reaches the region where $P = 1$ of RSU 1, there is no drop in P till the vehicle exits the RSU2's $P = 1$ region, i.e. P is always 1 as shown in Figure 5.12. From this observation it is clear that, this is the most reliable way of overlapping adjacent RSUs which ensures seamless handover. But this reliability comes at the cost of more overlapping distance as shown in the graph in Figure 5.12 and high interference issues as indicated in (Ganan et al., 2012) as both RSUs are in communication range of each other.

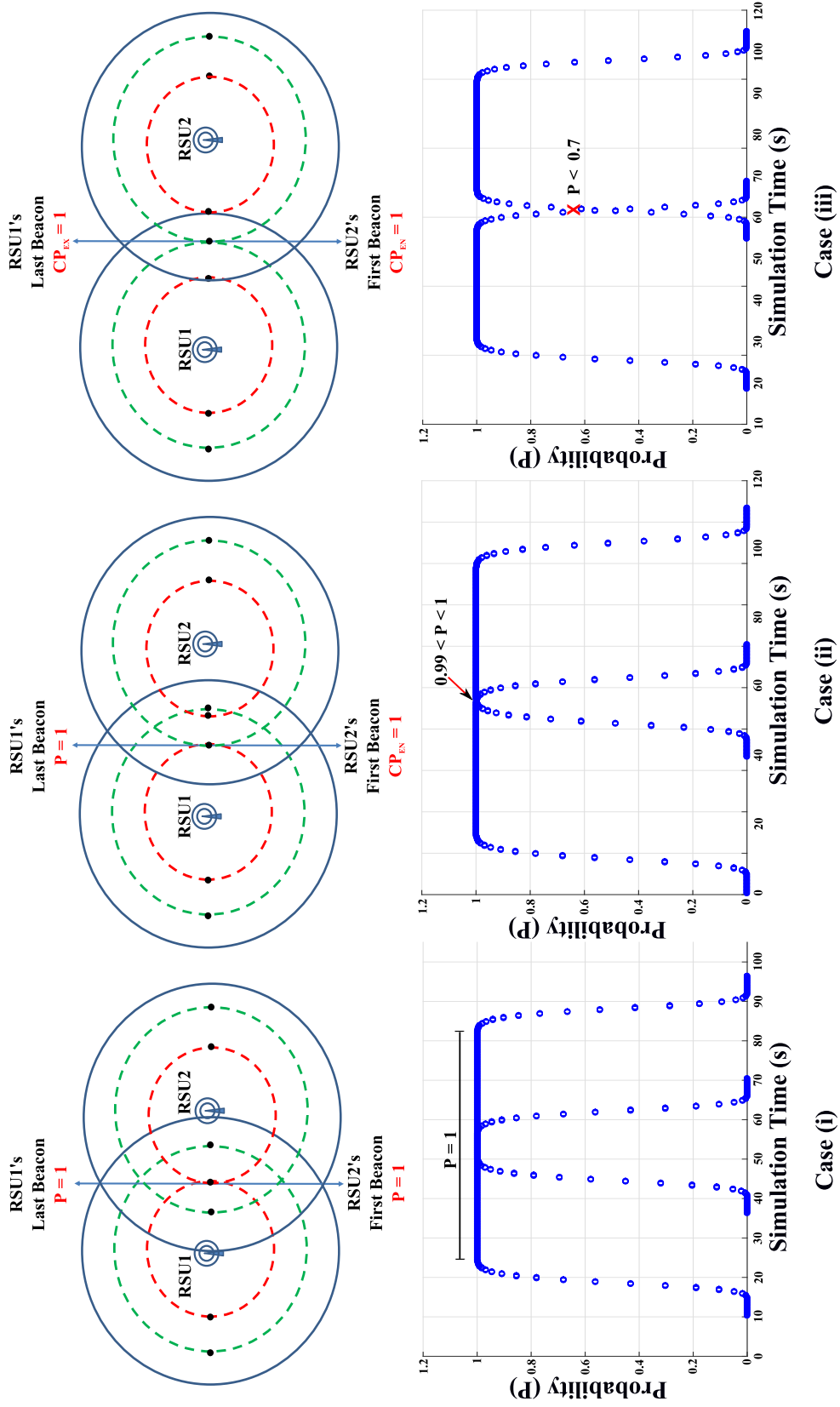


Fig. 5.12 Overlapping Scenarios

In Case (ii) as the RSUs are setup such that of RSU 1's last beacon with $P = 1$ and CP_{EN} of RSU2 is 1 at the overlapping region. This way of overlapping yields us less overlapping distance as shown in Figure 5.13 compared to case (i), however there is a very negligible amount of drop in P at the overlapping region i.e., $0.99 < P < 1$, Figure 5.12. According to (Vinel et al., 2009a) P should be greater than 0.99 for the safety related applications. Hence, case (ii) is equally reliable and also ensures seamless handover.

In Case (iii), the RSUs are setup considering CP_{EX} of RSU 1 and CP_{EN} of RSU2 for overlapping. This way of overlapping gives an advantage of a much smaller overlapping distance as compared to cases (i) and (ii). This also benefits the network with less interference as indicated in (Ganan et al., 2012). In the overlapping region, P reduces to less than 0.7 which is not suitable for seamless communication or safety critical applications.

As shown above case (ii) performs equally good as case (i), therefore this approach can be adopted for a scenario where critical life-safety application are given higher priority. By contrast, the Case (iii) approach is more suitable for a scenario where optimal coverage is required and where non-safety applications are used.

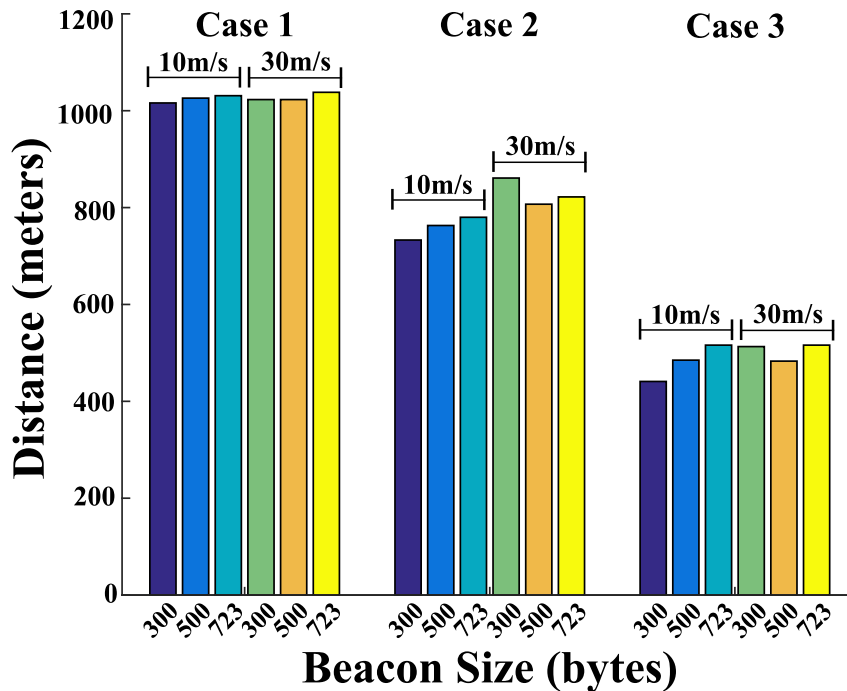


Fig. 5.13 Overlapping Distance.

In addition, the CP approach can be used to improve handover since $CP_{EN} = 1$ tells us when we are certain to have received at least one beacon from the new

RSU. Hence, we should ensure that handover can occur before $CP_{EN} = 1$. Similarly, $CP_{EX} = 1$ indicates when we are sure not to have heard a beacon from the current RSU and hence, we need to ensure that the MN should have been handed over to the next RSU before this point. It is therefore no longer necessary to manage handover using the hard handover circle as this probabilistic approach based on CP should yield more reliable results. Therefore, the CP approach should be incorporated into the handover mechanism for MNs.

5.5 Summary

In this Chapter, we investigated the impact of beaconing on Network Dwell Time using Cumulative probability and individual successful beacon reception. The results demonstrated that the size of the beacon directly affects the individual packet reception probability (i.e., the value of P changes), especially the probability distribution of the first packet P1 and hence it affects both single reception probability as well as the cumulative reception probability. However, our results also show that the frequency of the beacon only affects the cumulative probability and hence it verifies our argument that they affect different aspects of the probability space of with regard to the Network Dwell Time. Furthermore, we have shown how these results can be used to develop a probabilistic proactive handover approach based on cumulative effects of beaconing.

In the next Chapter, we will look at developing of approximate models for Communications in VANET Systems with respect to length of the beacon and velocity of the vehicle. This will then complete our investigation of communications in VANET systems at the network level which we have shown is dependant on the frequency of the beacon, the length of the beacon and the velocity of the vehicle.

Chapter 6

Development of an Approximate Model of Communications in VANET Systems

6.1 Introduction

From the previous Chapter, we showed how the dynamics of cumulative approach is needed to explore beaconing by taking into account the frequency and how the results suggested that a more probabilistic approach using cumulative probabilities to handover would give better understanding of how seamless handover can be achieved in highly mobile environments such as VANETs. In this Chapter, we focus on re-examining the calculations for Delta P (ΔP) equation. We then use key parameters of this analysis and apply them to the vehicular environment by comparing theoretical and measured values from simulation. An investigation is then performed to explain the differences obtained. This leads to a new model of the handover process based on cumulative probability, which is explored using an analytical model showing how communication changes as the vehicle approaches a new RSU. An approximate model is then developed to examine these issues further. These results clearly show the effects of length of the beacon, velocity of the vehicle and frequency of the beacon. This Chapter, further evaluates, that if at any given point velocity of the vehicle, the beacon length and the frequency are known then a formula can be modelled based on the results; also the rate of change of P can be calculated using the modelled formula. Further, with this rate of change being known the P and CP at any point can be calculated, which in turn can be used to predict the NDTr more accurately. In this Chapter, we investigate an approximate model, first by looking into the effects of how the

length of the beacon affects the individual beacon reception probability. In addition, we also highlight how the velocity of the vehicle affects the difference between the individual probability P and cumulative probability CP as the velocity increases. Finally, this Chapter summarises the need to develop a prototype VANET Testbed to test the simulation and analytical models and compels for a probabilistic approach based on accurate real-time values resulting from propagation models used in the Testbed.

6.2 The Essence of Signal-to-Noise Ratio (SNR) on ΔP with respect to Cumulative Probability

The simulation experiments in chapter 3 were conducted to analyse the change in P with respect to different velocities and different beacon frequencies. These results clearly show the effect of size of beacon, velocity of vehicle and frequency of beacon. If a formula is being modelled based on these results then for a given velocity of the vehicle, for a given beacon size and frequency; the rate of change of P can be calculated using the modelled formula. With this rate of change being known the P and CP at any point can be calculated, which in turn can be used to predict the NDT_r more accurately.

Differentiation of P (Equation 6.20) with respect to SNR (i.e., $\frac{dP}{dSNR}$) will yield us the ΔP for any given SNR which can be used to find the CP and when to Handover based on the prediction.

6.2.1 Full Calculations for: $\frac{dP}{dSNR}$

$$\begin{aligned} PacketReceptionProbability(PRPP) &= [1 - 1.5erfc(0.45\sqrt{SNR})]^L \\ BER &= 1.5erfc(0.45\sqrt{SNR}) \end{aligned} \quad (6.1)$$

So for a beacon of L Bits

$$PRPP = [1 - BER]^L \quad (6.2)$$

The complementary error function, denoted erfc, is defined as

$$\begin{aligned} erfc(x) &= 1 - erf(x) \\ &= \frac{2}{\sqrt{\pi}} \int_0^x e^{-t^2} dt \\ &= e^{-x^2} erfcx(x) \end{aligned} \quad (6.3)$$

$$\begin{aligned}\frac{d}{dx} \times \operatorname{erfc}(x) &= \frac{-2e^{-x^2}}{\sqrt{\pi}} \\ \frac{d}{dx}(\operatorname{erfc}(x)) &= \frac{-2e^{-x^2}}{\sqrt{\pi}}\end{aligned}\tag{6.4}$$

Where,

$$x = 0.45\sqrt{SNR}\tag{6.5}$$

Hence,

$$\Rightarrow P = [1 - 1.5\operatorname{erfc}(x)]^L\tag{6.6}$$

Now, Let

$$\Rightarrow z = (1 - 1.5\operatorname{erfc}(x))\tag{6.7}$$

Therefore,

$$\Rightarrow P = Z^L\tag{6.8}$$

$$\frac{dP}{dx} = \frac{dP}{dz} \times \frac{dz}{dx}\tag{6.9}$$

$$\frac{dP}{dx} = Lz^{L-1} \times \frac{dz}{dx}\tag{6.10}$$

$$\frac{dz}{dx} = \frac{1.5 \times 2e^{-x^2}}{\sqrt{\pi}}\tag{6.11}$$

$$\frac{dz}{dx} = Lz^{L-1} \cdot \frac{3e^{-x^2}}{\sqrt{\pi}}\tag{6.12}$$

$$\Rightarrow \frac{dP}{dSNR} = \frac{dP}{dx} \times \frac{dx}{dSNR}\tag{6.13}$$

$$\frac{dx}{dSNR} = \frac{0.45\sqrt{SNR}}{dSNR} = \frac{0.45(SNR)^{\frac{1}{2}}}{dSNR} \quad (6.14)$$

$$= 0.45 \times \frac{1}{2}(SNR)^{-\frac{1}{2}} \quad (6.15)$$

Therefore,

$$\frac{dP}{dSNR} = Lz^{L-1} \times \frac{3e^{-(0.45\sqrt{SNR})^2}}{\sqrt{\pi}} \times 0.45\frac{1}{2}(SNR)^{-\frac{1}{2}} \quad (6.16)$$

$$= Lz^{L-1} \times \frac{3e^{-(0.45^2 SNR)}}{\sqrt{\pi}} \times 0.45\frac{1}{2}(SNR)^{-\frac{1}{2}} \quad (6.17)$$

$$\frac{dP}{dSNR} = L(1 - 1.5\text{erfc}(0.45\sqrt{SNR}))^{L-1} \times \frac{3e^{-(0.45^2 SNR)}}{\sqrt{\pi}} \times 0.45\frac{1}{2}(SNR)^{-\frac{1}{2}} \quad (6.18)$$

$$\Rightarrow \frac{dP}{dSNR} = \frac{3L}{\sqrt{\pi}}(1 - 1.5\text{erfc}(0.45\sqrt{SNR}))^{L-1} \times \frac{3e^{-(0.45^2 SNR)}}{\sqrt{\pi}} \times 0.45\frac{1}{2}(SNR)^{-\frac{1}{2}} \quad (6.19)$$

$$\therefore \frac{dP}{dSNR} = L\frac{0.675}{\sqrt{\pi}}SNR^{-\frac{1}{2}}(1 - 1.5\text{erfc}(0.45\sqrt{SNR}))^{L-1}e^{-((0.45)^2 SNR)} \quad (6.20)$$

These analytical results are shown Figure 6.1 and compared with results from the simulation. From the Figure, there is a fairly close match between the results measured using the simulation and those calculated using the equation. Hence, we can explore the situation further using the analytical approach.

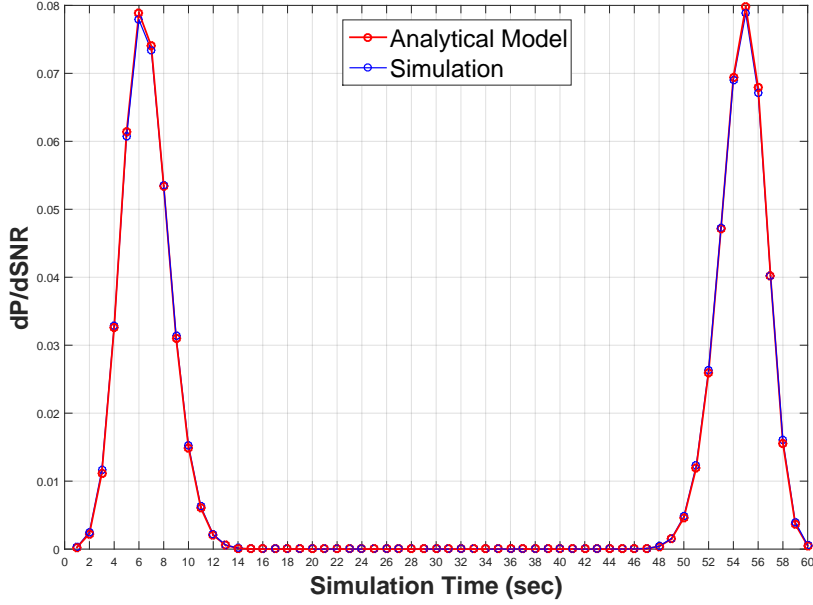


Fig. 6.1 Comparison of Simulation vs. Analytical Model.

6.3 The Impact of Beacon Length on Delta P (ΔP)

From both the simulation and calculated values of the $\frac{dP}{dSNR}$, we see that when P approaches 1, $\frac{dP}{dSNR}$ approaches 0. Furthermore, we know that as P approaches 1 i.e., $(1 - 1.5\text{erfc}(0.45\sqrt{SNR}))$ goes to 1. This means that in the region of interest is,

$$\frac{dP}{dSNR} \approx L \frac{0.675}{\sqrt{\pi}} SNR^{-\frac{1}{2}} e^{-((0.45)^2 SNR)} \approx 0 \quad (6.21)$$

This approximation is compared to the analytical model in Figure 6.2. The results clearly indicate that the approximate equation captures the change of SNR as the vehicle approaches the RSU.

We then use the approximate equation to compare the results for different packet lengths of 1556, 2856, 5456 bits (about 200, 325 and 752 bytes). The results are shown in Figure 6.3.

The graph in Figure 6.3 shows that the length of beacon does affect the rate of change of SNR but these values converge as the Packet OK approaches 1. However,

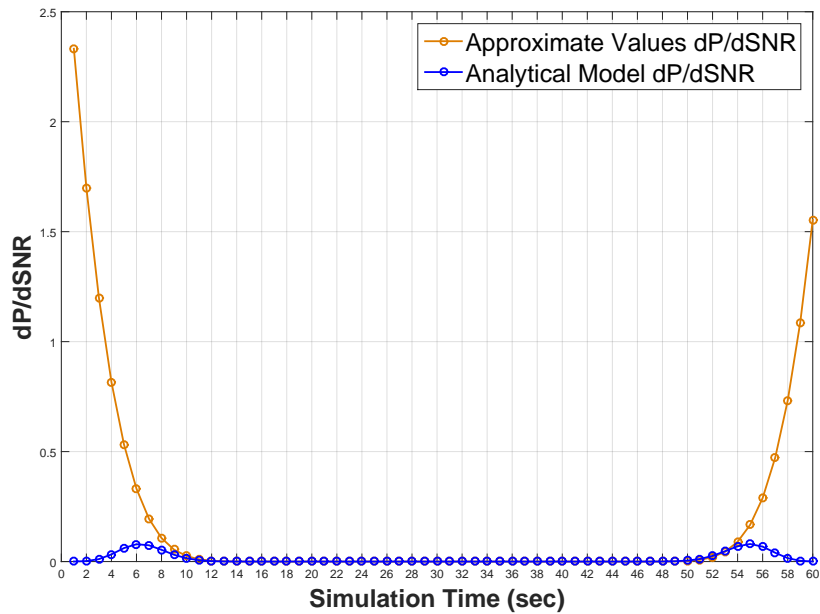


Fig. 6.2 Comparison of Analytical Model vs. Approximation.

when we plot $dP/dSNR$, approximate the rate of change of $dP/dSNR$ vs. Packet Length we get a straight line that indicates that there is a linear relationship between the rate of change of the SNR and the length of the beacon at those points in the network as the vehicle approaches the RSU. This line can be represented using a simple line equation (Equation 6.22)

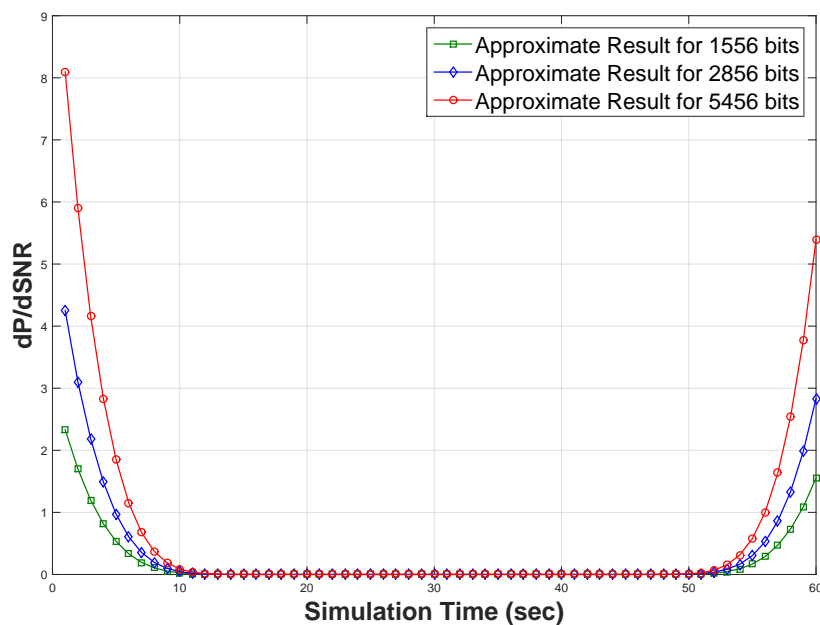


Fig. 6.3 Approximate with different Packet Lengths.

$$y = mx + b \quad (6.22)$$

where, x and y are the coordinates of the line, m is the slope of the line and b is the y intercept.

Equation 6.22 can be represented in terms of length of beacon and $dP/dSNR$ as shown in Equation 6.23.

$$dP/dSNR = mL + b \quad (6.23)$$

Here, L is the length of the beacon, $m = 6.1172E-11$ per bit and $b = -1.00E-13$ for $SNR = 100$ because according to equation in 6.21 $dP/dSNR$ is dependant on the instantaneous value of SNR .

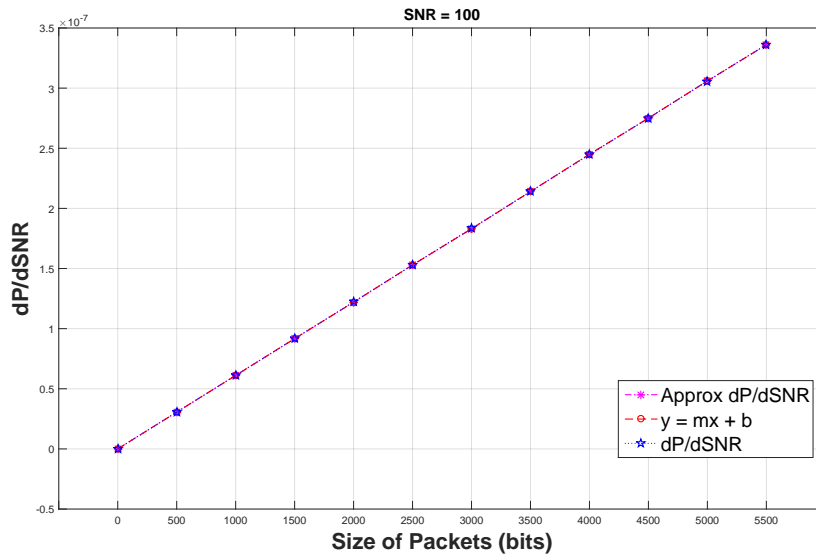


Fig. 6.4 Rate of change vs. Packet Length.

The result in Figure 6.4 where $SNR = 100$ shows that the $dP/dSNR$ of the approximation results are very close to the real results and hence the values of m , which is the change of $dP/dSNR$ per bit length of the beacon is an useful value to estimate the change of $dP/dSNR$ as the vehicle approaches the RSU.

We can define SNR by the following equation as defined in the next section

6.4 The relationship of Delta P with respect to velocity

In order to full investigate the effects of velocity, it is necessary to find out how P varies with the distance from the RSU given by radius (R). We begin by using our result for $dp/dSNR$ but since it possible using a propagation model to define the relationship between SNR and R, we can simply take the following approach.

$$\Rightarrow \frac{dP}{dSNR} = \frac{dP}{dx} \times \frac{dx}{dSNR} \quad (6.24)$$

$$\Rightarrow \frac{dP}{dR} = \frac{dP}{dSNR} \times \frac{dSNR}{dR} \quad (6.25)$$

Where, we know:-

$$SNR = \frac{P_S}{P_N} \quad (6.26)$$

$$P_S = \frac{P_T}{P_L} \quad (6.27)$$

$$\text{Hence, } SNR = \frac{P_T}{P_L P_N} \quad (6.28)$$

For Free Space Path Loss

$$\Rightarrow P_L = \left(\frac{4\pi r f}{c} \right)^2 \quad (6.29)$$

$$\Rightarrow SNR = \frac{P_T}{P_N} \left(\frac{c}{4\pi r f} \right)^2 \quad (6.30)$$

$$\therefore \frac{dSNR}{dR} = \frac{P_T}{P_N} \left(\frac{c}{4\pi f} \right)^2 \left(\frac{-2}{r^3} \right) \quad (6.31)$$

Therefore, the Full Equation:

$$\therefore \frac{dP}{dR} = \frac{3L}{\sqrt{\pi}} (1 - 1.5 \operatorname{erfc}(0.45\sqrt{SNR}))^{L-1} \times e^{-(0.45^2 SNR)} \sqrt{\pi} \times 0.45 \frac{1}{2} (SNR)^{-\frac{1}{2}} \times \frac{P_T}{P_N} \left(\frac{c}{4\pi f} \right)^2 \left(\frac{-2}{r^3} \right) \quad (6.32)$$

The graph in Figures 6.5 and 6.6 shows the relation of how delta P can be defined with respect to SNR and radius R from the equation defined in 6.20 and 6.32.

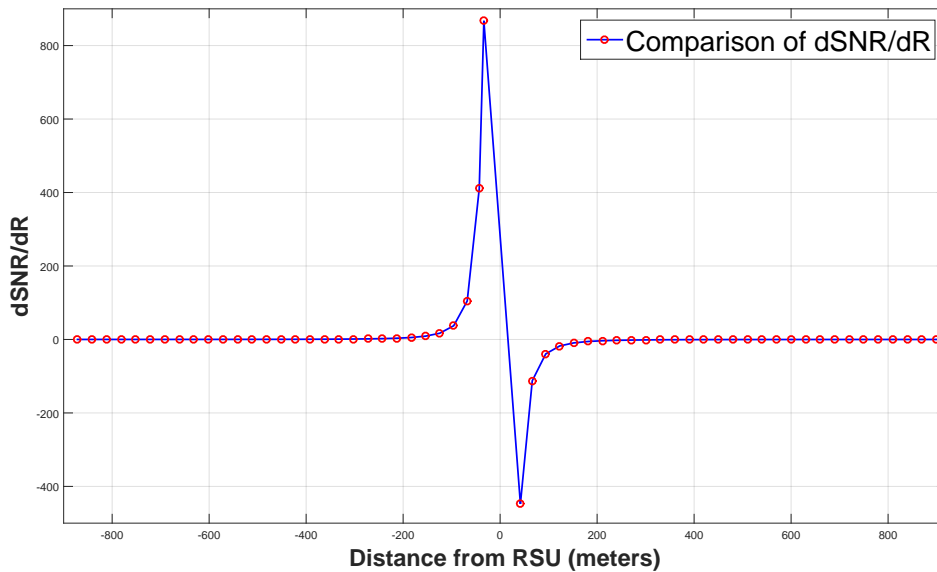


Fig. 6.5 Comparison of dSNR vs. dR.

However, the graph in Figures 6.5 and 6.6 model's the movement of the vehicle relative to the RSU as the vehicle tends to move to and away from the RSU. Thus, the distance needs to be on the x-axis in order to appropriately demonstrate the comparison of dSNR vs. dR and dP vs. dR (i.e. in meters, moving to and away from the RSU).

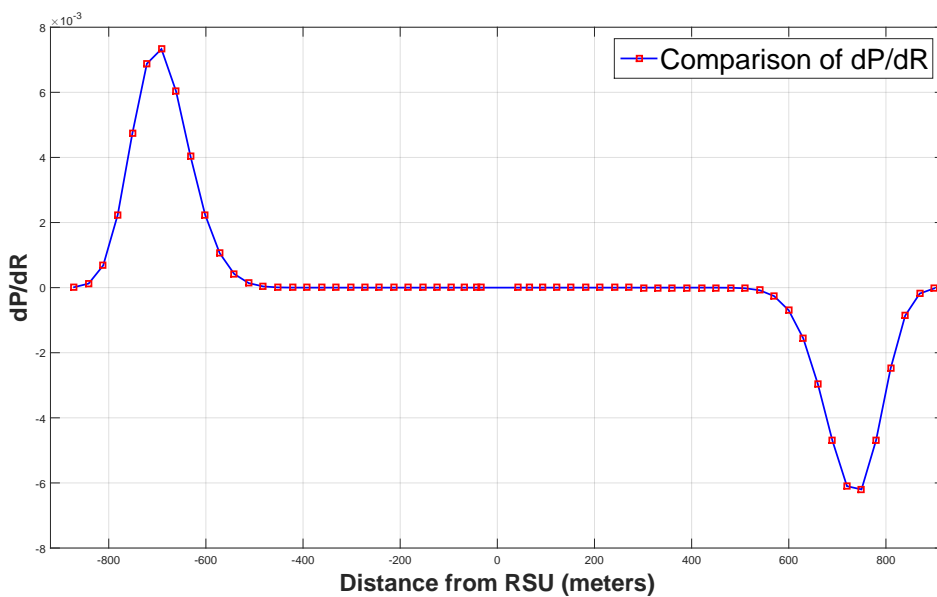


Fig. 6.6 Comparison of dP vs. dR.

6.4.1 Calculation for Probability P with respect to velocity using dP/dR

In order to model this we define the following parameters:

Let R_1 is the first the beacon is heard from a particular RSU in a new network that the vehicle is heading towards.

Let P_1 be the Probability of successful transmission at R_1 .

Let V be the velocity of the vehicle.

Let F be the frequency of the beacon as shown below:

$T = \text{Period of the Beacon}$ i.e., $T = \frac{1}{f}$, where $\frac{1}{f}$ is the frequency of the Beacon.

Let R_1 be the next time the beacon is heard, then:

$$R_2 = R_1 + VT$$

$$P_2 = P_1 + \int_{R_1}^{R_1+VT} \frac{dP}{dR}$$

Then at the third time of hearing the beacon:

$$R_3 = R_1 + 2VT$$

$$P_3 = P_1 + \int_{R_1}^{R_1+2VT} \frac{dP}{dR}$$

Hence, at the n^{th} time of hearing the beacon :

$$R_n = R_1 + (n - 1)VT$$

$$P_n = P_1 + \int_{R_1}^{R_1+(n-1)VT} \frac{dP}{dR}$$

Thus, the calculation for Cumulative Probability CP with respect to dP/dR is as follows:

where, $P_n = \left\{ P_1 + \int_{R_1}^{R_1+(n-1)VT} \frac{dP}{dR} \right\}$, hence the equation is represented as:

So, the Cumulative Probability at n:

$$\implies CP_n = P_1 + (1 - P_1)P_2 + (1 - P_1)(1 - P_2)P_3 + \dots + P_{n-1} \quad (6.33)$$

Thus, the series can be expanded in the form of:

$$\begin{aligned} \therefore CP_n = & \left\{ P_1 + (1 - P_1) \left(P_1 + \int_{R_1}^{R_1+VT} \frac{dP}{dR} \right) \right\} \\ & + \left\{ (1 - P_1) \left(1 - P_1 + \int_{R_1}^{R_1+VT} \frac{dP}{dR} \right) \left(P_1 + \int_{R_1}^{R_1+2VT} \frac{dP}{dR} \right) \right\} \\ & + \dots + \left\{ P_1 + \int_{R_1}^{R_1+(n-1)VT} \frac{dP}{dR} \right\} \end{aligned} \quad (6.34)$$

This analysis shows that both the individual probability as well as the cumulative probability is affected by the velocity of the vehicle when the beacon is heard. This is further discussed in the next section.

6.5 Impact of Velocity of the Vehicle on P and CP

This analysis above shows that both the individual probability as well as the cumulative probability are affected by the velocity of the vehicle when the beacon is heard. Thus, it is necessary to look at the impact of velocity on individual and cumulative probabilities at the times the beacon is heard. Therefore, it is necessary to focus on the number of times the beacon is heard before the individual probability and cumulative probability become 1 as shown in Figure 6.7.

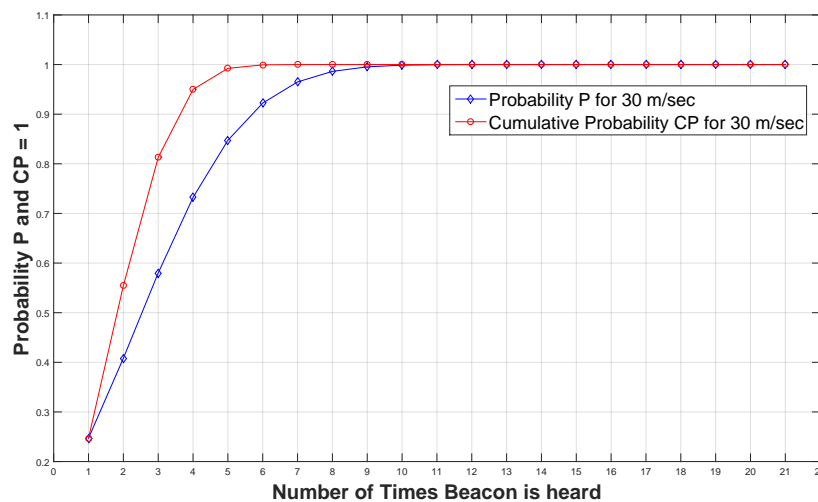


Fig. 6.7 Comparison of P and CP for 30 m/sec.

This graph clearly shows that the CP becomes 1 much earlier ($N = 5$) compared to the individual probability where ($N = 9$). Therefore, the difference in N between $CP = 1$ and $P = 1$ for different velocities is an appropriate way of investigating the effects of velocity on the overall system. We first look at the difference in N between P and CP when $P = 1$ and $CP = 1$ for 1Hz at different velocities.

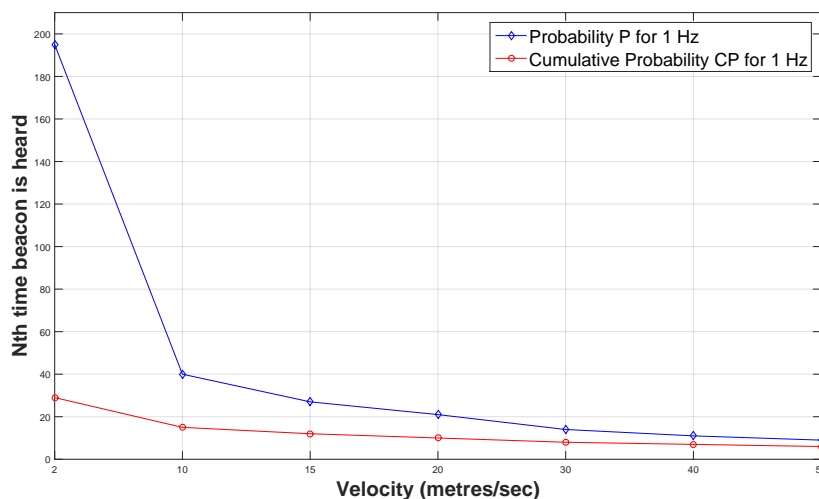


Fig. 6.8 Comparing P and CP for 1Hz.

The graph in Figure 6.8 clearly shows that for low speed there is a large difference. It is in the order of 165 beacons. However as the velocity increases this narrows significantly such that at 180 km/hr they are almost equal but at 360 km/hr they are exactly equal. This clearly shows that the benefits of cumulative frequency is reduced for greater speeds. Hence, for greater velocities we need to look at

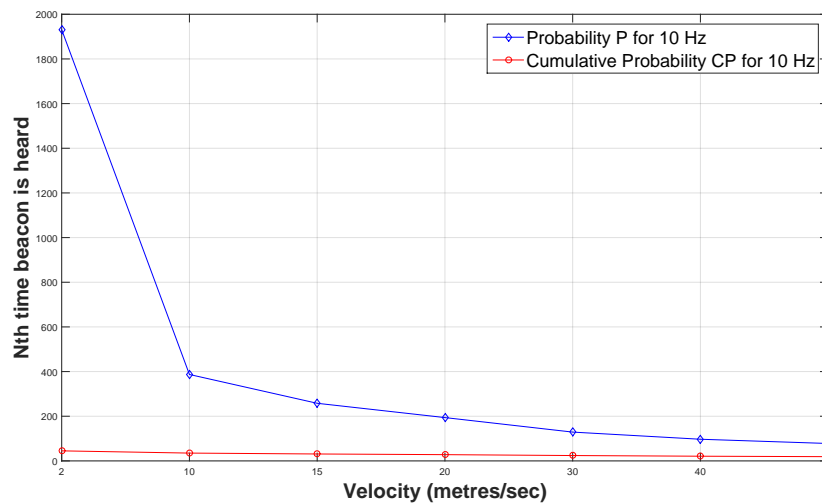


Fig. 6.9 Comparison of P and CP for 10Hz.

greater beacon frequency in order to negate the effect of velocity on the CP and this is shown in Figure 6.9.

We further compare the different values of P and CP at beaconing frequencies of 1 and 10Hz as shown in Figure 6.10, taking the value of the number of beacons heard when the probability (P) is 1. It should be noted that there is a more significant drop in the difference for individual probability at 1 and 10Hz respectively as the velocity increases.

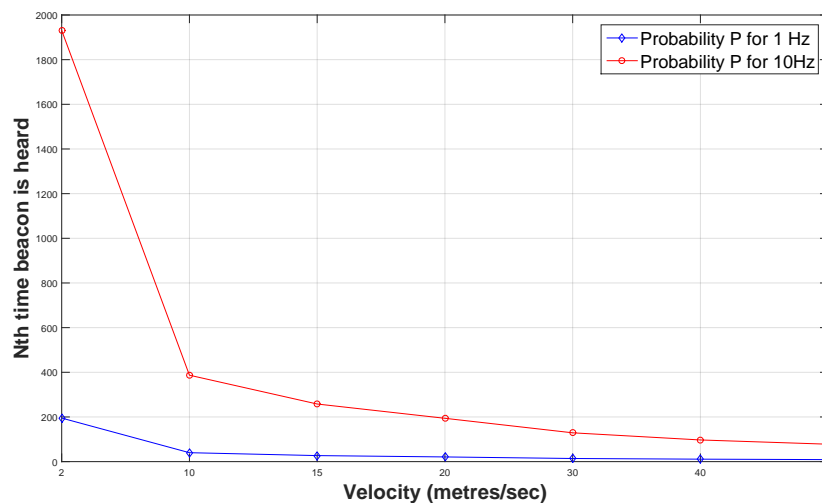


Fig. 6.10 Comparison of P of 1Hz and 10Hz.

This is not seen when we compare the CP at 1 and 10Hz respectively as the velocity increases as shown in graph in Figure 6.11.

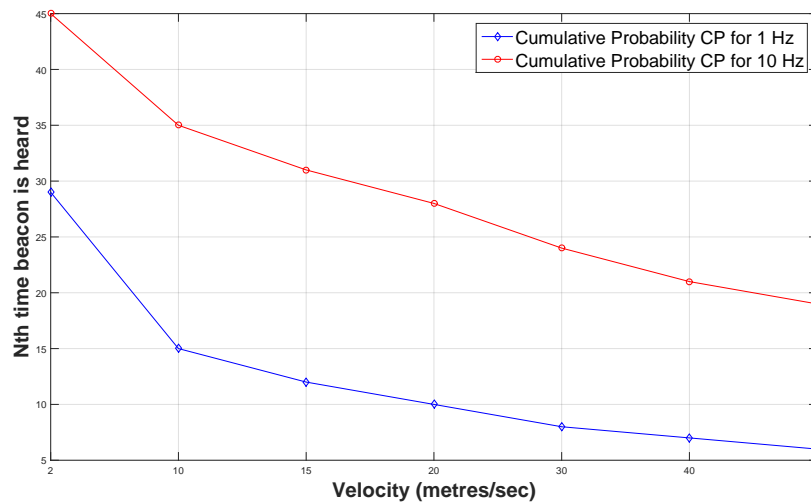


Fig. 6.11 Comparison of CP of 1Hz and 10Hz.

This indicates that in terms of velocity, the probabilistic approach to handover based on CP would represent a more stable handover policy over many velocities since the CP does not decrease much as the individual probability.

This result also verifies that in order to slow down the negative effects of high velocity between P and CP it is necessary to increase the frequency of beaconing. So the higher the velocity of the vehicle, the higher the beacon frequency, as we have previously noted.

6.6 Summary

In this Chapter, we investigated effects of the length of the beacon and the velocity of the vehicle. This was achieved by firstly looking at the Signal-to-Noise Ratio (SNR) on ΔP with respect to CP, i.e. $\frac{dP}{dSNR}$, where analytical results were presented. The results have shown that the length of the beacon contributes significantly to the rate of change of P (the individual probability) as the vehicle approaches the RSU.

Secondly, further investigation was carried out to explain the differences obtained in the analytical and simulation results. This led to a formation of a new mathematical model, which then explored how the communication changes as the vehicle approaches a new RSU.

Thirdly, this led to a new approximate model which further helped us to highlight the impact of the beacon length with respect to ΔP . This approximate model was then compared to the analytical model, which evidently indicated that

the approximate equation captures the change of SNR as the vehicle approaches the RSU. In addition, the result from the approximate model, the rate of change of $dP/dSNR$ vs. Packet Length, produced a straight line that indicated that there is a linear relationship between the rate of change of the SNR and the length of the beacon at those points, as the vehicle approaches the RSU.

Finally, in the case of the velocity of the vehicle, we have shown that there is also a strong relationship of ΔP with respect to the velocity of the vehicle i.e. dP/dR . Not only that, but the results from the comparison of dP/dR , suggested that there is a relation of how delta P can be defined with respect to SNR and radius R from the equations as defined in 6.20 and 6.32. In addition, we have also shown how the velocity of the vehicle affects the difference between the individual probability P and cumulative probability CP as the velocity increases.

Chapter 7

MDX-VANET TESTBED

7.1 Introduction

In the last Chapter, our analytical model for the system was shown to be dependant on the type of propagation model used. The Free Space Path Loss model was used in our calculations, but in order to get a more useful model it is necessary to explore propagation models for VANET systems based on real results. Hence, a testbed is needed to explore this phenomenon.

In this Chapter, we will look at deployment of RSUs as part of a VANET Testbed which is set-out at Middlesex University, Hendon Campus. This is to achieve a better understanding of VANET systems operating in an urban environment for capturing real-time constraints i.e., propagation models needed for highly mobile environments such as VANETs. In addition, environmental factors have to be taken into consideration for real-time deployment studies to see how they affect the performance of VANET systems under different scenarios. This eventually facilitates a comprehensive feasibility study in order to develop efficient propagation models for VANET systems. The MDX-VANET Testbed emphasises more on the infrastructure to vehicle (I2V) communications, since the data is being collected at a Middlesex University central server using the MDX network.

Additionally, two applications are developed based on the concept of Client-Server application model to facilitate communications between OBU and RSU. Previous papers have looked into simulation studies in VANET and very few papers focus on practical studies of VANET systems. This Chapter focuses on the deployment of VANET technology from the infrastructure point of view and the physical deployment of the RSUs around the Middlesex University, Hendon campus. It also highlights on the uniqueness of the testbed from previous VANET testbed studies

carried out by other academic institutions around the world. As well as focusing on physical constraints and real-time deployment aspects of the VANET technology.

In previous chapters, we had been more focused on carrying out several simulation experiments but in this Chapter we particularly compare our simulation and analytical results with the Testbed real-time measurements. The focus of this Testbed was to find out the coverage range of the RSUs in what is a very challenging environments in terms of complexity of building designs and street layouts.

7.2 MDX-VANET Testbed

In order to further explore the analytical and simulation models, a prototype VANET Testbed is being deployed at the Hendon Campus of Middlesex University as depicted in Figure 7.1. This testbed will enable us to correctly evaluate these models thus giving us better insight into the deployment of real transport networks.

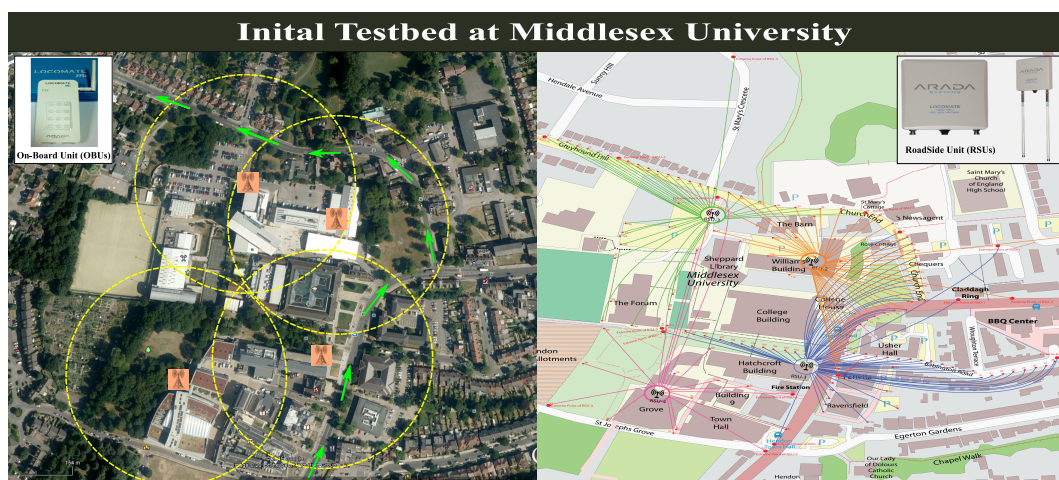


Fig. 7.1 MDX VANET Testbed.

7.3 Investigating previous deployments in VANET

To investigate and study VANET systems, a Test-bed environment is set-up at Middlesex University for the sole purpose of achieving real-time results. This includes outside field tests of VANET systems allowing us to achieve fundamental readings based on real-time results as well as exploring various parameters of VANET systems. Ultimately, we can make significant contributions to this emerging

technology. Middlesex University is one of the very few universities in the UK owning VANET systems and doing test experiments. A VANET infrastructure will be built that will consist of Road side Units (RSU) located at specific locations and On-Board Units (OBU) in vehicles. Previous research efforts as highlighted in (Gozalvez et al., 2012), where authors conducted extensive field trials around the city of Bologna in order to collect real-time data. These real-time datasets were collected in order to investigate the environmental factors affecting the IEEE 802.11p in order to achieve V2I communication. The authors aimed at analysing the impact of existing propagation models in an urban setting for RSU deployment strategy and how it affects the quality and reliability of communication. This work contains real-time experimental results of V2I communication ranges and how various urban environmental factors can affect the communication range in V2I scenario.

Additionally, computer simulation and comprehensive field trials were conducted in an internationally standardized laboratory, at the ARTC in Taiwan (Lin et al., 2012), to look at possible issues that occur in V2I communication scenarios. The results achieved gave us an indication of the performance of vehicular networks. The authors highlighted the computer simulation techniques which were used to analyse the relation between bit error rate performance along with signal to noise ratio. On the other hand, field trials were conducted on a simulated vehicular environment operating in a controlled laboratory to investigate the impact of DSCR communication; To do so, a variety of parameters were measured to look at communication performance such as packet loss, latency and spread delay.

In the past few years, many research efforts in relation to V2V, V2I and I2I have been investigated due to the fact that their roles are extremely crucial in the Intelligent Transport System (ITS). As a matter of fact, numerous VANET projects have been executed by different governments, academic institutions and industries around various parts of the world in the last decade (Zeadally et al., 2012).

Although propagation models is not one of the main focus of this research work, it has to be often taken into consideration for field trial studies in order to build a sustainable testbed. Thus factors like, line of sight, distance, wavelength, antenna height, velocity of vehicle, obstructions, topography of the road, and many other such factors can be calculated depending on what type of propagation model is used. Ideally, propagation models should take into account every of the necessary factors and potential hindrances(Rappaport, 2012).

7.4 Initial Steps before the Actual Deployment of the MDX VANET Testbed

VANET presents new technical challenges and unveils an exciting network environment to work in. However, one of the main characteristics of VANET systems is it encourages the concept of ubiquitous communication allowing us to have seamless connectivity and optimal coverage range (Ghosh et al., 2014b). Testing of VANET systems is carried out at Middlesex University. To do so, a VANET infrastructure was built which consists of Road Side Units (RSU) located at specific locations and On-Board Units (OBU) in vehicles. This initial coverage testing will greatly enhance our understandings of VANET in terms of performance e.g. we can find out the precise coverage area of a RSU. We believe that from the experiments and results we will be able to develop a better system and a model that we can apply to real world scenarios.

Real-time measurements from field tests for final deployment of VANET systems is crucial, allowing us to achieve fundamental readings based on real-time results as well as exploring various parameters of VANET systems, eventually, this will enable us to make significant contributions to this emerging technology. MDX VANET Testbed gives us the opportunity to demonstrate the important role of the vehicular testbed in validating such systems before deployment of large scale scenarios. Therefore, to further our understandings of VANET systems we undergo real-time testing around the university.

7.4.1 Initial scenario problem - The Effects of physical obstructions on wireless signal propagation

Wireless signal attenuation occurs due to physical obstructions, such as walls, blocking signals transmitted from one device to another, consequently, reduction of signal strength or in some cases a complete signal loss is experienced meaning communication cannot take place. Essentially one of the first issues we faced, as shown in the picture, was the two RSUs were not able to overlap each other due to the Sheppard library building, in-between the two device, blocking the signals of the two RSUs.

7.4.2 Initial testbed Coverage Analysis

The main priority of our testbed is to evaluate the performances of our systems in the form of V2I known as Infrastructure to Vehicle. In these experiments, a

single RSU is used on top of four different building while it continuously transmits beacons to the OBU which is moved around outside the campus. A laptop is used at the RSU to access and run the commands using command prompt to transmit data while another laptop is used at the other end with the OBU as an interface to see the data we receive at the OBU - the laptop communicates with the OBU via Bluetooth interface. The two performance characteristics we would like to explore during the testbed are:

- **Reliability:** This is the most important characteristics of the network as it makes the systems unique to other alternative networks. Transmitting high numbers of beacons make it possible for a reliable communication to take place between RSUs and OBUs.
- **Coverage Range:** The testbed enhances our understandings in terms of coverage range. We assume we get around 1 km range from our devices, however this testbed will prove that whether we are able to get such high coverage range.

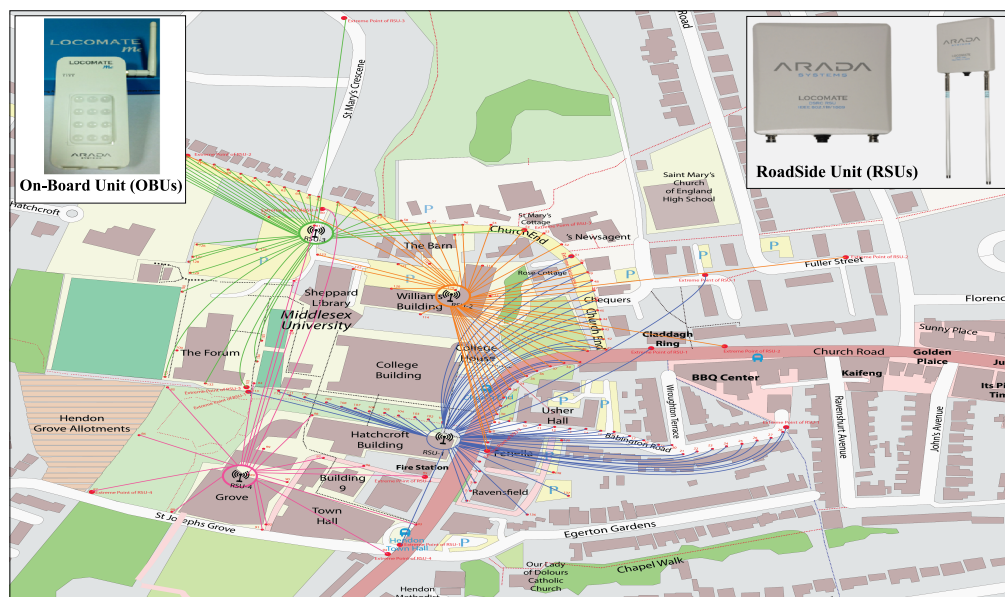


Fig. 7.2 Map with Coverage Range with respect to Spots of each RSUs.

7.4.3 Description of the testbed Deployment for the Field Study

After the RSU locations were decided, we conducted a field study for taking signal strength values of the initial RSU coverage at their existing locations. To do this,

instead of taking the reading of few spots, we took the Received Signal Strength Index (RSSI) values for every 10 meters till the signal strength dropped to 0. Moreover, this helped us to calculate the coverage distances between the four of the RSUs and the spots. Further to this, taking readings every 10 meters gives us an idea of where the signal was dropped and what was the main cause for instance any obstacle between the RSU and the vehicle. The map in Figure 7.2 shows a glimpse of the readings taken on each spots and the coverage area of the individual RSUs.

In each spot, we have taken three readings of the RSSI values, considering the fact that we need to take an average of the RSSI values and then convert it into dBm unit for comparison. The equipment, used for this experiment, is from a company called Arada Systems (AradaSystems, 2015) and according to Arada system's equipments specifications, in order to calculate the RSSI values in dBm, we need to adding -95 to the RSSI value which in turn should give us the received signal strength in dBm.

In this thesis, we compared the real time results against the calculated values from simple path loss models, which are used as the traditional propagation models in wireless communication. So far, to the best of our knowledge all the the propagation models used in this research work had been taken from the simulation and there are some active research going on using the same propagation models for real time field tests. This work, highlights some of the results by comparing the field test results against the propagation models, which will then enable us to have an understanding of how the traditional propagation models are different from the real-time values obtained from the field tests. And, hence the requirement for a a more modern and comprehensive propagation models for dense urban environments in VANET systems.

The results collected from the field test were then exported to put in tables for calculation purposes. During this field test, not only RSSI values were taken but considering the fact of how the RSSI values fluctuate between spots, therefore, each spot is uniquely identified with serial numbers and the location name. It also along with distances between each spot were recorded separately. But mostly spots were 10m away from each other. This was required for reasoning purposes in terms of how the line of sight and non line of sight affect such readings. Also additional information such as description of the spot or what was causing this NLOS. Finally, measurements as shown in tables 7.1, 7.2, 7.3, 7.4, 7.5, 7.6 and 7.7 a column containing distance information was provided in order to calculate the accurate distances between transmitter and receiver.

Table 7.1 VANET Field Test Measurements for RSU-1 on Hatchcroft Building.

Serial.NO	PLACE	DISTANCE	RSSI	RSSI	RSSI	dBm	dBm	Average	FSPL	ALTITUDE	LOS	NLOS	DISTANCE (M)	DISTANCE (KM)	fspl
1	RAVENS FIELD	10M	10	14	20	-85	-81	-75	85	83.43M		Y	71	0.071	-62
2	RAVENS FIELD SIGN BOARD	10M	28	30	32	-67	-65	-63	84	84.63M		Y	63.56	0.06356	-61
3	Ravens fields signage to 3rd pipe	10M	28	30	40	-67	-65	-65	83	84.21M		Y	57.5	0.0575	-60
4	Side walk between ravensfields	10M	30	33	37	-65	-62	-58	82	84.25M	Y		51.5	0.0515	-59
5	Start of fenella building	10M	39	45	48	-56	-54	-51	80	85.20M	Y*		39.31	0.03931	-57
6	Street light between Fenella building	10M	35	38	41	-60	-57	-54	79	85.11M	Y*		35.88	0.03588	-56
7	Street light between Fenella building-Bus Crossed	10M	35	26	0	-60	-69	-95	79	84.94M	Y*		35.88	0.03588	-56
8	Straight to RSU 10M from street light	10M	38	40	45	-57	-55	-50	79				35.2	0.0352	-56
9	Straight to RSU 10M from street light-Bus Crossed	10M	42	37	0	-53	-58	-95	79				35.2	0.0352	-56
10	Straight to RSU 10M from street light-Fire Truck	10M	36	24	0	-59	-71	-95	79				35.2	0.0352	-56
11	End of fenella building	10M	36	40	41	-59	-55	-54	79	86.22m	Y*		37.75	0.03775	-56
12	End of Usher Hall/starting of Usher hall	10M	46	47	50	-49	-48	-47	83		Y*		59.92	0.05992	-60
13	Fenella Building Entrance	10M	43	46	49	-52	-49	-46	85		Y*		69.89	0.06989	-62
14	Fenella Building Starting-in babington road	10M	41	43	45	-54	-52	-50	86		Y*		80.52	0.08052	-63
15	Opposite of fenella building car park	10M	46	48	50	-49	-47	-45	87		Y*		89.07	0.08907	-64
16	10M away From spot NO:15	10M	44	48	50	-51	-47	-45	88		Y*		99.07	0.09907	-65
17	Starting Point of Usher Hall	10M	42	45	47	-53	-50	-48	89		Y*		110	0.11	-66
18	Middle of Car Park	10M	40	41	43	-55	-54	-52	89		Y*		119.16	0.11916	-66
19	Usher Hall Car Park	10M	35	38	40	-60	-57	-55	90		Y*		129.58	0.12958	-67
20	Opposite of House NO:26	10M	26	27	32	-69	-68	-63	91		Y*		139.42	0.13942	-68
21	Opposite of House NO:32	10M	22	25	28	-73	-70	-67	91		Y*		149.3	0.1493	-68
22	House NO:36	10M	12	13	15	-83	-82	-80	92		Y*		158.95	0.15895	-69
23	House NO:40	10M	20	22	25	-75	-73	-70	92		Y*		169.84	0.16984	-69
24	House NO:44	10M	17	19	21	-78	-76	-74	93		Y*		180	0.18	-70
25	House NO:48	10M	6	9	10	-89	-86	-85	93		Y*		189.33	0.18933	-70
26	House NO:50 (Starting - Reliable Communication)	10M	3	5	6	-92	-90	-89	94		Y		199.01	0.19901	-71
27	House NO:54	10M	2	3	5	-93	-92	-90	94		Y		208.08	0.20808	-71
28	House NO:58	10M	1	2	4	-94	-93	-91	95		Y		218.04	0.21804	-72
29	House NO:62	10M	1	2	3	-94	-93	-92	95		Y		227.41	0.22741	-72
30	House NO:66	10M	1	2	3	-94	-93	-92	95		Y		238.14	0.23814	-72
31	West view Foot path signage	10M	1	2	3	-94	-93	-92	96		Y		247.4	0.2474	-73
32	Babington Road	10M	39	40	42	-56	-55	-53	81	85M	Y*		45.45	0.04545	-58
33	Usher hall Starting piont	10M	39	40	44	-56	-55	-51	82	84.90M	Y*		51.65	0.05165	-59
34	Opposite of MDX signage	10M	47	48	52	-48	-47	-43	83	85.4M	Y*		59.45	0.05945	-60
35	Usher hall signage	10M	37	39	41	-58	-55	-54	85	85.25M	Y*	one tree	68.2	0.0682	-62
36	Opposite of MDX bus stop	10M	37	40	41	-58	-55	-54	86	85.6M	Y*		77.9	0.0779	-63
37	Pathway of usher hall	10M	46	48	43	-49	-47	-52	87	85.95M	Y*		87.64	0.08764	-64
38	End of usher hall	10M	27	32	38	-68	-63	-57	88	85.71M	Y*		98	0.098	-65
39	MDX library gateway	10M	30	32	35	-65	-63	-60	88	83.96M	Y	one or two trees	107.2	0.1072	-65
40	Street camera opposite of MDX park	10M	33	37	40	-62	-58	-55	89	84.58M	Y	one or two trees	117.75	0.11775	-66
41	Start of Usher hall (10m from street cam)	10M	24	26	29	-71	-69	-66	90	85.3M	Y*		127.36	0.12736	-67
42	Street light after street camera	10M	35	37	40	-60	-58	-55	91	85.97M	Y*		135.75	0.13575	-68
43	End of MDX park	10M	29	32	32	-66	-63	-63	91	85.84M	Y		147.2	0.1472	-68
44	Church end road start	10M	23	0	0	-72	-95	-95	92	86.97M		Y	162.5	0.1625	-69
45	Church end road building starting piont	10M	16	18	20	-79	-77	-75	92	82.46M		Y	167.4	0.1674	-69
46	Opposite of Church end road 1st tree	10M	18	20	23	-77	-75	-72	93	86.42M		Y	174.3	0.1743	-70
47	End of Building	10M	8	10	13	-87	-85	-82	93	86.77M	Y		178.3	0.1783	-70
48	7.5M measured form chequers bar	7.5M	13	15	17	-82	-80	-78	93	86.74M	Y		184	0.184	-70
49	End of prince of wales close	10M	14	16	18	-81	-79	-77	93	85.93M	Y		188	0.188	-70
50	Chequers bar window	10M	14	18	20	-81	-77	-75	94	85.53M	Y		195.5	0.1955	-71
51	Starting point of chequers car park	10M	34	36	40	-61	-59	-55	94	87.96M	Y		202.2	0.2022	-71
52	End of Chequers Car park	10M	8	9	11	-87	-86	-84	94			Y	209.5	0.2095	-71
53	Snerriek House	10M	2	4	11	-93	-91	-84	95			Y	215.9	0.2159	-72
54	End of rsu range	10M	0	0	0	-95	-95	-95	95			Y	222	0.222	-72

Table 7.2 VANET Field Test Measurements for RSU-2 on Williams Building.

SerialNO	PLACE	DISTANCE	RSSI	RSSI	RSSI	dBm	dBm	Average dBm	FSPL	ALTITUDE	LOS	NLOS	DISTANCE (M)	DISTANCE (KM)	fspl dBm
52	Fennela Building Street light	10M	0	0	3	-95	-92	-94	93			Y	176.66	0.17666	-70
53	Opposite of RSU 1 (Hatch Croft Building)	10M	2	2	4	-93	-91	-92	92			Y	166.35	0.16635	-69
54	End of Fennela Building	10M	8	10	12	-87	-83	-85	92		Y	Y	153.3	0.1533	-69
55	Babington Road	10M	22	23	26	-73	-69	-71	91		Y	Y	140.95	0.14095	-68
56	Opposite of MDX signage	10M	22	23	23	-73	-72	-72	90		Y	Y	130.03	0.13003	-67
57	Usher Hall Signage	10M	14	16	20	-81	-79	-78	90		Y	Y	124.08	0.12408	-67
58	Opposite of MDX gate	10M	16	18	20	-79	-77	-77	89			Y	120.16	0.12016	-66
59	MDX gate toward library	10M	23	27	30	-72	-68	-68	89		Y*		115.21	0.11521	-66
60	10M away from S No:8	10M	25	29	34	-70	-66	-66	89		Y*		118.9	0.1189	-66
61	Next to Street camera	10M	34	37	10	-61	-58	-68	89		Y*		117.16	0.11716	-66
62	End of Usher hall	10M	21	23	25	-74	-72	-72	90		Y	Y	126.94	0.12694	-67
63	Church End road starting point	10M	19	20	21	-76	-74	-75	91		Y	Y	141.58	0.14158	-68
64	Church End road building starting point	10M	22	24	27	-73	-71	-71	91		Y	Y	136.32	0.13632	-68
65	Middle of the Building	10M	28	29	32	-67	-66	-65	90		Y	Y	130.31	0.13031	-67
66	Prince of Wales Close starting point	10M	32	35	37	-63	-60	-60	90		Y	Y	123.65	0.12365	-67
67	Front of Chequers Bar	10M	38	39	41	-57	-56	-56	90		Y	Y	120.99	0.12099	-67
68	Starting point of chuequers Car park	10M	24	25	32	-71	-69	-68	89			Y	116.4	0.1164	-66
69	End of Car Park	10M	22	26	28	-73	-71	-70	89			Y	115.91	0.11591	-66
70	Sherrick House	10M	21	22	24	-74	-73	-73	89			Y	116.98	0.11698	-66
71	Meritage Centre starting point	10M	8	10	12	-87	-85	-85	89			Y	111.06	0.11106	-66
72	Church House	10M	7	8	9	-88	-86	-87	88			Y	105.83	0.10583	-65
73	St Mary's Church	10M	28	30	31	-67	-64	-65	88		Y		102.81	0.10281	-65
74	Gray Hounded Pub	10M	25	27	30	-70	-68	-68	87		Y	Y	94.6	0.0946	-64
75	Opposite of Model Farm House	10M	30	31	32	-65	-63	-64	86		Y	Y	82.53	0.08253	-63
76	15m away from Model Farm house	15M	30	32	36	-65	-63	-62	86		Y	Y	79.43	0.07943	-63
77	Opposite of Farm Side	10M	33	36	39	-62	-59	-59	86		Y*		78.73	0.07873	-63
78	Sunny Hill Pathway	10M	40	45	47	-55	-48	-51	86		Y*		84.89	0.08489	-63
79	Start of House No:16	10M	27	29	30	-68	-66	-66	88		Y	Y	101.82	0.10182	-65
80	MDX Back Gate	10M	36	37	39	-59	-58	-58	89		Y	Y	116.4	0.1164	-66

Table 7.3 VANET Field Test Measurements for RSU-3 on MDX Car Park.

SerialNO	PLACE	DISTANCE	RSSI	RSSI	RSSI	RSSI	dBm	dBm	Average dBm	FSPL	ALTITUDE	LOS	NLOS	DISTANCE (M)	DISTANCE (KM)	fspl dBm
81	Sunny hill starting Point	10M	0	1	2	-95	-94	-93	-94	94	63.78		Y	205.92	0.20592	-71
82	Sunny Hill other side of the road	10M	0	0	0	-95	-95	-95	-95	94	64.43		Y	196.51	0.19651	-71
83	10M from Spot NO-2	10M	0	0	0	-95	-95	-95	-95	93	63.34		Y	187.62	0.18762	-70
84	Speed warning	10M	5	6	7	-90	-89	-88	-89	93	66.61		Y	176.9	0.1769	-70
85	10M from Spot NO-4	10M	5	6	7	-90	-89	-88	-89	92	66.39		Y	166.45	0.16645	-69
86	Digital Speed warning sign on Street light	10M	13	14	15	-82	-81	-80	-81	92	66.34		Y	157	0.157	-69
87	10M from Spot NO-6	10M	13	14	15	-82	-81	-80	-81	91	66.41	Y	Y	145.5	0.1455	-68
88	Front of House NO:40	10M	13	14	15	-82	-81	-80	-81	91	66.9	Y	Y	135.75	0.13575	-68
89	10M from Spot NO-8	10M	14	16	17	-81	-79	-78	-79	90	67.51		Y	127.25	0.12725	-67
90	10M from S:NO9 gate of Sunny Hill School	10M	14	16	17	-81	-79	-78	-79	89	68.65	Y	Y	117.6	0.1176	-66
91	House NO:34 10M away from S:NO 34	10M	16	16	18	-79	-79	-77	-78	89	69	Y	Y	108.49	0.10849	-66
92	10M from Spot NO-11	10M	16	16	18	-79	-79	-77	-78	88	69	Y	Y	99.2	0.0992	-65
93	10M from Spot NO-12	10M	13	13	15	-82	-82	-80	-81	87	71	Y		92.2	0.0922	-64
94	10M from spot NO 13	10M	15	17	18	-80	-78	-77	-78	86	72.4	Y	Y	83.73	0.08373	-63
95	House No 28- 10M away from S:NO-14	10M	23	25	28	-72	-70	-67	-70	85	73.14	Y	Y	75.8	0.0758	-62
96	House No 26- 10M away from S:NO-14	10M	30	36	40	-65	-59	-55	-60	85	74.9	Y	Y	68.3	0.0683	-62
97	10M away from House No:26	10M	35	37	42	-60	-58	-53	-57	84	75.66	Y*		61.55	0.06155	-61
98	St Mary's Crescent	10M	46	48	50	-49	-47	-45	-47	83	74.96	Y*		55.73	0.05573	-60
99	20M away from S:NO:18	20M	49	51	52	-46	-44	-43	-44	82	74.85	Y*		50.19	0.05019	-59
100	Opposire of MDX back gate	10M	38	47	48	-57	-48	-47	-51	82	77.47	Y*		48.45	0.04845	-59
101		10M	42	47	50	-53	-48	-45	-49	82	78.2	Y		49.43	0.04943	-59
102		10M	42	44	47	-53	-51	-48	-51	82	76.26	Y		51.9	0.0519	-59
103		10M	34	37	38	-61	-58	-57	-59	83	77.5		Y	56.55	0.05655	-60
104		10M	28	30	33	-67	-65	-62	-65	84	82		Y	62.55	0.06255	-61
105		10M	19	20	22	-76	-75	-73	-75	85	81.48		Y	68.78	0.06878	-62
106		10M	19	20	26	-76	-75	-69	-73	86	82.9		Y	77.8	0.0778	-63
107		10M	19	22	26	-76	-73	-69	-73	87	85.2		Y	88.25	0.08825	-64
108		10M	13	17	19	-82	-78	-76	-79	88	86.48		Y	97.65	0.09765	-65
109		10M	11	15	20	-84	-80	-75	-80	88	87.2		Y	107.3	0.1073	-65
110		10M	10	14	22	-85	-81	-73	-80	89	87.2		Y	118.3	0.1183	-66
111		10M	6	7	8	-89	-88	-87	-88	90	86.7		Y	127.82	0.12782	-67

Table 7.4 VANET Field Test Measurements for RSU-4 on Grove Building.

Serial.NO	PLACE	DISTANCE	RSSI	RSSI	dBm	Average dBm	FSPL	ALTITUDE	LOS	NLOS	DISTANCE (M)	DISTANCE (KM)	fspl dBm
112	MDX Back Gate	10M	6	7	8	-89	-88	-87	Y	Y	284.82	0.28482	-74
113	MDX Security box at back car park area	10M	13	14	15	-82	-81	-80	Y	Y	251.85	0.25185	-73
114	MDX Library Table area	10M	31	32	33	-64	-63	-62	Y	Y	201.7	0.2017	-71
115	Start of College Building	10M	14	15	16	-81	-80	-79	Y	Y	155.85	0.15585	-69
116	Real Tennis Court	10M	23	25	26	-72	-70	-69	Y	Y	93.07	0.09307	-64
117	Corner of football pitch	10M	27	29	31	-68	-66	-64	Y	Y	98.7	0.0987	-65
118	In between the park next to grove	10M	34	37	40	-61	-58	-55	Y	Y	74.67	0.07467	-62
119	End of the Park	10M	6	10	14	-89	-85	-81	Y	Y	96.5	0.0965	-65
120	End point of Grove(side Road st josephs road)	10M	13	14	16	-82	-81	-79	Y	Y	58.1	0.0581	-60
121	Entrance of Grove Building (under the RSU 4)	10M	34	35	36	-61	-60	-59	Y	Y	6	0.006	-40
122	Pathway between Townhall and Grove	10M	38	42	45	-57	-53	-50	Y	Y	34.75	0.03475	-56
123	Townhall building End point	10M	24	25	27	-71	-70	-68	Y	Y	67.81	0.06781	-61
124	Check post between Grove and Townhall	10M	9	10	13	-86	-85	-82	Y	Y	52.21	0.05221	-59
125	Between Townhall and Hendon Library	10M	26	27	30	-69	-68	-65	Y	Y	135.6	0.1356	-68
126	St Josephs Grove	10M	5	5	0	-90	-90	-95	Y	Y	128.25	0.12825	-67
127	Hendon Library in between fire station	10M	1	4	5	-94	-91	-90	Y	Y	144.33	0.14433	-68
128	Inside pathway between hatchcroft and town hall	10M	23	24	25	-72	-71	-70	Y	Y	97.02	0.09702	-65
129	Cycle locking area	10M	29	30	35	-66	-65	-60	Y	Y	53.12	0.05312	-59
130	Pathway between college building and hatchcroft	10M	22	23	26	-73	-72	-69	Y	Y	78.3	0.0783	-63
131	Grove middle Building	10M	27	28	31	-68	-67	-64	Y	Y	39.07	0.03907	-57
132	Middle of The Forum	10M	6	7	8	-89	-88	-87	Y	Y	147.86	0.14786	-68

Table 7.5 VANET Field Test Measurements for RSU-1 (Inside Pathway).

Serial.NO	PLACE	DISTANCE	RSSI	RSSI	RSSI	dBm	dBm	Average dBm	FSPL	ALTITUDE	LOS	NLOS	DISTANCE (M)	DISTANCE (KM)	fspl dBm
133	MDX gate between hatchcroft and college building	10M	40	42	45	-55	-53	-50	72		Y*		15.5	0.0155	-49
134	Barry office 3ed tree from left or 4th lamp post	10M	45	48	50	-50	-47	-45	74		Y*		19.2	0.0192	-51
135	Next to 5th lamp + 2.5 meter from 5th lamp	10M	39	40	45	-56	-55	-50	76		Y*		26	0.026	-53
136	7th lamp post	10M	35	37	39	-60	-58	-56	79		Y*		34.75	0.03475	-56
137	In between 8th and 9th lamp post	10M	30	32	34	-65	-63	-61	81		Y*		44.45	0.04445	-58
138	10th Lamp post	10M	31	35	37	-64	-60	-58	82		Y*		53.9	0.0539	-59
139	In between 11th and 12th Lamp post	10M	29	30	36	-66	-65	-59	84		Y*		63.33	0.06333	-61
140	13th Lamp post	10M	27	29	30	-68	-66	-65	85		Y*		73.5	0.0735	-62
141	In between 14th and 15th Lamp post	10M	13	15	17	-82	-80	-78	86			Y	83.1	0.0831	-63
142	16th Lamp post	10M	9	10	11	-86	-85	-84	87			Y	93.3	0.0933	-64
143	In between Grove Building	10M	9	11	13	-86	-84	-82	88			Y	102.8	0.1028	-65
144	In between Grove and Tennis Court	10M	4	5	7	-91	-90	-88	89			Y	112.7	0.1127	-66
145	Real Tennis Court	10M	1	0	0	-94	-95	-95	90			Y	122.5	0.1225	-67

Table 7.6 VANET Field Test Measurements for RSU-2 (Inside Pathway).

Serial.NO	PLACE	DISTANCE	RSSI	RSSI	RSSI	dBm	dBm	dBm	Average dBm	FSPL	ALTITUDE	LOS	NLOS	DISTANCE (M)	DISTANCE (KM)	fspl dBm
146	Williams building side gate	10M	28	30	33	-67	-65	-62	-65	76			Y	25.4	0.0254	-53
147	Williams building front	10M	28	30	33	-67	-65	-62	-65	82			Y	48.57	0.04857	-59
148	Williams building smoking area	10M	14	17	21	-81	-78	-74	-78	82			Y	50.83	0.05083	-59
149	RKTO Back Gate	10M	16	19	21	-79	-76	-74	-76	85			Y	75.28	0.07528	-62
150	RKTO front gate	10M	40	42	46	-55	-53	-49	-52	79		Y*		37.2	0.0372	-56
151	Williams building car park	10M	20	22	25	-75	-73	-70	-73	74		Y*		19.2	0.0192	-51
152	Williams/EFM	10M	7	9	12	-88	-86	-83	-86	80			Y	40	0.04	-57
153	MDX library edge	10M	30	35	37	-65	-60	-58	-61	82		Y		53.33	0.05333	-59
154	MDX library Car Park	10M	20	21	23	-75	-74	-72	-74	83		Y		59.95	0.05995	-60
155		10M	18	20	23	-77	-75	-72	-75	88		Y	Y	98.5	0.0985	-65

Table 7.7 VANET Field Test Measurements for RSU-3 (Inside Pathway).

Serial.NO	PLACE	DISTANCE	RSSI	RSSI	RSSI	dBm	dBm	Average	FSPL	ALTITUDE	LOS	NLOS	DISTANCE (M)	DISTANCE (KM)	fspl	dBm
156	MDX car Park Road side corner	10M	45	50	54	-50	-45	-41	80		Y*		39.63	0.03963	-57	
157		10M	31	30	36	-64	-65	-59	78		Y*		32.02	0.03202	-55	
158		10M	31	35	37	-64	-60	-58	85		Y*		73.38	0.07338	-62	
159		10M	27	30	32	-68	-65	-63	85		Y*		70.76	0.07076	-62	
160		10M	28	30	31	-67	-65	-64	86		Y*		80.84	0.08084	-63	
161		10M	25	27	32	-70	-68	-63	86		Y*		85.35	0.08535	-63	
162	Foot ball pitch starting point	10M	21	15	13	-74	-80	-82	87			Y	92.51	0.09251	-64	
163	End of foot ball pitch	10M	19	16	16	-76	-79	-79	93			Y	172.83	0.17283	-70	
164	Behind forum building	10M	11	9	5	-84	-86	-90	92			Y	168.25	0.16825	-69	
165		10M	7	9	10	-88	-86	-85	92			Y	161.7	0.1617	-69	
166		10M	12	14	15	-83	-81	-80	90		Y		135.23	0.13523	-67	
167		10M	22	24	30	-73	-71	-65	88		Y		99.8	0.0998	-65	
168	Ravensfield Car park corner	10M	16	18	20	-79	-77	-75	88			Y	106.73	0.10673	-65	
169		10M	20	22	24	-75	-73	-71	89		Y		111.81	0.11181	-66	
170	Fenella Building carpark	10M	27	30	33	-68	-65	-62	87			Y	90.93	0.09093	-64	
171		10M	29	30	33	-66	-65	-62	87			Y	87.15	0.08715	-64	

7.4.4 FSPL calculations for our MDX testbed

The Free Space Path Loss model used in mobile and wireless communication to predict the signal strength between the transmitter and receiver, where there is a clear line of sight (Rappaport, 2012). This propagation model will be compared with the real time result that we have collected during the testbed. The formula for free space path loss model are widely used in textbooks and online e.g.,(Christoph Sommer, 2014).

The diagram in Figure 7.3 shows a typical example of scenario with line of sight between transmitter and the receiver with no obstruction during transmission.

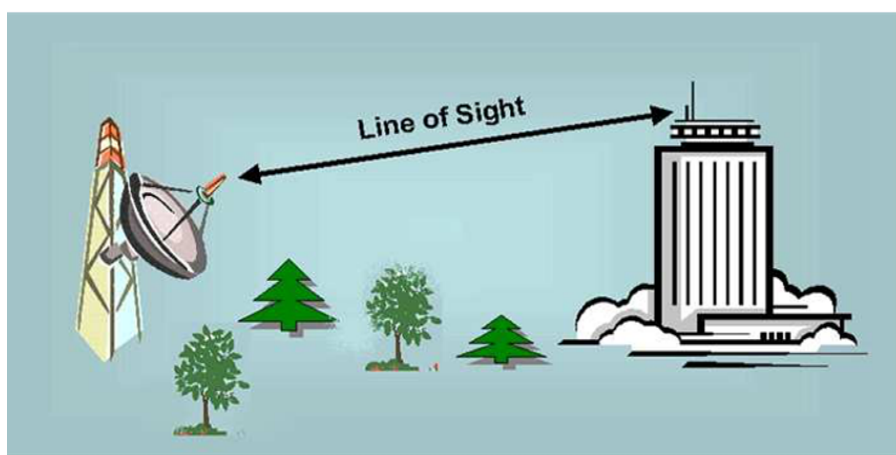


Fig. 7.3 An Example: Free Space Pathloss Model in Line-of-Sight (Rappaport, 2012).

$$\begin{aligned}
 FSPL &= \left(\frac{4\pi d}{\lambda} \right)^2 \\
 &= \left(\frac{4\pi df}{c} \right)^2
 \end{aligned} \tag{7.1}$$

where:

λ is the signal wavelength (in metres), in this case $\rightarrow \lambda = \frac{c}{f}$ or $c = f \times \lambda$,

f is the signal frequency (in hertz),

d is the distance from the transmitter (in metres),

c is the speed of light in a vacuum, 2.99792458×10^8 metres per second.

This equation is only accurate in the far field where spherical spreading can be assumed; it does not hold close to the transmitter.

The formula shown above will give the result in watts but our calculations are in dBm, Therefore, the results were converted to the same units, which included logarithmic conversions. This log based formula below was taken into consideration for calculating the path loss during transmission and to calculate the received power by adding the antenna gain to transmit power which is then subtracted by path loss to add the receiver gain to the path loss which in turn will give the received power in dBm.

$$\begin{aligned}
 FSPL(dB) &= 10\log_{10}\left(\left(\frac{4\pi df}{c}\right)^2\right) \\
 &= 20\log_{10}\left(\frac{4\pi df}{c}\right) \\
 &= 20\log_{10}(d) + 20\log_{10}(f) + 20\log_{10}\left(\frac{4\pi}{c}\right) \\
 &= 20\log_{10}(d) + 20\log_{10}(f) - 147.55
 \end{aligned} \tag{7.2}$$

where the units are as before.

For typical radio applications, it is common to find frequency (f) measured in units of GHz and the distance (d) in km, in which case the FSPL equation is represented as:

$$FSPL(dB) = 20\log_{10}(d) + 20\log_{10}(f) + 92.45 \tag{7.3}$$

- For d, f in meters and kilohertz, respectively, the constant becomes -87.55.
- For d, f in meters and megahertz, respectively, the constant becomes -27.55.
- For d, f in kilometers and megahertz, respectively, the constant becomes 32.45.

In order to use this formula the distance needed to be calculated in meters and the frequency in GHz, hence the constant becomes 92.45. But for our calculation purposes we used the distance in meters as VANET operates in the frequency band of 5.9 GHz. Therefore, in order to perform this calculation we had to convert the band of 5.9 GHz into MHz, therefore, the frequency becomes 5900 MHz and hence the constant changes to -27.55.

An Example of the calculation is illustrated below:

$$FSLP(dB) = 20\log_{10}(37.75) + 20\log_{10}(5900) + (-27.55) = 79.40 \quad (7.4)$$

Therefore, to calculate the received RSSI by the given formula:

Transmitted power (T_r) + antenna gain at transmitter (G_t) - path loss value (PL) + receiver antenna gain (G_r)

Hence,

$$RSSI = 23 + 0 - 79.40 + 0 = -56.4 \quad (7.5)$$

7.5 Analysis from the Initial Coverage Testing before Deployment

This part of the thesis is to analyse the results that have been collected during the field tests. The following parts will show how the free space path loss work when compared with real time results. Also it discusses how there is line of sight (LOS) and Non line of sight (NLOS) occurring and what is the reason for them to cause this occurrence?

7.5.1 Hatchcroft Building

Following graph in Figure 7.4 shows the average received power in dBm and it is then compared against Free Space Path Loss model along with the reading from the physical measured values from the VANET testbed.

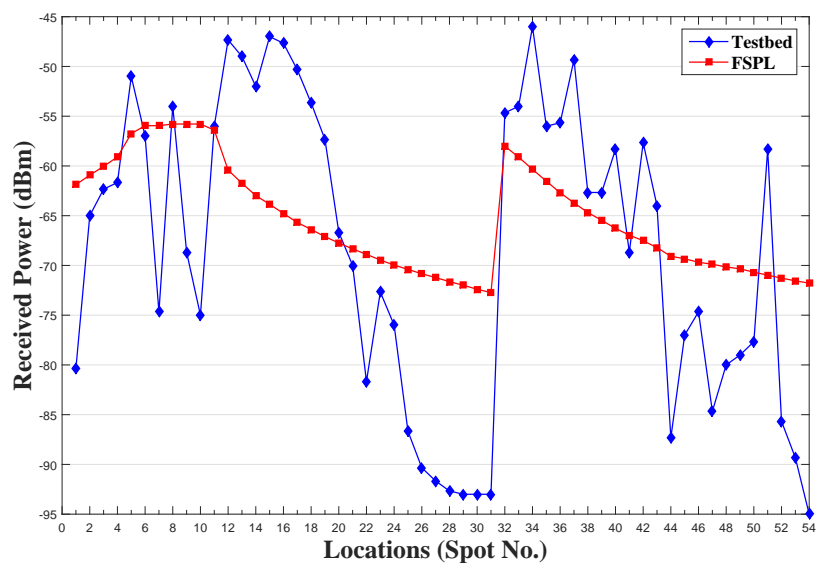


Fig. 7.4 Comparison of RSSI values from testbed and FSPL Model for Hatchcroft Building.

The Hatchcroft building reading were taken in two parts, the first part of the reading was taken on the main road and the graph show the result. Second reading was taken inside MDX pathway. The reason was to see the coverage distance and also to see how trees affecting the line of sight.

The graph in Figure 7.4 shows the combined results of received power from the testbed and Free Space Path Loss model predict received power. The spot where we started our experiment demonstrated a non line of sight (NLOS). This can also

be seen as the spot no: 1 received dBm was recorded at -80 dBm but according Free space path loss the power calculated is supposed to be -62 dBm, therefore, the NLOS affecting is about 18 dBm.

7.5.2 William Building

The second building where the RSU was deployed for testing purposes was William Building and the following graphs show the reading which has been taken from William building and also the Free Space Path Loss model graphs. The graph in Figure 7.5 shows the free space path loss dBm and actual real time reading together.

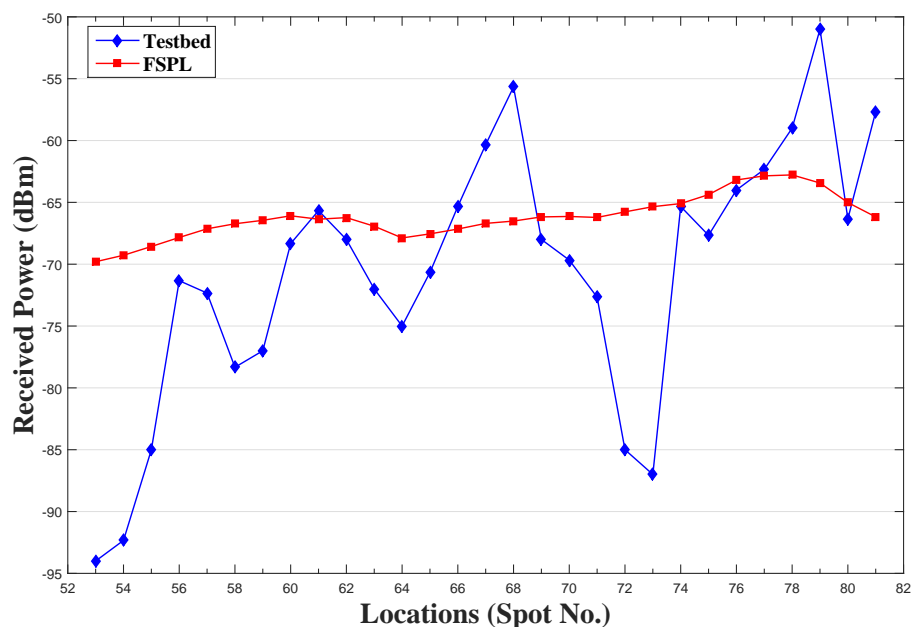


Fig. 7.5 Comparison of RSSI values from testbed and FSPL Model for Williams Building.

7.5.3 Middlesex University Car Park

The next RSU was placed on the car park area in Middlesex University and this RSU could cover the back area of the university. Another reason for us to place the RSU around the car park area was, to create an overlapping effect with the Williams building and the following graph in Figure 7.6 shows the comparison of the calculated Free Space Path Loss value and real time test-bed result.

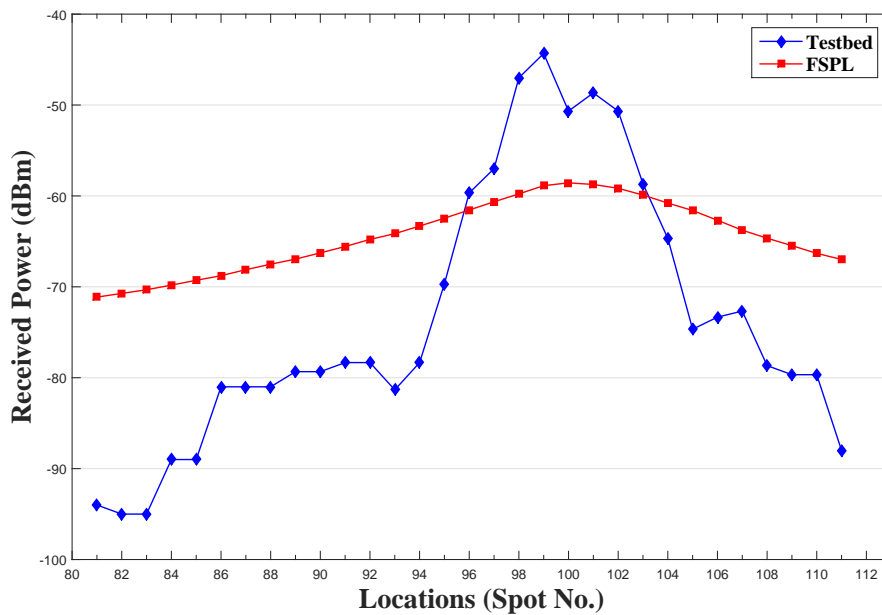


Fig. 7.6 Comparison of RSSI values from testbed and FSPL Model for Car Park.

7.5.4 Grove Building

Finally the fourth RSU was placed at Grove building at Middlesex University. The main purpose of this RSU to have a over lap region with other RSU. Also this RSU will cover most of the pathways inside the university. Most of the RSSI values collected inside the MDX University. The graph in Figure 7.7 shows the reading taken and also by looking at the graphs we can see where the line of site and non line of sight and compare with Free Space Path Loss model.

The first reading was taken near the back gate of MDX car park and it is bit far from the RSU and it was NLOS so, as expected, we received the dBm value as -89 and according to FSPL the dBm should be -74 that -15 dBm affect on the spot, due to NLOS. Picture 12 will shows NLOS below and most of the spots for this RSU are NLOS caused by trees and buildings.

The graph illustrated in Figures 7.4, 7.5, 7.6 and 7.7 where blue line represents the real-time measurements from the testbed, show some high peaks in the graphs. This is due to physical constraints and not due to the actual values, i.e. these effects are due to the multi-path spreads or fads (i.e. scattering effects of the signals).

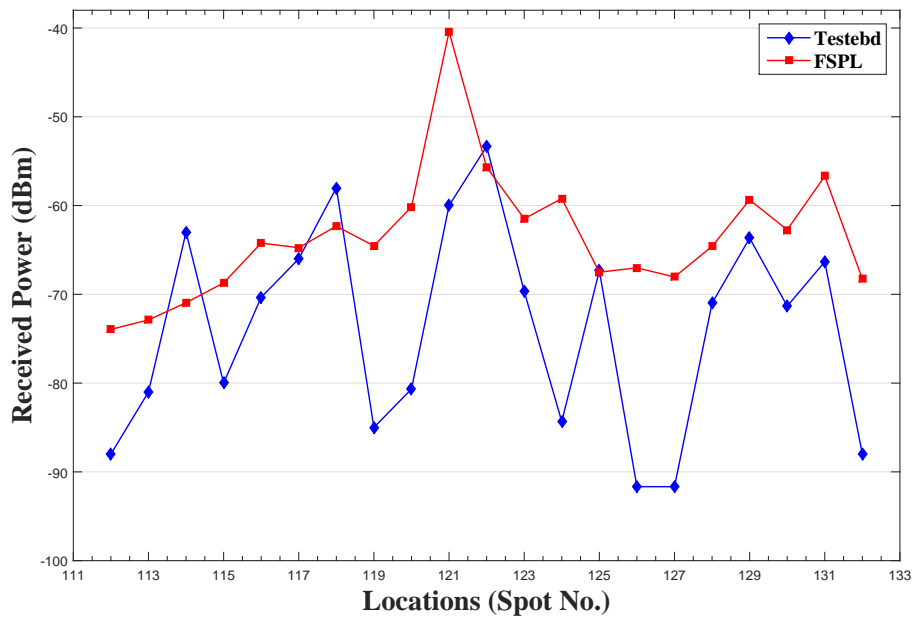


Fig. 7.7 Comparison of RSSI values from testbed and FSPL Model for Grove Building.

7.6 Overlapping Regions in MDX VANET testbed

One of the main goal of the testbed was to find out the coverage range of the RSU and if we know the coverage of the RSU we can come to a conclusion about the performances of the devices. RSUs were places at four different locations within the university with the sole purpose of providing full coverage for the entire campus. Three of the RSUs were places at height on three different buildings while the other one was places on ground level at the car park. There were less building around the car park so placing the RSU on ground level did not have a significant effect performance wise.

As shown in Figure 7.8 on the map above, each RSU has its own unique colour making each RSU different from one another. The map also shows the overlap regions in slightly darker colour. The most important thing to note is that each RSU is overlapping the coverage range of the other RSUs. This make for a well-planned testbed and also reflects on how strong the devices are as they are able to provide such a big coverage range, i.e. the RSU uses 200 mW transmission power. The testbed was successful as we managed to cover not only inside the university but the two main road which are The Borough Road and also coverage for the Church End Road - two roads which consistently have traffic and pedestrians around.



Fig. 7.8 Map with Overlapping Coverage Ranges of all RSUs.

In this thesis, some the previous testbed work had been carried out by members of the Middlesex University VANET team, taking into consideration the effect of the velocity, beacon frequency and size of the beacon. This was done making use of simulations, live test-beds and mathematical calculations. Therefore, from the given results derived from experiments carried out by MDX VANET team, it was observed that the Signal-to-Noise ratio which is totally dependent on the path-loss model used and this plays a highly important role in arriving at a mathematical equation to help calculate the packet delivery ratio which in turn provides a good prediction and reliable communication of the life-critical safety applications for the VANET systems, a potential solution for future intelligent transportation system. In addition, another very key observation was made from the results highlighted the packet delivery ratio, which was observed and highlighted in the previous chapters, that as soon as a the vehicle moves into the detection range of a RSU, the probability of successfully receiving a packet is very low but the probability gets closer to one as the distance between the vehicle and the RSU reduces. These observations forced us to believe that the Free Space Path Loss (FSPL) radio propagation model used for our MDX VANET testbed comparison is not 100% efficient and due to the high reliability needed for the safety messages, VANET can not afford to have any packet losses. Therefore, there is a significant need for an adaptive yet reliable radio propagation model for VANET systems.

7.7 The Final Deployment of the MDX VANET Testbed

The objective of this task was to design MDX VANET Research Testbed and this section details the challenges that were addressed. The first objective was to test the equipment in the laboratory conditions to ensure there was no interference with other communication systems and to understand the basic elements of the technology such as beaconing. The next challenge was to identify the best locations to mount the RSUs in order to cover most of the Hendon Campus and the surrounding roads. This involved making a detailed coverage map based on proposed locations of the RSUs. This was done manually and with the assistance of the undergraduate students. In order to determine the best location for the RSU, it was important to minimise the distance between the RSU and the router elements in the university network. This enabled us to directly backhaul data from the RSU to the central MDX VANET Server located in the basement of Sheppard's library using the university network.

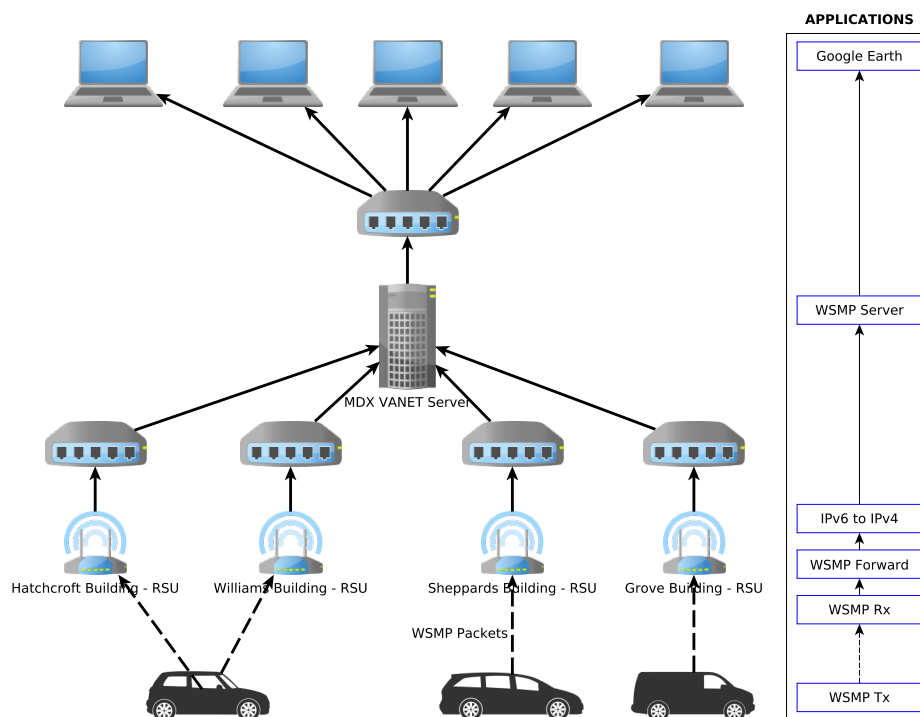


Fig. 7.9 NETWORK DIAGRAM.

Figure 7.9 shows the network diagram of the MDX VANET Testbed for the Hendon campus. Four RSUs have been deployed on top of the Hatchcroft building, Williams building, Sheppard's library building and Grove building. Figure 7.9 also shows the applications running at the respective devices. Wave Short Message Protocol (WSMP) Tx is an application used by the OBU to broadcast the packets containing Basic Safety Messages (BSM) and the RSU receives these packets using WSMP Rx application. The received packets are forwarded to the server using the WSMP Forward application via an IPv6 address of the server. Since, the MDX Network is not IPv6 enabled; an IPv6 to IPv4 conversion application was developed.

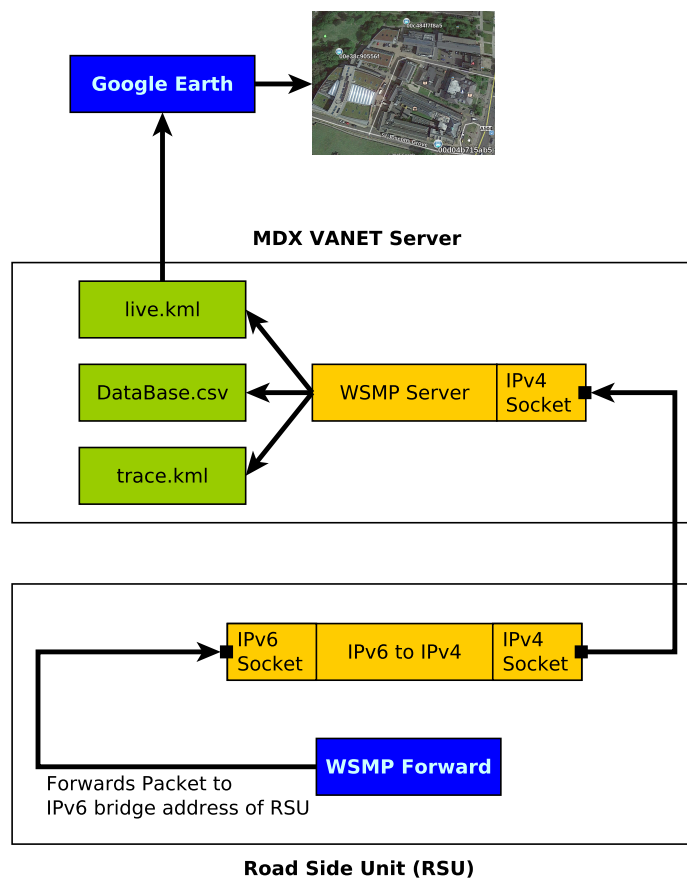


Fig. 7.10 Data forwarding from RSU to Server.

This application was made to run on the RSU and it receives the IPv6 addressed packets on the bridge address of the RSU and redirects the packets to the IPv4 address of MDX VANET Server's. The MDX VANET Server uses WSMP Server application to receive the packets and will save the data. At this stage additional information such as a timestamp and RSU's IP address are stored along with the

message received. The received data was saved in three different files: trace.kml, live.kml and Database.csv. trace.kml contains the whole trace of the GPS coordinates contained in the received packet, live.kml contains the live or current positions of each OBU through the packets received from those OBU and this file is saved in the Apache Web Server space for remote access as shown in Figure 7.10. Using Google earth, adding a network link to the live.kml file, the live tracking of the OBUs was achieved. The third file Database.csv contains the most of the available information in the packets such as the OBU's MAC address, the received signal strength indicator (RSSI) Value of the received packet, GPS coordinates along with the time stamp of the packet and IP address of the RSU by which the packet has been forwarded. Every day the Database.csv file was backed up for analysis through MySQL.

One of the major problem that had to be solved occurred when the RSU on the Williams Building was deployed and it was found not to be able to achieve the expected coverage area. We, therefore had to raise the height of the RSU by approximately five meters.

7.8 MDX VANET Trial

With the successful deployment of the Testbed it was now possible to move to the second objective of the project which was to conduct an extensive trial of the VANET Testbed. In order to do this, we first had to publicise the trial to obtain volunteered drivers who were willing to have OBUs placed in the cars for at least a day. This was achieved through the development of a VANET webpage (www.vanet.mdx.ac.uk), emails and the deployment of a blog via the University's website. The trial was originally intended to last for one week i.e., Jan 4th to Jan 11th 2016 but was extended to 15th Jan 2016.

Around ten people volunteered for the trial and OBUs were placed in their cars over several days. Each OBU contained very simple instructions about the trial showing how to operate such that successful readings could be obtained. In addition, an additional OBU was placed in a small utility vehicle belonging to the Middlesex University. This utility vehicle enabled us to obtain continuous readings of the vehicles position within the Hendon campus. However the other participants drove around different roads in the surrounding area including Watford Way (A41) at different times so as to obtain to get a picture of the traffic patterns in the area. Photos of the trial are shown in Figure 7.11.

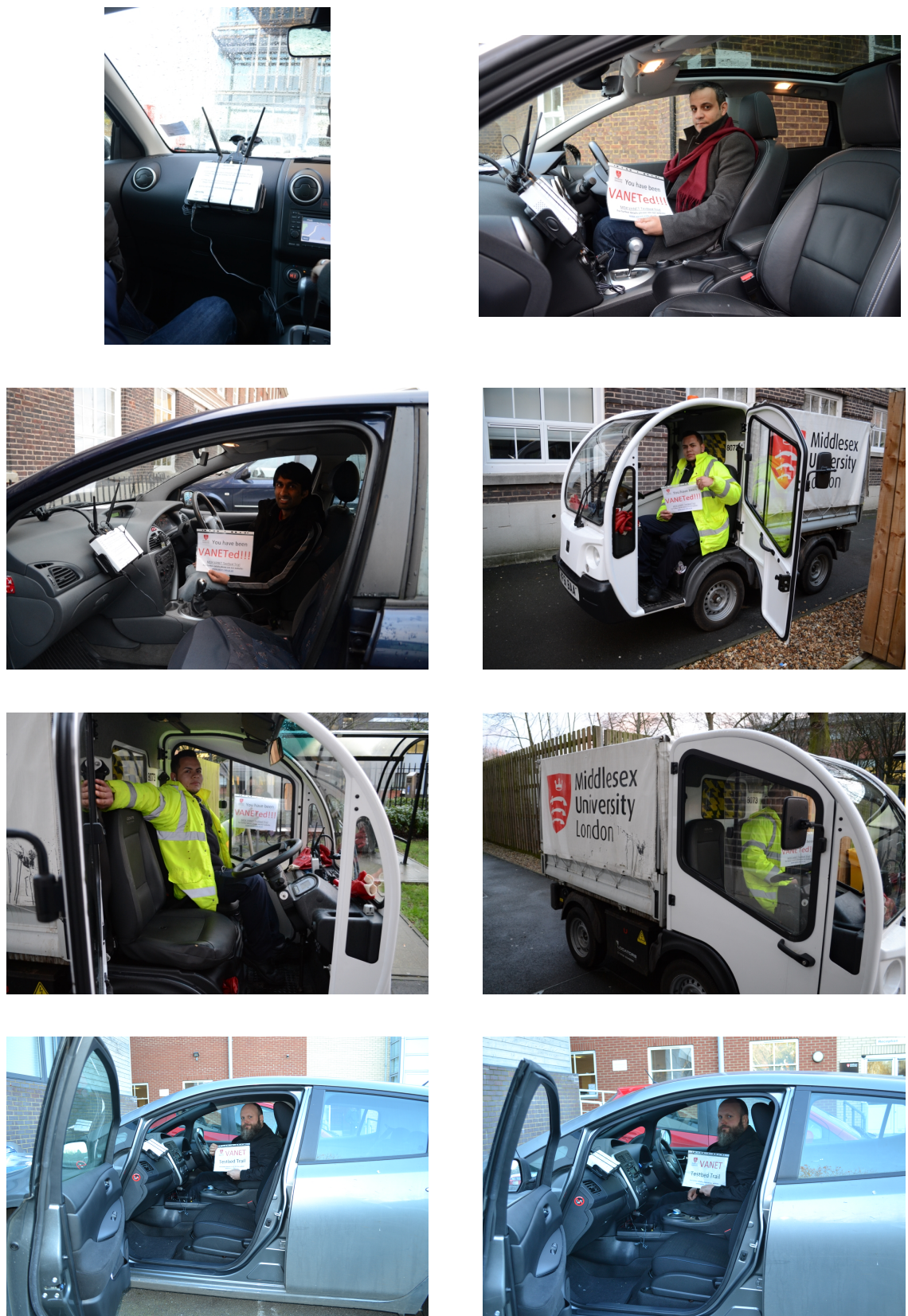


Fig. 7.11 MDX VANET Trial Photos.

7.9 Results - MDX VANET Testbed Deployment

7.9.1 Coverage Graph

The image in Figure 7.12 shows the unique GPS coordinates from the packets received by the MDX VANET Server, sent by the OBUs which were placed in the cars of the volunteers. Figure 7.12 displays the trial data for a 24 hour period which was collected on 8th January 2016 and a total of 390653 packets (around 17.14 MB) was received in that period. The coverage was better than anticipated but this was only because of the height of the RSU deployment. There are some blind spots that can be observed; these were purely due to effects of surrounding buildings. By these observations it is clear that we need more RSUs alongside the road to be deployed in an urban area, but if deployed on high raise buildings the advantages can be seen and might need less RSU. The dense line indicate very reliable communication and random spots indicate only few packets were received and not a continuous reliable communication is happening.

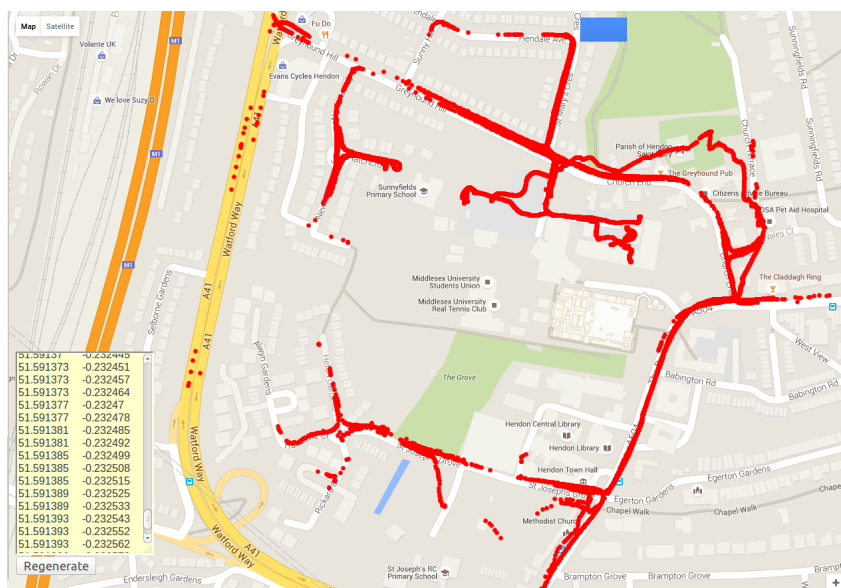


Fig. 7.12 Coverage Map.

The farthest point from where the packets were sent by the vehicles and successfully received by the RSU was approximately 1.15 Km from the Williams Building RSU to a point on the East side of Watford way close to where the A41 and A1 divide! This was achieved purely due to the very high elevation of the RSU on the Williams Building hence allowing Line of Sight communication over a great distance.

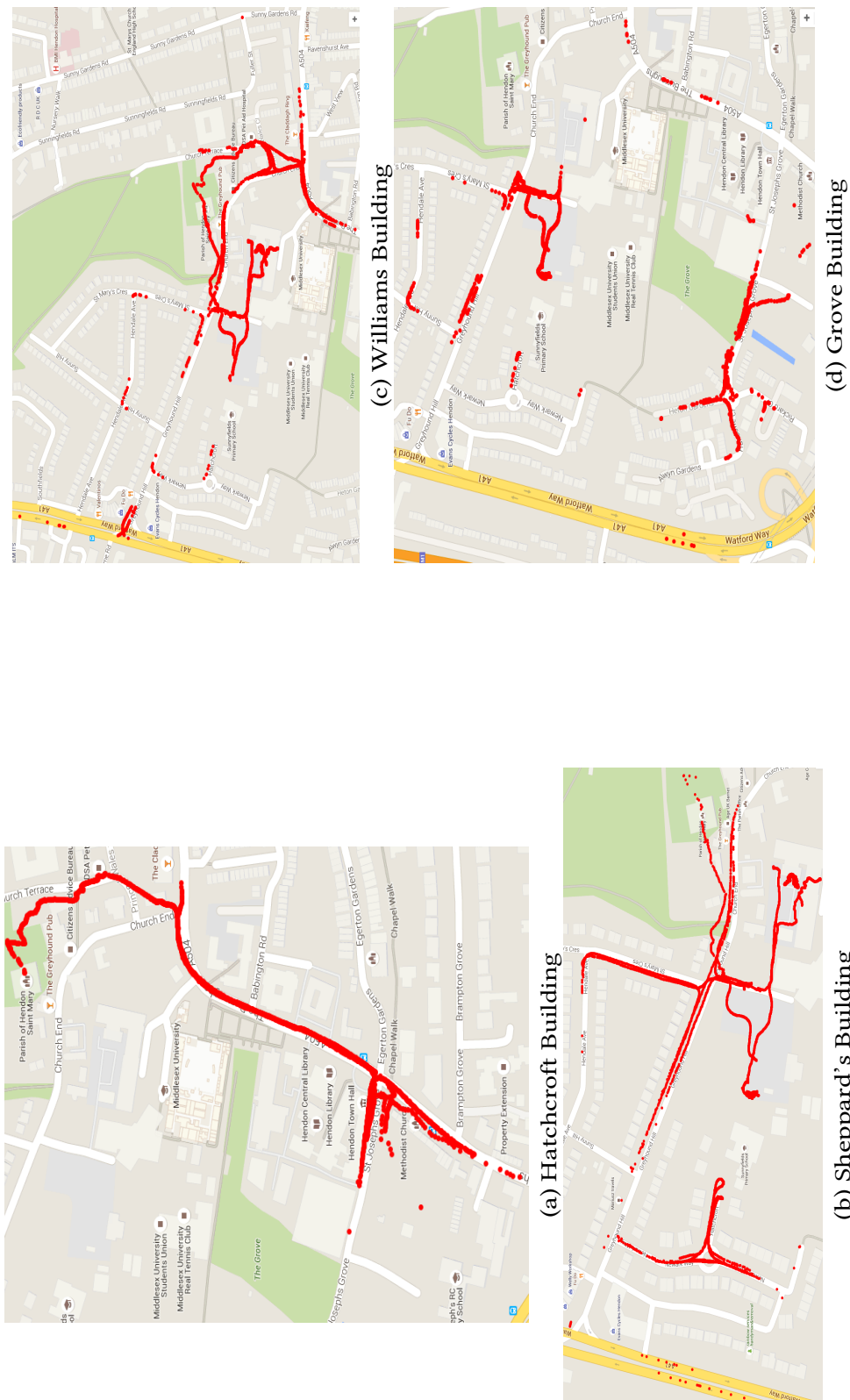


Fig. 7.13 Coverage of each RSU.

The Figure 7.13 shows the individual coverage achieved by the RSU located on each building. We can observe that the more coverage is achieved for the RSUs deployed at higher heights and also which have clear Line of Sight for the intended roads around. In Figure 7.13 we can observe some blind spots i.e., there are spots where the red dots are not continuous. For example the coverage map of RSU deployed at Grove building has almost no coverage on the A504 due to the blockade of signal propagation because of the buildings.

7.9.2 Live Vehicle Tracking

Figure 7.14 shows a screen shot with three cars moving around. Google Earth was used and the web address of the live.kml file was used for displaying and live tracking of multiple cars remotely. This test was performed by fixing an OBUs in one of our volunteer's car, one on the MDX Electric Cart which is used to collect rubbish inside university and one carried by a pedestrian. The movement of the vehicles was updated periodically every one second (least time interval that can be set in Google earth). Each vehicle was labelled and displayed with their respective MAC address of the OBU.

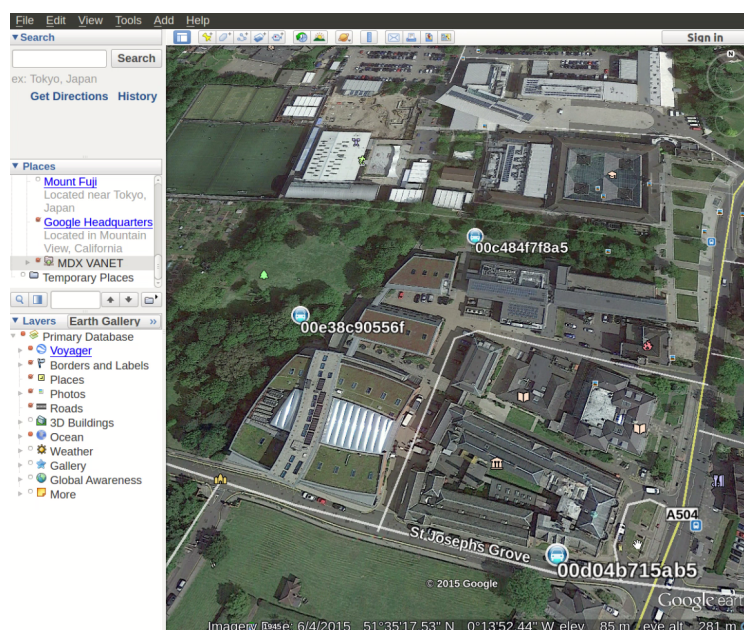


Fig. 7.14 Live Tracking Screen shot.

These were the primary results of the initial trial of the MDX VANET Testbed. Further observations are discussed in the next section.

7.10 General Observations from the MDX VANET Trial

For the most part, the technology worked in the sense that we got substantial readings over a large coverage area. However, there were some issues including the need for better cooperation between the various stakeholders of the project including Middlesex University, Barnet Council, Transport for London and the Department for Transport. This means that in order to take this research further in terms of a larger deployment, a powerful strategic team from all parties will be needed to significantly increase the scale of deployment of VANET technology.

The actual results were interesting on several levels. Firstly, we were surprised at the coverage of the RSUs that were mounted on the buildings of the Hendon campus because we were able to get readings from quite a far distance on Watford way (A41). This leads to the need to investigate both roadside and non-roadside locations for the RSU deployment. For example, it would be good to compare RSUs along the roadside with RSUs mounted on a conventional cellular mast.

In both cases however, this project clearly shows the need to better understand the communication/propagation models in order to work out the best position for the RSUs to achieve good coverage in all types of environments, both urban and motorway. In this trial, determining the best place of deployment of the RSUs was done manually, better communication/propagation models would allow us to semi automate this process leading to more rapid deployment.

In terms of hardware, we found that the firmware of the devices was not stable and we had to do various updates and sometimes we had to revert to older versions due to bugs being introduced because of lack of testing. This was time consuming because we did not have enough information, from manuals etc., to quickly fix the problem. A lot of these problems reflect the fact that VANET is still a very new technology hence, it will take some time for the hardware platform to work seamlessly. In addition, a low level software platform should be defined to drive the hardware functionality. In essence, we were too dependent on the manufacturers, in this case ARADA Systems, and so we were unable to get some program code for key functions on the RSU.

Because the equipment were purchased from ARADA Systems, which is a US based company, it was necessary to adjust the operational frequency parameters in order to comply with EU standard requirements. For this trial, this was a minor inconvenience, however, going forward the difference in Standards may have a significant impact on the applications since the EU Standard has dedicated service

channels for both safety critical and non-safety critical applications but the US standard does not. Hence, there will be a need to have one standard in the future.

7.11 Extended Testbed Project - Department for Transport (DfT)

This Project is innovative for several reasons, firstly it allows the deployment of new networking technology which will provide greater information about the use of the transport system and hence enable a platform for new algorithms to be developed to improve traffic efficiency. This technology integrates several networking technologies enabling a complete information platform within the vehicle such as GPS (less than 1 meter accuracy), Bluetooth and high-power 802.11p radios. It also allows simple integration with mobile phone technology. The information that can be provided from the vehicle to the central traffic management system include location data (GPS coordinates), speed of the vehicle, braking information and vehicle health data including engine efficiency and the state of electrical and electronic subsystems. In turn, the central system can provide information to the vehicle on transport infrastructure such traffic lights status, congestion, accidents and road management situations.

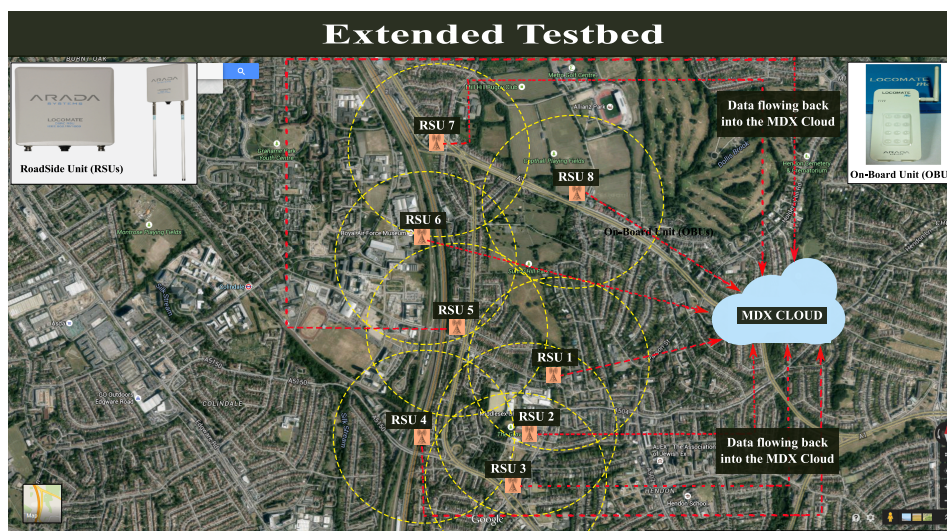


Fig. 7.15 Extended Scenario for MDX VANET testbed.

We at Middlesex University have taken the initiative and have currently deployed a VANET testbed on the Hendon Campus. However, we would like to extend the initial Middlesex testbed to cover more roads including the Burroughs (A504),

Greyhound Hill, the Barnet By-Pass (where the A1 and A41 converge) and along Watford way(A41) to A504 as shown in Figure 7.15.

7.11.1 Next Step/Recommendations for Future Testing and Implementation

It is quite clear that the next step for this project should be a deployment along a significant motorway in this country. This will allow a detailed understanding of VANET systems in such environments to be obtained leading to wide scale deployment of VANETs regionally and nationally.

Once the extended testbed has been built, we intend to conduct an extensive trial of road users and pedestrians as the extended network will have twenty OBUs. We intend to place these OBUs in the vehicles of different users; each OBU will be used for one day by one user. Hence, we intend to gather over 1250 sets of readings about day journeys in the area over the period of the trial. These readings will be housed on our dedicated storage server. This is a file server for applications and provides redundancy in the face of hardware and network failures. The Middlesex Cloud (MDX Cloud) is a Cloud system running OpenStack (which is a Cloud Management system) and Hadoop, which is used to process data on the Cloud, will be employed to generate real-time results. As previously mentioned this would require a complete roll-out strategy between all the stakeholders. If we consider London in particular, local Boroughs should be working with the Transport for London (TfL) and the Department for Transport (DfT) to do more trials on VANET technology.

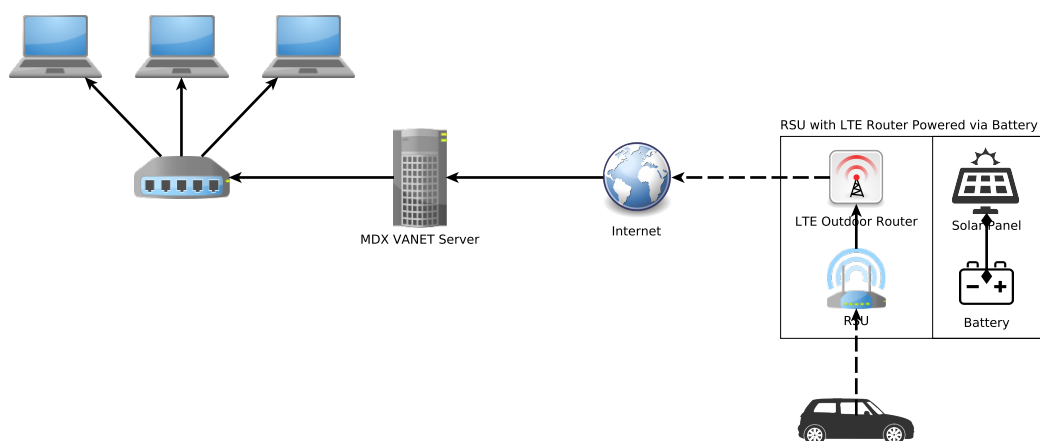


Fig. 7.16 Network Diagram of a LTE Backhauled Mobile RSU.

We are also building a Mobile RSU as shown in Figure 7.16 which will allow us to move the RSU setup anywhere required for future tests. The physical setup is shown in 7.17. In order to backhaul the data received by the RSU, an LTE Outdoor Router will be interfaced to the RSU. Hence, Internet will be used to forward the data to the MDX VANET Server. For powering both RSU and the LTE Outdoor Router, a battery along with a solar panel to recharge the battery will be customized, built and used. This further allows us to measure the power consumption and identify the challenges in building such green energy systems for ITS.

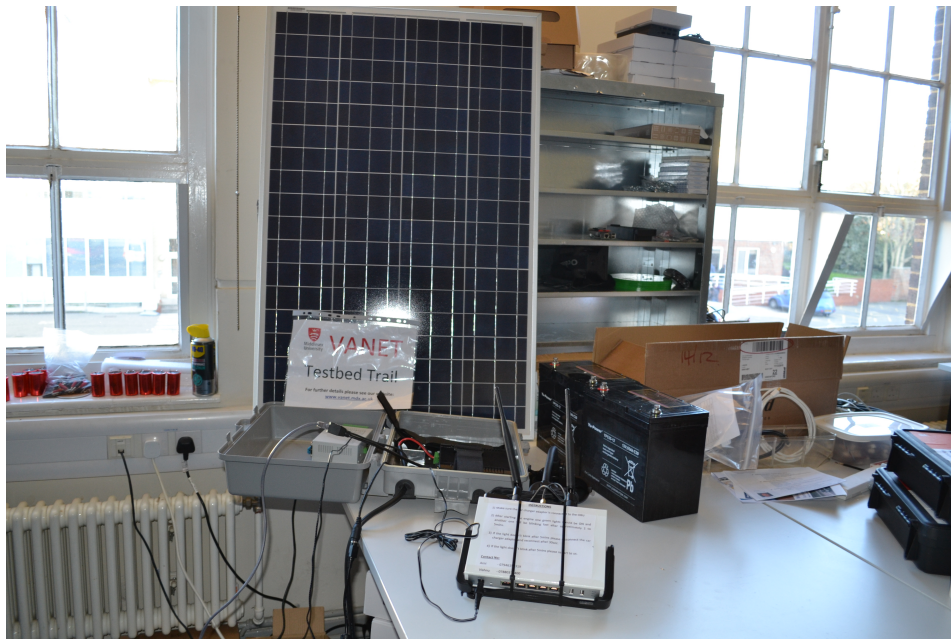


Fig. 7.17 Building LTE Backhauled Mobile RSU in Lab.

7.12 Summary

Intelligent Transport Systems (ITS) benefits a lot from VANET research and part of that progress relies on the simulation approach. Over time many tools have been developed to allow create various scenarios which have reduced costs of real-time tests. However there is still a limitation of a complete simulation software. Our experimentation shows that several tools have to be used in order to obtain close to real world results. The privilege of developing the MDX VANET TESTBED has led us to be a proving ground for VANET research.

At the MDX University, RSU were located at four different locations including one RSU on the ground floor. The highest coverage range we achieved in the testbed was 300 meters under None-line-of-sight. One of the aim of the testbed was to provide full RSU coverage for the campus. However, the results were beyond expectations as four RSU managed to provide coverage to surrounding outside the university such as The Burroughs Road and Church End Road. The OBU acts as a client while the RSU as a server. As a result we managed to successfully set-up a testbed and achieve communications between the devices using the applications developed.

Therefore, this chapter clearly shows that VANET technology can be used to form an Intelligent Information Platform for Smart Cities. It has also highlighted the weaknesses and strengths of this new technology and the key issues to be addressed in its wide scale deployment. Hence, the evolution of this technology and its potential to transform Smart Cities need to be fully understood by the transport authorities.

Chapter 8

Conclusion and Future Works

In this chapter, a complete summary of the work done in this thesis is given and the major contributions are highlighted. This is followed by conclusions resulting from this work and a discussion on the directions for future research is presented.

8.0.1 Summary of the Work Done

In this thesis, we have investigated the factors that affect seamless communication in VANET systems using the concepts of Network Dwell Time (NDT), Exit Times (ET) and Time Before Handover (TBH). Initial investigation showed that effects communication was dependent on the frequency, the length of the beacon and the velocity of the vehicle. These parameters were further investigated in detail to show how communication dynamics change with these parameters. The effect of frequency of the beacon was examined using cumulative probability approach. This resulted in the development of a new probabilistic handover mechanism. In addition, we have shown that the length of the beacon significantly affects the rate of change of the individual probability as the vehicle approaches the RSU. Furthermore, this work showed that the velocity of the vehicle affects the difference between the Cumulative and the individual probabilities. Finally, a new VANET Testbed was developed which highlighted the need for better propagation model for seamless communication in the urban environment.

8.0.2 Contribution to Knowledge

This research contribution of this thesis can be summarised as follows:

1. In Chapter 1, we began by motivating the need to look at VANET systems, and how it is being proposed as a long-term solution for Intelligent Transport

Systems. For this purpose, we first began to explore the use of simulation tools such as OMNeT++ and Veins framework (a framework used especially for Vehicles in Network Simulation) for highly mobile environments such as VANET systems. In Chapter 2, a thorough analysis of critical review of the literature was presented which opens new horizons for research by highlighting some of the key research questions. In addition, Chapter 2 also contained a detailed a literature survey of the standard and protocols in use, the state of art VANET applications and related work being used in this thesis. Some of the concepts used from the Y-Comm framework was explained in detail along with handover classification adapted from Y-Comm architecture.

2. In Chapter 3, preliminary investigations into communication mechanisms in VANETs were carried out to determine the parameters that affect the seamless communication because the current research has not adequately captured the real-world constraints in VANET handover techniques. The initial investigations was done by looking at a simple scenario to understand the communication mechanism in a VANET environment using ideal and measured values of the NDT. This showed that the communication dynamics was dependant on these three factors: the frequency and length of the beacon as well as the velocity of the vehicle.
3. In Chapter 4, a more in-depth analysis was conducted by investigating the effects of beacon size and beacon frequency as well as the velocity of the vehicle in order to achieve seamless handover. This was done by further exploration of the estimated Network Dwell Time for different beacon sizes, frequency and velocity of the vehicle. In this chapter, a PacketOK number is computed from the OMNeT++ simulation used. This PacketOK formula in this Chapter appears to directly take into account only the size of the beacon but the results from this chapter show that the frequency of the beacon and the velocity of the vehicle does also need to be taken into account. This work suggested that a cumulative probability approach is needed rather than just individual probabilities.
4. In Chapter 5, the cumulative approach and the analytical framework were examined in more detail. In Chapter 5, we further investigated the impact of beaconing on Network Dwell Time using the cumulative probability and the probability of individual successful beacon reception. However, the results also showed that the frequency of the beacon only affects the cumulative probability and hence it verifies the argument that they affect different aspects

of the probability space with regard to the Network Dwell Time. Comparative simulation results were presented in order to validate the accuracy of the models presented. Furthermore, these results can be used to develop a probabilistic proactive handover approach based on cumulative effects of beaconing. This was challenging because the probability of a successful reception increase as the vehicle get closer to the RSU and hence this is a non-stationary scenario.

5. Chapter 6, presented an important framework for the research by presenting an approximate model of communications in VANET systems with respect to length of the beacon and velocity of the vehicle. The equation for Delta P (ΔP) was re-examined with respect to the rate of change in the SNR (i.e., $dp/dSNR$). This showed that $dp/dSNR$ was directly proportional to length of the beacon as the vehicle approaches the RSU. The length of the beacon severely affects the individual probability as the vehicle approaches and moves away from the RSU. In addition, by looking at the difference in the number of beacons between $CP = 1$ and $P = 1$, allows us to capture the effects of velocity on the overall system. Our finding show that the difference in these two parameters decreases sharply as the velocity of the vehicle increases. Therefore, higher beacon frequencies are necessary to support handover for higher speeds.
6. In Chapter 7, we looked at deployment of RSUs as part of a VANET Testbed which is set-up at Middlesex University, Hendon Campus. This was done in order to achieve a better understanding of VANET systems operating in an urban environments for capturing real-time constraints i.e., propagation models needed for highly mobile environments such as VANETs. In addition, environmental factors needed to be considered for real-time deployment studies to see how they affect the performance of VANET systems under different scenarios. This was to eventually facilitate a comprehensive feasibility study in order to develop efficient propagation models for VANET systems. Our initial findings indicate the need for better propagation models because the Free Space Path Loss model does appear to capture all the parameters in the urban environment.

8.0.3 Thesis Contributions

Some of the significant contributions that have been highlighted in this thesis are as follows:

- To show the differences in the ideal NDT and the measured NDT based on the frequency and size of the beacon for two different velocities of vehicle.
- To investigate the relationship of cumulative probability distribution and its effect on measured NDT.
- To show that the frequency and size of the beacon have different effects on the cumulative and the individual probabilities.
- To investigate how the probability distribution of successful beacon reception changes with velocity.

Some of the key Research Questions that have been answered by way of contributions that have been highlighted in this thesis are as follows:

- To develop a comprehensive Analytical Model to model a realistic NDT.
- Implementation of an Analytical Model and comparison against simulation results to evaluate how realistic it is?
- To test the NDT Model in complex scenarios in terms of V2I communication types and also take into account density, Interference issues.
- To implement VANET-TESTBED for realistic comparison of results against theoretical NDT and simulation NDT.

For seamless communication we need NDT as we use Y-Comm concepts. Therefore our aim was to model the NDT for getting a realistic values and to find mechanism for seamless handover in order to achieve Seamless Communication in VANETs. Our main objective was to analytically model the NDT, which will suit a real-time scenario, in-line comparisons with simulation results and real-time calculations from the VANET Testbed at Middlesex University campus.

8.0.4 Summary

The research work demonstrated in this thesis suggests some important future directions in this field of study. The investigation clearly indicates that probabilistic approach based on cumulative probabilities can optimize the way handover is

currently dealt for achieving seamless connectivity in highly mobile environments such as VANETs. Thus, the analysis shown by means of simulation and an approximate model how the beaconing frequency, the length of the beacon and the velocity of the vehicle affect communication dynamics in highly mobile environments. The real-time experimental observations using the testbed demonstrated that there is a strong need to develop a more vibrant and focused propagation model for dense urban environments where buildings and objects are the main factors. In addition, the results obtained from the proposed models in this thesis, offer themselves as essential findings for identifying the key parameters to examine optimal coverage required for seamless connectivity. Also, these models which are helpful in understanding the complex interaction between the RSU and the vehicle, are vital factors such as handover and mobility.

8.1 Conclusion

In conclusion, the thesis showed a comprehensive analysis to identify the three main parameters i.e., the beacon frequency, the length of the beacon and the velocity of the vehicle which can be used to develop a probabilistic proactive handover approach based on cumulative effects of the beaconing. This was further proved by ways of extensive packet-level simulation and through our approximate models considering proactive handover phenomenon needed for seamless communication in VANET systems. The thesis provides a more comprehensive view of all three techniques used in order to conduct a strong research such as simulation techniques, developing analytical models and realistic values from the prototype VANET testbed, which answers the research questions in this thesis.

8.2 Suggestions for Future Work

Cooperative applications for VANET will require seamless communication between Vehicle to Infrastructure and Vehicle to Vehicle. In order to have seamless communication for these applications, it is necessary to look at handover as vehicles move between Road-side Units. Traditional models of handover used in normal mobile environments are unable to cope with the high velocity of the vehicle and the relatively small area of coverage with regard to vehicular environments. The Y-Comm framework has yielded techniques to calculate the Time Before Vertical Handover and the Network Dwell Time for any given network topology. Furthermore, by knowing these two parameters, it is also possible to improve channel allocation

and resource management in network infrastructure such as base-stations, relays, etc. In this thesis, we explained our overall approach by describing the VANET Testbed and show that in Vehicular environments it is necessary to consider a new handover model which is based on a probabilistic rather than a fixed coverage approach and show how the effects of the length of the beacon and the velocity of the vehicle are displayed.

The Future work has been highlighted below :-

1. This thesis has introduced the new concept of probabilistic handover based on cumulative entrance and exit probabilities. It is hoped that this work can be included in an overall system of handover techniques as explored in the Y-Comm architecture. This will help us in developing realistic techniques of estimating ΔP , P , CP and $NDTr$ which will be incorporated into the handover policy management mechanisms in mobile devices which will allow proactive seamless handover in both urban and motorway context.
2. This work points to the need to look at proactive handover for highly mobile environments and also their effects on the allocation of resources. This is being pursued by (Paranthaman et al., 2015).
3. This work concentrated on relatively a less complex scenario but going forward we need to look at more complex situations such as:
 - (a) For example, Vehicle-to-Vehicle (V2V) scenario and also Pedestrian-to-Infrastructure (P2I) scenario.
 - (b) To investigate the interference issues in the above mentioned scenarios.
 - (c) In the long term, we are seeking to develop a comprehensive framework that includes types of modulation being used as well as traffic density in order to handle seamless handover in both urban and motorway contexts.
4. To extend our Initial Testbed at Middlesex University in and around Barnet surrounding area in order to understand the urban context. And further extend the research by comparing the results attained from the extended testbed by comparing it against enhanced simulation experiments in order to examine new propagation models leading to more effective handover policies.

8.3 Final Statement

It is predicted that in the near future all the vehicles will be manufactured with an in-vehicle on-board system (On-Board Units) which will facilitate services like real-time traffic reporting, real-time vehicle navigation, social networking, video streaming, online-gaming, internet access and moreover vehicle safety applications preventing accidents. This phenomenon will not only revolutionize the automotive industry, but with the every growing interest of such technologies for vehicular communications, it is determined that about 50-70% of the vehicles by 2016 will be connected either by embedded systems or by using of in house apps developed for the auto industry. Global companies like Google (Google, 2016), Microsoft (Microsoft, 2016), Apple (Apple, 2016) and Blackberry (Blackberry, 2016) have already developed and released their mobile operating systems for the connected-cars theme.

Impelled by the increased demand and due to enormous market penetration of mobile apps as the current trend setter, it has now become a serious challenge for cellular industry to provide frameworks in order to meet this huge demand of vehicular networking. Therefore, it is envisioned that although the IEEE is committed to further optimise and enhance 802.11p as the main communications for vehicular networking. In addition, it would be worthwhile to consider cellular networks for providing the infrastructural support for the non-safety applications (i.e. infotainment applications) which require more bandwidth and the low-cost cellular networks to the vehicles.

Therefore, this will enable both vehicular and cellular networks achieve both scalable and cost-effective solutions for the future vehicle communications. This would also enable them to connect the vehicular networking environment to the existing Internet framework and applications, such as video streaming, content downloading via cloud computing. Further, this can be regarded as the most practical and convenient solution for enabling ubiquitous and reliable connection to vehicles in the densely urban environments. Therefore, this convergence of vehicular networking and existing cellular infrastructure will become one of the key issues for the next-generation networks efficiently.

References

- M. Almulla, Yikun Wang, A. Boukerche, and Zhenxia Zhang. Design of a fast location-based handoff scheme for IEEE 802.11 vehicular networks. *Vehicular Technology, IEEE Transactions on*, 63(8):3853–3866, Oct 2014. ISSN 0018-9545. doi: 10.1109/TVT.2014.2309677. URL <http://dx.doi.org/10.1109/TVT.2014.2309677>. 36
- Andras Varga. Omnet++: An extensible, modular, component-based C++ network simulation, Jan 2014. URL <http://www.omnetpp.org/>. 56, 64, 69, 71, 100
- Apple. Carplay: An app for Apple Auto iOS and iPhone, Jan 2016. URL <http://www.apple.com/uk/ios/carplay/>. 158
- AradaSystems. Arada systems, Dec 2015. URL <http://www.aradasystems.com>. 124
- Kamran Arshad, Ferdinand Katsriku, and Aboubaker Lasebae. An investigation of wave propagation over irregular terrain and urban streets using finite elements. In *Proceedings of the 6th WSEAS Int. Conference on Telecommunications and Informatics, TELE-INFO'07*, pages 105–110, Stevens Point, Wisconsin, USA, 2007. World Scientific and Engineering Academy and Society (WSEAS). ISBN 888-777-6666-55-4. URL <http://dl.acm.org/citation.cfm?id=1353841.1353861>. 51
- Maen M. Artimy, William Robertson, and William J. Phillips. *Vehicular Ad Hoc Networks: An Emerging Technology Toward Safe and Efficient Transportation*, pages 405–432. John Wiley & Sons, Inc., 2008. ISBN 9780470396384. doi: 10.1002/9780470396384.ch14. URL <http://dx.doi.org/10.1002/9780470396384.ch14>. 16, 17, 18, 19
- M. Augusto, R. Vanni, H. Guardia, M. Aiash, G. Mapp, and S. Moreira. Myhand: A novel architecture for improving handovers in NGNs, Jan 2014. URL http://www.thinkmind.org/index.php?view=article&articleid=aict_2013_9_40_10181. 36, 39, 40
- A. Autolitano, C. Campolo, A. Molinaro, R.M. Scopigno, and A. Vesco. An insight into decentralized congestion control techniques for VANETS from ETSI TS 102 687 v1.1.1. In *Wireless Days (WD), 2013 IFIP*, pages 1–6, Nov 2013. doi: 10.1109/WD.2013.6686471. URL <http://dx.doi.org/10.1109/WD.2013.6686471>. 8
- Fan Bai and B. Krishnamachari. Exploiting the wisdom of the crowd: localized, distributed information-centric VANETS [topics in automotive networking]. *Communications Magazine, IEEE*, 48(5):138–146, May 2010. ISSN 0163-6804. doi: 10.1109/MCOM.2010.5458375. URL <http://dx.doi.org/10.1109/MCOM.2010.5458375>. 10
- G.B. Baumgartner, H.V. Hitney, and R.A. Pappert. Duct propagation modelling for the integrated-refractive-effects prediction system (IREPS). *Communications*,

- Radar and Signal Processing, IEE Proceedings F*, 130(7):630–642, December 1983. ISSN 0143-7070. doi: 10.1049/ip-f-1.1983.0096. URL <http://dx.doi.org/10.1049/ip-f-1.1983.0096>. 51
- Michael Behrisch, Laura Bieker, Jakob Erdmann, and Daniel Krajzewicz. Sumo - simulation of urban mobility: An overview. In *in SIMUL 2011, The Third International Conference on Advances in System Simulation*, pages 63–68, 2011. 55
- Blackberry. The qnx car platform: A car platform for infotainment., Jan 2016. URL <http://www.qnx.com/products/qnxcar/index.html>. 158
- Annette Bohm and Magnus Jonsson. Handover in ieee 802.11p-based delay-sensitive vehicle-to-infrastructure communication. Technical Report IDE - 0924, Halmstad University, Embedded Systems (CERES), 2009. URL <http://www.diva-portal.org/smash/get/diva2:232276/FULLTEXT01.pdf>. 38
- C. Campolo and A. Molinaro. On vehicle-to-roadside communications in 802.11p/wave vanets. In *Wireless Communications and Networking Conference (WCNC), 2011 IEEE*, pages 1010–1015, March 2011a. doi: 10.1109/WCNC.2011.5779273. URL <http://dx.doi.org/10.1109/WCNC.2011.5779273>. 10
- C. Campolo and A. Molinaro. Improving v2r connectivity to provide its applications in ieee 802.11p/wave vanets. In *Telecommunications (ICT), 2011 18th International Conference on*, pages 476–481, May 2011b. doi: 10.1109/CTS.2011.5898972. URL <http://dx.doi.org/10.1109/CTS.2011.5898972>. 10
- C. Campolo, Y. Koucheryavy, A. Molinaro, and A. Vinel. Characterizing broadcast packet losses in ieee 802.11p/wave vehicular networks. In *Personal Indoor and Mobile Radio Communications (PIMRC), 2011 IEEE 22nd International Symposium on*, pages 735–739, Sept 2011a. doi: 10.1109/PIMRC.2011.6140063. URL <http://dx.doi.org/10.1109/PIMRC.2011.6140063>. 10
- C. Campolo, A. Vinel, A. Molinaro, and Y. Koucheryavy. Modeling broadcasting in ieee 802.11p/wave vehicular networks. *Communications Letters, IEEE*, 15(2): 199–201, 2011b. ISSN 1089-7798. doi: 10.1109/LCOMM.2011.122810.102007. URL <http://dx.doi.org/10.1109/LCOMM.2011.122810.102007>. 3, 69
- David R. Choffnes and Fabián E. Bustamante. An integrated mobility and traffic model for vehicular wireless networks. In *Proceedings of the 2Nd ACM International Workshop on Vehicular Ad Hoc Networks, VANET '05*, pages 69–78, New York, NY, USA, 2005. ACM. ISBN 1-59593-141-4. doi: 10.1145/1080754.1080765. URL <http://doi.acm.org/10.1145/1080754.1080765>. 57
- Christoph Sommer. Veins: Vehicles in network simulation, Jan 2014. URL <http://veins.car2x.org/>. 56, 64, 69, 71, 72, 132
- Jong-Moon Chung, Minseok Kim, Yong-Suk Park, Myungjun Choi, Sang Woo Lee, and Hyun seo Oh. Time coordinated v2i communications and handover for wave networks. *Selected Areas in Communications, IEEE Journal on*, 29(3): 545–558, March 2011. ISSN 0733-8716. doi: 10.1109/JSAC.2011.110305. URL <http://dx.doi.org/10.1109/JSAC.2011.110305>. 3, 38, 69
- Hugo Conceição, Luís Damas, Michel Ferreira, and João Barros. Large-scale simulation of v2v environments. In *Proceedings of the 2008 ACM Symposium on*

- Applied Computing*, SAC '08, pages 28–33, New York, NY, USA, 2008. ACM. ISBN 978-1-59593-753-7. doi: 10.1145/1363686.1363694. URL <http://doi.acm.org/10.1145/1363686.1363694>. 57
- K.H. Craig and M.F. Levy. Parabolic equation modelling of the effects of multipath and ducting on radar systems. *Radar and Signal Processing, IEE Proceedings F*, 138 (2):153–162, Apr 1991. ISSN 0956-375X. 51
- J. Deygout. Correction factor for multiple knife-edge diffraction. *Antennas and Propagation, IEEE Transactions on*, 39(8):1256–1258, Aug 1991. ISSN 0018-926X. doi: 10.1109/8.97368. URL <http://dx.doi.org/10.1109/8.97368>. 51
- J. Dias, A. Cardote, F. Neves, S. Sargento, and A. Oliveira. Seamless horizontal and vertical mobility in vanet. In *Vehicular Networking Conference (VNC), 2012 IEEE*, pages 226–233, Nov 2012. doi: 10.1109/VNC.2012.6407436. URL <http://dx.doi.org/10.1109/VNC.2012.6407436>. 38
- Dr.Glenford Mapp. Y-comm research, Jan 2014. URL http://www.mdx.ac.uk/research/science_technology/informatics/projects/ycomm.aspx. 33
- David Eckhoff and Christoph Sommer. A multi-channel iee 1609.4 and 802.11p edca model for the veins framework. In *5th ACM/ICST International Conference on Simulation Tools and Techniques for Communications, Networks and Systems (SIMUTools 2012): 5th ACM/ICST International Workshop on OMNeT++ (OMNeT++ 2012), Poster Session*, Desenzano, Italy, March 2012. ACM. URL <http://www.ccs-labs.org/bib/eckhoff2012multichannel/eckhoff2012multichannel.pdf>. 30
- MahmoudHashem Eiza, Qiang Ni, Thomas Owens, and Geyong Min. Investigation of routing reliability of vehicular ad hoc networks. *EURASIP Journal on Wireless Communications and Networking*, 2013(1):179, 2013. doi: 10.1186/1687-1499-2013-179. URL <http://dx.doi.org/10.1186/1687-1499-2013-179>. 2
- Paal E Engelstad and Olav N Østerbo. Queueing delay analysis of iee 802.11 e edca. In *WONS 2006: Third Annual Conference on Wireless On-demand Network Systems and Services*, pages 123–133, 2006. 41
- F. Esposito, A.M. Vegni, I. Matta, and A. Neri. On modeling speed-based vertical handovers in vehicular networks: Dad, slow down, i am watching the movie. In *GLOBECOM Workshops (GC Wkshps), 2010 IEEE*, pages 11–15, Dec 2010. doi: 10.1109/GLOCOMW.2010.5700126. URL <http://dx.doi.org/10.1109/GLOCOMW.2010.5700126>. 10
- ETSI-Std. Final draft etsi es 202 663 v1.1.0 - intelligent transport systems(its, 2009. URL http://www.etsi.org/deliver/etsi_es/202600_202699/202663/01.01.00_60/es_202663v010100p.pdf. 5, 6
- ETSI-Std. Draft etsi en 302 663 v1.2.0 - intelligent transport systems(its, 2011. URL http://www.etsi.org/deliver/etsi_en/302600_302699/302663/01.02.00_20/en_302663v010200a.pdf. 6
- European Standards Organization. Its: Intelligent transport systems by european telecommunicaitons standard institue (etsi), Dec 2015. URL <http://www.etsi.org/technologies-clusters/technologies/intelligent-transport>. 1, 2

- European Commission. Horizon 2020: The eu framework programme for research and innovation, Nov 2015. URL <http://ec.europa.eu/programmes/horizon2020/en/area/transport>. 1, 2, 18
- R. Fernandes and M. Ferreira. Scalable vanet simulations with ns-3. In *Vehicular Technology Conference (VTC Spring), 2012 IEEE 75th*, pages 1–5, May 2012. doi: 10.1109/VETECS.2012.6240251. URL <http://dx.doi.org/10.1109/VETECS.2012.6240251>. 57, 58
- R. Fernandes, P.M. d’Orey, and M. Ferreira. Divert for realistic simulation of heterogeneous vehicular networks. In *Mobile Adhoc and Sensor Systems (MASS), 2010 IEEE 7th International Conference on*, pages 721–726, Nov 2010. doi: 10.1109/MASS.2010.5663806. URL <http://dx.doi.org/10.1109/MASS.2010.5663806>. 57
- M. Fiore, J. Harri, F. Filali, and C. Bonnet. Vehicular mobility simulation for vanets. In *Simulation Symposium, 2007. ANSS ’07. 40th Annual*, pages 301–309, March 2007. doi: 10.1109/ANSS.2007.44. URL <http://dx.doi.org/10.1109/ANSS.2007.44>. 57
- P Fuxjager, A Costantini, D Valerio, P Castiglione, G Zacheo, T Zemen, and F Ricciato. Ieee 802.11 p transmission using gnuradio. In *Proceedings of the IEEE 6th Karlsruhe Workshop on Software Radios (WSR)*, pages 83–86, 2010. URL <http://userver.ftw.at/~valerio/files/wsr10.pdf>. 80, 97
- Carlos Ganan, Jonathan Loo, Arindam Ghosh, Oscar Esparza, Sergi Rene, and JoseL. Munoz. Analysis of inter-rsu beaconing interference in vanets. In Boris Bellalta, Alexey Vinel, Magnus Jonsson, Jaume Barcelo, Roman Maslennikov, Periklis Chatzimisios, and David Malone, editors, *Multiple Access Communications*, volume 7642 of *Lecture Notes in Computer Science*, pages 49–59. Springer Berlin Heidelberg, 2012. ISBN 978-3-642-34975-1. URL http://dx.doi.org/10.1007/978-3-642-34976-8_5. 3, 4, 8, 9, 68, 69, 72, 100, 102
- A. Ghosh, V. Vardhan, G. Mapp, O. Gemikonakli, and J. Loo. Providing ubiquitous communication using road-side units in vanet systems: Unveiling the challenges. In *ITS Telecommunications (ITST), 2013 13th International Conference on*, pages 74–79, Nov 2013. doi: 10.1109/ITST.2013.6685524. URL <http://dx.doi.org/10.1109/ITST.2013.6685524>. 3, 4
- A. Ghosh, V.V. Paranthaman, G. Mapp, and O. Gemikonakli. Providing ubiquitous communication using handover techniques in vanet systems. In *Ad Hoc Networking Workshop (MED-HOC-NET), 2014 13th Annual Mediterranean*, pages 195–202, June 2014a. doi: 10.1109/MedHocNet.2014.6849124. URL <http://dx.doi.org/10.1109/MedHocNet.2014.6849124>. 4
- A. Ghosh, V. Vardhan, G. Mapp, and O Gemikonakli. Exploring efficient seamless handover in vanet systems using network dwell time. *EURASIP Journal on Wireless Communications and Networking*, 2014(1):227, 2014b. ISSN 1687-1499. doi: 10.1186/1687-1499-2014-227. URL <http://jwcn.urasipjournals.com/content/2014/1/227>. 4, 99, 100, 122
- A. Ghosh, V.V. Paranthaman, G. Mapp, O. Gemikonakli, and J. Loo. Enabling seamless v2i communications: toward developing cooperative automotive applications in vanet systems. *Communications Magazine, IEEE*, 53(12):80–86,

- Dec 2015. ISSN 0163-6804. doi: 10.1109/MCOM.2015.7355570. URL <http://dx.doi.org/10.1109/MCOM.2015.7355570>. 97
- E. Giordano, R. Frank, G. Pau, and M. Gerla. Corner: a realistic urban propagation model for vanet. In *Wireless On-demand Network Systems and Services (WONS), 2010 Seventh International Conference on*, pages 57–60, Feb 2010. doi: 10.1109/WONS.2010.5437133. URL <http://dx.doi.org/10.1109/WONS.2010.5437133>. 49
- Google. Android auto: Android auto is an app that integrates with your car to use some of the main features of your android phone while driving, Jan 2016. URL https://www.android.com/intl/en_uk/auto/. 158
- J. Gozalvez, M. Sepulcre, and R. Bauza. Ieee 802.11p vehicle to infrastructure communications in urban environments. *Communications Magazine, IEEE*, 50(5):176–183, 2012. ISSN 0163-6804. doi: 10.1109/MCOM.2012.6194400. URL <http://dx.doi.org/10.1109/MCOM.2012.6194400>. 42, 121
- Huaqun Guo, Shen Tat Goh, N.C.S. Foo, Qian Zhang, and Wai-Choong Wong. Performance evaluation of 802.11p device for secure vehicular communication. In *Wireless Communications and Mobile Computing Conference (IWCMC), 2011 7th International*, pages 1170–1175, July 2011. doi: 10.1109/IWCMC.2011.5982706. URL <http://dx.doi.org/10.1109/IWCMC.2011.5982706>. 18, 19
- Martin PM Hall, Leslie W Barclay, and M Tim Hewitt. A review of: Propagation of radiowaves. *European Journal of Engineering Education*, 22(2):224–224, 1997. doi: 10.1080/03043799708928278. URL <http://dx.doi.org/10.1080/03043799708928278>. 51
- Chong Han, M. Dianati, R. Tafazolli, R. Kernchen, and Xuemin Shen. Analytical study of the ieee 802.11p mac sublayer in vehicular networks. *Intelligent Transportation Systems, IEEE Transactions on*, 13(2):873–886, June 2012. ISSN 1524-9050. doi: 10.1109/TITS.2012.2183366. URL <http://dx.doi.org/10.1109/TITS.2012.2183366>. 27, 28, 29, 30
- J. Harri, F. Filali, and C. Bonnet. Mobility models for vehicular ad hoc networks: a survey and taxonomy. *Communications Surveys Tutorials, IEEE*, 11(4):19–41, Fourth 2009. ISSN 1553-877X. doi: 10.1109/SURV.2009.090403. URL <http://dx.doi.org/10.1109/SURV.2009.090403>. 55, 57
- Aamir. Hassan and Tony. Larsson. On the requirements on models and simulator design for integrated vanet simulation. In *8th International Workshop on Intelligent Transport System*, pages 191–196, March 2011. URL http://www.diva-portal.org/smash/record.jsf?pid=diva23A437424&dswid=_new. 56
- M. Hatay. Empirical formula for propagation loss in land mobile radio services. *Vehicular Technology, IEEE Transactions on*, 29(3):317–325, Aug 1980. ISSN 0018-9545. doi: 10.1109/T-VT.1980.23859. URL <http://dx.doi.org/10.1109/T-VT.1980.23859>. 48
- Herbert V Hitney. Refractive effects from vhf to ehf. part a: Propagation mechanisms. In *In AGARD, Propagation Modelling and Decision Aids for Communications, Radar and Navigation Systems 13 p (SEE N95-14825 03-32)*, volume 1, 1994. 51

- IEEE-Std. Ieee standard for information technology–local and metropolitan area networks–specific requirements–part 11: Wireless lan medium access control (mac) and physical layer (phy) specifications - amendment 8: Medium access control (mac) quality of service enhancements, 2005. URL <http://dx.doi.org/10.1109/IEEESTD.2005.97890>. 7, 8, 71
- IEEE-Std. Ieee draft standard for wireless access in vehicular environments (wave) - multi-channel operation, 2010. URL <http://ieeexplore.ieee.org/servlet/opac?punumber=5511462>. 5, 6, 7, 9, 21, 22, 23, 24, 25, 26, 27, 71
- IEEE-Std. Ieee draft standard for local and metropolitan area networks – part 21: Media independent handover services - amendment 3: Optimized single radio handovers, Dec 2013. URL <http://ieeexplore.ieee.org/servlet/opac?punumber=6634307>. 39
- L. Vuokko J. Salo and P. Vainikainen. Why is shadow fading lognormal? In *International Symposium on Wireless Personal Multimedia Communications*, pages 522–526, Sept 2005. 46
- M. Jerbi, S.-M. Senouci, and M. Al Haj. Extensive experimental characterization of communications in vehicular ad hoc networks within different environments. In *Vehicular Technology Conference, 2007. VTC2007-Spring. IEEE 65th*, pages 2590–2594, April 2007. doi: 10.1109/VETECS.2007.533. URL <http://dx.doi.org/10.1109/VETECS.2007.533>. 42
- G. Karagiannis, O. Altintas, E. Ekici, G. Heijenk, B. Jarupan, K. Lin, and T. Weil. Vehicular networking: A survey and tutorial on requirements, architectures, challenges, standards and solutions. *Communications Surveys Tutorials, IEEE*, 13 (4):584–616, 2011. ISSN 1553-877X. doi: 10.1109/SURV.2011.061411.00019. URL <http://dx.doi.org/10.1109/SURV.2011.061411.00019>. 2
- F.K. Karnadi, Zhi Hai Mo, and Kun chan Lan. Rapid generation of realistic mobility models for vanet. In *Wireless Communications and Networking Conference, 2007.WCNC 2007. IEEE*, pages 2506–2511, March 2007. doi: 10.1109/WCNC.2007.467. URL <http://dx.doi.org/10.1109/WCNC.2007.467>. 57
- I. Khan and A. Qayyum. Performance evaluation of aodv and olsr in highly fading vehicular ad hoc network environments. In *Multitopic Conference, 2009. INMIC 2009. IEEE 13th International*, pages 1–5, Dec 2009. doi: 10.1109/INMIC.2009.5383121. URL <http://dx.doi.org/10.1109/INMIC.2009.5383121>. 51
- A. Köpke, M. Swigulski, K. Wessel, D. Willkomm, P. T. Klein Haneveld, T. E. V. Parker, O. W. Visser, H. S. Lichte, and S. Valentin. Simulating wireless and mobile networks in omnet++ the mixim vision. In *Proceedings of the 1st International Conference on Simulation Tools and Techniques for Communications, Networks and Systems & Workshops, Simutools '08*, pages 71:1–71:8, ICST, Brussels, Belgium, Belgium, 2008. ICST (Institute for Computer Sciences, Social-Informatics and Telecommunications Engineering). ISBN 978-963-9799-20-2. URL <http://dl.acm.org/citation.cfm?id=1416222.1416302>. 59
- Daniel Krajzewicz. Traffic simulation with sumo - simulation of urban mobility. In Jaume Barceló, editor, *Fundamentals of Traffic Simulation*, volume 145 of *International Series in Operations Research & Management Science*, pages 269–293. Springer New York, 2010. ISBN 978-1-4419-6141-9. doi: 10.1007/

- 978-1-4419-6142-6_7. URL http://dx.doi.org/10.1007/978-1-4419-6142-6_7. 56, 62, 63, 64
- Daniel Krajzewicz, Jakob Erdmann, Michael Behrisch, and Laura Bieker. Recent development and applications of SUMO - Simulation of Urban MObility. *International Journal On Advances in Systems and Measurements*, 5(3&4):128–138, December 2012. 62, 63
- Hyukjoon Lee, Young uk Chung, and Yong-Hoon Choi. A seamless handover scheme for ieee wave networks based on multi-way proactive caching. In *Ubiquitous and Future Networks (ICUFN), 2013 Fifth International Conference on*, pages 356–361, 2013. doi: 10.1109/ICUFN.2013.6614841. URL <http://dx.doi.org/10.1109/ICUFN.2013.6614841>. 39
- Yunxin(Jeff) Li. An overview of the dsrc/wave technology. In Xi Zhang and Daji Qiao, editors, *Quality, Reliability, Security and Robustness in Heterogeneous Networks*, volume 74 of *Lecture Notes of the Institute for Computer Sciences, Social Informatics and Telecommunications Engineering*, pages 544–558. Springer Berlin Heidelberg, 2012. ISBN 978-3-642-29221-7. doi: 10.1007/978-3-642-29222-4_38. URL http://dx.doi.org/10.1007/978-3-642-29222-4_38. 20, 22, 30, 31, 32, 33
- Jia-Chin Lin, Chi-Sheng Lin, Chih-Neng Liang, and Bo-Chiuan Chen. Wireless communication performance based on ieee 802.11p r2v field trials. *Communications Magazine, IEEE*, 50(5):184–191, May 2012. ISSN 0163-6804. doi: 10.1109/MCOM.2012.6194401. URL <http://dx.doi.org/10.1109/MCOM.2012.6194401>. 42, 121
- Christian Lochert, Andreas Barthels, Alfonso Cervantes, Martin Mauve, and Murat Caliskan. Multiple simulator interlinking environment for ivc. In *Proceedings of the 2Nd ACM International Workshop on Vehicular Ad Hoc Networks, VANET '05*, pages 87–88, New York, NY, USA, 2005. ACM. ISBN 1-59593-141-4. doi: 10.1145/1080754.1080771. URL <http://doi.acm.org/10.1145/1080754.1080771>. 59
- Atulya Mahajan, Niranjana Potnis, Kartik Gopalan, and Andy Wang. Modeling vanet deployment in urban settings. In *Proceedings of the 10th ACM Symposium on Modeling, Analysis, and Simulation of Wireless and Mobile Systems, MSWiM '07*, pages 151–158, New York, NY, USA, 2007. ACM. ISBN 978-1-59593-851-0. doi: 10.1145/1298126.1298154. URL <http://doi.acm.org/10.1145/1298126.1298154>. 51
- G. Mapp, F. Shaikh, M. Aiash, R.P. Vanni, M. Augusto, and E. Moreira. Exploring efficient imperative handover mechanisms for heterogeneous wireless networks. In *Network-Based Information Systems, 2009. NBIS '09. International Conference on*, pages 286–291, Aug 2009. doi: 10.1109/NBiS.2009.95. URL <http://dx.doi.org/10.1109/NBiS.2009.95>. 33, 35
- Glenford E. Mapp, Fatema Shaikh, David Cottingham, Jon Crowcroft, and Javier Baliosian. Y-comm: A global architecture for heterogeneous networking. In *Proceedings of the 3rd International Conference on Wireless Internet, WICON '07*, pages 22:1–22:5, ICST, Brussels, Belgium, Belgium, 2007. ICST (Institute for Computer Sciences, Social-Informatics and Telecommunications Engineering). ISBN 978-963-9799-12-7. URL <http://dl.acm.org/citation.cfm?id=1460047.1460075>. 35, 39
- Glenford E. Mapp, Ferdinand Katsriku, Mahdi Aiash, Naveen Chinnam, Rigolin Lopes, Edson dos Santos Moreira, Renata M. Porto Vanni, and Mario Augusto.

- Exploiting location and contextual information to develop a comprehensive framework for proactive handover in heterogeneous environments. *Journal Comp. Netw. and Communic.*, 2012, 2012. URL <http://dx.doi.org/10.1155/2012/748163>. 4, 5, 35, 36, 70, 75
- S. Marinoni and H.H. Kari. Ad hoc routing protocol performance in a realistic environment. In *Networking, International Conference on Systems and International Conference on Mobile Communications and Learning Technologies, 2006. ICN/ICONS/MCL 2006. International Conference on*, pages 96–96, April 2006. doi: 10.1109/ICNICONSMCL.2006.39. URL <http://dx.doi.org/10.1109/ICNICONSMCL.2006.39>. 51
- Francisco J. Martinez, Chai-Keong Toh, Juan-Carlos Cano, Carlos T. Calafate, and Pietro Manzoni. Realistic radio propagation models (rpms) for vanet simulations. In *Proceedings of the 2009 IEEE Conference on Wireless Communications & Networking Conference, WCNC'09*, pages 1155–1160, Piscataway, NJ, USA, 2009. IEEE Press. ISBN 978-1-4244-2947-9. URL <http://dl.acm.org/citation.cfm?id=1688345.1688552>. 45, 46
- Microsoft. Windows embedded automotive7: An operating system subfamily of windows embedded based on windows ce for use on computer systems in automobiles, Jan 2016. URL <http://www.microsoft.com/windowsembedded/en-us/windows-embedded-automotive-7.aspx>. 158
- J. Montavont and T. Noel. Ieee 802.11 handovers assisted by gps information. In *Wireless and Mobile Computing, Networking and Communications, 2006. (WiMob'2006). IEEE International Conference on*, pages 166–172, 2006. doi: 10.1109/WIMOB.2006.1696358. URL <http://dx.doi.org/10.1109/WIMOB.2006.1696358>. 38
- A. Mukunthan, C. Cooper, F. Safaei, D. Franklin, and M. Abolhasan. Studying the impact of the corner propagation model on vanet routing in urban environments. In *Vehicular Technology Conference (VTC Fall), 2012 IEEE*, pages 1–5, Sept 2012. doi: 10.1109/VTCFall.2012.6399132. URL <http://dx.doi.org/10.1109/VTCFall.2012.6399132>. 46, 50
- M. Nakagami. The m-distribution—a general formula of intensity distribution of rapid fading. In W.C. HOFFMAN, editor, *Statistical Methods in Radio Wave Propagation*, pages 3 – 36. Pergamon, 1960. ISBN 978-0-08-009306-2. doi: <http://dx.doi.org/10.1016/B978-0-08-009306-2.50005-4>. URL <http://www.sciencedirect.com/science/article/pii/B9780080093062500054>. 47, 51
- H. Noori and B.B. Olyaei. A novel study on beaconing for vanet-based vehicle to vehicle communication: Probability of beacon delivery in realistic large-scale urban area using 802.11p. In *Smart Communications in Network Technologies (SaCoNeT), 2013 International Conference on*, volume 01, pages 1–6, June 2013. doi: 10.1109/SaCoNeT.2013.6654589. URL <http://dx.doi.org/10.1109/SaCoNeT.2013.6654589>. 55, 56, 59
- Y. Okumura. Field strength and its variability in vhf and uhf land-mobile radio-services. *Review of the Electrical Communications Laboratory*, 16:825–873, September-October 1968. 47

- Tatsuaki Osafune, Yuki Horita, Nestor Mariyasagayam, and Massimiliano Lenardi. Effect of decentralized congestion control on cooperative systems. *International Journal of Intelligent Transportation Systems Research*, 13(3):192–202, 2015. ISSN 1348-8503. doi: 10.1007/s13177-014-0095-y. URL <http://dx.doi.org/10.1007/s13177-014-0095-y>. 8
- A. Paier, R. Tresch, A. Alonso, D. Smely, P. Meckel, Y. Zhou, and N. Czink. Average downstream performance of measured ieee 802.11p infrastructure-to-vehicle links. In *Communications Workshops (ICC), 2010 IEEE International Conference on*, pages 1–5, May 2010. doi: 10.1109/ICCW.2010.5503934. URL <http://dx.doi.org/10.1109/ICCW.2010.5503934>. 42
- Eun Kyoung Paik and Yanghee Choi. Prediction-based fast handoff for mobile w lans. In *Telecommunications, 2003. ICT 2003. 10th International Conference on*, volume 1, pages 748–753 vol.1, 2003. doi: 10.1109/ICTEL.2003.1191503. URL <http://dx.doi.org/10.1109/ICTEL.2003.1191503>. 38
- V. Paranthaman, G. Mapp, P. Shah, H. Nguyen, and A. Ghosh. Exploring markov models for the allocation of resources for proactive handover in a mobile environment. In *LCN 2015: 11th International Workshop on Performance and Management of Wireless and Mobile Networks*, Oct 2015. 157
- M. Piórkowski, M. Raya, A. Lezama Lugo, P. Papadimitratos, M. Grossglauser, and J.-P. Hubaux. Trans: Realistic joint traffic and network simulator for vanets. 2007. URL <http://infoscience.epfl.ch/record/114570?ln=en>. 57
- Theodore Rappaport. *Wireless Communications: Principles and Practice*. Prentice Hall PTR, Upper Saddle River, NJ, USA, 2012. ISBN 0130422320. 44, 45, 46, 121, 132
- Steele. Raymond and Hanzo. Lajos. *Mobile Radio Communications*. Wiley-IEEE Press, May 1999. URL <http://eu.wiley.com/WileyCDA/WileyTitle/productCd-047197806X,miniSiteCd-IEEE2.html>. 43
- R. Reinders, M. van Eenennaam, G. Karagiannis, and G. Heijenk. Contention window analysis for beaconing in vanets. In *Wireless Communications and Mobile Computing Conference (IWCMC), 2011 7th International*, pages 1481–1487, 2011. doi: 10.1109/IWCMC.2011.5982757. URL <http://dx.doi.org/10.1109/IWCMC.2011.5982757>. 3, 68, 69
- T. Salam, M. Ali, and M.-R. Fida. Seamless proactive vertical handover algorithm. In *Information Technology: New Generations (ITNG), 2011 Eighth International Conference on*, pages 94–99, 2011. doi: 10.1109/ITNG.2011.24. URL <http://dx.doi.org/10.1109/ITNG.2011.24>. 39
- F. Shaikh, G. Mapp, and A. Lasebae. Proactive policy management using tvbh mechanism in heterogeneous networks. In *Next Generation Mobile Applications, Services and Technologies, 2007. NGMAST '07. The 2007 International Conference on*, pages 151–157, 2007. doi: 10.1109/NGMAST.2007.4343414. URL <http://dx.doi.org/10.1109/NGMAST.2007.4343414>. 4, 39, 40, 70
- C.H. Shellman and NAVAL OCEAN SYSTEMS CENTER SAN DIEGO CA. *A New Version of MODESRCH Using Interpolated Values of the Magnetoionic Reflection Coefficients*. Defense Technical Information Center, 1986. URL <https://books.google.co.uk/books?id=CnzntgAACAAJ>. 51

- Jang-Ping Sheu, Chi-Yuan Lo, and Wei-Kai Hu. A distributed routing protocol and handover schemes in hybrid vehicular ad hoc networks. In *Parallel and Distributed Systems (ICPADS), 2011 IEEE 17th International Conference on*, pages 428–435, Dec 2011. doi: 10.1109/ICPADS.2011.4. URL <http://dx.doi.org/10.1109/ICPADS.2011.4>. 38
- Katrin Sjöberg, Johan Kåredal, Marie Moe, Øyvind Kristiansen, Runar Søråsen, Elisabeth Uhlemann, Fredrik Tufvesson, Knut Evensen, and Erik Ström. Measuring and using the rssi of ieee 802.11p. 2010. 97
- P.L. Slingsby. Modelling tropospheric ducting effects on vhf/uhf propagation. *Broadcasting, IEEE Transactions on*, 37(2):25–34, Jun 1991. ISSN 0018-9316. doi: 10.1109/11.86959. URL <http://dx.doi.org/10.1109/11.86959>. 51
- C. Sommer and F. Dressler. The dymo routing protocol in vanet scenarios. In *Vehicular Technology Conference, 2007. VTC-2007 Fall. 2007 IEEE 66th*, pages 16–20, Sept 2007. doi: 10.1109/VETEFC.2007.20. URL <http://dx.doi.org/10.1109/VETEFC.2007.20>. 59
- C. Sommer, Zheng Yao, R. German, and F. Dressler. Simulating the influence of ivc on road traffic using bidirectionally coupled simulators. In *INFOCOM Workshops 2008, IEEE*, pages 1–6, April 2008. doi: 10.1109/INFOCOM.2008.4544655. URL <http://dx.doi.org/10.1109/INFOCOM.2008.4544655>. 59
- C. Sommer, R. German, and F. Dressler. Bidirectionally coupled network and road traffic simulation for improved ivc analysis. *Mobile Computing, IEEE Transactions on*, 10(1):3–15, 2011. ISSN 1536-1233. doi: 10.1109/TMC.2010.133. URL <http://dx.doi.org/10.1109/TMC.2010.133>. 59, 99
- Christoph Sommer and Falko Dressler. Using the right two-ray model? a measurement based evaluation of phy models in vanets. In *17th ACM International Conference on Mobile Computing and Networking (MobiCom 2011), Poster Session*, Las Vegas, NV, September 2011. ACM. 45
- Chien-Chao Tseng, Kuang-Hui Chi, Ming-Deng Hsieh, and Hung-Hsing Chang. Location-based fast handoff for 802.11 networks. *Communications Letters, IEEE*, 9(4):304–306, 2005. ISSN 1089-7798. doi: 10.1109/LCOMM.2005.04010. URL <http://dx.doi.org/10.1109/LCOMM.2005.04010>. 38
- R. Uzcategui and G. Acosta-Marum. Wave: A tutorial. *Communications Magazine, IEEE*, 47(5):126–133, May 2009. ISSN 0163-6804. doi: 10.1109/MCOM.2009.4939288. URL <http://dx.doi.org/10.1109/MCOM.2009.4939288>. 6
- E. M. Van Eenennaam, G. Karagiannis, and G. J. Heijenk. Towards scalable beaconing in vanets. In *Fourth ERCIM workshop on eMobility, Lule?, Sweden*, pages 103–108, Lule?, Sweden, May 2010. Lule? University of Technology, Lule?, Sweden. URL <http://eprints.eemcs.utwente.nl/18015/>. 3, 38
- M. Van Eenennaam, W.K. Wolterink, G. Karagiannis, and G. Heijenk. Exploring the solution space of beaconing in vanets. In *Vehicular Networking Conference (VNC), 2009 IEEE*, pages 1–8, Oct 2009. doi: 10.1109/VNC.2009.5416370. URL <http://dx.doi.org/10.1109/VNC.2009.5416370>. 3, 69

- M. van Eenennaam, A. Remke, and G. Heijenk. An analytical model for beaconing in vanets. In *Vehicular Networking Conference (VNC), 2012 IEEE*, pages 9–16, Nov 2012. doi: 10.1109/VNC.2012.6407451. URL <http://dx.doi.org/10.1109/VNC.2012.6407451>. 41
- Anna Maria Vegni, Mauro Biagi, and Roberto Cusani. Smart vehicles, technologies and main applications in vehicular ad hoc networks. *Vehicular Technologies - Deployment and Applications*, 2013. ISSN 978-953-51-0992-1. doi: 10.5772/55492. URL <http://www.intechopen.com/books/vehicular-technologies-deployment-and-applications/smart-vehicles-technologies-and-main-applications-in-vehicular-ad-hoc-networks>. 17, 19
- A. Vinel. 3gpp lte versus ieee 802.11p/wave: Which technology is able to support cooperative vehicular safety applications? *Wireless Communications Letters, IEEE*, 1(2):125–128, April 2012. ISSN 2162-2337. doi: 10.1109/WCL.2012.022012.120073. URL <http://dx.doi.org/10.1109/WCL.2012.022012.120073>. 41
- A. Vinel, V.M. Vishnevsky, and Y. Koucheryavy. A simple analytical model for the periodic broadcasting in vehicular ad-hoc networks. In *GLOBECOM Workshops, 2008 IEEE*, pages 1–5, Nov 2008. doi: 10.1109/GLOCOMW.2008.ECP.73. URL <http://dx.doi.org/10.1109/GLOCOMW.2008.ECP.73>. 40
- A. Vinel, D. Staehle, and A. Turlikov. Study of beaconing for car-to-car communication in vehicular ad-hoc networks. In *Communications Workshops, 2009. ICC Workshops 2009. IEEE International Conference on*, pages 1–5, June 2009a. doi: 10.1109/ICW.2009.5208066. URL <http://dx.doi.org/10.1109/ICW.2009.5208066>. 10, 40, 102
- Alexey Vinel, Yevgeni Koucheryavy, Sergey Andreev, and Dirk Staehle. Estimation of a successful beacon reception probability in vehicular ad-hoc networks. In *Proceedings of the 2009 International Conference on Wireless Communications and Mobile Computing: Connecting the World Wirelessly, IWCMC '09*, pages 416–420, New York, NY, USA, 2009b. ACM. ISBN 978-1-60558-569-7. doi: 10.1145/1582379.1582470. URL <http://doi.acm.org/10.1145/1582379.1582470>. 10
- S.Y. Wang, C.L. Chou, Y.H. Chiu, Y.S. Tzeng, M.S. Hsu, Y.W. Cheng, W.L. Liu, and T.W. Ho. Nctuns 4.0: An integrated simulation platform for vehicular traffic, communication, and network researches. In *Vehicular Technology Conference, 2007. VTC-2007 Fall. 2007 IEEE 66th*, pages 2081–2085, Sept 2007. doi: 10.1109/VETEFCF.2007.437. URL <http://dx.doi.org/10.1109/VETEFCF.2007.437>. 59
- E. Weingartner, H. vom Lehn, and K. Wehrle. A performance comparison of recent network simulators. In *Communications, 2009. ICC '09. IEEE International Conference on*, pages 1–5, June 2009. doi: 10.1109/ICC.2009.5198657. URL <http://dx.doi.org/10.1109/ICC.2009.5198657>. 57
- Chengshan Xiao, Yahong R. Zheng, and N.C. Beaulieu. Statistical simulation models for rayleigh and rician fading. In *Communications, 2003. ICC '03. IEEE International Conference on*, volume 5, pages 3524–3529 vol.5, May 2003. doi: 10.1109/ICC.2003.1204109. URL <http://dx.doi.org/10.1109/ICC.2003.1204109>. 45, 46

REFERENCES

- J. Yoon, M. Liu, and B. Noble. Random waypoint considered harmful. In *INFOCOM 2003. Twenty-Second Annual Joint Conference of the IEEE Computer and Communications. IEEE Societies*, volume 2, pages 1312–1321 vol.2, March 2003. doi: 10.1109/INFCOM.2003.1208967. URL <http://dx.doi.org/10.1109/INFCOM.2003.1208967>. 59
- Sherali Zeadally, Ray Hunt, Yuh-Shyan Chen, Angela Irwin, and Aamir Hassan. Vehicular ad hoc networks (vanets): status, results, and challenges. *Telecommunication Systems*, 50(4):217–241, 2012. ISSN 1018-4864. doi: 10.1007/s11235-010-9400-5. URL <http://dx.doi.org/10.1007/s11235-010-9400-5>. 121

Appendix A

A.1 Equations

A.1.1 Full derivation of $\frac{dP}{dSNR}$ with respect to radius (R)

$$\begin{aligned} PacketReceptionProbability(PRP) &= [1 - 1.5erfc(0.45\sqrt{SNR})]^L \\ BER &= 1.5erfc(0.45\sqrt{SNR}) \end{aligned} \quad (A.1)$$

So for a beacon of L Bits

$$PRP = [1 - BER]^L \quad (A.2)$$

The complementary error function, denoted erfc, is defined as

$$\begin{aligned} erfc(x) &= 1 - erf(x) \\ &= \frac{2}{\sqrt{\pi}} \int_0^x e^{-t^2} dt \\ &= e^{-x^2} erfcx(x) \end{aligned} \quad (A.3)$$

$$\begin{aligned} \frac{d}{dx} \times erfc(x) &= \frac{-2e^{-x^2}}{\sqrt{\pi}} \\ \frac{d}{dx}(erfc(x)) &= \frac{-2e^{-x^2}}{\sqrt{\pi}} \end{aligned} \quad (A.4)$$

Where,

$$x = 0.45\sqrt{SNR} \quad (A.5)$$

Hence,

$$\Rightarrow P = [1 - 1.5\text{erfc}(x)]^L \quad (\text{A.6})$$

Now, Let

$$\Rightarrow z = (1 - 1.5\text{erfc}(x)) \quad (\text{A.7})$$

Therefore,

$$\Rightarrow P = Z^L \quad (\text{A.8})$$

$$\frac{dP}{dx} = \frac{dP}{dz} \times \frac{dz}{dx} \quad (\text{A.9})$$

$$\frac{dP}{dx} = Lz^{L-1} \times \frac{dz}{dx} \quad (\text{A.10})$$

$$\frac{dz}{dx} = \frac{1.5 \times 2e^{-x^2}}{\sqrt{\pi}} \quad (\text{A.11})$$

$$\frac{dz}{dx} = Lz^{L-1} \cdot \frac{3e^{-x^2}}{\sqrt{\pi}} \quad (\text{A.12})$$

$$\Rightarrow \frac{dP}{dSNR} = \frac{dP}{dx} \times \frac{dx}{dSNR} \quad (\text{A.13})$$

$$\frac{dx}{dSNR} = \frac{0.45\sqrt{SNR}}{dSNR} = \frac{0.45(SNR)^{\frac{1}{2}}}{dSNR} \quad (\text{A.14})$$

$$= 0.45 \times \frac{1}{2}(SNR)^{-\frac{1}{2}} \quad (\text{A.15})$$

Therefore,

$$\frac{dP}{dSNR} = Lz^{L-1} \times \frac{3e^{-(0.45\sqrt{SNR})^2}}{\sqrt{\pi}} \times 0.45 \frac{1}{2}(SNR)^{-\frac{1}{2}} \quad (\text{A.16})$$

$$= Lz^{L-1} \times \frac{3e^{-(0.45^2 SNR)}}{\sqrt{\pi}} \times 0.45 \frac{1}{2}(SNR)^{-\frac{1}{2}} \quad (\text{A.17})$$

$$\frac{dP}{dSNR} = L(1 - 1.5\text{erfc}(0.45\sqrt{SNR}))^{L-1} \times \frac{3e^{-(0.45^2 SNR)}}{\sqrt{\pi}} \times 0.45 \frac{1}{2} (SNR)^{-\frac{1}{2}} \quad (\text{A.18})$$

$$\therefore \frac{dP}{dSNR} = \frac{3L}{\sqrt{\pi}} (1 - 1.5\text{erfc}(0.45\sqrt{SNR}))^{L-1} \times \frac{3e^{-(0.45^2 SNR)}}{\sqrt{\pi}} \times 0.45 \frac{1}{2} (SNR)^{-\frac{1}{2}} \quad (\text{A.19})$$

$$\Rightarrow \frac{dP}{dR} = \frac{dP}{dSNR} \times \frac{dSNR}{dR} \quad (\text{A.20})$$

We know,

$$SNR = \frac{P_S}{P_N} P_S = \frac{P_T}{P_L} \quad (\text{A.21})$$

For Free Space Path Loss

$$P_L = \left(\frac{4 \cdot \pi \cdot r \cdot f}{c} \right)^2 \quad (\text{A.22})$$

$$\therefore SNR = \frac{P_T}{P_L \cdot P_N} \quad (\text{A.23})$$

$$SNR = \frac{P_T}{P_N} \left(\frac{c}{4 \cdot \pi \cdot r \cdot f} \right)^2 \quad (\text{A.24})$$

$$\therefore \frac{dSNR}{dR} = \frac{P_T}{P_N} \left(\frac{c}{4 \cdot \pi \cdot f} \right)^2 \cdot \left(\frac{-2}{r^3} \right) \quad (\text{A.25})$$

Therefore, the Full Equation:

$$\therefore \frac{dP}{dR} = \frac{3L}{\sqrt{\pi}} (1 - 1.5\text{erfc}(0.45\sqrt{SNR}))^{L-1} \times e^{-(0.45^2 SNR)} \sqrt{\pi} \times 0.45 \frac{1}{2} (SNR)^{-\frac{1}{2}} \times \frac{P_T}{P_N} \left(\frac{c}{4 \cdot \pi \cdot f} \right)^2 \cdot \left(\frac{-2}{r^3} \right) \quad (\text{A.26})$$

A.1.2 Calculation for Probability P with respect to velocity using dP/dR

In order to model this we define the following parameters:

Let R_1 is the first the beacon is heard from a particular RSU in a new network that the vehicle is heading towards.

Let P_1 be the Probability of successful transmission at R_1 .

Let V be the velocity of the vehicle.

Let F be the frequency of the beacon as shown below:

$T = \text{Period of the Beacon}$ i.e., $T = \frac{1}{f}$, where $\frac{1}{f}$ is the frequency of the Beacon.

Let R_1 be the next time the beacon is heard, then:

$$R_2 = R_1 + VT$$

$$P_2 = P_1 + \int_{R_1}^{R_1+VT} \frac{dP}{dR}$$

Then at the third time of hearing the beacon:

$$R_3 = R_1 + 2VT$$

$$P_3 = P_1 + \int_{R_1}^{R_1+2VT} \frac{dP}{dR}$$

Hence, as the n_{th} time of hearing the beacon :

$$R_n = R_1 + (n - 1)VT$$

$$P_n = P_1 + \int_{R_1}^{R_1+(n-1)VT} \frac{dP}{dR}$$

Thus, the calculation for Cumulative Probability CP with respect to dP/dR is as follows:

where, $P_n = \left\{ P_1 + \int_{R_1}^{R_1+(n-1)VT} \frac{dP}{dR} \right\}$, hence the equation is represented as:

So, the Cumulative Probability at n:

$$\implies CP_n = P_1 + (1 - P_1)P_2 + (1 - P_1)(1 - P_2)P_3 + \dots + P_{n-1} \quad (\text{A.27})$$

Thus, the series can be expanded in the form of:

$$\begin{aligned} \therefore CP_n = & \left\{ P_1 + (1 - P_1) \left(P_1 + \int_{R_1}^{R_1+VT} \frac{dP}{dR} \right) \right\} \\ & + \left\{ (1 - P_1) \left(1 - P_1 + \int_{R_1}^{R_1+VT} \frac{dP}{dR} \right) \left(P_1 + \int_{R_1}^{R_1+2VT} \frac{dP}{dR} \right) \right\} \\ & + \dots + \left\{ P_1 + \int_{R_1}^{R_1+(n-1)VT} \frac{dP}{dR} \right\} \end{aligned} \quad (\text{A.28})$$

The calculated analysis shows that both the individual probability as well as the cumulative probability is affected by the velocity of the vehicle when the beacon is heard. This has further been explained in chapter 6.

Appendix B

B.1 Abstract of Publications

Abstracts of the published conference papers & journals:

Building a Prototype VANET Testbed to Explore Communication Dynamics in Highly Mobile Environments (Springer/EAI Endorsed Transactions on Future Internet)

Applications for VANETs will require seamless communication between vehicle-to-infrastructure and vehicle-to-vehicle. However, this is challenging because it is being done in the context of a highly mobile environment. Therefore, traditional handover techniques are inadequate due to the high velocity of the vehicle and the small coverage radius of Road-side Units. Hence in order to have seamless communication for these applications, a proactive approach needs to be carefully investigated. This requires measurements from a real testbed in order to enhance our understanding of the communication dynamics. This paper is about building and evaluating a prototype VANET network on the Middlesex University Hendon Campus, London to explore these issues. The testbed is being used to investigate better propagation models, road-critical safety applications as well as algorithms for traffic management. In addition, the Network Dwell Time of vehicles traveling in the coverage of the RSUs is measured to explore proactive handover and resource allocation mechanisms.

Enabling Seamless V2I Communications: Towards Developing Cooperative Automotive Applications in VANET Systems (IEEE Communications Magazine)

Cooperative applications for VANET will require seamless communication between Vehicle to Infrastructure and Vehicle to Vehicle. IEEE 802.11p has been developed to facilitate this effort. However, in order to have seamless communication for these applications, it is necessary to look at handover as vehicles move between Road-side Units. Traditional models of handover used in normal mobile environments are unable to cope with the high velocity of the vehicle and the relatively small area of coverage with regard to vehicular environments. The Y-Comm framework has yielded techniques to calculate the Time Before Vertical Handover and the Network Dwell Time for any given network topology. Furthermore, by knowing these two parameters, it is also possible to improve channel allocation and resource management in network infrastructure such as base-stations, relays, etc. In this article we explain our overall approach by describing the VANET Testbed and show that in Vehicular environments it is necessary to consider a new handover model which is based on a probabilistic rather than a fixed coverage approach. Finally, we show a new performance model for proactive handover which is then compared with traditional approaches.

Exploring Seamless Connectivity and Proactive Handover Techniques in VANET System (Springer - Book Chapter)

In order to provide Dependable Vehicular Communications for Improved Road Safety, it is necessary to have reliable Vehicular-to-Infrastructure (V2I) and Vehicle-to-Vehicle (V2V) communication. Such requirements demand that the handover process as vehicles move between adjacent Roadside Units (RSUs) be examined in detail to understand how seamless communication can be achieved. Since the use of beacons is a key part of VANETs, it is necessary to investigate how the beaconing process affects the opportunities to effect handovers. A framework is needed to be able to calculate the regions of overlap in adjacent RSU coverage ranges to guarantee ubiquitous connectivity. A highly mobile environment, therefore, makes this a serious challenge and points to the need to look at proactive handover techniques. This chapter, therefore, explores the development of the proactive handover mechanisms required to provide seamless connectivity and dependable communication in VANET environments.

Exploring Markov Models for the Allocation of Resources for Proactive Handover in a Mobile Environment (IEEE - 40th Local Computer Networks (LCN) Conference)

Proactive handover, in which mobile nodes attempt to determine the best time and place to handover to local networks, has been studied in the context of new architectures such as the Y-Comm Framework. Y-Comm research has yielded techniques to calculate the Time Before Vertical Handover and the Network Dwell Time, for any given network topology. However, by knowing Time Before Vertical Handover and Network Dwell Time for mobile nodes as they move around, it is also possible to improve channel allocation and resource management in network infrastructure such as base-stations, relays, etc. This should greatly enhance overall system efficiency including the physical and medium access control layers of mobile networks, such as LTE. In this paper queuing models based on Markov chains are explored to represent channel allocation in proactive handover scenarios. The results are compared with classical handover queuing models. The results indicate that the proactive model is beneficial over a wide range but it is necessary to explore an operational space in which proactive handover techniques can be used in real networks.

Exploring Efficient Seamless Handover in VANET Systems Using Network Dwell Time (EURASIP Journal)

Vehicular Ad Hoc Networks are a long-term solution contributing significantly towards Intelligent Transport Systems in providing access to critical life-safety applications and services. Although Vehicular Ad Hoc Networks are attracting greater commercial interest, current research has not adequately captured the real-world constraints in Vehicular Ad Hoc Network handover techniques. Therefore, in order to have the best practice for Vehicular Ad Hoc Network services, it is necessary to have seamless connectivity for optimal coverage and ideal channel utilization. Due to the high velocity of vehicles and smaller coverage distances, there are serious challenges in providing seamless handover from one Road Side Unit to another. Though other research efforts have looked at many issues in VANET networks, very few research work have looked at handover issues. Most literature assume that handover does not take a significant time and does not affect the overall VANET operation. In our previous work, we started to investigate these issues. This journal provides a more comprehensive analysis involving the beacon frequency, size of beacon and the velocity of the vehicle. We used some of the concepts of Y-Comm architecture such as Network Dwell Time, Time before Handover and Exit Time to provide a framework to investigate handover issues. Further simulation studies were used to investigate the

relation between beaconing, velocity and the Network Dwell Time. Our results show that there is a need to understand the cumulative effect of beaconing in addition to the probability of successful reception as well as how these probability distributions are affected by the velocity of the vehicle. This provides more insight into how to support life critical applications using proactive handover techniques.

Providing Ubiquitous Communication Using Handover Techniques in VANET Systems (IEEE/IFIP - 13th International Med-Hoc-Nets Conference)

Vehicular Ad hoc Networks are a long-term solution contributing significantly towards Intelligent Transport Systems in providing access to critical life-safety applications and services. Although Vehicular Ad hoc Networks are attracting greater commercial interest, current research has not adequately captured the real-world constraints in Vehicular Ad hoc Network handover techniques. This is necessary in order to provide seamless connectivity for optimal coverage and ideal channel utilization. Our previous work highlighted the challenges in providing ubiquitous communication using Road Side Unit in Vehicular Ad hoc Network. We used some of the concepts of the Y-Comm architecture such as Network Dwell Time, Time before Handover and Exit Time to provide a framework to investigate handover issues concentrating on essential parameters such beaconing and velocity of the vehicle. The results clearly showed that the Network Dwell Time was affected by the size and frequency the beacon and as well as the velocity of the vehicle. In this paper we conducted simulation studies to further examine the relation between these parameters. Simulation of VANET systems depends critically upon the calculation of the probability of a successful transmission. The current formulas used to calculate this parameter do not take into account the frequency of the beacon or velocity of the vehicle. This paper shows that these factors are significant and point to the need for a more complete analytical model for estimating the Network Dwell Time.

Providing Ubiquitous Communication Using Road Side Units in VANET systems: Unveiling the Challenges (IEEE - 13th International ITST Conference)

Vehicular Ad-Hoc Networks (VANETs) are a long-term solution contributing significantly towards Intelligent Transport Systems (ITS) in providing access to critical life-safety applications and services. Although Vehicular Ad Hoc Networks (VANETs) are attracting greater commercial interest, current research has not adequately captured the real-world constraints in VANET handover techniques. Therefore, in order to have the best practice for VANET services, it is necessary to have seamless connectivity for optimal coverage and ideal channel utilization: this comes at the cost of overlapping

signals of adjacent RSUs. This overlapping effect can be investigated using concepts such Network Dwell Time, Time Before Handover and Exit Times. In this simulation study we investigate the feasibility and benefits of providing a ubiquitous communication in VANET under different mobile environments. We also study the impact of beacon frequency and velocity on Network Dwell Time, Time Before Handover and Exit Times, which will help us to predict the handover times and thus make proactive handover possible. Therefore understanding handover issues is critical in supporting life-safety applications and services in VANETs.

Analysis of Inter-RSU Beaconing Interference in VANETs (Springer - Lecture Notes in Computer Science Series)

Vehicular ad Hoc Networks (VANETs) have emerged as a key technology serving community of peoples in various applications. Providing infotainment and safety services requires the existence of roadside units (RSU) to access to the desired resources. Ideally, the infrastructure should be deployed permeatively to provide continuous connectivity and optimal coverage. This deployment technique increases capacity and coverage at expenses of increasing interference that can severely degrade the performance of the VANET. Moreover, malicious vehicles could mimic the signals of RSUs causing significant performance degradation. In this paper we study the impact of the inter-RSU interference on the beacon broadcasting due to both inefficient deployment and potential RSU emulation attacks (REA). Extensive packet-level simulations have been performed to support the observations made.